UNIVERSITÉ DE REIMS CHAMPAGNE-ARDENNE

ÉCOLE DOCTORALE SCIENCES TECHNOLOGIE SANTE (547)

THÈSE

Pour obtenir le grade de

DOCTEUR DE L'UNIVERSITÉ DE REIMS CHAMPAGNE-ARDENNE

Discipline : ***SCIENCES DE LA VIE ET DE LA SANTE***

Spécialité : Médecine - STS

Présentée et soutenue publiquement par

CHRISTIAN GARBAR

Le 6 juillet 2018

MUC1/EGFR/IL17 et l'autophagie sont associés dans la résistance à la chimiothérapie et aux thérapies ciblées dans les cancers du sein triple négatif.

Thèse dirigée par **YACINE MERROUCHE ET FRANK ANTONICELLI**

JURY

Mme Anne MARIE-CARDINE,	Directeur de Recherche,	INSERM Hôpital Saint Louis, PARIS,	Président
M. Yacine MERROUCHE,	Professeur,	Université de Reims Champagne Ardenne	Directeur de thèse
M. Frank ANTONICELLI,	Professeur,	Université de Reims Champagne Ardenne,	Co-Directeur de thèse
Mme Hélène Le BUHANEC,	Chargé de Recherche HDR,	INSERM Hôpital Saint Louis, PARIS,	Rapporteur
M. Armand BENSUSSAN,	Directeur de Recherche,	INSERM, Hôpital Saint Louis, PARIS,	Invité
M. Stéphanie SERVAGI-VERNAT,	Maître de Conférences HDR,	Université de Reims Champagne Ardenne,	invité

UNIVERSITÉ DE REIMS CHAMPAGNE-ARDENNE

ÉCOLE DOCTORALE SCIENCES TECHNOLOGIE SANTE (547)

THÈSE

Pour obtenir le grade de

DOCTEUR DE L'UNIVERSITÉ DE REIMS CHAMPAGNE-ARDENNE

Discipline : ***SCIENCES DE LA VIE ET DE LA SANTE***

Spécialité : Médecine - STS

Présentée et soutenue publiquement par

CHRISTIAN GARBAR

Le 6 juillet 2018

MUC1/EGFR/IL17 et l'autophagie sont associés dans la résistance à la chimiothérapie et aux thérapies ciblées dans les cancers du sein triple négatif.

Thèse dirigée par **YACINE MERROUCHE ET FRANK ANTONICELLI**

JURY

Mme Anne MARIE-CARDINE,	Directeur de Recherche, INSERM Hôpital Saint Louis, PARIS, Président
M. Yacine MERROUCHE,	Professeur, Université de Reims Champagne Ardenne, Directeur de thèse
M. Frank ANTONICELLI,	Professeur, Université de Reims Champagne Ardenne, Co-Directeur de thèse
Mme Hélène Le BUHANEC,	Chargé de Recherche HDR, INSERM Hôpital Saint Louis, PARIS, Rapporteur
M. Armand BENSUSSAN,	Directeur de Recherche, INSERM, Hôpital Saint Louis, PARIS, invité
Mme. Stéphanie SERVAGI-VERNAT,	Maître de Conférences HDR, Université de Reims Champagne Ardenne, invité

REMERCIEMENTS

Merci aux membres du jury et mes directeurs de thèse, le Professeur Yacine Merrouche, le Professeur Frank Antonicelli, le Docteur Anne Marie-Cardine, le Docteur Hélène le Buanec, le Docteur Stéphanie Servagi-Vernat et le Docteur Armand Bensussan, pour avoir partagé leurs précieux temps pour la lecture, les commentaires et la participation au Jury de cette thèse.

Lors de la réalisation de ces lignes, j'ai une pensée émue à tous ceux qui m'ont poussé à ce travail et en particulier, à deux Directeurs de l'Institut Jean Godinot : le Professeur Yacine Merrouche et le Professeur Hervé Curé. Je n'oublie pas, non plus, le Docteur Armand Bensussan qui fut mon lecteur principal et ma motivation au long de ces trois années de travail.

Plus encore dans le passé, je n'oublie pas le Professeur Charles van Ypersele de Strihou, le Professeur Michel Jadoul et le Professeur Henry Noel des Cliniques Universitaires Saint-Luc (Université Catholique de Louvain, Bruxelles) pour m'avoir donné la passion de la recherche et les outils pour la publier. Merci pour ces travaux sur l'amylose du dialysé.

Difficile d'oublier le Professeur Mia Pipeleers-Marichal (Vrij Universiteit van Brussel) qui fut certainement la pierre fondatrice de ma carrière. Merci pour ta confiance durant ces 13 années fragmentées à l'AZ !

En écrivant une thèse sur l'autophagie, il est difficile de ne pas souligner ma formation rigoureuse de médecin à l'Université Catholique de Louvain et, particulièrement des cours de biochimie et de physiologie cellulaire des Professeurs Baudhuin P., Beaufay H., Berthet J., Hers H. et Masson P., équipe du Pr Christian de Duve, prix Nobel de médecine pour la découverte du lysosome et du peroxysome, ainsi que du concept de l'autophagie. Merci à tous mes professeurs de l'UCL.

Merci à mes filles pour leur soutien.

Pour finir, merci à mon épouse et technicienne Corinne Mascaux pour son travail technique exceptionnel et rigoureux, base de cette thèse que je partage avec toi, et surtout pour ta patience.

Je terminerai par une citation du Professeur Christian de Duve, prix Nobel de Médecine 1974 : conseil aux jeunes chercheurs ***« N'hésitez pas à suivre votre curiosité plutôt que de rester liés à un programme préétabli. »***

RESUMES

MUC/EGFR/IL17 et l'autophagie sont associés à la résistance à la chimiothérapie ou aux thérapies ciblées dans les cancers du sein triple négatif.

Résumé :

Le cancer du sein triple négatif (TN) est un cancer présentant des résistances aux agents de chimiothérapie. Malgré la forte expression de l'EGFR, il est aussi résistant aux agents anti-EGFR. Ces mécanismes de résistance ne sont pas connus.

MUC1 est une protéine transmembranaire largement glycosylée. Sa fonction extracellulaire est impliquée dans la régulation des récepteurs membranaires, dont l'EGFR. Comme les autres glycoprotéines membranaires, son unité extracellulaire (MUC1-N) peut moduler la réponse cellulaire immune par hypersialylation. Son unité intracellulaire (MUC1-C) possède des sites de phosphorylation impliqués dans plusieurs voies de signalisation telles que PI3K/AKT/mTOR ou RAS/RAF/MEK/ERK. Ces dernières régulent l'autophagie qui est un mécanisme de survie cellulaire associé à la résistance aux agents de chimiothérapie.

Nous avons démontré que les TN présentaient des modifications quantitatives et qualitatives de l'expression de MUC1, altérant probablement les régulations des voies associées à MUC1/EGFR dont l'autophagie. L'activation de l'autophagie explique la résistance aux traitements des agents de chimiothérapie. L'IL17 est un facteur pro-inflammatoire secrété par du microenvironnement tumoral et associé également à la résistance des agents de chimiothérapie des TN, par activation de la voie MEK/ERK, suggérant son implication à activer l'autophagie.

En conclusion, nos travaux permettent d'émettre l'hypothèse que l'inhibition de l'autophagie et/ou MUC1 et/ou IL17 pourrait augmenter la sensibilité aux traitements de chimiothérapie ou des thérapies ciblées dirigées contre les TN.

Mots clés : MUC1, EGFR, IL17, autophagie, triple-négatif, sein, cancer

MUC1/EGFR/IL17 and autophagy are associated in resistance of chemotherapy or targeted therapy in triple negative breast cancer.

Resume

Triple negative breast cancer (TN) is often associated to chemioresistance. Despite an EGRF over-expression, TN is also resistant to anti-EGFR drugs. These resistance mechanisms are not known yet.

MUC1 is a transmembrane broadly glycosylated protein. Its extracellular unit (MUC-N) is involved to membrane receptor regulations, as EGFR. As other membrane glycoproteins, MUC1 could modulate, by over-sialylation, the immune cellular response. Its intracellular unit (MUC-C) presents phosphorylation sites involved in numerous signal pathways such as PI3K/AKT/mTOR or RAS/RAF/MEK/ERK. Both pathways regulate autophagy which is a survival cellular mechanism associated to resistance of chemotherapy drugs.

We showed that TN presents quantitative and qualitative MUC1 alterations, likely associated with dys-regulation of autophagy/MUC1/EGFR pathways. The activation of autophagy explains the chemotherapy resistance. IL17 is a pro-inflammatory interleukin secreted by the tumor microenvironment. In TN, IL17 is also associated to chemiorestistance throughout the MEK/ERK pathways, suggesting its involving activating autophagy.

In conclusion, our work allows us to hypothesize that inhibition of autophagy and/or MUC1 and/or IL17 could be increasing the sensibility to chemotherapy or targeted therapies against TN.

Key words : MUC1, EGFR, IL17, autophagy, triple-negative, breast, cancer

UNITES DE RATTACHEMENT

EA-7509 DERM-IC

UFR Médecine Reims

51095 Reims Cedex

INSTITUT DE CANCEROLOGIE JEAN-GODINOT

Départements de Biopathologie et de Recherche

1, rue du Général Kœnig – CS 80014

51726 Reims Cedex.

TABLE DES MATIERES

Remerciements p2

Résumés p3

Table des matières p6

Table des illustrations p7

Abréviations p9

Corps du texte

1. Introduction p10
2. Théorie
    a. Les cancers du sein p12
    b. MUC1 : sa structure, MUC1-N et la glycosylation, MUC1-C et les voies de signalisation p13
    c. Relation entre MUC1, EGFR et/ou IL17 p25
    d. Autophagie p26
3. Publications et travaux
    a. But de cette thèse p29
    b. Avant-propos p30
    c. Apports personnels p31
    d. Publications p32
    e. Perspectives p93
4. Discussion p96
5. Conclusion générale p99

Bibliographie p101

Annexes : nos travaux de collaboration en relation avec la thèse p113

1. Publication sur l'hétérogénéité des cancers du sein triple négatif.
2. Découverte de MUC1-ARF
3. Publications concernant IL17 dans les cancers du sein triple négatif

TABLE DES ILLUSTRATIONS

- figure 1 : classification moléculaire des cancers du sein selon Pérou p12

- figure 2 : classification des mucines p14

- figure 3 : structure de MUC1 p15

- figure 4 : structure de MUC1-ARF p16

- figure 5 : mécanismes de la glycosylation p18

- figure 6 : O-glycosylation normale de MUC1-N p19

- figure 7 : sialylation de MUC1-N dans le cancer p20

- figure 8 : cibles thérapeutiques de MUC1-N p21

- figure 9 : trois sites de phosphorylation de MUC1-C p22

- figure 10 : voies de signalisation impliquées avec MUC1-C :
PI3K/AKT/mTOR et RAS/RAF/MEK/ERG p23

- figure 11 : MUC1-C et les voies d'internalisation des récepteurs
et des signaux intracellulaires, voie d'activation de l'AMPK p24

- figure 12 : l'autophagie p26

- figure 13 : voies de régulation de l'autophagie impliquée à MUC1-C p28

- figure 14 : expression de MUC1 dans le tissu normal et le cancer du sein p33

- figure 15 : corrélation entre Bécline1 et PI3Kp110β dans les TN p51

- figure 16 : corrélation entre Bécline1 et MUC1-N dans les TN p51

- figure 17 : corrélation entre PI3Kp110β et MUC1-C dans les TN p52

- figure 18 : corrélation entre MUC1-N et MUC1-C dans les TN p52

- figure 19 : autophagie dans les cellules MCF7 (LUM) p67

- figure 20 : autophagie dans les cellules MDA-MB231 (TN) p67

- figure 21 : expression de ST6Gal-I dans les cancers du sein p82

- figure 22 : expression de ST6Gal-II dans les cancers du sein p82

- figure 23 : expression de ST6GalNac-I dans les cancers du sein p82

- figure 24 : corrélation ST6Gal-I et CTL dans les HER2 p83

- figure 25 : corrélation ST6Gal-II et ST6GalNac-I et CTL dans les TN p84

- figure 26 : double marquage MUC1-C et EGFR dans une glande normale p93

- figure 27 : double marquage MUC1-ARF et EGFR dans un LUM p94

- figure 28 : double marquage MUC1-ARF et EGFR dans un TN p95

ABBREVIATIONS

ABL	Abelson leukemia virus
AKT	nom d'une souche de souris
AMP	adénosine monophosphate
AMPK	AMP kinase
ARNm	acide ribonucléique messager
ATG	autophagy related gene
ATP	adénosine triphosphate
BAX	BCl2 associated X protein
Bcl2	B-cell lymphoma 2
CK	cytokératine
CTL	cytotoxic T lymphocytes
DIN	ductal in-situ neoplasia
EGF	epidermal growth factor
EGFR	epidermal growth factor receptor
ErbB	de erythrobastose B virus, famille des récepteurs de croissance épithéliaux
ERK	extracellular signal-regulated kinase
FFPE	formol fixation parafin embebbed
FGFR	fibroblastic growth factor receptor
GRB2	growth factor receptor binding protein 2
GSK3β	synthetase kinase 3 beta glycogen
HER2	Human epidermal growth factor 2
HER2	Cancer du sein surexprimant HER2
HIF	hypoxy induced factor
HSP	Heat shock protein
IGFR	insulin-like growth factor receptor
IL17	interleukine 17
JAK	janus kynase
Ki67	marqueur de la prolifération cellulaire
LAMP	lysosome associated membrane protein
LC3	microtubule light chaine 3
LUM	cancer du sein luminal
MAPK	mitogen-activated protein kinase
MEK	MAPK-ERK kinase
MET	mesenchymial-epithelial transition factor receptor tyrosine kinase
mTOR	mammalian target of rapamycin
MUC1	mucin 1
MUC1-C	unité COOH de MUC1
MUC1-CT	domaine intracytoplasmique carboxy-terminale.
MUC1-N	unité NH2 de MUC1
NFκN	nuclear factor kappa N
PDGFR	platelet-derived growth factor
PI3K	Phosphoinositide 3-kinase
PIP2	phosphatidylinositol diphosphate
PIP3	phosphatidylinositol triphosphate
RAF	rat fibrosarcoma virus
RAS	Rat sarcoma virus
RO	récepteur aux œstrogènes
RP	récepteur à la progestérone
SEA	sperm enterokinase and agrine
Sia	acide sialique
Src	Sarcoma virus
sT	forme sialylisée de l'antigène T
ST6Gal	galactosamine sialyltransférase
ST6GalNAc	N-acétyl galactosamine sialyltransférase
STAT	signal transducer and activator of transcription
sTn	forme sialylisée de l'antigène Tn
T	antigène de Thomsen-Fridenreich
TAA	tumor-associated antigen
TMA	tissue micro area
TN	Triple-négatif, cancer du sein triple négatif
Tn	antigène Tn
TNM	classification clinique Tissu/Node/Metastase
ULK	unc like activating kinase
VEGFR	vascular endothelial growth factor receptor
VNTR	variable number of tandem repeats

CORPS DU TEXTE

1) INTRODUCTION

Ce travail a été initié à la suite d'un programme de recherche de l'Institut de cancérologie Jean Godinot sur les cancers du sein triple négatifs (TN) qui a débuté, il y a 8 ans, lors d'une réunion de travail composée de pathologistes, d'oncologues et de chercheurs immunologistes. En effet, pour l'oncologue ces tumeurs TN incitent un sentiment d'impuissance, car elles répondent peu aux traitements de chimiothérapie classique. Leur pronostic est donc très péjoratif.

Pour l'immunologiste, une des voies possibles de cet échappement se trouve dans le stroma et le microenvironnement tumoral. Les signaux effecteurs entre les cellules immunes et les cellules tumorales pourraient, en partie expliquer la résistance aux traitements. Par exemple, les interleukines comme IL6 et IL8 influencent cette relation entre les cellules immunes et les cellules tumorales. Il est aussi admis que les lymphocytes associés aux tumeurs du sein TN sont l'un des facteurs pronostics favorables à la réponse aux traitements de chimiothérapie. De plus, parmi ce groupe de lymphocytes, on décrit une sous-population de lymphocytes T intra-tumoraux (Th17) secrétant de l'interleukine 17 A.(37) Notre équipe de recherche en immunologie a principalement étudié IL17 et ses variantes. (voir annexes)

En dehors du diagnostic, pour le pathologiste les voies d'étude sont nombreuses. Nous nous sommes spécialement intéressés à MUC1, une mucine transmembranaire MUC1 que nous avons démontrés dans les tumeurs urologiques de la prostate et de la vessie. (21-22) L'étude de la littérature concernant MUC1, nous a d'emblée intriguée par la possibilité de MUC1 de se lier aux récepteurs de croissance tels que l'EGFR. En effet, l'EGFR est largement exprimé par les cancers du sein TN, contrairement aux autres types de cancers du sein. Par ailleurs, l'un des cofacteurs principaux de l'EGFR est la PI3K de classe 1, une kinase assez complexe qui active la voie AKT/mTOR. Nous avons étudié l'expression de la sous-unité p110β de PI3K, car elle intervient comme régulateur « fin » de l'action de PI3K de classe 1, mais aussi comme un facteur influençant de l'autophagie.

L'autophagie est le mécanisme cellulaire de survie de la cellule lors d'une agression telle que l'hypoxie, la privation glucidique, les radiations ionisantes, mais surtout les agents de chimiothérapies. Elle intervient certainement dans les résistances aux traitements des cancers du sein TN. De plus, sa régulation est

associée à mTOR, l'un de ses inhibiteurs principaux (voie PI3K/AKT/mTOR) et ERG (voie RAS/RAF/MEK/ERK) ou l'hypoglycémie (voie AMPK, p53), comme activateurs.

MUC1 est aussi intimement lié à la voie d'EGFR et peut d'ailleurs être phosphorylé par plusieurs kinases dont EGFR lui-même et PI3K. Son rôle sur l'autophagie pourrait se faire indirectement par ses régulations sur EGFR, sur PI3K (voie de mTOR), sur GRB2 (voie RAS/RAFMEK/ERK) ou encore sur la glycolyse (AMPK).

Concomitamment à ce travail, nos équipes d'immunologistes ont récemment démontré que l'IL17A intervient aussi dans la résistance de la chimiothérapie des cancers TN par activation de la voie d'ERK1/2, cette même voie activatrice de l'autophagie.

La question était donc posée : « ***Existe-t-il une relation entre MUC1-EGFR-IL17 et l'autophagie dans les cancers du sein triple négatif ? Et dans ce cas, quel en est le rôle dans la chimiorésistance induite par ces tumeurs ?*** »

2) THÉORIE

a) Le cancer du sein.

Le cancer du sein est la première cause de mortalité par cancer dans nos pays occidentaux. Le traitement actuel se base sur une classification génétique et moléculaire proposée par Perou *et al.* (75-76). Schématiquement, cinq sous-types sont décrits (figure 1) :

- le luminal A (LUM) exprimant les récepteurs aux œstrogènes (RO+) et à la progestérone (RP+), mais pas le récepteur de facteur de croissance épidermique 2 (HER2 -) et présentant un indice de prolifération faible (Ki67 < 14 %),
- le luminal B exprimant RO+ et RP+, mais pas HER2- et présentant un indice de prolifération élevé (Ki67>14),
- le luminal C caractérisé par RO+RP+/-HER2+,
- Les HER2 surexprimés qui montrent une amplification génétique du gène HER2 associée à la surexpression de sa protéine et l'absence de récepteurs hormonaux : RO- RP- HER2+
- TN qui sont négatifs pour tous ces récepteurs : RO-RP-HER-

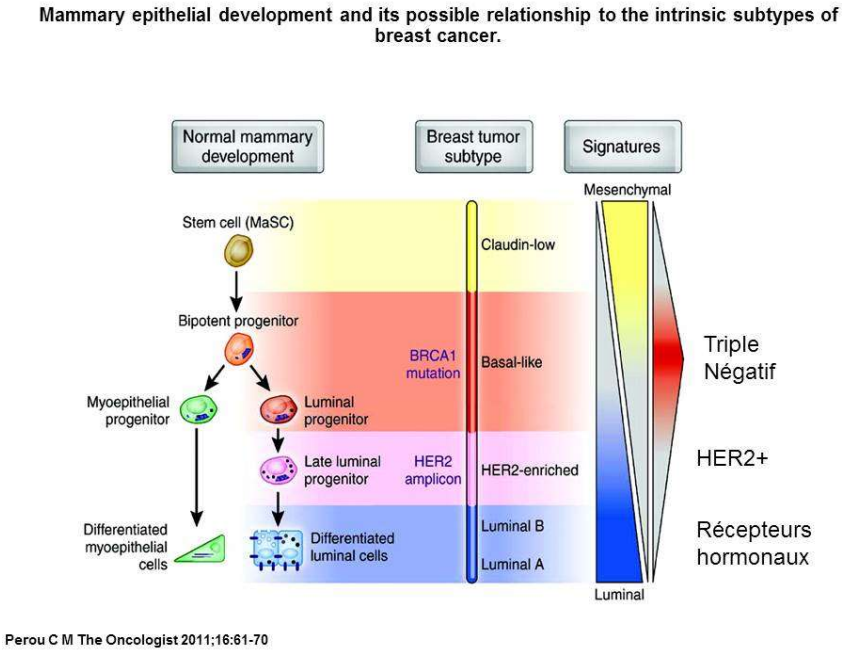

Figure 1 : Classification moléculaire des cancers du sein selon Pérou C. et al. (Voir texte)

En général, le traitement des cancers du sein repose sur l'administration d'anti-estrogènes et/ou d'anti-HER2 selon l'expression de ces récepteurs par les cellules tumorales. A cela s'ajoute une chimiothérapie classique si la tumeur présente un indice élevé de prolifération (Ki67).

Les patientes souffrant un cancer TN, sont plus difficiles à traiter par ces cibles thérapeutiques classiques. En effet, ce type de cancer n'exprime ni les récepteurs hormonaux, ni HER2. De plus, ce groupe de tumeurs est très hétérogène d'un point de vue moléculaire et de comportement clinique. La conséquence est que ces tumeurs ont souvent une évolution et un pronostic variables.

Bien que de nombreuses sous-classes ont été décrites, les TN sont divisés actuellement en deux sous-groupes : l'un dit « basal-like » qui est le plus fréquent - secrétant l'EGFR et les cytokératines basales (CK5/6 et CK14) - et les non-basal-likes n'exprimant pas ces marqueurs. (annexes) En pratique, la distinction entre basal-likes et non basal-likes semble cependant purement académique.

Rappelons que la majorité des TN, contrairement aux LUM (ce type de cancer nous servira de groupe témoin), exprime fortement EGFR. Curieusement les traitements anti-EGFR (cetuximab, erlutibine…), pour une raison encore inconnue, sont rarement très efficaces contre les TN.

Concernant MUC1, celui-ci est décrit comme fortement secrété dans les cancers du sein, est peu secrétéé voir absent dans les TN, expliquant partiellement les limites des quelques essais thérapeutiques cliniques d'immunothérapie anti-MUC1 sur ces tumeurs.

Les chapitres suivants résument la description moléculaire de MUC1 et ses fonctions cellulaires les plus importantes.

b) Structure et fonctions de MUC1

Les mucines ont d'abord été décrites comme des glycoprotéines de lubrification et de protections mécanique et antimicrobienne de l'épithélium de revêtement comme celui des bronches ou du tube digestif. Par la suite, on s'est rendu compte qu'elles étaient secrétées ubiquitairement dans quasi tous les organes glandulaires.

Les travaux de ces dernières décennies ont montré que leur rôle ne s'arrêtait pas en une simple fonction mécanique, mais qu'elles intervenaient comme messager intermédiaire entre le milieu extracellulaire - par modifications de sa structure glycosylée externe - et le milieu intracellulaire - par phosphorylation de ses domaines intracytoplasmiques. (74)

MUC1 est fortement altérée dans les cancers, surtout dans ses domaines glycosylés. La plupart des antigènes de glycosylation anormale de MUC1 sont d'ailleurs des antigènes associés aux tumeurs (« tumor-associated antigens » ou TAA), non exprimés par les cellules normales. Les TAA sont donc de sérieux candidats à la thérapie ciblée.

« The Human Genome Nomenclature Committee » décrit actuellement une famille de 18 gènes dont 11 codent pour des protéines membranaires. La plus étudiée des mucines transmembranaires est MUC1. (46) (figure 2)

	Localisation	Chromosome	Répétition (nombre d'acides aminés)	Taille de l'ARN (kb)
Mucines sécrétées				
MUC2	Côlon (LS174T)	11p15	23	14-16
MUC5AC	Trachée	11p15	8	17-18
MUC5B	Trachée	11p15	29	17,5
MUC6	Estomac	11p15	169	16,5-18
Mucines membranaires				
MUC1	Sein, pancréas	1q21-24	20	4-6, 8
MUC4	Trachée	3q29	16	16,5-24
MUC3 (A, B)	Intestin grêle	7q22	17	17-17,5
MUC11	Côlon	7q22	?	?
MUC12	Côlon	7q22	?	?
MUC17	Recherche informatique	7q22	59	?
Inclassables ou non mucines ?				
MUC7	Glandes salivaires	4q13-q21	23	2,7
MUC8	Trachée	12q24.3	14	?
MUC9	Oviducte	1p13	?	?
Muc 10 (murin)	Glandes salivaires	?	13	0,85
MUC13	Recherche informatique	3q13	28	3,2
Muc14 (murin)	Endothélium	3	?	1,3
MUC15	Lait	11p14	?	?
MUC16	Cancer de l'ovaire (CA 125)	19p13	165	?
MUC18	Mélanocytes	?	?	3,3

Figure 2 : Classification des mucines.

i) Structure de la molécule MUC1

Le gène de MUC1 contient 8 exons et occupe 4,4 kbp sur le locus 1q21. Sept variants ARNm de MUC1 sont transcrits en un seul polypeptide, et un certain nombre ARNm subissent un épissage, ou même une protéolyse ultérieure de la portion extracellulaire. La partie intracellulaire de la molécule est relativement constante chez les mammifères, soulignant son caractère fonctionnel important dans la phylogenèse. (2, 6, 67)

Le polypeptide de MUC1 est ensuite clivé au niveau du SEA module (domaine du Sperm Enterokynase and Agrine) en deux sous unités, une partie extracellulaire amino-terminale, dite sous-unité α (synonymes : MUC1, *MUC1-N*, MUC1-VNTR) et une partie transmembranaire carboxy-terminale dite β (synonymes : *MUC1-C*, MUC1-CT). L'ensemble formant un complexe protéique hétérodimère lié par une liaison non covalente. (51,52 ,88) (figure 3)

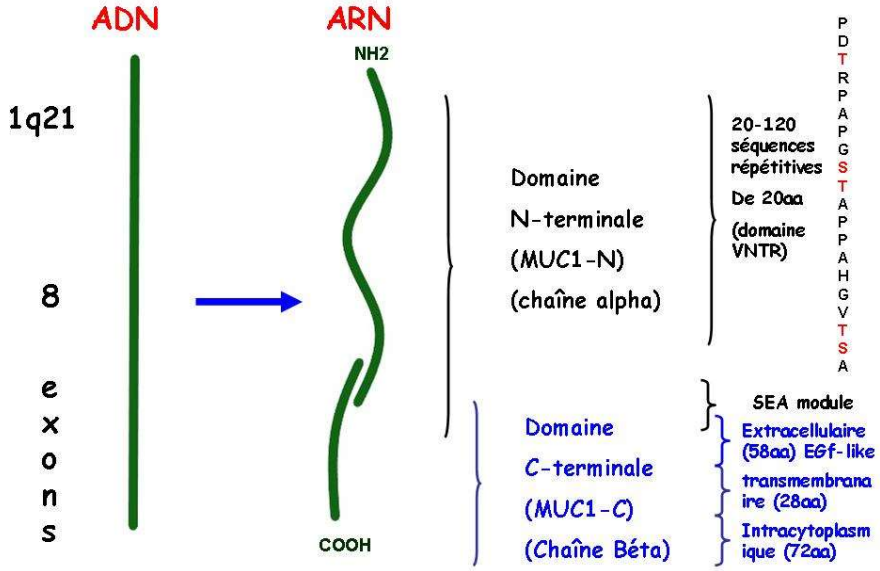

Figure 3 : Structure de l'hétérodimère de MUC1. (voir texte)

Plusieurs transcrits de la forme classique de MUC1 sont décrits avec de grandes variations de l'unité MUC1-N. En effet, MUC1-N (extracellulaire) est composée par un volumineux domaine de 25 à 125 séquences répétitives, dite tandem (domaine VNTR) formées d'une succession de 20 acides aminés riches en sérine et thréonine (séquence PD**T**RPAPG**ST**APPAHGV**TS**A). La sérine et la thréonine sont

des sites connus pour des liaisons O-glycosidiques qui seront, par conséquent, abondantes sur la partie extracellulaire de MUC1. (16, 94)

Dans le tissu normal, MUCI-N est fortement glycosylée et représente 50 à 90 % de la masse moléculaire. Cette partie glycosylée est fortement altérée dans le cancer et exprime de nombreux antigènes tumoraux (TAA).

Récemment, un nouveau transcrit de MUC1, pour lequel nous avons modestement collaboré, *MUC1-ARF* a été décrit. (figure 4) Celui-ci consiste en une molécule non clivée contenant 175 aa en C-terminal, environ une quinzaine de séquences VNTR (300aa), 49 aa en N-terminal. Cette molécule ne possède pas le domaine SEA. Par contre, MUC1-ARF possède de nombreux domaines SH3 pouvant s'associer à de nombreuses protéines comme l'EGFR (docking site). MUC1-ARF est observée dans le cytoplasme et le noyau des cellules normales et tumorales, mais, contrairement à la molécule dimère de MUC1, elle n'est pas retrouvée au niveau membranaire. Son transfert nucléaire est favorisé par des cytokines du milieu extracellulaire (IL6 et IL8), soulignant l'influence des interleukines secrétées par le milieu sur le métabolisme de MUC1. Les fonctions de MUC1-ARF restent encore à découvrir. (12) (annexes).

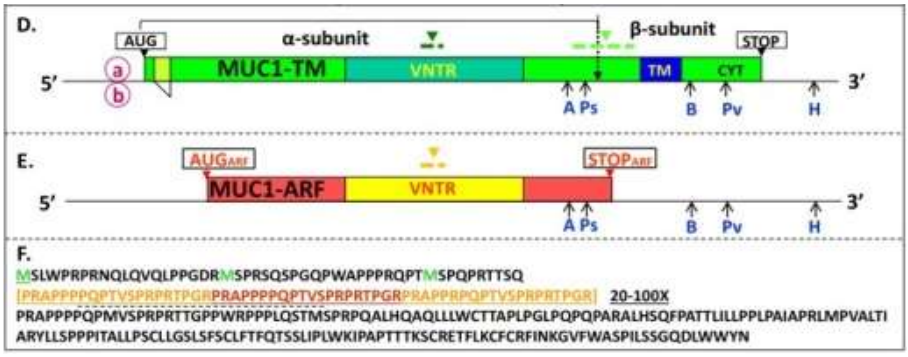

Figure 4 : Structure de MUC1-ARF. Cette molécule est non clivée, ne contient pas de sous-unité bêta et possède moins de VNTR que le MUC1 transmembranaire. On la retrouve dans le cytoplasme et le noyau des cellules. Il n'y a pas d'expression membranaire. (voir annexe 2)

L'unité MUC1-C (intracellulaire) contient un domaine extracellulaire de 58 acides aminés, un domaine hydrophobe transmembranaire de 28 aa et un domaine intracytoplasmique de 72aa ou C-Terminal dénommé MUC1-CT. (61)

MUC1-C est connue pour former un complexe à la surface des cellules, avec la famille des ErbB (récepteurs des facteurs de croissance épithéliaux) par liens non covalents avec son domaine EGF-like.(48-49)

MUC1-CT est un polypeptide intéressant, composé de 72 aa présentant 6 à 7 sites de tyrosine, capables d'être phosphorylés et donc d'initier de nombreuses voies métaboliques. Cependant comme MUC1 est dépourvu d'activité enzymatique, MUC1 ne peut pas être considéré comme une tyrosine kinase. (92,106) Le contrôle de ces phosphorylations serait réalisé par épissure de l'ARNm.(100)

De plus, la partie intracytoplasmique de MUC1-C est capable de se détacher et de se dimériser dans le cytoplasme. Ce dimère libre est un stabilisateur de plusieurs récepteurs ou messagers intracellulaires en bloquant leur dégradation par le protéosome. Il permet également leurs transferts vers le noyau. (98-99)

ii) MUC1-N et la glycosylation

La glycosylation est un mécanisme fréquent post-transcriptionnel intervenant sur les glycoprotéines ou les glycolipides. C'est un phénomène non statique, contrôlé enzymatiquement par la cellule. Le changement de la composition glucidique impacte la fonction de la protéine. La glycosylation est probablement plus fréquente que la phosphorylation. Elle est également fortement altérée dans la cellule cancéreuse. (68) MUC1 étant largement glycosylée surtout sur son domaine extracellulaire (MUC1-N), nous résumerons ci-dessous les mécanismes principaux de la glycosylation associée à MUC1.

Deux voies principales de la glycosylation des protéines sont connues (figure 5): celle retrouvée sur MUC1-N est la O-glycosylation dans laquelle le premier sucre ajouté par les glycosyltransférases, se réalise sur des résidus OH d'une sérine ou d'une thréonine. La seconde est la N-glycosylation dans laquelle un polysaccharide entier est transféré sur le groupe NH2 d'un résidu d'asparagine. Les altérations de ces glycoprotéines sont très fréquentes dans les cellules cancéreuses et se corrèlent à leur comportement invasif et métastatique.

Les modifications glycoprotéiques du cancer font intervenir des altérations mutationnelles des enzymes qui y sont impliqués (tels que les glycosyltansférases, les protéines chaperones…), mais également des altérations épigénétiques. (93)

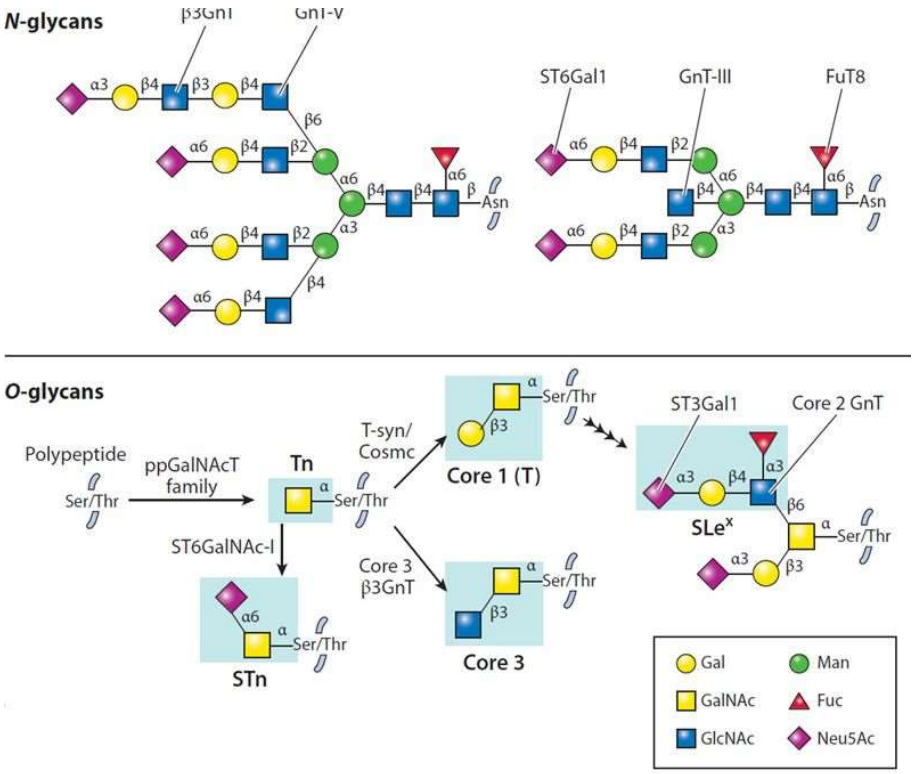

Figure 5 : Deux mécanismes de glycosylation : la N-glycosylation s'effectue sur un résidu d'Asparagine. La plupart des sialylations des N-glyco-protéines est réalisée par la ST6gal-I ; les protéines O-glycolysées développent leurs glycans sur des résidus de sérine ou thréonine (domaine VNTR de MUC1). La sialylation se fait par plusieurs enzymes dont ST6GalNac-I en est la principale.

Concernant MUC1, la O-glycosylation est initiée par une famille d'enzymes, les N-acétyl-galactosamine-transférases, ajoutant un sucre N-acétyl-galactosamine (GalNac) sur un résidu sérine ou thréonine des domaines VNTR de MUC1-N. (figure 6) Il en résulte une structure appelée antigène Tn. Le transfert d'un sucre de galactosamine (Gal) à Tn est effectué par la T-synthétase si elle est protégée de la dégradation protéosomique par la protéine chaperone COSMC. Le premier complexe glucidique formé est le core, appelé également l'antigène T ou épitope de Thomsen-Friedenreich. Ce dernier est le précurseur de l'extension de la chaîne glycosylée.

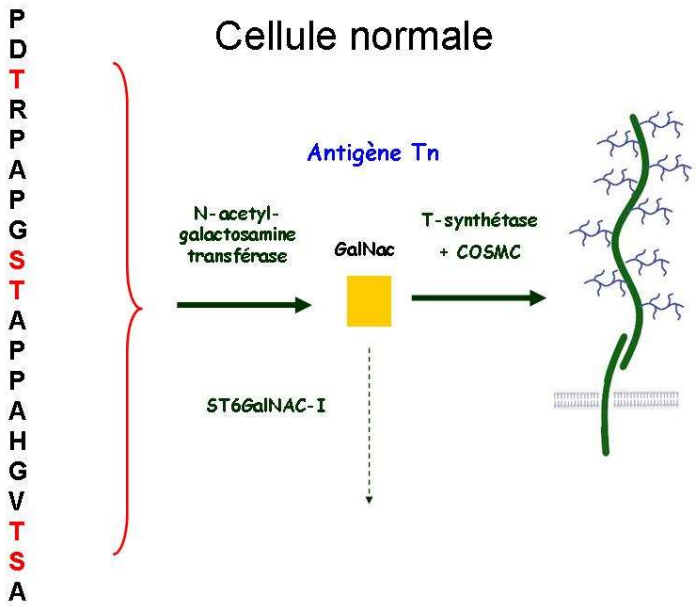

Figure 6 : O-glycosylation normale des domaines VNTR de MUC1-N fait intervenir le couple T-synthétase et sa protéine chaperone de stabilisation COSMC qui ajoute à l'antigène Tn une galactosamine pour former l'antigène T. Celui-ci est la base des longues chaînes glycosylées. L'antigène Tn ne peut donc pas être sialylisé par ST6GalNAc-I.

Dans le cancer, les chaines O-glycosylées sont tronquées et contiennent de nombreux résidus sialylisés des antigènes T et Tn.(8) Cette hypersialylisation, c'est-à-dire l'ajout d'un acide sialique (Sia) est le produit de la dérégulation et de l'hyper activation de l'enzyme α-6-N-acétyl-sialyltransférase I ou ST6GalNac-I, transférant le Sia sur Tn en sTn.(93)

Un autre mécanisme fait également intervenir l'inactivation de COSMC par hyperméthylation. COSMC stabilise la T-synthétase et empêche sa dégradation par le protéosome. Le dérèglement de la réaction est en faveur de la suractivation de ST6GalNAC-I. Le produit résiduel ou sTn qui est un signal de fin d'allongement de la chaîne glycosylée, est donc très abondant sur la cellule cancéreuse, le caractérisant comme un TAA. (98)

Tn et sTn sont également connus comme des marqueurs de dédifférenciation et de mauvais pronostic dans le cancer du sein, du côlon, de la prostate, de la vessie et du pancréas. (9, 21, 30, 35) (figure 7)

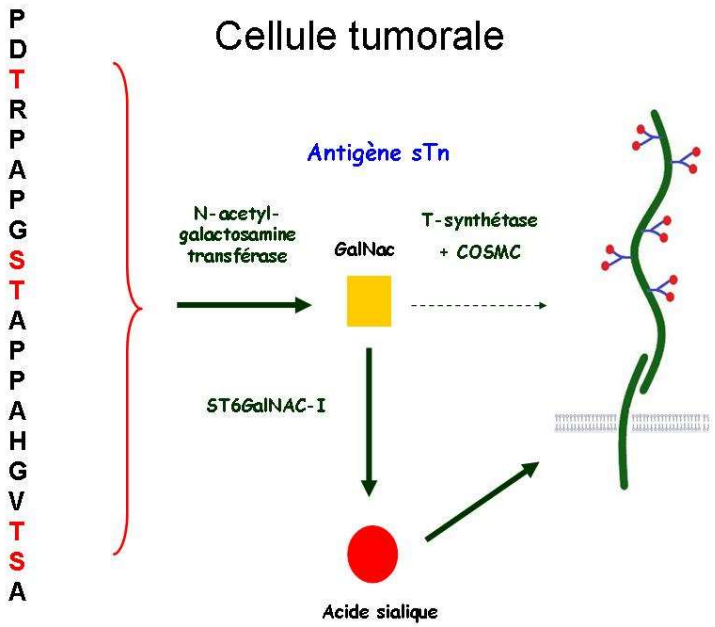

Figure 7 : Sialylation anormale de MUC1-N dans la cellule cancéreuse par inactivation de la T-synthétase et/ou de sa protéine chaperone COSMC, aboutissant à un excès de résidus d'acide sialique. La présence d'acide sialique empêche l'allongement des chaînes glycosylées qui seront tronquées et courtes, laissant à nu la protéine core. Les antigènes protéiques de cette dernière sont alors accessibles aux anticorps.

Une autre sialyltransférase, moins spécifique pour MUC1, la ST6Gal-I est corrélée avec une perte d'adhésion entre les cellules tumorales, car elle modifie la charge électrostatique négative générée par l'ensemble des résidus Sia. La résultante induit une répulsion intercellulaire ou des protéines de la matrice extracellulaire comme la fibronectine et les intégrines. (46,53, 68,104)

Cette hypersialylation de MUC1 et des autres protéines de membranes permet également aux cellules cancéreuses d'interagir avec les sialoadhésines (siglecs) présentes sur la majorité des macrophages tissulaires. Ces derniers produisent alors des pro-cytokines inflammatoires qui moduleront l'action des cellules T cytotoxiques. (4, 11, 28)

Dans le cancer du sein, la forme hypoglycosylée de MUC1 est surexprimée dans 90 % avec perte de sa polarisation membranaire apicale normale. L'expression anormale d'antigènes comme les antigènes Tn ou sTn, et la mise à nu du core protéique VNTR par la perte de glycosylation propre au cancer, ont fait de MUC1 un bon candidat à l'immunothérapie anti-cancéreuse. Actuellement, une vingtaine de vaccins anticancéreux (Stimuvax, TG4019, Panvac…) ont été actuellement produits et testés cliniquement. (26, 35) (figure 8)

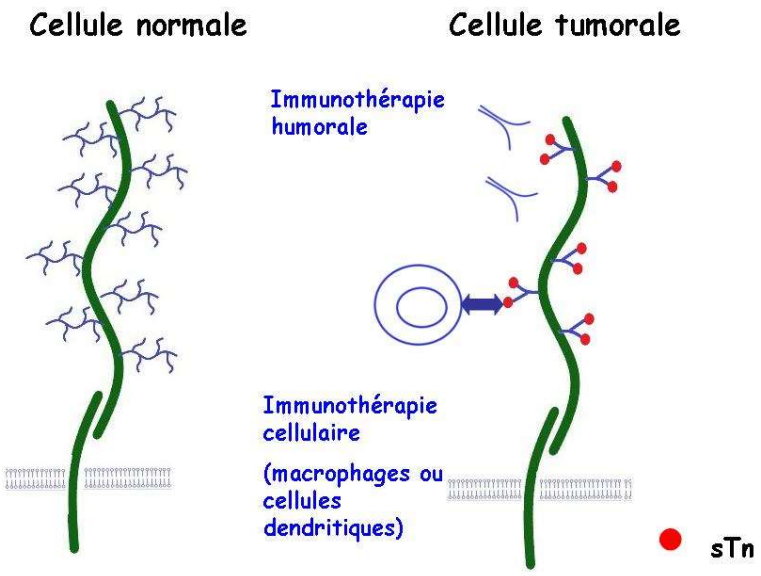

Figure 8 : Cibles thérapeutiques de MUC1-N dirigées contre la protéine core mise à nu ou contre les TAA sialylisés comme sT et sTn.

MUC-C présente aussi cinq sites potentiels de N-Glycosylation localisés sur la partie C-terminale de MUC1-N. Ces derniers interviennent dans la stabilité de la molécule. (74) Leurs altérations sont moins bien connues.

En dehors de MUC1, de nombreuses autres protéines membranaires, dont des récepteurs de facteurs de croissance, sont également régulées par glycosylation et altérées par sialylation (en particulier par ST6Gal-I ou ST6Gal-II). Parmi ces protéines, soulignons EGFR, FGFR, PDGFR, MET, IGFR, VEGFR… suggérant la complexité de la glycosylation dans la régulation des récepteurs de membrane, leurs altérations associées au cancer et les possibilités thérapeutiques. (34)

iii) **MUC1-C et les voies de signalisations**

Comme nous l'avons exprimé précédemment, la partie MUC1-C (transmembranaire et intracellulaire) est plus complexe, car elle possède de nombreux sites de phosphorylation qui sont impliqués dans plusieurs voies de signalisation. Son interaction la plus connue est celle des récepteurs de croissance épithéliale (ErbB) et en particulier EGFR, dont elle partage une affinité par son domaine extracellulaire EGF-like. Il est actuellement admis que MUC1 est un site de stockage membranaire

capable de moduler le signal transmembranaire de nombreux récepteurs, par accumulation, internalisation et transport vers le noyau. (49,87, 91) Par exemple, pour EGFR on sait que le complexe MUC1-N/MUC1-C est exprimé normalement à la partie apicale de la membrane plasmique des cellules épithéliales et inversement, EGFR est localisé baso-latéralement. (5,46). Dans la cellule tumorale ou lors d'un stress cellulaire, la perte de la polarité conduit à un repositionnement et un contact intime entre l'EGFR et MUC1-C, probablement suite à une N-glycosylation de MUC1 en Asp-36 et un couplage intermédiaire possible par le galectine-3. (85) Cette interaction augmente l'internalisation et le cycle intracellulaire et membranaire de l'EGFR en empêchant son ubiquitination par le protéosome. (60,77)

Pour la compréhension de ce travail, trois sites de phosphorylation de MUC1-C et un site riche en cystéine de MUC1-C méritent d'être mentionnés, car ils font intervenir quatre voies importantes de signalisation. (figure 9)

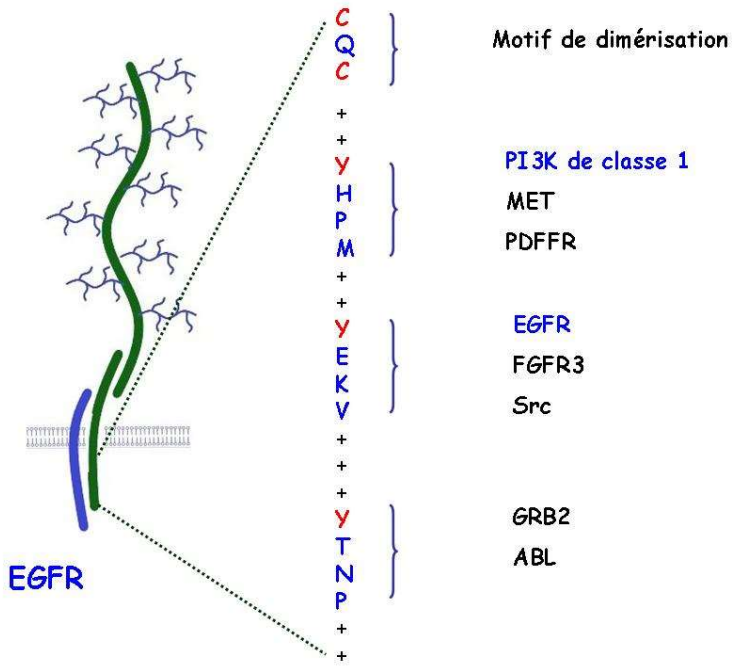

Figure 9 : Un site riche en cystéine (CQC) et trois sites importants de phosphorylation (y) de MUC1-C qui sont à l'origine de quatre voies de signalisation.

<u>La première voie de signalisation</u> (figure 10) intéresse l'interaction entre MUC1-C et EGFR qui facilite l'activation de la voie EGFR/PI3K/AKT/mTOR. (83) Cette voie fait intervenir le domaine **Y**HPM de MUC1-C. Elle est directement associée à p85 du complexe PI3K. La voie PI3K/AKT est une voie majeure impliquant la croissance, la survie cellulaire et le métabolisme des cellules cancéreuses. Les PI3Ks sont une

famille de kinases lipidiques servant de second stimulus vers diverses autres voies. Elles sont divisées en trois classes selon leurs substrats spécifiques. La classe I est activée par les récepteurs des tyrosines kinases (EGFR, HER2…). Elle est composée d'unités catalytique p110α et régulatrice p85. MUC1-C induit le recrutement membranaire de la p85 qui, à son tour, recrute la p110α générant, à partir du PIP2, un PIP3 activateur d'AKT et de ses voies métaboliques. (32,39, 97) Par contre, la p110β est l'une des sous-unités régulatrices de ce complexe PI3K activé. Comme on le décrira ci-dessous, le PI3K de classe III et l'unité régulatrice p110β de PI3K de classe I, sont aussi des activateurs de l'autophagie.

La deuxième voie de signalisation (figure 10) est celle du domaine **Y**TNP phosphorylé par GRB2, un activateur de la voie RAS/MEK/ERK. Cette phosphorylation serait tributaire de l'interaction entre MUC1 et EGFR (80-83) Ainsi, certains auteurs ont démontré une corrélation entre la surexpression de MUC1-C et l'activation de ERK. ERK participe ensuite à la régulation de MUC1. (25, 89, 95)

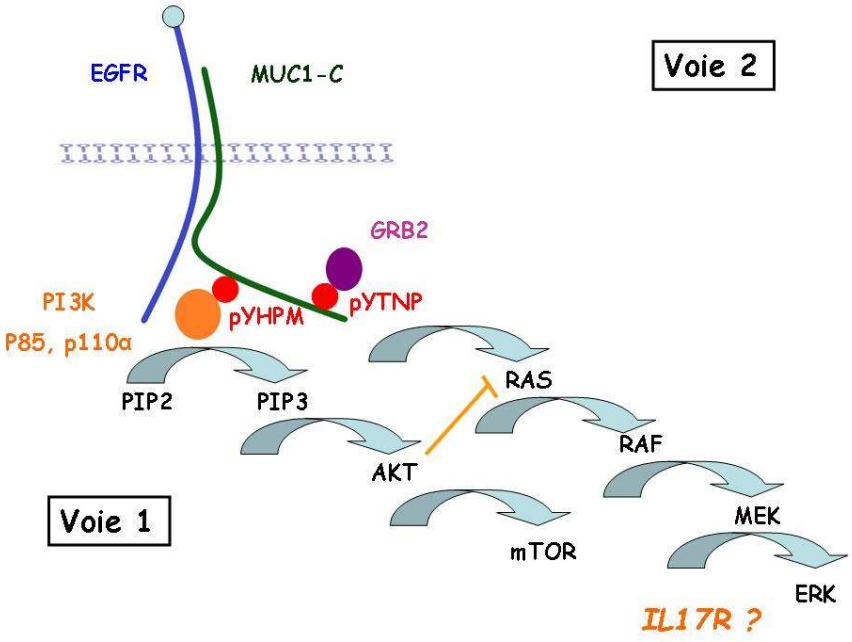

Figure 10 : Voies de signalisations PI3K/AKT/mTOR (voie 1, associée au domaine YHPM) et RAS/RAF/MEK/ERG (voie 2, associée au domaine YTNP). L'activation de ERK peut-être associée à IL17.

La troisième voie de signalisation (figure 11) de MUC1-C comprend le domaine de phosphorylation **Y**EKV également associé à l'EGFR. pYEKV est un lien pour le domaine SH2 de Src. Cette phosphorylation induit une interaction entre MUC1-C et la β-cathénine. Ce lien nécessite la forme dimère de MUC1-C. La conséquence de ce couplage est le largage de l'inhibiteur la β-cathénine, la GSK3β. Dans le noyau le complexe MUC1-C/β-cathénine coactive aussi l'expression de la cycline D1 et donc la prolifération cellulaire. (48, 84, 86, 89, 91)

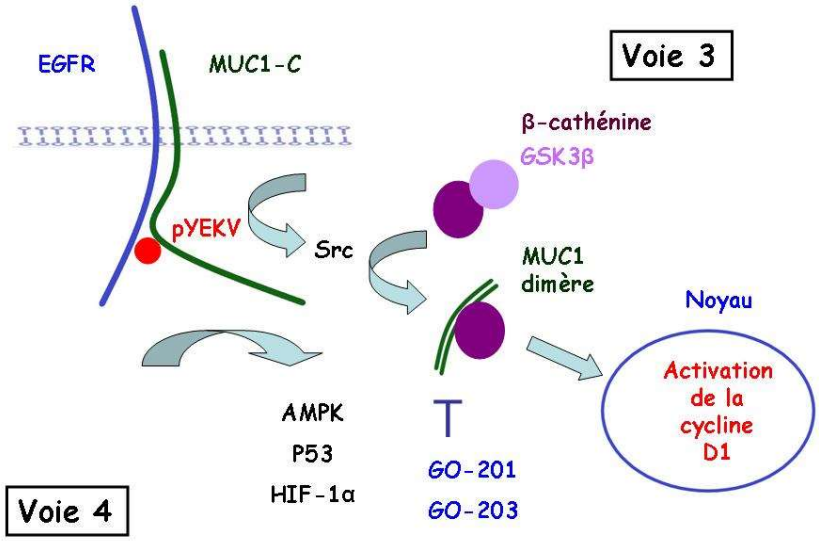

Figure 11 : Internalisation des récepteurs et effecteurs comme la β-cathénine (voie 3, associée au domaine YEKV et la dimérisation de MUC1-C), et la voie d'activation de l'AMPK lors de l'hypoglycémie (voie 4).

Comme pour la β-cathénine, MUC1-C est nécessaire au transfert de l'EGFR vers le noyau. En effet, MUC1 permet le recyclage de l'EGFR à la membrane s'il n'est pas lié à son ligand EGF. Par contre, quand EGFR est lié à l'EGF, il se lie à MUC1-C dimérisé, et par l'intermédiaire de la β-importine, est transférée dans le noyau où il active la cycline D1. En l'absence de MUC1, EGFR est dégradé par protéolyse, non recyclée et inactif. (5) Curieusement, nous avons également décrit une voie important l'EGFR stimulé vers le noyau qui serait associé aux récepteurs de l'IL17. (62)

Cette voie de dimérisation de MUC1 permettant le transfert vers le noyau, est dépendante de la présence de motifs cystéine-glutamine-cystéine (CQC). (42, 81, 99) La forme dimérisée permet également l'internalisation et le transfert vers le noyau de divers cofacteurs interagissant avec de nombreuses voies de signalisation : EGFR,

MET, Src, GSK3β, protéine kinase C, Abl, p53, NFκN, STAT3, BAX, récepteurs à œstrogènes… (1, 45) Récemment, ces domaines CQC peuvent être bloqués par des agents chimiques expérimentaux à visée thérapeutiques : GO-201 et GO-203 . (80, 96)

Enfin, la quatrième voie de signalisation (figure 11) fait intervenir le métabolisme du glucose. En effet, MUC1 est capable de moduler les régulateurs de la glycolyse en activant la signalisation des gènes de transcription impliqués dans cette voie métabolique comme a voie PI3K/AKT/mTOR, p53, HIF-1α. De même en cas de privation de glucose MUC1 active la voie AMPK et donc l'autophagie. (59)

c) Relation MUC1, EGFR et IL17

Nous avons illustré que MUC1 est une protéine de communication entre la cellule et le milieu extracellulaire et peut interagir avec de nombreuses voies de signalisation. Nous nous sommes surtout intéressés aux interactions entre MUC1/EGFR et la possibilité des interactions avec l'autophagie qui nous semble être une voie possible de la résistance à la chimiothérapie. En effet, une des voies activatrices principales de l'autophagie est celle de l'ERK qui, comme nous l'avons démontré plus haut, est co-activée par MUC1 et EGFR. (figure 10)

Cette voie est intéressante, car notre équipe a également montré une relation entre la résistance à la chimiothérapie et la phosphorylation d'ERK induite par l'interleukine 17 A. Rappelons que l'IL17A est produite par les lymphocytes intratumoraux (TIL). De plus, nous avons aussi illustré que les cellules tumorales du sein exprimaient les récepteurs à IL17. (13) (annexes)

En dehors d'ERK, la relation entre MUC1 et IL17 n'est cependant pas évidente. Une piste possible est celle de la voie des STATs (voie des cytokines et JAK Kinases) dont on sait qu'elles interagissent à la fois avec MUC1 et IL17. D'autres auteurs ont démontré une surexpression de MUC1-C dans des cultures de cellules épithéliales malignes sous l'influence de l'IL-1β, IL6 et TNFα induisant aussi le transfert de MUC1-C vers le noyau. (1, 12) Curieusement, nous avons également montré que l'IL17E et l'IL17B internalisaient l'EGFR dans le noyau comme le fait MUC1-C. (62) (annexes) La relation entre MUC1-C, EGFR et les récepteurs à IL17 reste toutefois, hypothétique.

d) Autophagie

L'autophagie est un mécanisme de survie ou de maintien de l'homéostasie cellulaire. Elle permet à la cellule de digérer une partie de ses constituants ou organites afin de fournir une source interne d'énergie, en réponse à un stress comme l'hypoxie, l'hypoglycémie, les infections, les radiations, les toxines et les agents de chimiothérapie.

L'activation de l'autophagie est complexe et fait intervenir une vingtaine de protéines contrôlées par les gènes ATG (pour autophagy related genes). Schématiquement, on distingue quatre phases : l'induction, nucléation, la maturation et la fusion aux lysosomes. (figure 12)

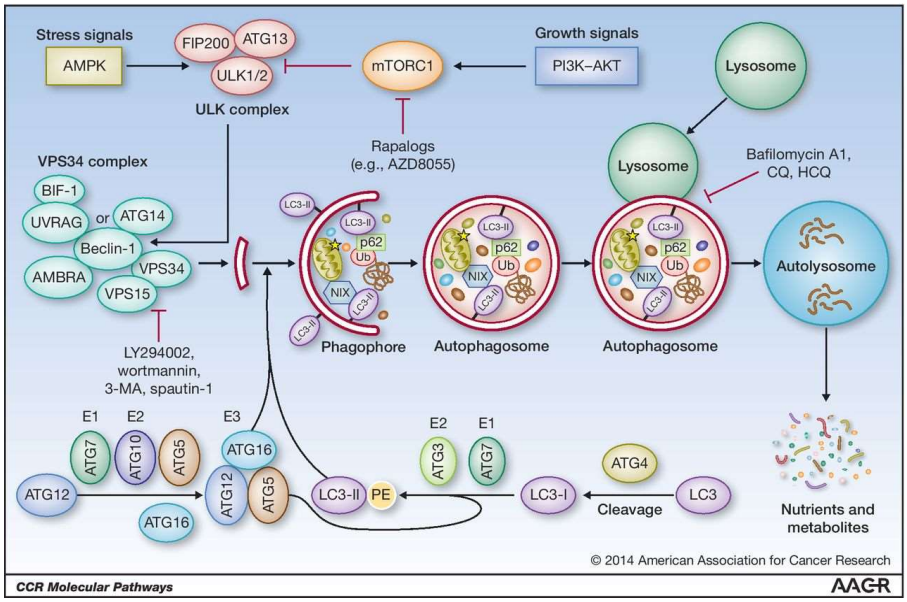

Figure 12 : Mécanisme d'activation de l'autophagie. L'activation du complexe ULK par l'AMPK et son inhibition par mTOR. ULK initialise l'activation du complexe de la Bécline-1. LC3 stabilise l'autophagosome.

L'initiation fait intervenir l'activation d'ATG1 (ULK1/2), ATG13 par l'intermédiaire de l'inhibition de mTOR et/ou l'activation de l'AMPK (AMP kinase).

La nucléation est contrôlée par la PI3K de classe III (ou Vps-34), ATG14 et la Bécline1 (ATG6). Ce complexe enzymatique activé conduit à la formation de l'autophagosome ou vésicule contenant les organites à digérer.

La maturation est régulée par LC3-I/II qui est clivé au niveau de la membrane en LC3-II par l'intervention d'ATG5-ATG16. Tous ces complexes protéiques seront retirés de l'autophagosome à l'exception de LC3 qui sera transporté vers le compartiment lysosomial.

Le dernier évènement qui est la fusion aux lysosomes, fait intervenir la LAMP2 (lysosome associated membrane protein 2). (29, 64)

L'autophagie est régulée par de nombreuses voies de signalisation dans lesquelles peut intervenir MUC1 dont on décrit deux voies principales : l'une inhibitrice et l'autre activatrice. (figure 13)

La première voie de signalisation est inhibitrice qui est souvent impliquée dans le cancer : c'est la voie PI3K de classe-I/AKT/mTOR qui comme on l'a vu précédemment, est activée par les ErbB comme EGFR et HER2. mTOR est un inhibiteur puissant du complexe ULK et donc de l'autophagie. L'activation d'AKT inhibe et régule la voie activatrice au niveau de RAS.

La voie activatrice principale est celle de RAS/RAF/MEK/ERK dont nous avons décrit précédemment sa relation avec MUC1-C. (71)

D'autres voies activatrices de l'autophagie peuvent encore être associées à MUC1. Par exemple, la voie PI3K/AKT/mTOR est aussi un activateur paradoxal de l'autophagie. En effet, cette voie active également la protéine p110β qui est protéine de la régulation « fine » de PI3K de classe-I. Celle-ci est également un activateur de l'autophagie, car elle possède une action positive sur la Bécline1 et Vps34 (ou PI3K de classe III), favorisant ainsi la libération de la Bécline1 de sa protéine inhibitrice BCL2 et ainsi son activation. (17-18)

L'activation de l'autophagie peut aussi s'effectuer par l'AMPK qui est aussi un inhibiteur de mTOR. AMPK est activée quand la cellule est en souffrance énergétique conduisant à un haut niveau d'AMP par dégradation de sa réserve d'énergie, l'ATP. Un autre activateur de l'AMPK est aussi la p53 (15, 29, 57, 73) La p53 est curieusement liée directement à MUC1 et facilite le transport du p53 vers la mitochondrie. (59,103)

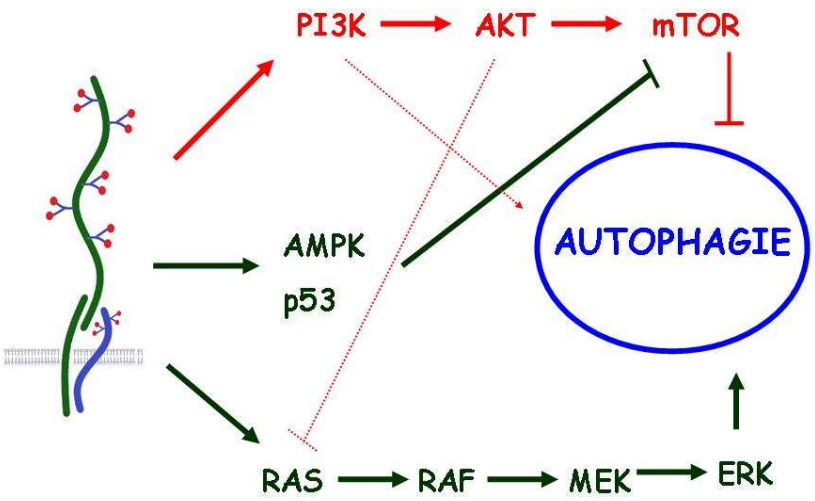

Figure 113 : La voie PI3K/AKT/mTOR inhibitrice. La voie RAS/RAF/MEK/ERK est activatrice comme celle faisant intervenir AMPK et p53. Toutes ces voies ont des relations avec MUC1 et sont souvent activées par son association et phosphorylation avec EGFR.

La relation entre l'autophagie et IL17 semble moins évidente. Cependant l'autophagie est connue comme un modulateur de l'inflammation, dont l'importance en carcinogenèse n'est plus à démontrer. L'autophagie influence la réponse adaptative des cellules immunes du stroma, entre autres des lymphocytes T (y compris les Th17, producteur de l'IL17A) par l'induction de production d'interleukines. (71)

Par exemple, dans la fibrose pulmonaire, on sait que l'IL17A régule la phosphorylation de GSK3β (aussi impliqué comme inhibiteur de la β-cathénine) qui perd ainsi son interaction avec BCL2. La BCL2, inhibiteur de l'autophagie est ainsi libérée et perd son activité par dégradation du protéosome.

IL17A serait également impliqué dans l'autophagie des cardiomyocytes ou dans les cellules malignes hépatocytaires par la voie de RAS/RAF/MEK/ERK. (27, 55,105)

Rappelons que nos travaux ont démontré que les cellules tumorales TN en culture soumises à l'IL17A induisent la phosphorylation d'ERK, voie activatrice de l'autophagie, et ainsi la résistance au docetaxel (chimiothérapie). (Annexe 3).

3. PUBLICATIONS ET TRAVAUX

a. But de cette thèse

Le but de ce travail consiste à étudier la résistance à la chimiothérapie des cancers du sein TN et si cette relation peut être liée à MUC1 ou EGFR. Nos observations ont conduit à conclure que MUC1 est peu exprimé dans les TN par comparaison à l'EGFR (trois premiers articles). L'une des causes de la chimiorésistance pourrait être l'autophagie, connue pour être régulée par MUC1 et EGFR (deuxième et troisième articles). Nos travaux collaboratifs démontrent une relation entre IL17 et la chimiorésistance sur des voies métaboliques communes avec l'autophagie. Dans la littérature quelques travaux émettent une association possible entre IL17 et l'autophagie par l'intermédiaire du système immunitaire. Enfin, notre dernier article suggère une influence de la modification des protéines glycosylées - dont MUC1 est l'une des plus représentées- infliées aux lymphocytes tumoraux.

Chronologiquement :

- Le premier article (MUC1/CD227 immunohistochemistry in routine practice is a useful biomarker in breast cancer) met en relation l'expression de MUC1 dans les cancers du sein in situ et invasifs (toutes classes confondues) en comparaison avec les tissus non tumoraux sur des prélèvements de patientes opérées à l'Institut Jean Godinot. Nous avons étudié les corrélations avec certains facteurs cliniques d'agressivité tumorale. Un petit groupe de patientes TN montrait une diminution possible d'expression de MUC1. Cette observation sera confortée par ce second article.
- Le second article (Autophagy is decrease in triple-negative breast cancers involving likely the MUC1-EGFR-NEU1 signaling pathway) s'intéresse à l'expression de MUC1 et/ou EGFR des tumeurs du sein de patientes TN et leurs relations probables avec l'autophagie. Le groupe de comparaison est formé de patientes présentant un cancer du sein LUM.
- Le troisième article (Chemotherapy treatment induces an increase of autophagy in luminal breast cancer cells MCF7 but not in triple-negative MDA-MB231) décrit un modèle de cultures cellulaires LUM et TN,

démontrant les variations possibles entre MUC1, EGFR, IL17RA, IL17RB et LC3 (autophagie) sous chimiothérapie.

- Enfin, le quatrième article (Triple-negative and HER2-overexpressing breast cancer cell sialylation impacts tumor microenvironment T lymphocyte subset recruitment: A possible mechanism of tumor escape) est une étude sur les sialyltransférases connues pour modifier la composition de la partie glycosylée de MUC1 et/ou EGFR et l'association avec les lymphocytes tumoraux. Ces derniers sont associés à la réponse aux agents de chimiothérapie.

b. Avant-propos

Cette thèse, n'a pas l'ambition d'être un travail de biologie fondamentale, mais bien un travail translationnel dont les résultats pourraient avoir des retombées sur la pratique clinique, le diagnostic, le pronostic ou au mieux thérapeutique.

Les techniques utilisées sont celles habituelles des laboratoires d'anatomie et de cytologie pathologiques de routine, à savoir des prélèvements tissulaires de tumeur humaine provenant de rebus de nos pièces chirurgicales ou de cultures cellulaires épithéliales humaines commerciales qui seront traitées par fixation dans du formol tamponné à 4 % et inclus classiquement en paraffine (formol fixation paraffin embebbed ou FFPE).

Les protéines étudiées sont mises en évidence par immunohistochimie en utilisant notre automate de routine (Dako®/ Agilent®). En dehors des examens classiques hormonaux (RO et RP) et de récepteurs de croissance (HER2), la plupart des anticorps de ce travail sont des anticorps de recherche, habituellement non utilisés en pratique clinique.

Sur les prélèvements de tumeurs humaines, nous avons parfois utilisé la technique de Tissue Micro Area (TMA) qui permet une meilleure standardisation des résultats.

Sur les cultures cellulaires, nous proposons un modèle dynamique de cultures cellulaires avec ou sans chimiothérapie et sur lesquelles nous réalisons des prélèvements FFPE. Ces prélèvements peuvent, comme ceux de la routine clinique, être stockés facilement, voire quasi indéfiniment. De plus, les cultures en FFPE présentent comme avantage qu'elles peuvent être étudiées par des techniques identiques à celles utilisées sur les tissus humains.

Finalement, nous avons mis au point sur les prélèvements FFPE des techniques d'immunofluorescence, ouvrant des perspectives de double voire triples marquages. Elles seront des techniques morphologiques complémentaires à celles de la biologie de recherche comme le Western blot ou l'ELISA. Ces mises au point en fluorescence seront également utiles au développement de la technique PLA (Duolink®), mettant en évidence la localisation intime de deux antigènes associés à des macromolécules différentes.

c. Apports personnels

Les projets ont été discutés conjointement avec moi et le Dr Armand Bensussan.

Ma formation initiale de technicien de laboratoire m'a permis, en collaboration étroite avec Me Mascaux Corinne (technicienne en ACP), de mettre au point les immuno-marquages non encore développés en routine dans notre laboratoire et de confectionner les TMA.

Les coupes histologiques, les immuno-marquages de production et les blocs cellulaires ont été réalisés par Me Mascaux Corinne.

Les cultures cellulaires ont été initiées par Me Malherbe (technicienne en ACP) avec une aide précieuse de Dr Salesse Stéphanie (MCU à l'URCA).

Les quantifications ont été réalisées par moi-même et Me Mascaux Corinne. La quantification digitale (programme Image-J) étant faite par moi-même.

L'analyse des données, la recherche des données cliniques, les statistiques, la rédaction, les figures ou photographies de tous les articles de cette thèse, sont réalisés par moi-même. Je remercie le Dr Bensussan Armand pour les premières lectures et critiques judicieuses.

d. Publications

Dans ce paragraphe, nous résumerons des résultats principaux à la compréhension de nos observations. Pour plus d'informations, je conseille au lecteur de se référer à l'article qui suit chaque travail.

i. MUC1 dans le cancer du sein

But de ce travail :

Par nos travaux sur les tumeurs urologiques, nous avons montré que MUC1 était surexprimée dans ces tumeurs et que son expression était anormale par rapport à la cellule épithéliale non tumorale.

Question posée : **« MUC1 est-il exprimé dans le cancer du sein invasif ou in situ (non invasif) ? »**

Matériel et méthode :

Nous utiliserons des prélèvements de routine provenant de 123 blocs FFPE de 111 patients différents. Nous avons sélectionné 31 tissus normaux, 21 cancers in situ (DIN) et 71 cancers invasifs (LUM, HER2 et TN). 22 métastases ganglionnaires sont également étudiées.

La technique consiste en des examens immunohistochimiques de routine utilisant des anticorps contre les récepteurs hormonaux (RO et RP), le facteur de prolifération Ki67 et MUC1-N.

Résultats principaux:

MUC1 perd son caractère polarisé apical dans les DIN et dans les carcinomes invasifs quand ils sont dédifférenciés. MUC1 devient alors membranaire circonférentiel et cytoplasmique. (figure 14)

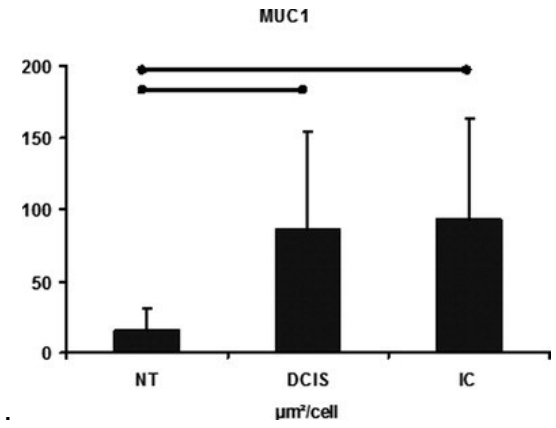

FIGURE 14 : L'expression de MUC1 dans le tissu normal du sein (NT) est moins importante que dans les cancers canalaires in situ (DCIS) ou les cancers invasifs (IC).

Curieusement quelques rares cellules expriment MUC1 dans le noyau.

Les corrélations des critères cliniques pronostiques ne montrent pas de différence statistique entre MUC1 et le score de Scarff et Bloom (score histologique de malignité) ou le TNM (score clinique d'agressivité). Par contre les tumeurs très agressives, à haute expression de Ki67, présentent une faible expression de MUC1-N (p=0.001). Dans ces cancers à Ki67 élevé, il y avait 10 cancers TN.

Conclusion :

MUC1-N est bien surexprimé dans 90 % des cancers invasifs et dans les cancers in situ du sein. Cependant, l'intensité de cette expression traduit des comportements biologiques différents.

En effet, l'expression morphologique permet de discerner les cancers invasifs ou in situ associés à un haut grade histologique ou à haut potentiel d'agressivité biologique. Autrement exprimé, plus les cellules sont malignes, ou peu différenciées, plus elles perdent leur sécrétion membranaire localisée au pôle apical des cellules et plus elles sous-expriment MUC1.

Cette observation implique que l'expression de MUC1 pourrait être un marqueur clinique de mauvais pronostic. De plus, MUC1 est associé à la chimiorésistance au trastuzumab (anti HER2) ou tamoxifen (anti-œstrogène).

D’un point de vue thérapeutique, la recherche développe actuellement des cibles inhibitrices contre la partie intra-cytoplasmique MUC1-C mais également des vaccins antitumoraux dirigés contre la partie extracellulaire, ou MUC1-N. Comme nous l’avons illustré dans cette étude, les tumeurs très agressives comme les TN montrent une expression de MUC1 plus faible, laissant présager un échappement possible à ces thérapies. Dans ce contexte, la stratégie de thérapie ciblée contre MUC1 ne pourra être efficace que si elle intègre l’immunohistochimie comme test compagnon.

Pour conclure, MUC1 pourrait être un biomarqueur appréciable pour la pratique clinique et l’évaluation des tumeurs du sein invasives et in situ.

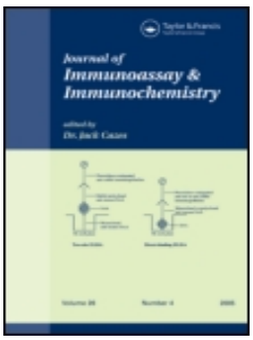

Journal of Immunoassay and Immunochemistry

ISSN: 1532-1819 (Print) 1532-4230 (Online) Journal homepage: http://tandfonline.com/loi/ljii20

MUC1/CD227 IMMUNOHISTOCHEMISTRY IN ROUTINE PRACTICE IS A USEFUL BIOMARKER IN BREAST CANCERS

Christian Garbar , Corinne Mascaux , Hervé Curé & Armand Bensussan

To cite this article: Christian Garbar , Corinne Mascaux , Hervé Curé & Armand Bensussan (2013) MUC1/CD227 IMMUNOHISTOCHEMISTRY IN ROUTINE PRACTICE IS A USEFUL BIOMARKER IN BREAST CANCERS, Journal of Immunoassay and Immunochemistry, 34:3, 232-245, DOI: 10.1080/15321819.2012.699491

To link to this article: https://doi.org/10.1080/15321819.2012.699491

Accepted author version posted online: 13 Jun 2012.
Published online: 13 Jun 2012.

Journal of Immunoassay and Immunochemistry, 34:232–245, 2013

ISSN: 1532-1819 print/1532-4230 online
DOI: 10.1080/15321819.2012.699491

Taylor & Francis
Taylor & Francis Group

MUC1/CD227 IMMUNOHISTOCHEMISTRY IN ROUTINE PRACTICE IS A USEFUL BIOMARKER IN BREAST CANCERS

Christian Garbar,[1] Corinne Mascaux,[1] Hervé Curé,[2] and Armand Bensussan[1]

[1]*Institut Jean Godinot, Biopathology, Reims, France*
[2]*Institut Jean Godinot, Oncology, Reims, France*

□ *Over-expression of MUC1/CD227 is observed in 90% of breast tumors. Classical morphologic description and semi-quantitative digital measurement of MUC1 were performed from immunohistochemical stained slides of 123 routine histological samples. Measures of MUC1 expression showed statistical differences between non tumoral (NT) breast tissue and Ductal Carcinoma In Situ (DCIS) or infiltrating carcinoma (IC), $p < 0.0001$. Loss of MUC1 was correlated with high Ki67 index ($p = 0.001$) and loss of hormonal receptors ($p = 0.03$), whereas no correlations were found with HER2 expression. High-grade DCIS or IC showed increasing loss of apical polarised and cytoplasmic expression of MUC1.*

Keywords Biomarker, breast cancer, cancer prognosis, cancer therapy, CD227, immunohistochemistry, MUC1, Mucins

INTRODUCTION

Breast cancer is the most common cause of cancer mortality in women. The knowledge of potential biomarkers is essential to understand the pathophysiology of the disease and to improve its treatment and the survival of patients.

Mucins are heterogeneous large O-glycosylated proteins containing numerous repetitive regions and many highly glycosylated serines and threonines amino acides. MUC1/CD227 is a transmembranaire insoluble mucin that plays an important role in cell protection and cell-cell or cell-matrix interactions.[1] Many carcinomas present an overexpression of MUC1. Most of them show severe alterations of the MUC1 glycosylation, contributing to local invasion of tumors and its capacity of metastasis.[2]

Address correspondence to Christian Garbar, Institut Jean Godinot, Biopathology, 1, Avenue du G. Koenig, BP171, Reims, 51056 France. E-mail: christian.garbar@reims.unicancer.fr

Recently, numerous experimental research demonstrated that MUC1 is a transmembrane heterodimeric protein with a cytoplasmic tail transducing signals recruiting various pathways including growth, apoptosis, and migration, therefore potentially involved in the carcinogenesis.[3]

Expression of MUC1/CD227 is observed in 90% of breast tumors and its over-expression is inversely correlated with a poor prognosis.[4] Furthermore, to date, several new pharmaceutical molecules against the cytoplasmic domain of MUC1/ CD227 were also developed in vitro.[5,6] Consequently, MUC1/CD227 appeared as an interesting biomarker.

Nevertheless, most of the histological studies concerning MUC1/ CD227 were performed retrospectively in experimental research using Tissue Micro Array (TMA) slides constructions.

The originality of this present study is to demonstrate that MUC1/ CD227 immunohistochemistry, with a commercially available monoclonal antibody termed Ma695, is routinely feasible and constant from fine needle biopsies and surgical samples and could give some clinical and diagnostic information. Therefore, we described morphological patterns of MUC1/ CD227 and its quantification, by an immunohistological method in Infiltrating Breast Carcinoma (IC), Ductal Carcinoma In Situ (DCIS), and Non Tumor breast tissue (NT). Also, we discuss the need of morphological evaluation of MUC1/CD227 to evaluate the appropriate treatment against this biomarker.

MATERIALS AND METHODOLOGY

Patient Population

A total of 123 routine histological analyses were performed in 111 different patients, without particular selection (mean +/− SD of age: 57.8 +/ − 12.8 years). Histological samples were needle biopsies or surgical tumorectomies (respectively, 8 and 23 for NT, 17 and 4 for DCIS, 36 and 35 for IC). Diagnosis classification was made according the WHO classification for tumors of the breast and the TNM classification of malignant tumors.[7,8] Normal tissue was composed of fibrocystic changes ($n = 8$) and normal breast lobules in breast surgical reductions ($n = 11$) or in normal breast tissues of tumorectomies for tumors, far of cancerous tissue ($n = 12$). To exclude the same tumor cell clone in DCIS and IC in the same sample, only DCIS from patients without IC were selected. To evaluate TNM, post-surgical and pathological reports were available in 55 patients and nodal status was known in 44 patients. Twenty-two patients had node metastasis. MUC1 status was studied retrospectively in 12 patients (8 patients had too small node metastasis and 2 patients were not treated in our hospital). As the number was too small and not statistical

TABLE 1 Clinical and Immunohistological Characteristics

	N	Age			Ki67			ER			PR			HER2		
Non Tumor breast tissue	31	**55,6**	+/−	10,5												
Normal Breast	23	**55,5**	+/−	11,3												
Fibrocystic Change	8	**56,0**	+/−	8,7												
Ductal Intraepithelial Neoplasia	21	**56,7**	+/−	11,3				**7,0**	+/−	2,5	**5,1**	+/−	3,5	**1,8**	+/−	1,0*
DIN1	3	**54,7**	+/−	5,5				**6,0**	+/−	2,8	**6,0**	+/−	2,8	**5,0**	+/−	0,7
DIN2	4	**58,0**	+/−	20,9				**8,0**	+/−	0,0	**8,0**	+/−	0,0	**1,0**	+/−	0,8
DIN3	14	**56,8**	+/−	9,6				**4,1**	+/−	3,7	**4,1**	+/−	3,7	**2,1**	+/−	0,8
Infiltrating Carcinoma	71	**59,0**	+/−	13,3	**32,1**	+/−	26,3	**6,3**	+/−	3,1	**4,9**	+/−	3,5	**0,8**	+/−	1,0*
Ductal Carcinoma	55	**57,5**	+/−	12,6	**36,2**	+/−	27,2*	**5,9**	+/−	3,4	**4,9**	+/−	3,7	**0,9**	+/−	1,0
Lobular Carcinoma	16	**64,3**	+/−	14,8	**15,1**	+/−	12,7*	**7,9**	+/−	1,0	**5,1**	+/−	2,7	**0,3**	+/−	0,6
Histological Grading																
Grade 1	10	**62,9**	+/−	9,5	**5,6**	+/−	1,9*	**7,9**	+/−	0,3*	**8,0**	+/−	0,1*	**0,6**	+/−	0,8
Grade 2	23	**59,1**	+/−	9,9	**26,9**	+/−	15,7*	**6,9**	+/−	2,7*	**5,6**	+/−	3,3*	**0,8**	+/−	0,8
Grade 3	22	**53,3**	+/−	15,2	**53,9**	+/−	25,7*	**4,0**	+/−	3,7*	**2,6**	+/−	3,6*	**1,2**	+/−	1,3
Clinical Stage																
T1	33	**60,7**	+/−	13,3	**22,6**	+/−	20,0	**6,6**	+/−	2,9	**5,4**	+/−	3,3	**0,5**	+/−	0,8
T2	18	**57,9**	+/−	13,0	**41,9**	+/−	27,8	**6,5**	+/−	3,1	**4,8**	+/−	3,5	**0,9**	+/−	1,1
T3	4	**42,3**	+/−	5,6	**43,0**	+/−	39,0	**4,8**	+/−	3,6	**3,3**	+/−	3,9	**1,3**	+/−	1,5
N0	22	**61,3**	+/−	11,8	**31,7**	+/−	25,3	**6,0**	+/−	3,4	**4,0**	+/−	3,7	**0,6**	+/−	0,8
N+	22	**55,3**	+/−	13,4	**33,0**	+/−	29,0	**5,5**	+/−	3,6	**4,6**	+/−	3,6	**0,9**	+/−	1,2

N: number of cases; Age: mean +/− SD (years); Ki67: mean +/− SD (%); ER: mean +/− SD of Allred's score for oestrogen receptors; PR: mean +/− SD of Allred's score for progesterone receptors; score of HER2: mean +/− SD of HER2 score.

Significant difference are notified by * ($p < 0.01$).

significant, one lobular intraepithelial neoplasia (LIN) and 2 micropapillary IC were discarded. Details of clinical information were described in Table 1.

Immunohistochemical Methods

All specimens were fixed in 4% formaldehyde solution between 8–24 hr for needle biopsies and between 24–48 hr for surgical samples. Specimens were then imbedded in paraffin and cut to 4 μm.

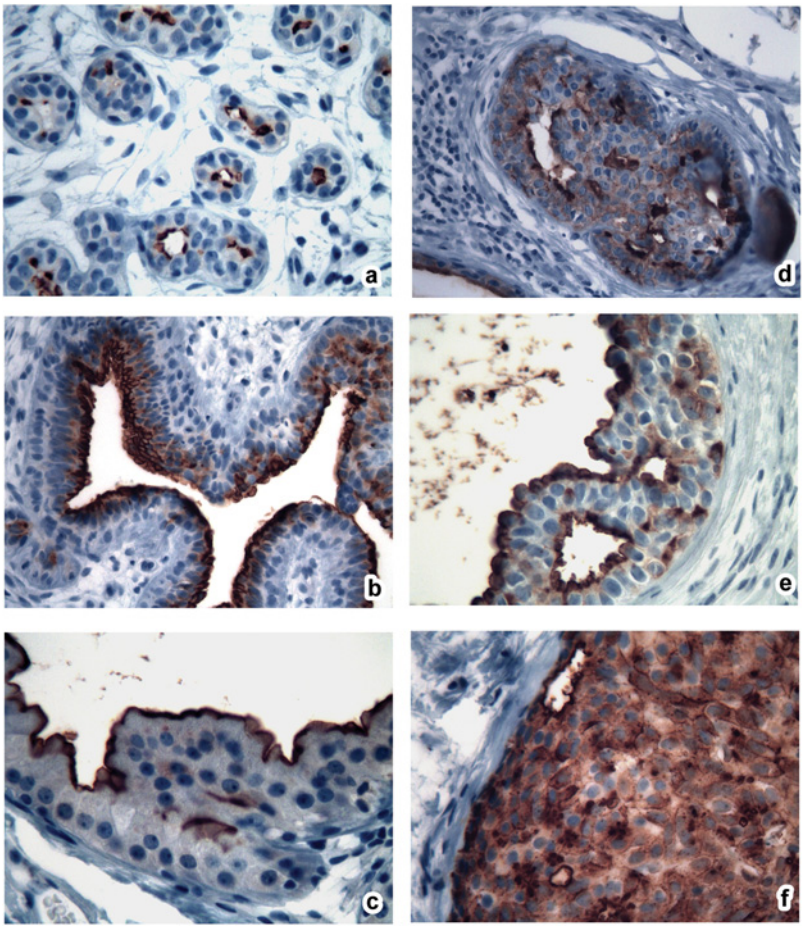

FIGURE 1 Comparison of MUC1/CD227 immuno-staining patterns (MUC1/Ma695) monoclonal antibody in normal tissue and non invasive breast lesions (60x magnification). Non tumour breast tissue: (a) normal lobules; (b) ductal ectasia; (c) cystic change with apocrine metaplasia; (d) usual ductal hyperplasia: (e) low-grade DCIS; and (f) high-grade DCIS. Benin lesions and low-grade DCIS show only apical polarized MUC1/CD227-positivity (a, b, c, d, e). Cytoplasmic and circumlferential membrane MUC1/Cd227-positivity are observed only in high-grade DCIS (color figure available online).

Immunohistological staining were performed with the Automated Slide Stainers Benchmark XT (Roche diagnostics/Vantana Medical System Inc, Meyland, France), according to the manufacture's instructions and described previously.[9] The following commercial monoclonal antibodies were used: anti- MUC1/CD227 (clone Ma695; diluted at 1:100; Novocastra, Newcastle upon Tyne, UK), anti-estrogens receptors (clone SP1; ready to use; Roche Diagnostics, Meland, France), anti-progesterone receptors (clone PGR636; ready to use; Roche Diagnostics), anti- HER2 (4B5, Roche Diagnostics), and anti-Ki67 (clone Mib-1; diluted at 1:75; Dako, Glostrup, Denmark).

Morphologic Methods

Manual selections of five areas of each patient slide were chosen at random. Pictures were made with a PC digital image camera (Nikon Digital Sight DS-Fi1c; Nikon, Illrich, France) mounted on a Nikon Eclipse 50i microscope with a 40x objective (Nikon). A mean of 275 +/− 114 cells per case were analyzed. We observed six morphological parameters: diffuse

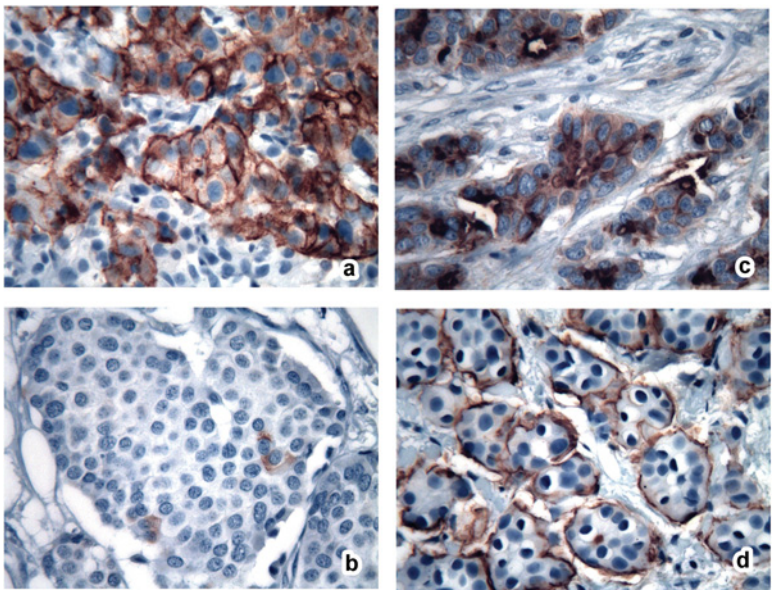

FIGURE 2 Comparison of MUC1/CD227 immuno-staining patterns (MUC1/Ma695) monoclonal antibody in invasive breast lesions (60x magnification). (a) Partial or cironferential membrane MUC1/CD227-positive tumoral cells Infiltrating Breast Carcinoma; (b) MUC1/CD227-negative tumoral cells; (c) cytoplasm MUC1/CD227-positive tumoral cells with Golgi's dot expression; and (d) micropapillary carcinoma presenting a peripheric membrane MUC1/CD227- positivity (color figure available online).

cytoplasm (Figure 1f, Figure 2c), intracytoplasmic vacuole, apical and polarized positive signal (Figure 1a–e, Figure 2c), partial or complete circumferential membrane positive signal (Figure 2a and d), and Golgi's dot and nuclear (Figure 2c).

Ki67 index and Hormonal Receptors were manually calculated with a cell counter, in two different fields. Scoring of HER2 was calculated according the American Pathologists Guideline.[10] Estrogens (ER) and progesterone receptors (PR) were subsequently scored according the Allred score that consists to sum of intensity and proportion of the nuclear immunostaining.[11]

For automated parametric measures of MUC1/CD227 we used the NIH Image-J method (Image-J 1,44p; NIH, Bethesda, MD, USA) for automated selection of DAB-labelled tissue in one picture.[9] The measurements gave the global positive area, in μm^2, for each case picture. To discarded stromal tissue, we calculated manually with the cell counter, the number of epithelial cells in each picture. Final result was expressed as positive area per cell, in μm^2/cell. Nonparametric or global MUC1 positivity was calculated in mean of a ROC curve between NT and IC, with a cut-off of 30 μm^2/cell (sensitivity of 83.1% and specificity of 83.9%).

Statistics

The results were expressed by percentage of observations and means +/− SD. Annova or Fisher's exact tests were performed. A p value <0.05 was considered significant. The Analyse-it 2.22 (Analyse-it Software, Leeds, UK) and Excel 2003 (Microsoft Corp., Redmond, WA, USA) programs were used for statistical analysis. This study was made according the approval of an ethics committee.

RESULTS

Clinical and Immunohistochemical Characteristics

Table 1 shows the main clinical and histological characteristics. We found no statistical significance for age of patient's groups, except for patients with T1 tumors in comparison with T3 tumors (Table 1, $p = 0.01$).

Ki67 index increased with the modified histological grade of Elston and Ellis (Table 1, $p < 0.001$). Similarly, correlations were also seen between Allred's scores of ER or PR and histological grade (Table 1, $p < 0.001$) except for ER between grade1 and grade2 tumors (Table 1, p = ns). Furthermore, we observed a differences of Ki67 index between ER-negative and ER-positive (60.3 +/−25.3% vs. 25.3 +/−22.3%; $n = 7$ vs. $n = 29$;

$p = 0.0034$) and between PR-negative and PR-positive (54.8 +/−25.3%. vs. 19.3 +/−16.6%; $n = 13$ vs. $n = 23$; $p = 0.0003$). Score of HER2 showed significant differences between DCIS and IC (Table 1, $p = 0.0003$) or between Ductal IC and Lobular IC (Table 1, $p = 0.03$). There was also a relationship of ER Allred's score between HER2-negative and HER2-positive (6.7 +/− 2.7 vs. 4.2 +/− 3.8; $n = 80$ vs. $n = 10$; $p = 0.013$). Similarly, PR Allred's score for HER2-negative and HER2-positive was also significant (5.4 +/− 3.3 vs. 1.6 +/− 3.2; $n = 80$ vs. $n = 10$; $p = 0.0012$).

MUC1/CD227 Immuhistochemistry

Table 2, Figure 1, and Figure 2 summarized morphological patterns of MUC1/CD227 expression in NT, DCIS, and IC (ductal $n = 55$ and lobular $n = 16$). Although considering the cytoplasm or global MUC1/CD227-positive expression, IC and DCIS are significantly more often positive than NT tissues (Table 2, pictures in Figure 1 and Figure 2). The same result was observed for the MUC1/CD227 digital parametric measures (respectively, 93 +/− 70, 86 +/− 68 and 16 +/− 15 μm^2/cell, $p < 0.001$; Figure 3). MUC1/CD227-positive circumferential membrane (Figure 1f and Figure 2a) or MUC1/CD227- positive diffuse cytoplasmic (Figure 1f and Figure 2c) were more specific for DCIS and IC as compared to NT tissues (Figure 1a–d). Polarized apical MUC1/CD227-positive expression pleaded for NT (Table 2: NT vs. DCIS, $p = 0.027$; DCIS vs. IC, $p = 0.001$; Figure 1a–e). No statistical differences were found about nuclear or Golgi-dot area positive expression (Figure 2c). MUC1/CD227-positive intracytoplasmic vacuoles were observed in IC and were more specific of

TABLE 2 Morphologic Patterns of MUC1/CD227 Immunostaining

	Non Tumoral	DIN	Infiltrating Carcinoma
No.cases	31	21	71
Global positivity (cutt-off > 30 μm^2/cell)	**16%**	**95%**	**84%***
	5/31	20/21	60/71
Cytoplasm	**3%**	**85%**	**92%***
	1/31	18/21	66/71
Apical	**96%**	**71%**	**22%***
	30/31	15/21	16/71
Cytoplasmic membrane	**0%**	**42%**	**57%***
	0/31	9/21	41/71
Golgi Area	**35%**	**66%**	**57%**
	11/31	14/21	37/71
Nuclear	**19%**	**33%**	**9%**
	6/31	7/21	7/71
Intracytoplasmic vacuole	**0%**	**4%**	**25%***
	0/31	1/21	18/71

Significant difference are notified by * ($p < 0.01$).

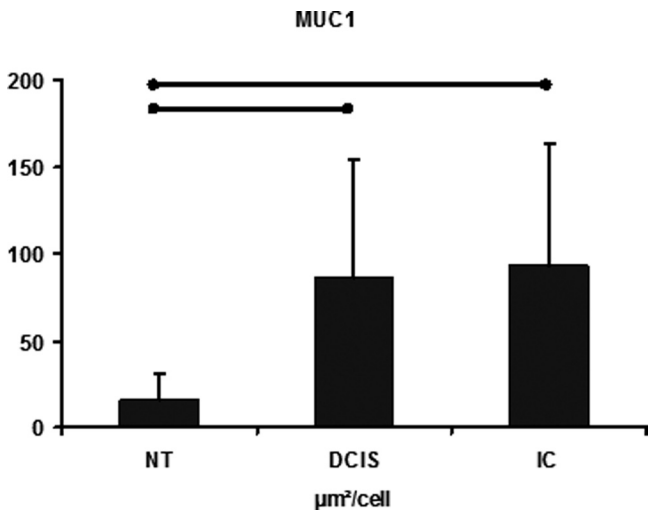

FIGURE 3 Positive area measures of MUC1/CD227 in non tumor breast cell (NT), ductal carcinoma in situ (DCIS), and infiltrating breast carcinoma (IC). Prospective study. There is a significant statistical difference between NT (x) and DCIS (*) or IC (*), $p < 0.0001$.

lobular carcinoma than ductal carcinoma: respectively 16.3% (9/55) vs. 56.2% (9/16), with $p = 0.0054$.

The morphologic comparison between the 12 patients with both primary tumor and node metastasis showed no statistical difference for MUC1/CD227-positive cytoplasm (respectively, 83.3% or 10/12 vs. 91.6% or 11/12, p = ns), MUC1/CD227-positive circumferential membrane (50.0% or 6/12 vs. 58.3% or 7/12, p = ns), polarized apical MUC1/CD227-positive expression (33.3% or 4/12 vs. 8.3% or 1/12, p = ns), Golgi-dot positivity (58.3% or 7/12 vs. 58.3% or 7/12, p = ns), or nuclear expression (25.0% or 3/12 vs. 0% or 0/12, p = ns). Interestingly, we found a statistical difference ($p = 0.01$) between positive area per cell in primary tumor (84 +/− 60 μ^2/cell) and in comparison with its metastasis (163 +/− 81 μ^2/cell, Figure 4).

Correlations Between Clinical Information and MUC1/CD227

Semi-quantitative results showed a tendency of loss of MUC1/CD227 immunostaining (positive area per cell) associated with the aggressive behaviour of IC, without obvious statistical differences, such as for Elston and Ellis's histological grade (grade1 = 80 +/− 44 μm^2/cell; grade2 = 98 +/− 57 μm^2/cell; grade3 = 92 +/− 97 μm^2/cell; p = ns) or for TNM classification (T1 = 96 +/− 55 µm/cell^2; T2 = 86 +/− 62μm^2/cell; T3 = 83 +/− 59 μm^2/cell, p = ns; N0 = 90 +/− 64 μm^2/cell; N1 = 83 +/− 57μm^2/cell; p = ns). In case of triple negative carcinoma, we observed decreasing

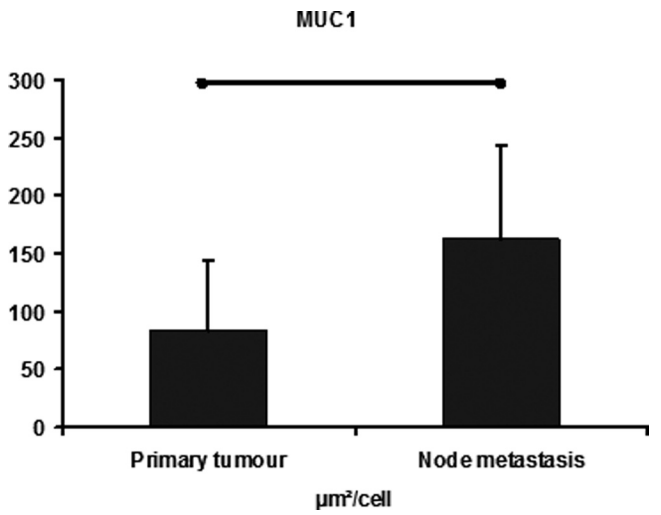

FIGURE 4 Positive area measures of MUC1/CD227 in primary tumor breast cell (NT) and its node metastasis. Retrospective analysis of 12 patients. There is a significant statistical difference, $p < 0.01$.

MUC1/CD227 intensity between basal-like and non basal-like carcinoma (respectively, 51 +/− 73 vs 75 +/−70 μm^2/cell for n = 4 vs. n = 6), however we could not establish significant statistical differences due to the small

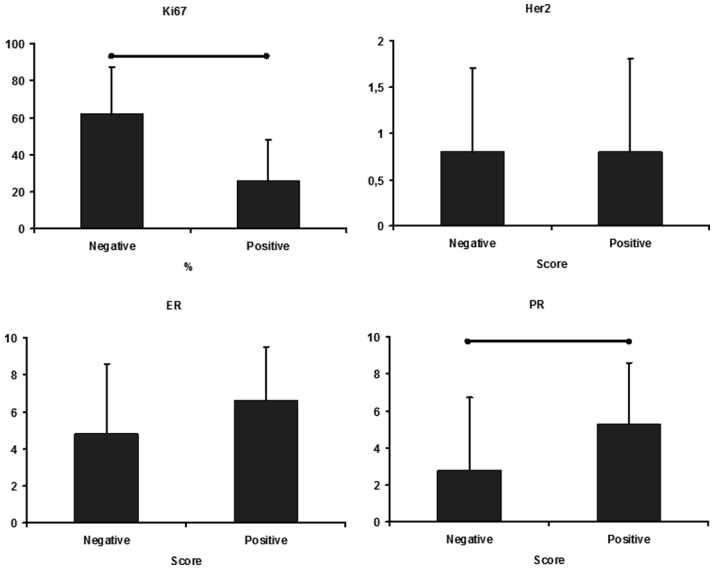

FIGURE 5 Comparison of immunostaining between negative or positive MUC1/CD227 invasive tumoral cells (μm^2/cell) and Ki67 index, HER2 (score), PR, and ER (Allred's score). There were significant results between MUC1/CD227-negative and MUC1/CD227-positive for the Ki67 index ($p = 0.0012$) or hormonal receptors (PR, $p = 0.03$). No correlation was observed for HER2 and ER.

number of cases. Ki67 index and PR Allred's score presented a positive correlation between global cellular MUC1/CD227positive signal respectively with $p = 0.0012$ and $p = 0.03$, as illustrated in Figure 5 (number of cases for MUC1/CD227-negative = 11 and for MUC1/CD227-positive = 60). No correlation was found between HER2 or ER and MUC1/CD227 (Figure 5).

DISCUSSION

To date, routine immunohistochemical studies of MUC1 in breast cancer giving a clinical or pathological data are relatively rare. Most of them were realized retrospectively from TMA method and in experimental researches. Mukhopadhyay et al. reviewed recently only 2 prospective immunohistochemical studies over MUC1 in breast cancer.[12] Our study was performed from routine sample using a commercially available MUC1/CD227 monoclonal antibody Ma695. The results showed that our technical procedure was constant and standardized. We also demonstrated that expression of MUC1/CD227 is higher in breast cancer cells, both for DCIS or IC, than in NT. In cancer cells, MUC1/CD227 expression was however heterogeneous but more often observed with loss of apical (or luminal) polarized localization, mainly positive in cytoplasm and/or in periphery of cytoplasmic membrane. In a recent work, we already reported this particular pattern in urological tumors of the bladder and the prostate and we proposed that this pattern could be helpful for distinguishing between non tumor tissue from cancerous cells.[9,13] Here, the loss of MUC1/CD227 expression could be a potential marker for aggressive tumor behavior of breast cancers such as high histological grade or high TNM, although we found no statistical correlation. Nevertheless, using the aggressive prognosis marker Ki67 index, we found that it was inversely correlated with the MUC1/CD227 expression (Figure 5). Also, Rakha et al.[4], with a large TMA series of 1447 patients, reported that the apical cellular localization was an indicator of intact MUC1/CD227 pathway and a normal differentiation of tumor breast cells. Similarly to our findings, they reported 91% of MUC1/CD227-positive breast carcinoma and they demonstrated an inverse association in favor of highly aggressive cancer. They also proved, by means of Kaplan-Meier curves for survival and disease free, that apical positive phenotype showed a better prognostic than cytoplasmic or membranous MUC1/CD227 positive phenotype. Van der Vegt et al.[14] with a same methodology of TMA pointed out the MUC1/CD227-negative expression of breast cancer as an independent risk factor for poor relapse-free survival and overall survival, besides classical prognostic indicators. Further, in agreement with our results these authors found an association between MUC1/CD227-negative cells and negative hormonal receptors status.[4,14]

For pathologists, MUC1/CD227-positive intracytoplasmic vacuoles are an interesting pattern to diagnosis lobular to ductal carcinoma. These vacuoles were already described in the literature.[15] Moreover, we observe also a distinct MUC1/CD227 pattern in 2 cases of micropapillary carcinoma (Figure 2d, this cases are discarded because small number of cases) consisting to an inversed basal membrane MUC1/CD227-positive expression.[16,17] MUC1/CD227 pattern was also a good tool to discriminate low and high grade DIN (Figure 1). We already showed the usefulness of MUC1/CD227 for the diagnosis of low- and high-grade non invasive papillary tumors of the bladder.[8] The same pattern could be also applying for DIN in breast carcinoma. Mommers et al.[18] described that membrane expression of underglycosylated MUC1/CD227 was found only in poorly differentiated DIN. Ours observations over high-grade DIN associated with loss of MUC1/CD227 apical expression and cytoplasmic or membrane MUC1/CD227-positive DIN was already reported in the literature.[12,19,20] Also, we agree to the suggestion of de Ross et al.[18] that the MUC1/CD227 pattern of DCIS could be helpful for distinguishing between different grades of DCIS.

It is well known that MUC1/CD227-C intracellular subunit is involved in several cellular signalling pathways that may induce cell cancer transformation and promote growth or survival cancerous cells by apoptosis suppression. MUC1/CD227-C shows interaction with ErbB family (particularly ErbB1 and FGFR3), beta-catenin, ER-alpha, PI3 K, AKT, p53, Bcl-Xl, SrC, heat shock protein 90 chaperon.[3,5,21–24] Interestingly, MUC1/CD227 is also associated to the resistance of trastuzumab or tamoxifen.[12,25,26] Recent in vitro studies show that interactions between MUC1-C and these cellular pathways could be inhibited by several small molecule inhibitor, creating likely novel approaches for the breast cancer chemotherapy.[5,6,30–32] Bitler et al. postulated that MUC1/CD227-C regulates nuclear localisation and function of EGFR in a transgenic mouse model of breast cancer.[33] Also, we found no association between MUC1/CD227 and HER2 but it is well known that, contrary to EGRF (HER1), MUC1/CD227 is not directly associated with HER2 receptors.[3]

In cancer, MUC1/CD227-N extracellular domain shows aberrant glycosylation leading to the exposure of repetitive core peptide epitopes that are good targets for immunotherapy. Also, MUC1/CD227-N is overexpressed on tumor cells membrane altering cell-cell and cell-matrix adhesion of E-cadherin and is a ligand for ICAM-1/CD54.[3,5,26,27] Others suggested a possible role of MUC1/CD227 in the modulation of VEGF and the tumoral angiogenic response.[28,29] These mechanisms could explain the role of MUC1/CD227 in cancer progression and your observation of over-expression of MUC1 in metastatsis (Figure 4). Vaccines against MUC1/CD227-N have been actually extensively studied in phase I/II. Some

modest clinical responses have been reported but new synthetic MUC1/CD227-N vaccines are now available and seem to be promising.[5,34] Recently, Mensdorff-Pouilly et al. demonstrated the ability of natural anti–MUC1/CD227 antibodies to bind tumor cells over-expressing MUC1/CD227 and to recruit effector cytotoxic NK lymphocytes.[35] These findings open also an alternative therapeutic approach using MUC1/CD227 as a target for breast cancer monoclonal antibody therapies.

CONCLUSIONS

MUC1/CD227 is secreted in about 90% of infiltrating breast cancer and intraepithelial breast neoplasia. The pattern of cellular MUC1/CD227 expression is very important to discriminate the aggressive grade of IC or DCIS and is therefore an interesting helpful for the pathologist. For clinicians, MUC1/CD227 expression seems to be an independent poor prognostic marker, sometimes associated with chemoresitance of trastuzumab or tamoxifen. To date, new therapeutic molecules against the cytoplasmic domain of MUC1 are studied and new vaccines against extracellular domain of MUC1 are developed. Because breast cancers show heterogeneous expression of MUC1 in intensity and/or in patterns, immuno-histological evaluation of MUC1 will play likely an important role for selection of patient under future potential anti-MUC1 treatment.

REFERENCES

1. Dall'olio, F. Protein glycosylation in cancer biology: An overview. *Clin. Mol. Pathol.* **1996**, *46*, M126–135.
2. Springer, G. F.; Heather, M. T and Tn pancarcinoma markers: Autoantigenic adhesion molecules in pathogenesis, prebiopsy carcinoma-detection, and long term breast carcinoma immunotherapy. *Crit. Rev. Oncol.* **1995**, *6*, 57–85.
3. Bafna, S.; Kaur, S.; Batra, S. K. Membrane-bound mucins: The mechanistic basis for alterations in the growth and survival of cancer cells. *Oncogene* **2010**, *29*(20), 2893–2904.
4. Rakha, E.; Boyce, R.; El-Rehim, D.; Kurien, T.; Green, A.; Paish, E.; Robertson, J.; Ellis, I. Epression of mucins (MUC1, MUC2, MUC3, MUC4, MUC5AC and MUC6) and their prognostic significance in human breast cancer. *Mod. Pathol.* **2005**, *18*, 1295–1304.
5. Senapati, S.; Das, S.; Batra, S. Mucin-interacting protein: From function to therapeutics. *Trends Biochem. Sci.* **2010**, *35*(4), 236–245.
6. Zhou, Y.; Rajabi, H.; Kufe, D. MUC1-C Oncoprotein is a target for small molecule inhibitors. *Molec. Pharmacol.* **2011**, *79*(5), 886–893.
7. Ellis, I.; Tavossoli, F.; MacGrogan, G.; Bussolati, G.; Tavasolli, F. A.; Eusibi, V.; Peters, J. L.; Mukai, K.; Tabar, L.; Jacquemier, J.; Cornelisse, C. J.; Sasco, A. J.; Kaaks, R.; Pisani, P.; Goldgar, D. E.; Devilee, P.; Cleton-Jansen, M. J.; Borrensen-Dale, A. L.; van't Veer, L.; Sapino, A. Pathology and Genetics. In *Tumours of the Breast and Female Genital Organs*; Tavassoli, F.; Devilee, P., Eds; IARC Press: Lyon, 2003; pp. 13–85.
8. Sobin, L. H.; Gospodarowicz, M. K.; Wittekind, C. H. *TNM Classification of Malignant Tumours*, 7th Ed.; Wiley-Backwell: Chichester, UK, 2009; pp. 181–193.

9. Garbar, C.; Mascaux, C. Expression of MUC1 (Ma695) in noninvasive papillary urothelial neoplasm according the 2004 World Health Organization Classification of the noninvasive urothelial neoplasm. *Anal. Quant. Cytol. Histol.* **2011**, *33*, 277–282.
10. Wolff, A. C.; Hammond, M. E.; Schwartz, J. N.; Hagerty, K. L.; Allred, D. C.; Cote, R. J.; Dowsett, M.; Fitzgibbons, P. L.; Hanna, W. M.; Langer, A.; McShane, L. M.; Paik, S.; Pegram, M. D.; Perez, E. A.; Press, M. F.; Rhodes, A.; Sturgeon, C.; Taube, S. E.; Tubbs, R.; Vance, G. H.; van de Vijver, M.; Wheeler, T. M.; Hayes, D. F. American society of clinical oncology/college of American pathologists guideline recommendations for human epidermal growth factor receptor 2 testing in breast cancer. *J. Clin. Oncol.* **2007**, *25*, 118–145.
11. Allred, D. C.; Havey, J. M.; Berardo, M.; Clark, F. M. Prognostic and predictive factors in breast cancer by immunohistochemical analysis. *Mod. Pathol.* **1998**, *11*, 155–168.
12. Mukhopadhyay, P.; Chakraborty, S.; Ponnusamy, M.; Lakshmanan, I.; Jain, M.; Batra, S. Mucins in the pathogenesis of breast cancer: Implications in diagnosis, prognosis and therapy. *Biochim. Biophys. Acta* **2011**, *1815*(2), 224–240.
13. Garbar, C.; Mascaux, C.; Wespes, E. Expression of MUC1 and sialyl-Tn in benign prostatic glands, high-grade prostate intraepithelial neoplasia and malignant prostatic glands: A preliminary study. *Anal. Quant. Cytol. Histol.* **2008**, *30*, 71–77.
14. van der Vegt, B.; de Roos, M. A.; Peterse, J. L.; Patriarca, C.; Hilkens, J.; de Bock, G. H.; Wesseling, J. The expression pattern of MUC1 (EMA) is related to tumour characteristics and clinical outcome of invasive ductal breast carcinoma. *Histopathology* **2007**, *51*(3), 322–325.
15. Yu, J.; Bhargava, R.; Dabbs, D. Invasive lobular carcinoma with extracellular mucin production and HER2 overexpression: A case report and further case studies. *Diag. Pathol.* **2010**, *5*, 36–43.
16. Nassar, H.; Pansar, V.; Zhang, H.; Che, M.; Sakr, W.; Ali-Fehmi, R.; Grignon, D.; Sarkar, F.; Cheng, J.; Adsay, V. Pathogenesis of invasive micropapillary carcinoma: Role of MUC1 glycoprotein. *Mod. Pathol.* **2004**, *17*, 1045–1050.
17. Acs, G.; Esposito, N. N.; Rakosy, Z.; Laronga, C.; Zhang, P. J. Invasive ductal carcinoma of the breast showing partial reversed cell polarity are associated with lymphatic tumor spread and may represent part of a spectrum of invasive micropapillary carcinoma. *Amer. J. Surg. Pathol.* **2010**, *34*(11), 1637–1646.
18. Mommers, E. C.; Leonhart, A. M.; von Mensdorff-Pouilly, D. J.; Schol, D. J.; Hilgers, J.; Meijer, C. J.; Baak, J. P.; van Diest, P. J. Aberrant expression of MUC1 mucin in ductal hyperplasia and ductal carcinoma in situ of breast. *Int. J. Cancer* **1999**, *84*(5), 466–469.
19. Diaz, L. K.; Wiley, E. L.; Morrow, M. Expression of epithelial mucin MUC1, MUC2, and MUC3 in ductal carcinoma in situ of the breast. *Breast J.* **2001**, *7*(1), 40–45.
20. de Roos, M. A.; van der Vegt, B.; Peterse, J. L.; Patriarca, C.; de Vries, J.; de Bock, G. H.; Wesseling, J. The expression pattern of MUC1 (EMA) is related to tumour characteristics and clinical outcome in pure ductal carcinoma in situ of the breast. *Histopathology* **2007**, *51*(2), 227–238.
21. Raina, D.; Kharbanda, S.; Kufe, D. The MUC1 Oncoprotein activates the anti-apoptotic phosphoinositide 3-kinase.akt and bcl-xl pathways in rat 3Y1 fibroblasts. *J. Biol. Chem.* **2004**, *279*, 20607–20612.
22. Horn, G.; Gaziel, A.; Wreshner, D. H.; Smorodinsky, N. L.; Ehrlich, M. ERK and PI3 K regulate different aspect of the epithelial to mesenchymal transition of mammary tumor cells induced by truncated MUC1. *Exp. Cell Res.* **2009**, *315*(8), 1490–1504.
23. Bernier, A.; Zhang, J.; Lillehoj, E.; Shaw, A.; Guasekara, N.; Hugh, J. Non-cysteine linked MUC1 cytoplasmic dimmers are required for Src recruitment and ICAM-1 bnding induced cell invasion. *Mol. Cancer* **2011**, *10*, 93–111.
24. Zaretsky, J. Z.; Barnea, I.; Aylon, Y.; Gorivodsky, M.; Wreschner, D. H.; Keydar, I. MUC1 gene overexpressed in breast cancer: Structure and transcriptional activity of the MUC1 promoter and role of estrogens receptor alpha (ERalpha) in regulation of MUC1 gene expression. *Mol. Cancer* **2006**, *5*, 57.
25. Pitroda, S. P.; Khodarev, N. N.; Beckett, M. A.; Kufe, D. W.; Weichselbaum, R. R. MUC1-induced alterations in a lipid metabolic gene network predict response of human breast cancers to tomoxifen treatment. *Proc. Natl. Acad. Sci. USA* **2009**, *106*(14), 5837–5841.
26. Fessler, S. P.; Wotkowicz, M. T.; Mahanta, S. K.; Bamdad, C. MUC1* is a determinant of trastuzumab (Herceptin) resistance in breast cancer cells. *Breast Cancer Res. Treat.* **2009**, *118*(1), 113–124.
27. Borsig, L. Selectins facilitate carcinoma metastasis and heparin can prevent them. *News Physiol. Sci.* **2004**, *19*, 16–21.

28. Zanetti, J.; Soave, D.; Oliveira-Costa, J.; Da Silveira, G.; Ramalho, L.; Garcia, S.; Zucoloto, S.; Ribeiro-Silva, A. The role of tumor hypoxia in MUC1-positive breast carcinomas. *Virschows Arch.* **2011**, *459*, 367–375.
29. Woo, J.; Choi, Y.; Jeong, J.; Choi, D.; Seo, H.; Kim, C. Mucin 1 enhances the tumor angiogenic response be activation of the AKT signalling pathway. *Oncogene* **2011**, *31*(17), 2187–2198.
30. Smith, J. S.; Colon, J.; Madero-Visbal, R.; Isley, B.; Konduri, S. D.; Baker, C. H. Blockade of MUC1 expression by glycerol guaicolate inhibits proliferation of human breast cancer cells. *Anticancer Agents Med. Chem.* **2010**, *10*(8), 644–650.
31. Bitler, B. G.; Menzl, I.; Huerta, C. L.; Sands, B.; Knowlton, W.; Chang, A.; Schroeder, J. A. Intracellular MUC1 peptides inhibit cancer progression. *Clin. Cancer Res.* **2009**, *15*(1), 100–109.
32. Hiscox, S.; Jordan, N. J.; Smith, C.; James, M.; Morgan, L.; Taylor, K.; Green, T. P.; Nicholson, R. I. Dual targeting of Src and ER prevents acquired antihormone resistance in breast cancer cells. *Breast Cancer Res. Treat.* **2009**, *115*, 57–67.
33. Bitler, B. G.; Goverdhan, A.; Schroeder, J. A. MUC1 regulates nuclear localization of epidermal growth factor receptor. *J. Cell. Sci.* **2010**, *123*(pt10), 1716–1723.
34. Coveler, A.; Bates, N.; Disis, M. Progress in the development of a therapeutic vaccine for breast cancer. *Breast Cancer Res. Treat.* **2010**, *2*, 25–36.
35. von Mensdorff-Pouilly, S.; Moreno, M.; Verheijen, R. Natural and induced humoral responses to MUC1. *Cancers* **2011**, *33*, 3073–3103.

ii. MUC1/EGFR et l'autophagie dans le cancer du sein de patientes triple négatif.

But du travail :

Les cancers TN sont composés d'un groupe hétérogène de cancers du sein exprimant à plus de 75 % l'EGFR. Ce sont des cancers agressifs souvent résistants à la chimiothérapie et ne répondant pas ou quasiment pas aux anti-EGFR.

L'autophagie est un mécanisme de survie cellulaire impliqué dans la résistance à la chimiothérapie. Elle peut être activée par la voie de signalisation EGFR/PI3K dont MUC1 a été décrit comme associée.

Les questions posées sont : **« l'autophagie est-elle activée dans les TN ? Si oui, quelle est l'implication de MUC1 ou EGFR ? »**

Matériel et méthode :

Des TMA sont construits à partir de matériel FFPE de 48 patientes TN et de 39 patientes LUM servant de groupe contrôle.

Les expressions de l'EGFR, MUC1-N, MUC1-C, PI3Kp110β, Bécline-1 sont évaluées.

Résultats :

Comme dans nos observations précédentes sur les tissus humains, nous confortons sur cette série différente, la diminution d'expression de MUC1-N et de MUC1-C dans les cancers TN par comparaison aux LUM (respectivement $p = 0.002$ et $p < 0.0001$).

EGFR n'est quasiment pas observé dans les LUM ($p < 0.001$).

Bécline1 et PI3Kp110β sont plus faiblement exprimées dans les TN que dans les LUM ($p < 0.0001$, $p < 0.0001$).

Dans les TN, une corrélation positive est calculée entre PI3Kp110β et la Bécline1, démontrant une association probable entre les 2 molécules dans la voie de l'autophagie. (figure 15)

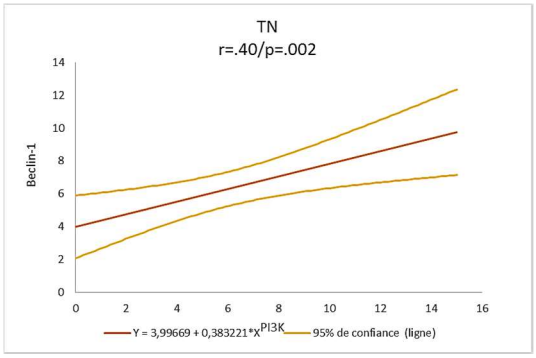

FIGURE 15 : Corrélation positive entre Bécline1 et PI3Kp110β dans les TN, suggérant que les 2 molécules sont liées dans le même mécanisme d'autophagie.

Dans les LUM et les TN, on observe une corrélation positive entre MUC1-N (MUC1-VNTR) et Bécline-1 : elle est cependant négative pour les LUM et positive pour les TN. (figure 16) MUC1-C est positivement corrélé avec PI3Kp110β, uniquement dans les TN. (figure 17).

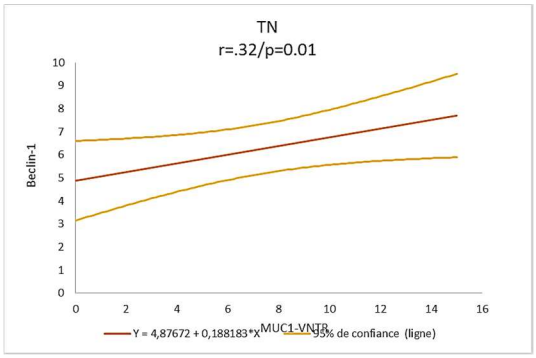

FIGURE 16 : corrélation positive entre Bécline1 et MUC1-N dans les TN, illustrant l'association possible entre MUC1 et l'autophagie.

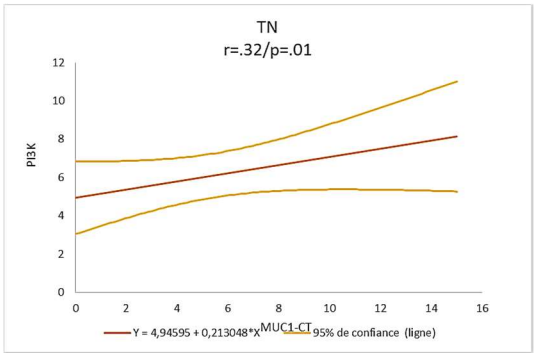

FIGURE 17 : Corrélation positive entre MUC1-C et PI3Kp110β dans les TN, illustrant également la possibilité d'association entre MUC1 et l'autophagie.

Aucune relation entre EGFR et les autres anticorps étudiés n'a pas été démontrée.

Une observation importante est la corrélation positive entre MUC1-C et MUC1-N uniquement décrite dans les TN ($p<0.0001$) suggérant que la molécule transcrite MUC1 reste intacte dans les TN et n'est pas modifiée par des phénomènes épigénétiques (internalisation principalement et splicing intracellualre…), contrairement aux LUM. Rappelons que MUC1-C est l'une des voies d'internalisation de l'EGFR, suggérant que l'EGFR s'accumule à la membrane par défaut de ce mécanisme. (figure 18)

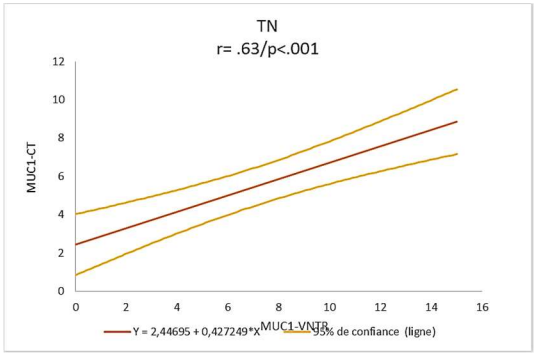

FIGURE 18 : Corrélation entre MUC1-C et MUC1-N dans les TN, suggérant un proportion identique entre les deux parties de MUC1 et que, par conséquent, MUC1 est sous une forme native peu modelée par internalisation successive.

Conclusion :

Les diminutions de Bécline1 et de PI3Kp110β dans les TN suggèrent que l'autophagie jouerait un important rôle dans ce groupe hétérogène de tumeurs TN, connu pour la résistance à la chimiothérapie ou aux thérapies ciblées contre EGFR.

De plus, nous démontrons, également dans les TN, une association positive entre Bécline-1 ou PI3Kp110β et MUC1-N ou MUC1-C, suggérant l'implication de MUC1 dans la voie de l'autophagie.

L'association entre MUC1 et EGFR est démontrée depuis plusieurs années et a fait l'objet de nombreuses publications. Le complexe moléculaire MUC1/EGFR n'est plus à remettre en doute. Par contre, l'association entre MUC1/EGFR/NEU1 a été récemment décrite. NEU1 est un enzyme lysosomiale capable d'enlever les acides sialiques des glycoprotéines comme MUC1 ou EGFR. Ce processus de sialylation/désialylation serait un important modulateur des fonctions de ces macromolécules. NEU1 a également montré une interaction moléculaire avec EGFR. Son interaction avec MUC1 reste cependant encore hypothétique.

Nos observations illustrent aussi que MUC1 est moins exprimée dans les TN et qu'elle se présente dans une forme moins remodelée, c'est-à-dire intacte sans phénomène de « splicing » (corrélation positive MUC1-N et MUC1-C). Cette différence peut s'expliquer par un défaut de l'internalisation de MUC1, suggérant que l'accumulation de l'EGFR à la membrane des TN est due également à un défaut d'internalisation du couple MUC1/EGFR et, par conséquent, une accumulation d'EGFR à la membrane. Ceci expliquant la présence excessive de l'EGFR dans les cellules TN par comparaison aux cellules LUM.

Pour conclure, nous pensons que l'autophagie est altérée dans les TN impliquant le complexe moléculaire de MUC1/EGFR et probablement NEU1.

Int J Clin Exp Pathol 2015;8(5):4344-4355
www.ijcep.com /ISSN:1936-2625/IJCEP0007525

Original Article

Autophagy is decreased in triple-negative breast carcinoma involving likely the MUC1-EGFR-NEU1 signalling pathway

Christian Garbar[1,2], Corinne Mascaux[1,2], Jérôme Giustiniani[1,2], Stéphanie Salesse[3], Laurent Debelle[3], Frank Antonicelli[2], Yacine Merrouche[1,2], Armand Bensussan[4]

[1]Institut Jean Godinot-Unicancer, 1 rue du Général Koenig CS80014, Reims 51726, France; [2]Derm-I-C EA7319, UFR Médecine, Université de Reims Champagne Ardenne, 51 rue Cognacq Jay Reims 51095, France; [3]Umr cnrs/urca 7369 MEDyC, UFR Sciences Exactes et Naturelles, Université de Reims Champagne Ardenne, Moulin de la Housse, BP1039, 51687 Reims Cedex 2, France; [4]Institut National de la Santé et de la Recherche Médicale (INSERM) UMR-S 976, Hôpital Saint Louis, Paris 75010, France and Université Paris Diderot, Sorbonne Paris Cité, Laboratoire Immunologie Dermatologie & Oncologie, UMR-S 976, Paris 75475, France

Received March 3, 2015; Accepted Aprily 15, 2015; Epub May 1, 2015; Published May 15, 2015

Abstract: Triple-negative breast carcinoma (TN) is a heterogeneous cancer type expressing EGFR in 75% of cases. MUC1 is a large type I sialylated glycoprotein comprising two subunits (α and β chains, also called respectively MUC1-VNTR and MUC1-CT), which was found to regulate EGFR activity through endocytic internalisation. Endocytosis and autophagy use the lysosome pathway involving NEU1. Recently, a molecular EGFR-MUC1-NEU1 complex was suggested to play a role in EGFR pathway. In the aim to understand the relationship between EGFR-MUC1-NEU1 complex and autophagy in breast carcinoma, we compared triple negative (TN) showing a high-EGFR expression with luminal (LUM) presenting low-EGFR level. We studied the expression of MUC1-VNTR, MUC1-CT and NEU1 in comparison with those of two molecular actors of autophagy, PI3K (p110β) and Beclin1. A total of 87 breast cancers were split in two groups following the immunohistochemical classification of breast carcinoma: 48 TN and 39 LUM. Our results showed that TN presented a high expression of EGFR and a low expression of MUC1-VNTR, MUC1-CT, NEU1, Beclin-1 and PI3Kp110β. Moreover, in TN, a positive statistical correlation was observed between Beclin-1 or PI3Kp110β and MUC1-VNTR or NEU1, but not with EGFR. In conclusion, our data suggest that autophagy is reduced in TN leading likely to the deregulation of EGFR-MUC1-NEU1 complex and its associated cellular pathways.

Keywords: Breast, carcinoma, EGFR, MUC1, NEU1, PI3K, beclin-1, autophagy

Introduction

Breast cancers are the most common cause of cancer mortality in women. Most of them are routinely treated following their estrogen receptors (ER), progesterone receptors (PR) and human epidermal growth factor receptor type 2 (HER2) expressions. According to this clinical approach, a biological classification has been recently proposed by Perou *et al* and adopted by the St Galen International Expert Consensus. Briefly, this classification proposes three main molecular subtypes: luminal (ER+PR+HER2-), overexpressed HER2 (ER-PR-HER2+) and triple negative (ER-PR-HER2-) carcinomas [1-3]. However, triple negative breast carcinoma (TN) corresponds to a heterogeneous cancer subtype leading to difficulties to assign an appropriate treatment [4]. Interestingly, about 75% of TN expressed high amount of type 1 epidermal growth factor receptor (EGFR). Unfortunately, the treatments by a monoclonal anti-EGFR alone (Cetuximab) or in combination with carboplatin, were associated with a low rate of clinical response suggesting a complex signalling pathway [5-7].

MUC1, or CD227, is a large trans-membrane O-glycosylated protein affiliated to the insoluble mucin family. Structurally, MUC1 is a heterodimer consisting of a large extracellular α-subunit containing 20 to 125 tandem repeats of 20

amino acids broadly glycosylated (MUC1-VNTR), and a β-subunit containing the transmembrane domain and a cytoplasmic tail (MUC1-CT) [8-10]. Many breast cancers and other epithelial cancers over-express MUC1 presenting severe alterations of their glycosylation pattern leading to the exposure of repetitive peptide core epitopes that may represent potential targets for immunotherapy [11-14]. Kawaguchi *et al* demonstrated that MUC1 glycosylation changes are correlated to the tumoral capacity to develop metastasis [15]. Among the glycosylation processes, sialylation is crucial for a variety of cellular functions such as cell adhesion signal recognition, and biological stability of glycoproteins. Sialylation of glycoproteins is regulated by two opposing enzymatic activities: sialyltransferases and sialidases [16, 17]. It is interesting to mention that NEU1, a well-known lysosome sialidase, has been proposed to regulate EGFR and MUC1 signalling (ref Lillehoj et *al)*. Moreover, NEU1 forms a complex with both EGFR and MUC1 [18]. The β-subunit part of MUC1, MUC-CT, is involved in several cellular signalling pathways that could potentially induce cancerous transformation by either growth/survival pathways induction or apoptosis inhibition [19, 20]. Some authors demonstrated a colocalisation between MUC1-CT and EGFR both at the cell membrane and in the nucleus, involving internalisation of EGFR and activation of the EGFR-PI3K-AKT pathway [20-22].

The phosphoinositide 3-kinases (PI3K) constitute a family of lipid kinases that can be activated by extracellular stimuli. PI3K are involved in tumour cell survival, proliferation and differentiation. They are grouped into three classes of isoforms mainly based on their substrate specificity. The two ubiquitously expressed PI3K isoforms p110α and p110β play different roles in cellular signalling. The p110α isoform promotes the main response of EGFR stimulation, whereas p110-β seems to finely tune this response [23, 24]. Importantly, p110β is also involved in the endocytosis of EGFR and/or to promote autophagy by activation of the Rab5-Vps34-Vps15-Beclin-1 complex [25, 26]. Interestingly, MUC1 expression is associated with increased lysosomal turnover of the autophagic maker LC3-II by stimulation of the AMP-activated protein kinase (AMPK), therefore highlighting the involvement of MUC1 in the regulation of autophagy [21, 27]. Autophagy is a cellular degradation pathway involving double-membrane vesicles and the lysosome machinery, including catabolic enzymes such as NEU1. Autophagy is activated upon cellular stress in order to maintain cell homeostasis. Autophagy plays a role in differentiation, aging, immunity and tumour suppression [28]. Intriguingly, autophagy is also associated with resistance to chemotherapy [29, 30].

To understand the relationship between EGFR-MUC1-NEU1 complex and autophagy in breast carcinoma, we compared TN showing a high-EGFR expression, with LUM presenting low-EGFR level. We studied the expression of MUC1-VNTR, MUC1-CT and NEU1 in comparison with those of PI3K (p110β) and Beclin1.

Materials and methodology

Patient population

Between 2010 to 2013, archival paraffin embedded surgical material and clinical data of 48 triple negative breast carcinomas (TN, age = 61.1 ± 14.9 years) and 39 luminal carcinoma (LUM, age = 60.4 ± 12.4 years, P = ns) using as control group, were available for this study. All cases were classified following the immunohistochemical classification in mean of a preliminary immunohistochemical study confirmed by the tissue microarray (TMA) [1-3]. Among those, 19 patients presented lymph node metastasis (LUM = 15/39 (38.4%) vs. TN = 4/48 (10.4%), *P* = 0.0008) and 15 had haematogenous metastasis (mainly lung, liver and brain; LUM = 1/39 (2.5%) vs. TN = 14/48 (29.1%), *P* = 0.0007). Tumour recurrence was described in 13 patients (LUM = 2/39 (5.1%) vs. TN = 11/48 (22.9%), *P* = 0.02). No neo-adjuvant chemotherapy was performed. The mean of follow-up was 101.6 ± 60.4 weeks.

This study was made according to the approval of the local ethic committee, and all patients were informed and agreed to contribute to this study.

Histological procedures and Tissue Micro Array (TMA) construction

All surgical specimens were initially fixed in 4% buffered formaldehyde solution for 8 to 48

Table 1. Primary antibodies, dilution, antigenic retrieval, incubation times and abbreviations used in this study

Antibodies	Clone	Abbreviation	Manufacture	Dilution	Retrievial	Incubation (minutes)
Beclin-1	H-300	Beclin-1	Santa Cruz	1:50	Citrate, pH 6	60
EGFR wild-type	DAK-H1-WT	EGFR	Dako	1:200	EDTA, pH 9	30
α-Estrogen Receptor	SP1	ER	Dako	RTU	EDTA, pH 9	20
HER2	c-erB-2	HER2	Dako	1:800	Citrate, pH 6	30
MUC1 core glycoprotein	Ma552	MUC1-VNTR	Novocastra	1:50	EDTA, pH 9	10
MUC1-ter C	ARP41446	MUC1-CT	Aviva System Biology	1:400	EDTA, pH 9	60
Neuraminidase1	NEU1	ARP44186_T100	Aviva System Biology	1:1000	EDTA, pH 9	60
Pi3K p110 β	N/A	PI3K	Spring	1:100	Citrate, pH 6	30
Progesterone Receptor	PgR636	PR	Dako	RTU	EDTA, pH 9	20

hours, then embedded in paraffin and cut into 4 µm thick slides. The slides were stained with a classical haematoxylin-eosin stain to perform the initial diagnosis. From these archival formol/paraffin blocs, we built a TMA receive paraffin block that could be used for all immunohistochemical slides. We used an automated TMA device (Minicore2, Mitogen UK) associated with a needle core of 0.6 mm diameter. We chose 3 distant core needle samples of each donor tumour paraffin block. The final TMA receive paraffin block was cut in serial slides. These slides were consecutively used for immunohistochemistry.

Immunohistochemical methods

Immunohistological staining was performed with a Dako Autostainer Link 48® immunostaing system (Dako Glostrub, Denmark). After dewaxing, antigenic retrieval were performed using citrate buffered (pH 6) or EDTA buffered (pH 9) antigenic retrieval solution at 99°C in a warm bath (EnVision Flex Target Retrieval solutions high and low pH, Dako). Endogen peroxydase were inhibiting with a hydrogen peroxide phosphate buffered solution (EnVision Flex Peroxydase Blocking Reagent, Dako). After the incubation of the primary antibodies, the immunological reaction was revealed by a polymer dextran coupled with secondary antibody and peroxydase for 15 min (EnVision Flex HRP, Dako) and diaminobenzidine for 10 minutes (EnVision DAB + chromogen, Dako). Counterstain was made with haematoxylin for 10 min (EnVision Flex haematoxylin, Dako). Negative controls were obtained using mouse IgG1 (Negative Control Mouse, Dako) diluted at 1:100, in place of primary antibodies. Primary antibodies, dilution and antigenic retrieval are described in **Table 1**.

Classification of breast cancers by immunohistochimestry

HER2 immunostaining were considered positive as described in the Guideline of College of American Pathologists and controlled by a FISH technique for all cases (HercepTest® Dako) [31]. ER and PR were subsequently scored using a score consisting to sum the intensity and proportion of the nuclear immunostaining. A result superior to 2 was considered as positive [32]. According the St Galen guideline [3] and the results of these immunostainings, all cases were classified following the immunohistochemical classification [1, 2].

Immunostaining quantification

Staining results were evaluated by CG and CM, based on the intensity and percentage of staining tumour cells, with agreement reached. The parametric results were edited as a score by a multiplication of intensity (0 = none, 1 = weak, 2 = intermediated, 3 = strong) and the percentage of tumour cells (0 = none, 1 = 1%, 2 = between 1% to 10%, 3 = between 10% to 33%, 4 = between 33% to 66% and 5 = between 66 to 100%) [modified from 32].

Statistics

T-test and Spearman's test were performed. A p value < 0.05 was considered significant. The WinSTAT® version 2012 (Fitch Software, Bad Krozinger, Germany) and Excel 2013 (Microsoft Corp., Redmond, Washington U.S.A.) programs were used for statistical analysis. The results were expressed in means and standard error.

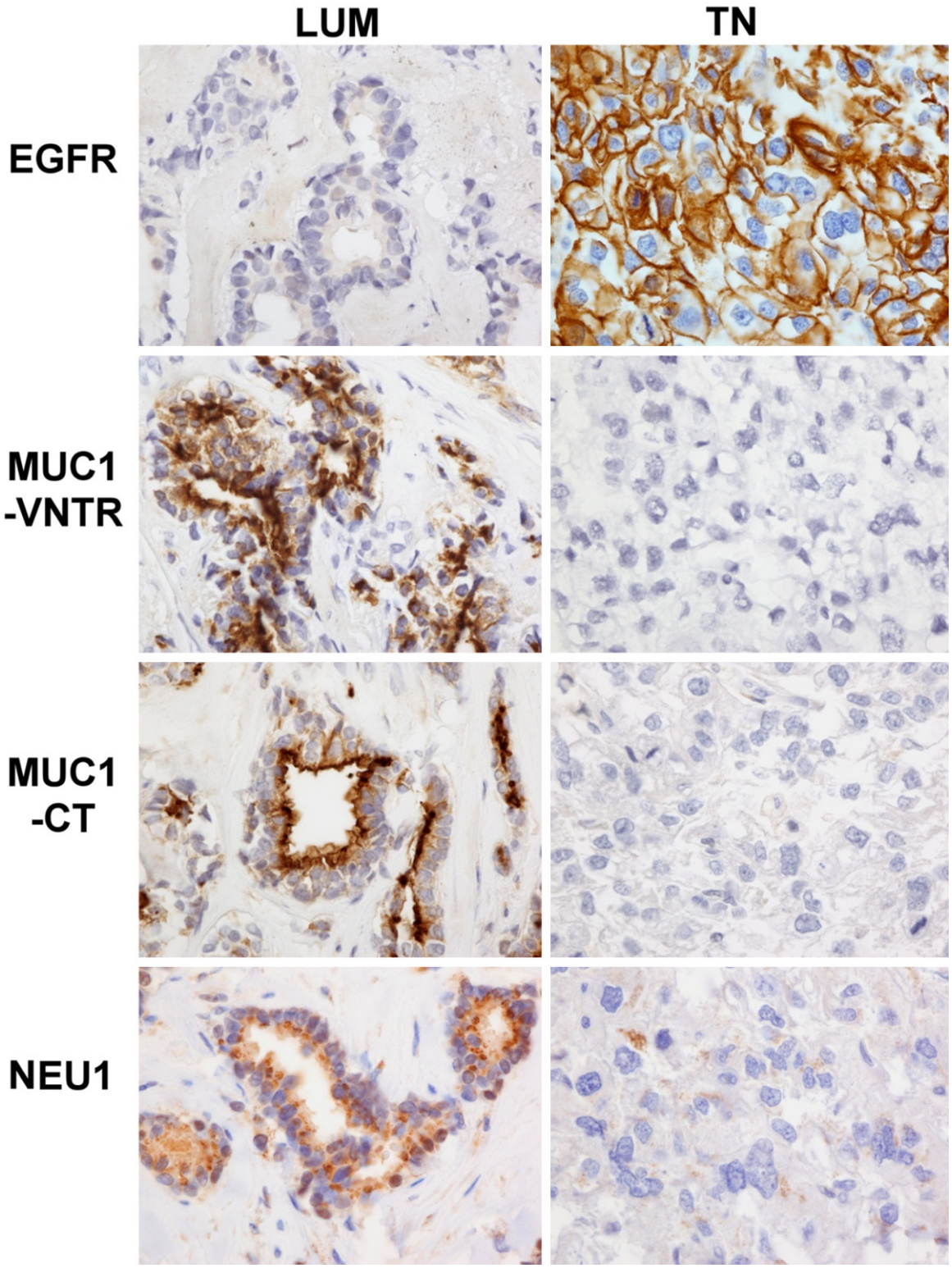

Figure 1. EGFR, MUC1-VNTR, MUC1-CT and NEU1 difference and morphological distribution between luminal (LUM) and triple-negative (TN) breast carcinoma. EGFR is negative in LUM and positive in only membrane in this TN case/ MUC1-VNTR and MUC-CT are positive in cytoplasm of LUM and negative in TN/NEU1 is positive in cytoplasm of LUM and negative in TN. This figure illustrated observations described in **Table 2**: the low-expression of MUC1-VNTR, MUC1-CT, NEU1 and the high-expession of EGFR in TN, suggesting that the EGFR/MUC1/NEU1 molecular complex could be deregulated in breast cancers. Immunohistochemistry on the same LUM and TN cases. Magnification 400×.

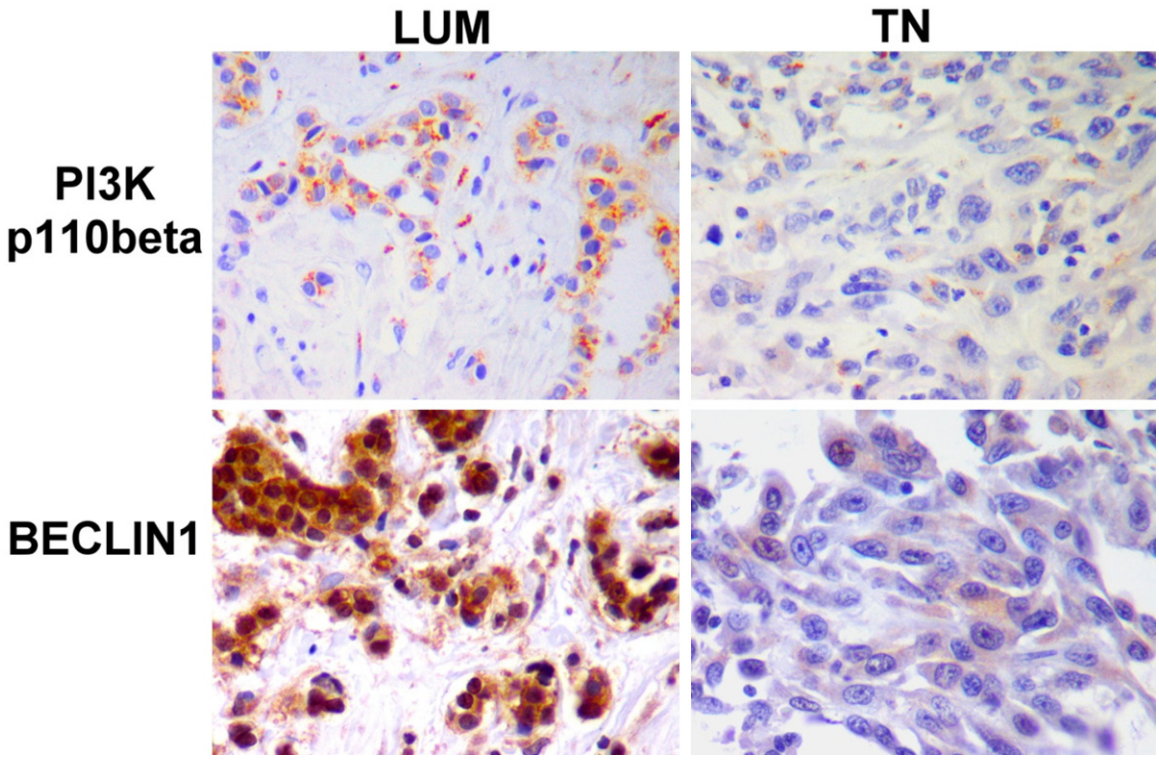

Figure 2. PI3Kp110β and Beclin-1 difference and morphological descriptions between luminal (LUM) and triple-negative (TN) breast carcinoma. PI3Kp110β and Beclin-1 are high-positive in LUM and low-positive in TN. This figure illustrated observations described in **Table 2**: the low-expression of Beclin-1 and PI3Kp110β in TN, suggesting a low action of autophagy. Immunohistochemistry on the same LUM and TN cases. Magnification 400×.

Results

Characteristics of patients with TN and LUM breast carcinomas

In this retrospective study, we analysed data from 87 patients prognosticated either with triple negative breast carcinomas (TN, n = 48, age = 61.1 ± 14.9 years) or with luminal breast carcinoma (LUM, n = 39, age = 60.4 ± 12.4 years, *P* = ns) [1-3]. Among the whole population of breasts cancer patients, those diagnosed with lymph node metastasis was significantly higher in the LUM group compared to the TN group (15/39 (38.4%) vs. TN = 4/48 (10.4%), respectively, P = 0.0008). Conversely, the number of patients with haematogenous metastasis (mainly lung, liver and brain) was lower within the LUM group than in the TN group (LUM = 1/39 (2.5%) vs. TN = 14/48 (29.1%), *P* = 0.0007). Tumour recurrence was described in 13 patients (LUM = 2/39 (5.1%) vs. TN = 11/48 (22.9%), *P* = 0.02). No neo-adjuvant chemotherapy was performed. The mean of follow-up was 101.6 ± 60.4 weeks.

Morphological differences between TN and LUM

First, we studied the morphological cell distribution of EGFR, MUC1-VNTR, MUC1-CT and of NEU1 (**Figure 1**), PI3Kp110β and Beclin-1 (**Figure 2**) in the 48 TN in comparison with the 39 LUM. To that aim, we compared the immunohistological score obtained for each antibody in the TN and LUM groups (**Table 2**). Interestingly, all immunostainings presented a significant statistical difference between LUM and TN, suggesting an important biological difference between these 2 groups of breast tumours. Globally, TN showed a lower expression of MUC1-VNTR (*P* = 0.002), MUC1-CT (*P* < 0.0001), NEU1 (*P* = 0.03), PI3Kp110β (*P* < 0.0001) and Beclin-1 (*P* < 0.0001) as compared to LUM. A higher expression of EGFR (*P* < 0.0001) was observed in TN. Although TN breast cancers are well-known to highly express EGFR, in this study 14 TN were EGFR-negative and 2 LUM were EGFR-positive. However, no change within our data was observed if these cases were discarded EGFR is expressed both in the cytoplasm and the cell membrane.

Table 2. Biological difference between LUM and TN antigenic expressions. Results are expressed in mean and standard deviation of histological score

	LUM	TN	P
N	39	48	
EGFR	0.35 ±1.18	6.60 ± 5.04	< 0.0001
MUC1-VNTR	10.71 ± 4.89	7.14 ± 5.76	0.002
MUC1-CT	9.53 ± 4.62	5.50 ± 4.18	< 0.0001
NEU1	8.05 ± 3.16	6.06 ± 5.01	0.03
PI3Kp110β	9.55 ±4.09	6.10 ± 3.96	< 0.0001
BECLIN1	9.65 ± 4.26	6.23± 3.77	< 0.0001

Then, we investigated the morphological localisation of these molecules. As we previously described, MUC1-VNTR is expressed both at the cytoplasm membrane and in the cytoplasm [33]. MUC1-CT showed the same expression pattern. Importantly, we noted that MUC1-VNTR and MUC1-CT expression were not always observed at the cell membrane of each patient group, indicating that MUC1 epitopes are not always accessible for a target therapy using monoclonal antibodies. NEU1 and PI3Kp110β were localized mainly in the cytoplasm. Beclin-1 was observed either in the cytoplasm or in the nuclei.

Relative expression of the EGFR/MUC1/NEU1 complex molecules

Although MUC1 expression has been well illustrated in breast carcinoma, to date the comparison of MUC1-VNTR and MUC1-CT in TN and LUM is still not described in the literature. Here, we found a positive correlation between MUC1-VNTR and MUC1-CT within the TN group ($P < 0.0001$, r = 0.64) but not for the LUM group, suggesting that in TN, MUC1-VNTR and MUC1-CT were produced at the same rate (**Figure 3**). Previous studies suggested the possibility of a MUC1-EGFR-NEU1 molecular complex [18, 34]. We then sought a relationship between the expressions of EGFR with each one of these two forms of MUC1 in the two groups of breast cancers. In contrast to the previous documented studies, we did not observe a positive correlation neither between EGFR and MUC1-VNTR, nor with MUC1-CT whatever the breast cancer group analysed (data not shown). Likewise, EGFR expression was not positively correlated to Neu1 expression. Furthermore, in the setting of the above-mentioned results in

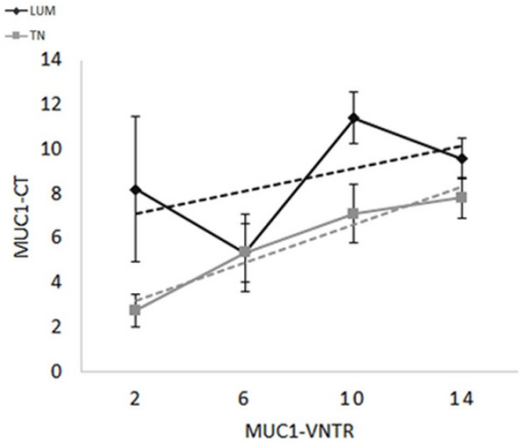

Figure 3. Histological score relationship between MUC1-VNTR and MUC1-CT in LUM (grey, P = ns) or TN (black, $P < 0.0001$). The linear positive correlation between MUC1-VNTR and MUC1-CT observed only in TN, suggests that these both antigens were produced in the same concentration. Consequently, MUC1 seems less modified in TN than in LUM.

Figure 1, we also questioned the possibility of an inverse correlation between EGFR and MUC1 or NEU1. Though, no correlation was found between these molecules. Conversely, MUC1-VNTR was statistically and positively correlated to NEU1 expression in the TN group (P = 0.04; r = 0.25), but not in the LUM group (**Figure 4**). No correlation was observed with the intracellular MUC1 domain (MUC1-CT) (**Figure 4**). These results suggest that only an interaction between NEU1 and the extracellular domain of MUC1 may occur in the TN group.

Autophagy and TN breast cancer

Autophagy has been involved in breast cancer [29, 30]. We studied two different proteins involved in the autophagy pathway: the subunit PI3Kp110β and Beclin-1 [26-28]. Our results indicate a positive correlation between PI3Kp110β and Beclin-1 either in LUM (P = 0.001, r = 0.41) and TN (P = 0.002, r = 0.40), demonstrating the relationship between the two proteins. TN presented a low-level of both PI3Kp110β and Beclin-1 suggesting a decreasing of autophagy (**Table 2**). Moreover, NEU1 presented a positive correlation for PI3Kp110β and Beclin-1 in TN (respectively P = 0.0003, r =0.48 and P = 0.01, r = 0.31) (**Figure 5**). In the LUM group, NEU1 was positively correlated to PI3Kp110β (P = 0.04, r = 0.29) but not with beclin-1 (**Figure 5**). These observations pointed

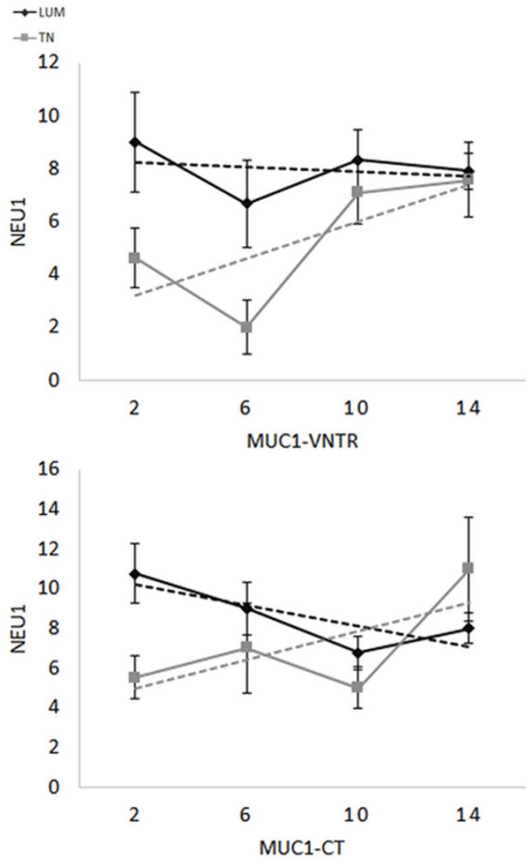

Figure 4. Histological score relationship between NEU1 and MUC1-VNTR in LUM (grey, *p*=ns) or TN (black, *p*=0.04) or MUC1-CT for LUM (grey, *P* = ns) or TN (black, *P* = ns). Correlations between MUC1-VNTR or MUC1-CT and NEU1 were only significant between MUC1-VNTR and NEU1 in TN (*P* = 0.04) suggesting that the extracellular chain of MUC1 is associated with NEU1 only in TN.

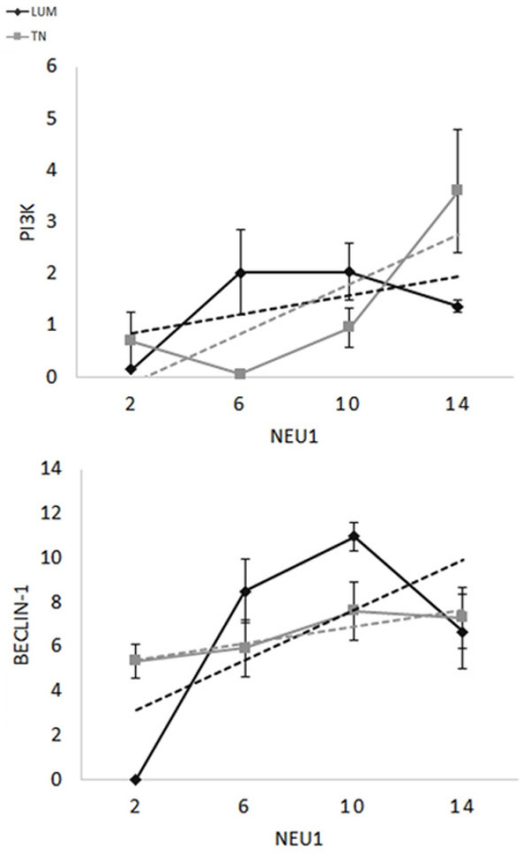

Figure 5. Histological score relationship between NEU1 and PI3Kp110β for LUM (grey, *P* = 0.04) or TN (black, *P* = 0.0003) or Beclin1 for LUM (grey, *P* = ns) or TN (black, *P* = 0.01). NEU1 presented a positive correlation with the two antigens of autophagy: PI3K (p110β) (for TN *P* = 0.01 and for LUM *P* = 0.04) and Beclin-1 (For Tn *P* = 0.0003 and for LUM P = ns). This suggests that the lysosomial enzyme NEU1 is involved in the autophagy pathway.

out the implication of NEU1 in the autophagy through the lysosomal machinery. MUC1-VNTR also showed positive correlations in TN for both PI3Kp110β (*P* = 0.009, r = 0.32) and Beclin 1 (*P* = 0.01, r = 0.32). MUC1-CT was only correlated with PI3Kp110β in the TN group (*P* = 0.04) but not with Beclin-1 (**Figure 6**), suggesting that MUC1-VNTR was the main MUC1 subunit involved in the autophagy process in TN (**Figure 7**). This relationship was less obvious in LUM. We concluded that autophagy is reduced in TN involving likely MUC1-VNTR and NEU1.

Discussion

Recently on routine histological material, we have demonstrated that MUC1 protein was associated with the tumour aggressive biological behaviour of breast carcinoma [33]. Several authors also illustrated the secretion of MUC1 by breast cancer cells [35-37]. Most of them were mainly interested by the extracellular α-subunit of the MUC1 (MUC1-VNTR) because in tumour cells, the antigenic sides of the α-subunit protein core are specifically denuded by an aberrant lack of glycosylation. The core protein is then more exposed and constitutes a potential target for immunotherapy [38]. Deepening the knowledge of breast carcinomas, we here showed an important heterogeneity, both in the quantitative and the qualitative expression of MUC1 in luminal and triple negative breast carcinomas. In agreement with our data, Siroy *et al had already* showed that 67% of early stage basal-like triple negative

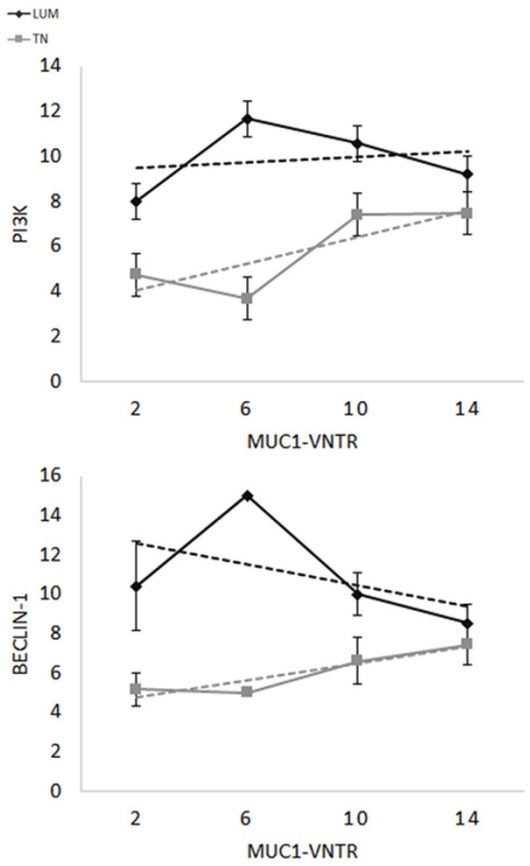

Figure 6. Histological score relationship between MUC1-VNTR and PI3Kp110β for LUM (grey, $P = 0.04$) or TN (black, $P = 0.009$) or Beclin-1 for LUM (grey, $P = 0.01$) or TN (black, $P = 0.01$). Only MUC1-VNTR is correlated with two antigens of autophagy (Beclin-1 and PI3Kp110β) (P = ...) in TN and in LUM. This suggests that the extracellular part of MUC1 could be played a role in the autophagy of breast carcinoma.

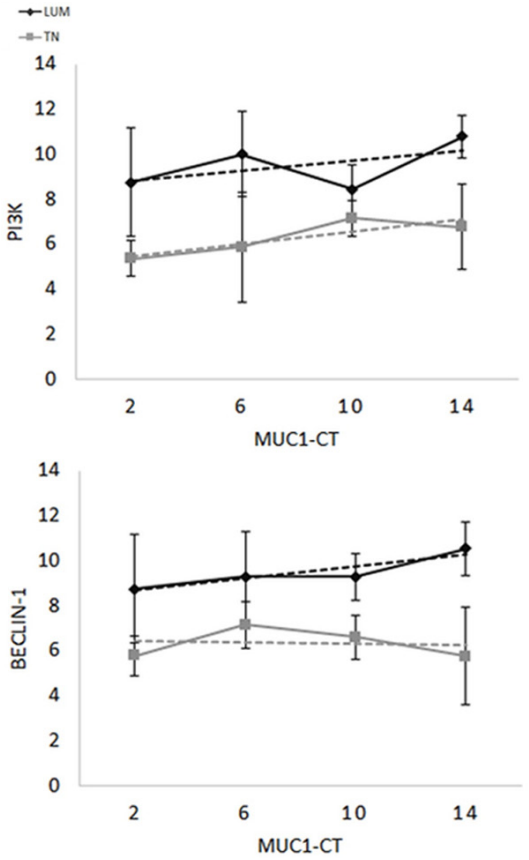

Figure 7. Histological score realtionship between MUC1-CT and PI3Kp110β for LUM (grey, P = ns) or TN (black, $P = 0.04$) or Beclin-1 for LUM (grey, P = ns) or TN (black, P = ns). Only MUC1-CT is only correlated PI3K (p110β) in TN ($P = 0.04$). This suggests that the intracellular part of MUC1 is less involved in the autophagy pathway than the extracellular part of MUC1. As illustrated in the **Figure 2**, MUC1 is less modified by the MUC1-VNTR splicing in TN, suggesting that an independent action of the extracellular MUC1-VNTR and the intracellular MUC1-CT.

breast cancers strongly expressed MUC1, 27% showed a weak secretion and 6% were negative [37]. Our study also supports a previous report on MUC1-VNTR expression in a small group of patients (10 cases) [33]. Such variability is of clinical interest. Indeed, we here showed that both MUC1 subunits (MUC1-VNTR and MUC1-CT), and thereof epitopes exposure, are less expressed in TN than in LUM breast cancers.

Lillehoj et al suggested the possibility of a MUC1-EGFR-NEU1 molecular complex [18]. Consequently, we looked at the association between MUC1, EGFR and/or NEU1 in the two groups of breast cancers. However, we did not find any correlation between EGFR and MUC1-VNTR, MUC1-CT or NEU1. We even found that while TN was expressed a high level of EGFR, both MUC1-VNTR and MUC1-CT were down-regulated in TN as compared to LUM breast cancer. These results are discordant with those of Neeraja Dharmanarj *et al* who recently demonstrated a statistical correlation between MUC1 and EGFR and concluded that the activation of EGFR stimulates MUC1 expression in multiple cellular contexts [39], but are in setting with those of others authors who showed that EGFR stimulation promotes the cleavage α-subunit MUC1 [20, 40, 41]. Such discrepancies highlight the importance to define *in situ* the expression of these molecules according to the type of cancer. *In vitro* study on breast cell lines demonstrated that MUC1 and EGFR are associ-

ated in a molecular complex in breast cancers and that MUC1 inhibits EGFR down-regulation and endocytosis [34]. Based on our *in situ* results, we then hypothesize that EGFR overexpression observed in TN is the result of EGFR accumulation in the cytoplasm or cell membrane rather than EGFR-overproduction.

Our results demonstrate that the expression of MUC1-VNTR and MUC1-CT were only correlated in TN, suggesting that the MUC1 is not cleaved yet, and therefore that MUC1 endocytosis is reduced in TN. Accordingly, Wreschner et al demonstrated that full length MUC1 is modified following a limited proteolysis event of its extracellular part (MUC1-VNTR) by the recycling of MUC1 by endocytosis [34, 38]. Subsequently, Crose et al showed that MUC1-CT constitutes a better indicator of MUC1 production than MUC1-VNTR because it does not depend on the MUC1 proteolysis [42]. Therefore, the positive correlation between MUC1-VNTR and MUC1-CT observed in TN, is the indirect reflect of the lack of MUC1 recycling. Reduced recycling of MUC1 in TN therefore bound to a reduced level of MUC1 glycosylation supports the fact that MUC1 epitopes could be better recognized in this type of breast cancer. Furthermore, because MUC1-CT is not or less altered or glycosylated, it constitutes a better indicator of the primary secretion of the MUC1 [42]. This also supports our above mentioned hypothesis that EGFR accumulates in TN.

The high level of EGFR and our hypothesis that MUC1 is not cleaved suggest that EGFR-MUC1 pathway is deregulated in TN. The membrane associated PI3K plays an important role in the EGFR intracytoplasmic signalling. Using conditional gene knockout mice deficient in the class IA PI3K p110α or p110β catalytic subunit, Dou *et al* demonstrated that p110β subunit promotes autophagy by activation of the complex Rab5-Vps34-Vps15-Beclin-1, independently of its kinase activity [26]. This pathway seems to be independent of EGFR stimulating pathway which is associated with the cascade of PI3K p110α/AKT/mTOR, well-known as an inhibitor of autophagy [23, 43]. Our observation of the low expression of both Beclin-1 and PI3Kp110β confirms that the autophagy pathway is reduced in TN breast cancer. In these cancers, the positive correlation between MUC1-VNTR with both PI3K p110β and Beclin-1, strongly advocates for a link between MUC1-VNTR and autophagy [45]. Then, our in situ results support a previous in vitro study showing that MUC1 promotes autophagy in human tumour cells in response to glucose deprivation [27].

Autophagy is an adaptive phenomena widely used by tumour cells using the lysosomial machinery [44]. Debnath *et al* pointed out the important role of autophagy in breast carcinogenesis. Indeed, reduced autophagy can promote tumour development by genomic instability. We found that EGFR was highly expressed in TN. Interestingly, in a series of 107 TN, Tilch *et al* did not identify any mutation of the EGFR gene suggesting that EGFR protein is physiologically normal [45]. In the setting of a reduced level of autophagy in TN breast cancer, it is worth to note that IL17A has been described to attenuate the autophagy process by regulation of PI3K [46]. Recently, in 3 of our patients presenting a TN breast cancer, Cochaud *et al* showed a high production of IL17A, supporting the implication of IL17A as inhibitor of autophagy in TN [47]. Furthermore, EGFR activation in TN surely plays a role in Beclin-1 phosphorylation and, consequently on autophagy suppression. Indeed, Wei *et al* demonstrated that this mechanism could contribute to tumour progression and chemoresistance in lung carcinoma [48]. Another interesting regulator of autophagy is the oncoprotein p53 which is often mutated in TN. Of note, genetically altered p53 was also demonstrated to inhibit autophagy [49-51]. Interestingly, we also observed a high level of p53 in TN (data not show).

Tumour cells are also able to activate autophagy in diverse conditions such as hypoxia, extracellular matrix fragmentation or other metabolic modifications [52]. The recycling of MUC1 through the cytoplasm and the cellular membrane and its cleavage and release in the extracellular matrix are well documented in the literature [34, 38]. Although NEU1 has been recently suggested to be associated with the EGFR-MUC1 membrane complex, we found that NEU1 is less expressed in TN than LUM. Nevertheless, in TN NEU1 was positively correlated with the extracellular MUC1 domain or MUC1-VNTR ($P = 0.04$, $r = 0.25$) but not with the intracellular MUC1 domain (MUC1-CT). Interestingly, NEU1 is a lysosome enzyme that is able to de-sialylate several macromolecules such as MUC1 or EGFR. NEU1 is known as a modulator of cell

receptors, and has been involved in endocytosis and MUC1 regulation [18]. It can activate phagocytosis in macrophages and dendritic cells through de-sialylation of surface receptors [53, 54]. NEU1 is also involved in processing extracellular matrix fragmentation signals such as elastin peptides [55]. Gilmour *et al* showed that matrix metalloproteinase-9 and NEU1 form a complex with EGFR on the cell surface [56]. These observations suggest that the extracellular matrix could play an important role in the engagement of the molecular complex EGFR-NEU1-MUC1 and its associated intracellular signals.

To conclude, we demonstrated that autophagy is reduced in TN breast cancers leading likely to deregulation of the EGFR-MUC1-NEU1 complex and associated cellular pathways. Nevertheless, further studies will be needed to show the co-localizations of EGFR-MUC1-NEU1 and the close regulations of these molecular actors in different type of breast cancers.

Disclosure of conflict of interest

None

Abbreviations

TN, triple-negative breast carcinoma; LUM, luminal type of breast carcinoma; MUC1-VNTR, α-subunit of MUC1; MUC1-CT, β-subunit of MUC1; TMA, tissue micro-array; NEU1, neuraminidase-1; EGFR, human epidermal growth factor receptor type 1; HER2, human epidermal growth factor receptor type 2; ER, Estrogen receptors; PR, progesterone receptors; CK, cytokeratin; PI3K, phosphoinositide 3-kinases.

Address correspondence to: Christian Garbar, Department of Biopathology, Institut Jean Godinot-Unicancer, 1 rue du Général Koenig CS80014, Reims 51726, France. Tel: +33 326 504 266; Fax: +33 326 504 274; E-mail: Christian.garbar@reims.unicancer.fr

References

[1] Perou CM. Molecular stratification of triple-negative breast cancers. Oncologist 2011; 16 Suppl 1: 61-70.

[2] Strehl JD, Wachter DL, Fasching PA, Beckmann MW, Hartmann A. Invasive Breast Cancer: Recognition of Molecular Subtypes. Breast Care (Basel) 2011; 6: 258-264.

[3] Goldhirsch A, Winer EP, Coates AS, Gelber RD, Piccart-Gebhart M, Thürlimann B, Senn HJ; Panel members. Personalizing the treatment of women with early breast cancer: highlights of the St Gallen International Expert Consensus on the Primary Therapy of Early Breast Cancer 2013. Ann Oncol 2013; 24: 2206-23.

[4] Rivenbark AG, O'Connor SM, Coleman WB. Molecular and cellular heterogeneity in breast cancer: challenges for personalized medicine. Am J Pathol 2013; 183: 1113-24.

[5] Carey LA, Rugo HS, Marcom PK, Mayer EL, Esteva FJ, Ma CX, Liu MC, Storniolo AM, Rimawi MF, Forero-Torres A, Wolff AC, Hobday TJ, Ivanova A, Chiu WK, Ferraro M, Burrows E, Bernard PS, Hoadley KA, Perou CM, Winer EP. TBCRC 001: randomized phase II study of cetuximab in combination with carboplatin in stage IV triple-negative breast cancer. J Clin Oncol 2012; 30: 2615-23.

[6] Baselga J, Gómez P, Greil R, Braga S, Climent MA, Wardley AM, Kaufman B, Stemmer SM, Pêgo A, Chan A, Goeminne JC, Graas MP, Kennedy MJ, Ciruelos Gil EM, Schneeweiss A, Zubel A, Groos J, Melezínková H, Awada A. Randomized phase II study of the anti-epidermal growth factor receptor monoclonal antibody cetuximab with cisplatin versus cisplatin alone in patients with metastatic triple-negative breast cancer. J Clin Oncol 2013; 31: 2586-92.

[7] Lehmann BD, Pietenpol JA. Identification and use of biomarkers in treatment strategies for triple-negative breast cancer subtypes. J Pathol 2014; 232: 142-50.

[8] Baruch A, Hartmann M, Zrihan-Licht S, Greenstein S, Burstein M, Keydar I, Weiss M, Smorodinsky N, Wreschner DH. Preferential expression of novel MUC1 tumor antigen isoforms in human epithelial tumors and their tumor-potentiating function. Int J Cancer 1997; 71: 741-9.

[9] Joshi MD, Ahmad R, Yin L, Raina D, Rajabi H, Bubley G, Kharbanda S, Kufe D. MUC1 oncoprotein is a druggable target in human prostate cancer cells. Mol Cancer Ther 2009; 8: 3056-65.

[10] Rubinstein DB, Karmely M, Ziv R, Benhar I, Leitner O, Baron S, Katz BZ, reschner DH. MUC1/X protein immunization enhances cDNA immunization in generating anti-MUC1 alpha/beta junction antibodies that target malignant cells. Cancer Res 2006; 66: 11247-53.

[11] Senapati S, Das S, Batra SK. Mucin-interacting proteins: from function to therapeutics. Trends Biochem Sci 2010; 35: 236-45.

[12] Coveler AL, Bates NE, Disis ML. Progress in the development of a therapeutic vaccine for breast cancer. Breast Cancer (Dove Med Press) 20104; 2: 25-36.

[13] Limacher JM, Quoix E. TG4010: A therapeutic vaccine against MUC1 expressing tumors. Oncoimmunology 2012; 1: 791-792.
[14] Pillai K, Pourgholami MH, Chua TC, Morris DL. MUC1 as a Potential Target in Anticancer Therapies. Am J Clin Oncol 2013; 38: 108-18.
[15] Kawaguchi T, Takazawa H, Imai S, Morimoto J, Watanabe T. Lack of polymorphism in MUC1 tandem repeats in cancer cells is related to breast cancer progression in Japanese women. Breast Cancer Res Treat 2005; 92: 223-30.
[16] Harduin-Lepers A, Vallejo-Ruiz V, Krzewinski-Recchi MA, Samyn-Petit B, Julien S, Delannoy P. The human sialyltransferase family. Biochimie 2001; 83: 727-37.
[17] Monti E, Preti A, Venerando B, Borsani G. Recent development in mammalian sialidase molecular biology. Neurochem Res 2002; 27: 649-63.
[18] Lillehoj EP, Hyun SW, Feng C, Zhang L, Liu A, Guang W, Nguyen C, Luzina IG, Atamas SP, Passaniti A, Twaddell WS, Puché AC, Wang LX, Cross AS, Goldblum SE. NEU1 sialidase expressed in human airway epithelia regulates epidermal growthfactor receptor (EGFR) and MUC1 protein signaling. J Biol Chem 2012; 287: 8214-31.
[19] Bafna S, Kaur S, Batra SK. Membrane-bound mucins: the mechanistic basis for alterations in the growth and survival of cancer cells. Oncogene 2010; 29: 2893-904.
[20] Raina D, Kharbanda S, Kufe D. The MUC1 oncoprotein activates the anti-apoptotic phosphoinositide 3-kinase/Akt and Bcl-xL pathways in rat 3Y1 fibroblasts. J Biol Chem 2004; 279: 20607-12.
[21] Bitler BG, Goverdhan A, Schroeder JA. MUC1 regulates nuclear localization and function of the epidermal growth factor receptor. J Cell Sci 2010; 123: 1716-23.
[22] Kufe DW. MUC1-C oncoprotein as a target in breast cancer: activation of signaling pathways and therapeutic approaches. Oncogene 2013; 32: 1073-81.
[23] Jia S, Roberts TM, Zhao JJ. Should individual PI3 kinase isoforms be targeted in cancer? Curr Opin Cell Biol 2009; 21: 199-208.
[24] Utermark T, Rao T, Cheng H, Wang Q, Lee SH, Wang ZC, Iglehart JD, Roberts TM, Muller WJ, Zhao JJ. The p110α and p110β isoforms of PI3K play divergent roles in mammary gland development and tumorigenesis. Genes Dev 2012; 26: 1573-86.
[25] Dbouk HA, Backer JM. Novel approaches to inhibitor design for the p110β phosphoinositide 3-kinase. Trends Pharmacol Sci 2013; 34: 149-53.
[26] Dou Z, Pan JA, Dbouk HA, Ballou LM, DeLeon JL, Fan Y, Chen JS, Liang Z, Li G, Backer JM, Lin RZ, Zong WX. Class IA PI3K p110β subunit promotes autophagy through Rab5 small GTPase in response to growth factor limitation. Mol Cell 2013; 50: 29-42.
[27] Yin L, Kharbanda S, Kufe D. MUC1 oncoprotein promotes autophagy in a survival response to glucose deprivation. Int J Oncol 2009; 34: 1691-9.
[28] Sinha S, Levine B. The autophagy effector Beclin 1: a novel BH3-only protein. Oncogene 2008; 27 Suppl 1: S137-48.
[29] Yoon JH, Ahn SG, Lee BH, Jung SH, Oh SH. Role of autophagy in chemoresistance: regulation of the ATM-mediated DNA-damage signaling pathway through activation of DNA-PKcs and PARP-1. Biochem Pharmacol 2012; 83: 747-57.
[30] Ajabnoor GM, Crook T, Coley HM. Paclitaxel resistance is associated with switch from apoptotic to autophagic cell death in MCF-7 breast cancer cells. Cell Death Dis 2012; 3: e260.
[31] Wolff AC, Hammond ME, Schwartz JN, Hagerty KL, Allred DC, Cote RJ, Dowsett M, Fitzgibbons PL, Hanna WM, Langer A, McShane LM, Paik S, Pegram MD, Perez EA, Press MF, Rhodes A, Sturgeon C, Taube SE, Tubbs R, Vance GH, van de Vijver M, Wheeler TM, Hayes DF; American Society of Clinical Oncology; College of American Pathologists. American Society of Clinical Oncology/College of American Pathologists guideline recommendations for human epidermal growth factor receptor 2 testing in breast cancer. J Clin Oncol 2007; 25: 118-45
[32] Allred DC, Harvey JM, Berardo M, Clark GM. Prognostic and predictive factors in breast cancer by immunohistochemical analysis. Mod Pathol 1998; 11: 155-68.
[33] Garbar C, Mascaux C, Curé H, Bensussan A. Muc1/Cd227 immunohistochemistry in routine practice is a useful biomarker in breast cancers. J Immunoassay Immunochem 2013; 34: 232-45.
[34] Wreschner DH, McGuckin MA, Williams SJ, Baruch A, Yoeli M, Ziv R, Okun L, Zaretsky J, Smorodinsky N, Keydar I, Neophytou P, Stacey M, Lin HH, Gordon S. Generation of ligand-receptor alliances by "SEA" module-mediated cleavage of membrane-associated mucin proteins. Protein Sci 2002; 11: 698-706.
[35] Mukhopadhyay P, Chakraborty S, Ponnusamy MP, Lakshmanan I, Jain M, Batra SK. Mucins in the pathogenesis of breast cancer: implications in diagnosis, prognosis and therapy. Biochim Biophys Acta 2011; 1815: 224-40.
[36] van der Vegt B, de Roos MA, Peterse JL, Patriarca C, Hilkens J, de Bock GH, Wesseling

J. The expression pattern of MUC1 (EMA) is related to tumour characteristics and clinical outcome of invasive ductal breast carcinoma. Histopathology 2007; 51: 322-35.
[37] Siroy A, Abdul-Karim FW, Miedler J, Fong N, Fu P, Gilmore H, Baar J. MUC1 is expressed at high frequency in early-stage basal-like triple-negative breast cancer. Hum Pathol 2013; 44: 2159-66.
[38] Litvinov SV, Hilkens J. The epithelial sialomucin, episialin, is sialylated during recycling. J Biol Chem 1993; 268: 21364-71.
[39] Neeraja Dharmaraj, Engel BJ, Carson DD. Activated EGFR stimulates MUC1 expression in human uterine and pancreatic cancer cell lines. J Cell Biochem 2013; 114: 2314-22.
[40] Lau SK, Shields DJ, Murphy EA, Desgrosellier JS, Anand S, Huang M, Kato S, Lim ST, Weis SM, Stupack DG, Schlaepfer DD, Cheresh DA. EGFR-mediated carcinoma cell metastasis mediated by integrin αvβ5 depends on activation of c-Src and cleavage of MUC1. PLoS One 2012; 7: e36753.
[41] Pochampalli MR, Bitler BG, Schroeder JA. Transforming growth factor alpha dependent cancer progression is modulated by Muc1. Cancer Res 2007; 67: 6591-8.
[42] Croce MV, Isla-Larrain MT, Rua CE, Rabassa ME, Gendler SJ, Segal-Eiras A. Patterns of MUC1 tissue expression defined by an anti-MUC1 cytoplasmic tail monoclonal antibody in breast cancer. J Histochem Cytochem 2003; 51: 781-8.
[43] Kang R, Zeh HJ, Lotze MT, Tang D. The Beclin 1 network regulates autophagy and apoptosis. Cell Death Differ. 2011; 18: 571-80.
[44] Barth JM, Köhler K. How to take autophagy and endocytosis up a notch. Biomed Res Int 2014; 2014: 960803.
[45] Altschuler Y, Kinlough CL, Poland PA, Bruns JB, Apodaca G, Weisz OA, Hughey RP. Clathrin-mediated endocytosis of MUC1 is modulated by its glycosylation state. Mol Biol Cell 2000; 11: 819-31.
[46] Tilch E, Seidens T, Cocciardi S, Reid LE, Byrne D, Simpson PT, Vargas AC, Cummings MC, Fox SB, Lakhani SR, Chenevix Trench G. Mutations in EGFR, BRAF and RAS are rare in triple-negative and basal-like breast cancers from Caucasian women. Breast Cancer Res Treat 2014; 143: 385-92.
[47] Liu H, Mi S, Li Z, Hua F, Hu ZW. Interleukin 17A inhibits autophagy through activation of PIK3CA to interrupt the GSK3B-mediated degradation of BCL2 in lung epithelial cells. Autophagy 2013; 9: 730-42.
[48] Cochaud S, Giustiniani J, Thomas C, Laprevotte E, Garbar C, Savoye AM, Curé H, Mascaux C, Alberici G, Bonnefoy N, Eliaou JF, Bensussan A, Bastid J. IL-17A is produced by breast cancer TILs and promotes chemoresistance and proliferation through ERK1/2. Sci Rep 2013; 3: 3456.
[49] Wei Y, Zou Z, Becker N, Anderson M, Sumpter R, Xiao G, Kinch L, Koduru P, Christudass CS, Veltri RW, Grishin NV, Peyton M, Minna J, Bhagat G, Levine B. EGFR-mediated Beclin 1 phosphorylation in autophagy suppression, tumor progression, and tumor chemoresistance. Cell 2013; 154: 1269-84.
[50] Balaburski GM, Hontz RD, Murphy ME. p53 and ARF: unexpected players in autophagy. Trends Cell Biol 2010; 20: 363-9.
[51] Shah SP, Roth A, Goya R, Oloumi A, Ha G, Zhao Y, Turashvili G, Ding J, Tse K, Haffari G, Bashashati A, Prentice LM, Khattra J, Burleigh A, Yap D, Bernard V,McPherson A, Shumansky K, Crisan A, Giuliany R, Heravi-Moussavi A, Rosner J, Lai D, Birol I, Varhol R, Tam A, Dhalla N, Zeng T, Ma K, Chan SK, Griffith M, Moradian A, Cheng SW, Morin GB, Watson P, Gelmon K, Chia S, Chin SF, Curtis C, Rueda OM, Pharoah PD, Damaraju S, Mackey J, Hoon K, Harkins T, Tadigotla V,Sigaroudinia M, Gascard P, Tlsty T, Costello JF, Meyer IM, Eaves CJ, Wasserman WW, Jones S, Huntsman D, Hirst M, Caldas C, Marra MA, Aparicio S. The clonal and mutational evolution spectrum of primary triple-negative breast cancers. Nature 2012; 486: 395-9.
[52] Morselli E, Tasdemir E, Maiuri MC, Galluzzi L, Kepp O, Criollo A, Vicencio JM, Soussi T, Kroemer G. Mutant p53 protein localized in the cytoplasm inhibits autophagy. Cell Cycle 2008; 7: 3056-61.
[53] Debnath J. The multifaceted roles of autophagy in tumors-implications for breast cancer. J Mammary Gland Biol Neoplasia 2011; 16: 173-87.
[54] Seyrantepe V, Iannello A, Liang F, Kanshin E, Jayanth P, Samarani S, Szewczuk MR, Ahmad A, Pshezhetsky AV. Regulation of phagocytosis in macrophages by neuraminidase 1. J Biol Chem 2010; 285: 206-15.
[55] Pshezhetsky AV, Hinek A. Where catabolism meets signalling: neuraminidase 1 as a modulator of cell receptors. Glycoconj J 2011; 28: 441-52.
[56] Duca L, Blanchevoye C, Cantarelli B, Ghoneim C, Dedieu S, Delacoux F, Hornebeck W, Hinek A, Martiny L, Debelle L. The elastin receptor complex transduces signals through the catalytic activity of its Neu-1 subunit. J Biol Chem 2007; 282: 12484-91.
[57] Gilmour AM, Abdulkhalek S, Cheng TS, Alghamdi F, Jayanth P, O'Shea LK, Geen O,Arvizu LA, Szewczuk MR. A novel epidermal growth factor receptor-signaling platform and its targeted translation in pancreatic cancer. Cell Signal 2013; 25: 2587-603.

iii. MUC1/EGFR/IL17 et l'autophagie dans les cultures cellulaires de cancer du sein triple négatif sous chimiothérapie

But du travail :

Mettre au point un modèle dynamique d'étude de la chimiothérapie en FFPE sur des cultures cellulaires de cellules de cancer du sein TN et LUM (groupe contrôle).

Question posée : **« quelles sont les variations d'expression de MUC1, EGFR, IL17A, IL17RA, IL17RB et de l'autophagie (LC3) sur ces cellules sous chimiothérapie ? »**

Matériel et méthode :

Des cultures MDA-MD231 (TN) et MCF7 (LUM) sont soumises à des doses sublétales d'agents de chimiothérapie : épirubicine, docetaxel, 5-fluorouracil, cyclophosphamide. Un test métabolique Rotitest Vital® est utilisé pour calibrer la concentration sublétale d'agents de chimiothérapie. Des groupes contrôles sans traitement sont également observés.

Une technique de cytologie cytoblock® est réalisée pour effectuer des prélèvements FFPE à partir de ces cultures et sur lesquels nous effectuons les examens immunohistochimiques : MUC1-N, MUC1-C, EGFR, IL17A, IL17RA, IL17RB, LC3.

Résultats principaux ;

Nous confirmons nos observations sur tissus humains : les MDA-MD231 (TN) sont MUC1 négatifs et EGFR positifs à l'inverse des MCF7 (LUM).

Nous confirmons aussi les études de l'IL17 effectuées par nos équipes à savoir que l'IL17A n'est pas secrétée par les cellules épithéliales et que, par contre, les récepteurs de l'IL17 (IL17RA et RB) sont présents dans le cytoplasme ou au niveau de la membrane plasmique de nos 2 cultures.

Aucune variation d'expression n'est observée sous chimiothérapie pour MUC1, EGFR, IL17RA et IL17RB.

Le niveau basal d'autophagie est élevé significativement pour les MDA-231 et ne varie pas sous les agents de chimiothérapie, contrairement au MCF7. (figure 19, figure 20)

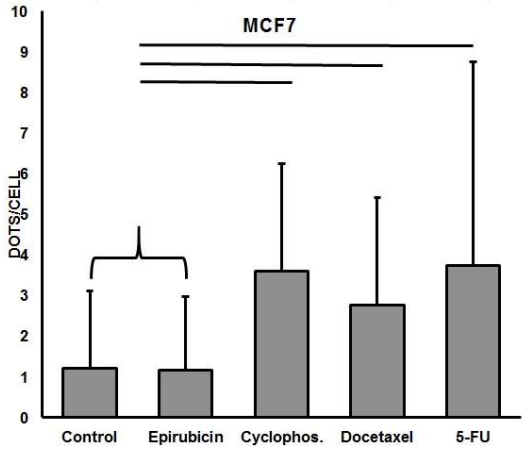

FIGURE 19 : dans les LUM, l'autophagie (mesurée en dots/cellules de marquage LC3) est augmentée sous cyclophosphamide, docétaxel et 5-flourouracil. L'épirubicine est un inhibiteur de l'autophagie montre le même niveau de base que celui du groupe contrôle, suggérant que l'autophagie n'est pas activée dans les LUM.

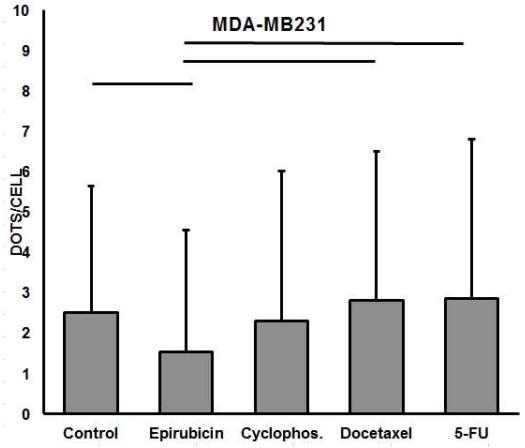

FIGURE 20 : dans les TN (MDA-MB231), l'autophagie basale (mesurée en dots/cellules de marquage LC3) est maximale même sans traitement (cultures contrôles) et identique à celui des cultures sous cyclophosphamide, docétaxel et 5-flourouracil. L'épirubicine est un inhibiteur de l'autophagie, diminue son niveau à celui des cultures contrôles MCF7 (LUM) suggérant que l'autophagie est activée initialement dans les TN.

Conclusion :

Dans cette étude, nous avons mis au point un modèle morphologique dynamique basée sur des cultures cellulaires, permettant des études immunohistochimiques ou de biologie moléculaire proches de celles pouvant être effectuées sur des prélèvements fixés au formol et enchâssés dans la paraffine provenant de pièces chirurgicales. Cette technique possède comme avantages de moduler les traitements des cellules en culture et surtout d'économiser les prélèvements de tumeurs des patientes.

Nos résultats montrent que les MDA-MD231 (TN) et les MCF7 (LUM) présentent une stratégie de défense différente lorsqu'elles sont soumises aux agents de chimiothérapie. Les TN ayant une activation basale optimale contrairement aux LUM. Autrement dit, les TN ont une autophagie déjà enclenchée, pouvant expliquer la résistance de ces cellules aux agents de chimiothérapie. L'épirubicin, connu comme un inhibiteur de l'autophagie, réduit l'activité de celle-ci au niveau de celui des cancers LUM.

Les cancers LUM montrent un mécanisme inverse : un niveau d'autophagie quiescent et une activation par l'agression des agents de chimiothérapie.

Concernant, MUC1 ou EGFR comme voie potentielle de régulation de l'autophagie, nous n'avons pas observé de modification qualitative d'expression. Cependant, les MDA-MB231 (TN) — associé à une autophagie active — n'expriment pas MUC1 et surexpriment EGFR. Les cellules MCF7 (LUM) dont l'autophagie est inactive montrent une image inverse. Notre méthodologie ne peut certainement pas mettre en évidence les mécanismes fins de la régulation de l'autophagie.

Nous avons également fait l'hypothèse que l'IL17 pourrait avoir un potentiel régulateur de l'autophagie. Même si les certains travaux de la littérature le démontrent dans des pathologies inflammatoires, nos résultats ne le confirment pas. Par contre, nous avons illustré nos publications précédentes sur IL17 par notre technique morphologique.

En conclusion, l'inhibition de l'autophagie par des agents spécifiques ou par association de l'épirubicine pourrait lever la chimiorésistance particulière des TN.

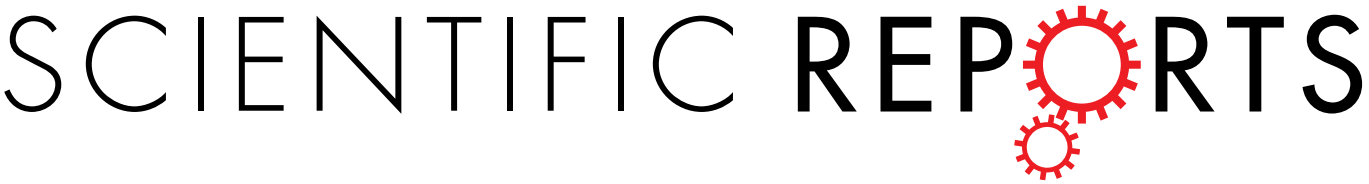

OPEN

Chemotherapy treatment induces an increase of autophagy in the luminal breast cancer cell MCF7, but not in the triple-negative MDA-MB231

Received: 15 February 2017
Accepted: 27 June 2017
Published online: 03 August 2017

Christian Garbar[1,4], Corinne Mascaux[1,4], Jérôme Giustiniani[3,4], Yacine Merrouche[2,4] & Armand Bensussan[5,6]

Autophagy is one of the chemotherapy resistance mechanisms in breast cancer. The aim of this study was to determine the level of recruitment of the autophagy pathway in the triple-negative breast cancer (TNBC) cell line MDA-MB231 compared with that in the control luminal breast cancer cell line MCF7 before and after treatment with chemotherapy drugs. Furthermore, we investigated the relationship between autophagy and EGFR, MUC1 and IL17-receptors as activators of autophagy. Immunohistochemistry was performed in cell culture blocks using LC3b, MUC1-C, EGFR, IL17A, IL17-RA and IL17-RB antibodies. We found that the basal autophagy level in MDA-MB231 was high, whereas it was low in MCF7. However, in contrast to MDA-MB231, the autophagy level was increased in MCF7 upon treatment with chemotherapy agents. Interestingly, we observed that the expression levels of MUC1-C, EGFR, IL17-RA, and IL17-RB were not modified by the same treatments. Furthermore, the chemotherapy treatments did not increase autophagy in TNBC cells without affecting the expression levels of MUC1-C, EGFR, IL17-RA or IL17-RB.

Perou's biological and clinical classification of breast cancers (BCs) was proposed by the St Galen International Expert Consensus and is currently widely used in the clinic. This classification system proposes the following three main molecular subtypes: luminal (LUM) BC, which expresses hormonal estrogen and progesterone receptors (ER+ and PR+) but no human epidermal growth receptor 2 (HER2-); overexpressed HER2 BC (ER+/− PR+/− HER2+); and triple negative (TN) BC, which lacks these receptors HER2, ER and PR[1,2].

LUM BC benefits from anti-estrogen therapy, such as tamoxifen, which is an aromatase inhibitor, and HER2 BC is treated with targeted anti-HER2 (i.e., trastuzumab) therapy. Treatments of TN BC remain more challenging and are mainly based on cytotoxic chemotherapy, such as docetaxel, cyclophosphamide, fluorouracil, and epirubicine[3–5].

Autophagy is an adaptive cellular mechanism to external stress and contributes to cell survival and homeostasis. Autophagy is a complex pathway involving multiple proteins. First, autophagosomes consisting of an isolated membrane in the cytosol are activated by class I PI3K and Atg complexes, leading to nucleation, which involves Beclin-1. Finally, LC3 proteins (microtubule-associated protein 1 light chain 3) control the elongation phase, which stabilizes the autophagosomes. LC3 proteins are stable and persistent and are widely used to monitor

[1]Biopathology Department, Institut Jean Godinot–Unicancer, 1 rue du Général Koenig CS80014, 51726, Reims, France. [2]Oncology Department, Institut Jean Godinot–Unicancer, 1 rue du Général Koenig CS80014, 51726, Reims, France. [3]Research Department, Institut Jean Godinot–Unicancer, 1 rue du Général Koenig CS80014, 51726, Reims, France. [4]DERM-I-C EA7319, Université de Reims Champagne Ardenne, 51 rue Cognacq Jay, 51095, Reims, France. [5]Institut National de la Santé et de la Recherche Médicale (INSERM) U976, Hôpital Saint Louis, 75010, Paris, France. [6]Université Paris Diderot, Sorbonne Paris Cité, Laboratoire Immunologie Dermatologie & Oncologie, UMR-S 976, 75475, Paris, France. Correspondence and requests for materials should be addressed to C.G. (email: christian.garbar@reims.unicancer.fr)

autophagy[6]. Tumor cells exhibit a basal level of autophagy activity that could be increased upon exposure to anoxia, starvation, chemical agents and radiation.

Chemotherapy resistance is due to multiple mechanisms, including autophagy. For example, in breast cancer, epirubicin reduces autophagy and protects cells from chemotherapy-induced apoptosis. Moreover, in colorectal cancer, oxaliplatin and 5-fluorouracil were found to have an improved efficiency in the presence of an anti-autophagy agent, whereas in lung cancer, anti-EGFR agents (i.e., gefitinib or erlotinib) activate autophagy and induce drug resistance[7].

MUC1 is a large transmembrane O-glycosylated heterodimer protein that consists of a large, broadly glycosylated extracellular α-subunit containing 20 to 125 tandem repeats of 20 amino acids (MUC1-VNTR) and a β-subunit containing the transmembrane domain and a cytoplasmic tail (MUC1-C)[8–10]. The β-subunit is involved in several cellular signaling pathways, such as growth/survival pathways and the induction or inhibition of apoptosis[11,12]. Moreover, MUC1 expression is associated with an increased lysosomal turnover of the autophagy maker LC3 after stimulation of the AMP-activated protein kinase (AMPK), which is involved in the regulation of autophagy[13]. Some authors have demonstrated that the β-subunit of MUC1 and EGFR are both co-localized in the cell membrane and nucleus and are involved in the internalization of EGFR and the activation of the EGFR-PI3K-AKT-mTOR pathway[14–17]. Interestingly, this pathway is a key regulator of autophagy, and activated mTOR inhibits autophagy[7].

ERK1/2 is an autophagy activator. Additionally, our team has recently shown that IL17A is produced by BC TILs and plays a role in docetaxel chemoresistance and proliferation through the ERK1/2 pathway[18]. We also reported that IL17A and IL17B receptor transcripts are overexpressed in BCs and that the activation of the IL17E receptor, i.e., the heterodimer of IL17A and IL17B receptors, induces EGFR phosphorylation and migration to the nucleus. We have also suggested that the inhibition of IL17E could enhance the efficacy of anti-EGFR chemotherapy[19,20].

To better understand the relationship between autophagy and the chemotherapy resistance of TN BC, we used a cell culture model consisting of a TNMDA-MB231 cell line and an MCF7 LUM control cell line with or without a treatment with sub-lethal concentrations of chemotherapy agents. We then performed immunohistochemistry to measure the expression levels of LC3b, which is an autophagy marker, and the targeted antigens MUC1, EGFR, IL17RA and IL17RB, which are known to be involved in autophagy and chemoresistance.

Results

Basal autophagy level is high in MDA-MB231 cells and is not influenced by chemotherapy drugs. The MDA-MD231 cell line consists of triple-negative breast cancer cells that do not express estrogen and progesterone receptors or HER2. These characteristics are conserved in the cells upon exposure to chemotherapy agents (data not shown). When cultured in the control medium, LC3b staining was higher in the in MDA-MD231 cells than in the MCF7 cells (Fig. 1). Compared with cells cultured in the control medium, cells cultured with epirubicin exhibited a significantly decreased basal level of autophagy. Importantly, the autophagy level in the MDA-MD231 cells cultured with cyclophosphamide, docetaxel and 5-FU was similar to that in the MDA-MD231 cells cultured in the control culture (Fig. 2).

Basal autophagy is low and increases with chemotherapy drugs in MCF7 cells. MCF7 cells are a luminal cancer cell line expressing estrogen and progesterone receptors but not HER2. These characteristics were conserved upon exposure to chemotherapy agents (data not shown). Interestingly, as shown in Fig. 3, MCF7 cells treated with the autophagy inhibitor epirubicin still had the same low basal level of autophagy as the MCF7 cells cultured in the control medium (control medium MCF7 vs control medium MDA-MB231: $p = 0.006$, control medium MCF7 vs epirubicin MDA-MB231: $p = 0.45$) and that treatments with cyclophosphamide, docetaxel and 5-fluorouracil (5-FU) significantly enhance the level of autophagy.

Expression levels of MUC1, EGFR, IL17-RA and IL17-RA are not influenced by chemotherapy. We have recently described that luminal breast cancer cells widely express MUC1 and exhibit a low level of EGFR *in situ*, whereas triple-negative breast cancer cells are negative for MUC1 and positive for EGFR[21]. Here, we confirmed these results using the luminal breast cancer cell line MCF7 and the triple-negative breast cancer cell line MDA-MB231. Interestingly, we observed no differences in the expression of MUC1 or EGFR in the MCF7 or MDA-231 cell cultures treated with the control medium alone, the autophagy inhibitor epirubicin, or chemotherapy drugs (Figs 4 and 5).

IL17A is known to inhibit autophagy[22]. We have previously demonstrated that IL17A transcripts are not detected in breast cancer cell lines, although these cell lines do express IL17RA and IL17RB transcripts[19]. In the present work, specific antibodies were used for the first time, and we confirmed our previous results: IL17A is not expressed in any culture cells (Fig. 6) comparatively to IL17-RA (Fig. 7). Moreover, we also observed a lower level of IL17RB in the MDA-MD231 cells than in the MCF7 cells (Fig. 8). Interestingly, the expression of IL17RA and IL17RB was not influenced by the chemotherapy drugs (Figs 7 and 8), and IL17A remained negative (Fig. 6)

Discussion

In the present study, we performed an analysis investigating the recruitment of the autophagy pathway in triple-negative cancer cells. The luminal cancer cells showed a low level of autophagy, which was increased by chemotherapy drugs. However, epirubicin, which is a known autophagy inhibitor, failed to induce this enhancement[7]. By contrast, the triple-negative cancer cells showed a high level of autophagy, which was not influenced by the chemotherapy drugs. Interestingly, epirubicin reduced the basal level of autophagy.

This high level of autophagy in TN BC has already been observed *in vitro* and *in vivo* by Lefort S. *et al*. in a large cohort of BC cells. These authors demonstrated that TN BC shows significantly more autophagosomes

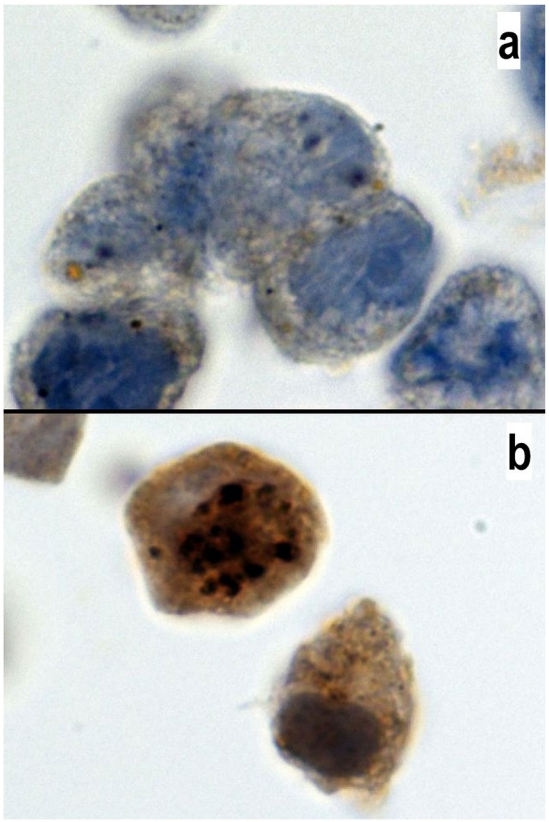

Figure 1. Expression of LC3b in MCF7 and MDA-MB231 cells. LC3b antibody staining in MCF7 (**a**) and MDA-MB231 (**b**) cells. Positive staining is characterized by a cytoplasmic dot signal. Note the low basal level in MCF7 cells and the high basal level in MDA-MB231 cells. The LC3b antibody was diluted 1/400 (100x magnification).

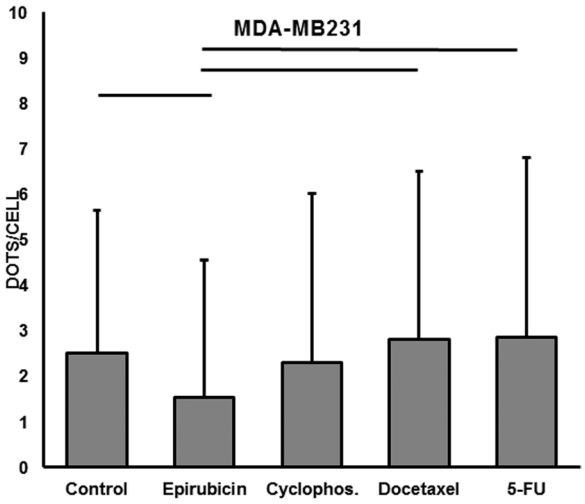

Figure 2. Quantification of autophagy in MDA-MB231. Mean and SD of the cytoplasmic dot signals of LC3b in 100 cells from each MDA-MB231 culture. Line illustrates a p-value <0.05 (Mann-Whitney test). Significant differences were observed between the control and epirubicin-, docetaxel- or 5-FU-treated cultures.

(measured by LC3b) than LUM or HER2 BC. Furthermore, these authors demonstrated that the LC3b protein is a marker of a poor prognosis in TN BC patients using immunohistochemistry on paraffin embedded biopsy tissue[23]. Using a mouse model, chloroquine, which is an autophagy inhibitor, was demonstrated to potentiate chemotherapy against human TN BC[23].

The aim of our present work was to establish a kinetic cell culture model to better understand chemoresistance. We found that TN BC (MDA-MB231) and LUM (MCF7) cells exhibit a different strategy against

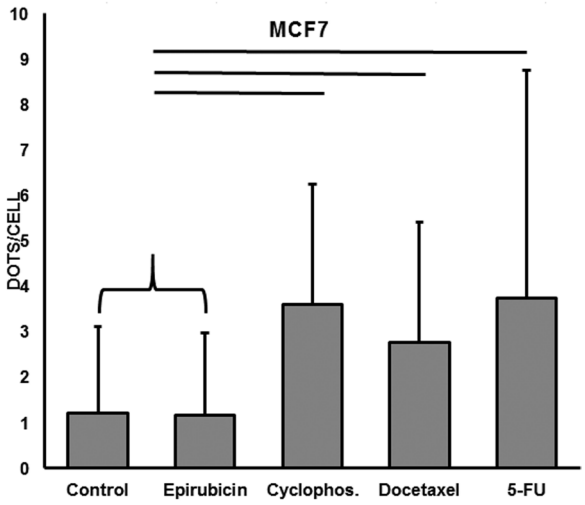

Figure 3. Quantification of autophagy in MCF7 cells. Mean and SD of cytoplasmic dot signals of LC3b in 100 cells from each MCF7 culture. Line indicates $p < 0.05$ (Mann-Whitney test). Significant differences were observed between the control and cyclophosphamide, docetaxel, 5-FU or epirubicin treated cells.

chemotherapy drugs. TN BC has an already high initial level of autophagy, whereas LUM exhibits increased autophagy in response of chemotherapy. These cell strategy differences could be explained by the dual paradoxical role of autophagy against therapeutic anticancer drugs, which either induce cell death or promote cell survival[7]. It is easy to understand that treatment against autophagy will yield different results in the same tumors and across tumor subtypes, leading to a true targeted therapy.

The ERK1/2 signaling pathway is a key component of autophagy. Sivaprasad U *et al.* demonstrated that TNF activates autophagy in MCF7 BC and that the pharmacological inhibition of ERK1/2 was associated with a decrease in TNF-induced autophagy (LC3b)[24]. In similar cell models using MCF7 and MDA-MB231 cell lines, Shen P. *et al.* demonstrated that gemcitabin induces autophagy with a cytotoxic effect in MCF7 cells and a cytoprotective effect in MDA-MB231 cells. The cytotoxic effect in MCF7 cells is attributed to the cascade of estrogen receptor-ERK-p62, which could be inactivated by specific siRNA. Furthermore, these authors showed that gemcitabin is able to induce mTOR-independent autophagy in MDA-MB231 cells also via the ERK1/2 pathway[7,25,26].

Interestingly, our team demonstrated that IL17A promotes chemoresistance to docetaxel and proliferation through ERK1/2 signaling in the MCF7, T47D, BT20, MDA468 and MDA157 cell lines[18,19]. We also showed that IL17A is produced by tumor-infiltrating lymphocytes isolated in biopsies from six patients with TN BC. The mechanism of this chemoresistance is not currently understood, but inhibition of the autophagy pathway in TN BC is likely the best candidate. Indeed, Zhou Y. *et al.*, using a hepatocellular carcinoma cell culture model, demonstrated that IL17A promotes the migration of tumor cells and prevents autophagic cell death[22]. Our previous studies also demonstrated that MCF7 and MDA-MD231 cells do not express IL17A mRNA, but do express the transcripts of its receptor IL17RA. Furthermore, we found that MCF7 cells expressed IL17RB mRNAs, whereas MDA-MB231 cells only expressed a low level of IL17RB mRNA[19]. The present study confirmed these observations using immunohistochemistry. We recently described the possible synergy between EGF and IL17RE to confer resistance against anti-EGFR therapy[20]. Here, we illustrated that protein expression of IL17RA, IL17RB, EGFR and MUC1 is not altered by chemotherapy and, consequently, that these proteins could be accessible for specific targeted therapy. It should be noted that in this study, we also confirmed *in vitro* our previous *in vivo* observations indicating that TN BC cells present a low level of MUC1 and a high level of EGFR and that LUM BC cells show the opposite pattern[21]. Moreover, MUC1 expression is correlated with an increased lysosomal turnover of the autophagic maker LC3, suggesting that MUC1 plays a role in the regulation of autophagy[27].

Recently, Hiraki M *et al.* demonstrated, using the TN BC cell line MDA-MB468, that MUC1-C activated the MEK-ERK and PI3K-AKT pathways, and both activated autophagy. These authors concluded that targeting MUC1-C is a potential strategy for reversing resistance in TN BC[28]. We do not completely agree with this hypothesis because in our experience, both *in vivo and in vitro*, TNBC shows no or low levels of MUC1-C[21]. Another study using MCF7 and ZR-75-1 cell lines treated with an inhibitor of MUC1-C (GO-203) demonstrated an increase in the apoptotic response to Taxol and doxorubicin[29]. It is known that the MUC1-C cytoplasmic domain interacts with numerous regulator proteins, such as NF-B, p53 and PI3k[30]. As discussed above, the PI3K-AKT-mTOR pathway is involved in autophagy. Recently, we have demonstrated that PI3K-p110β and MUC1-C are more highly expressed in LUM than in TN BC[21]. This finding suggests that BC cell autophagy activation strategies could involve the MUC1-PI3K-AKT pathway in LUM BC and the IL17-ERK pathway in TN BC.

In conclusion, this study illustrated the different strategies of inducing autophagy in MDA-MB231 and MCF7 cells in response to chemotherapy. Further studies should be performed to confirm our hypothesis and identify the ideal strategy for anti-autophagy adjuvant therapy to avoid chemotherapy resistance in each BC subtype.

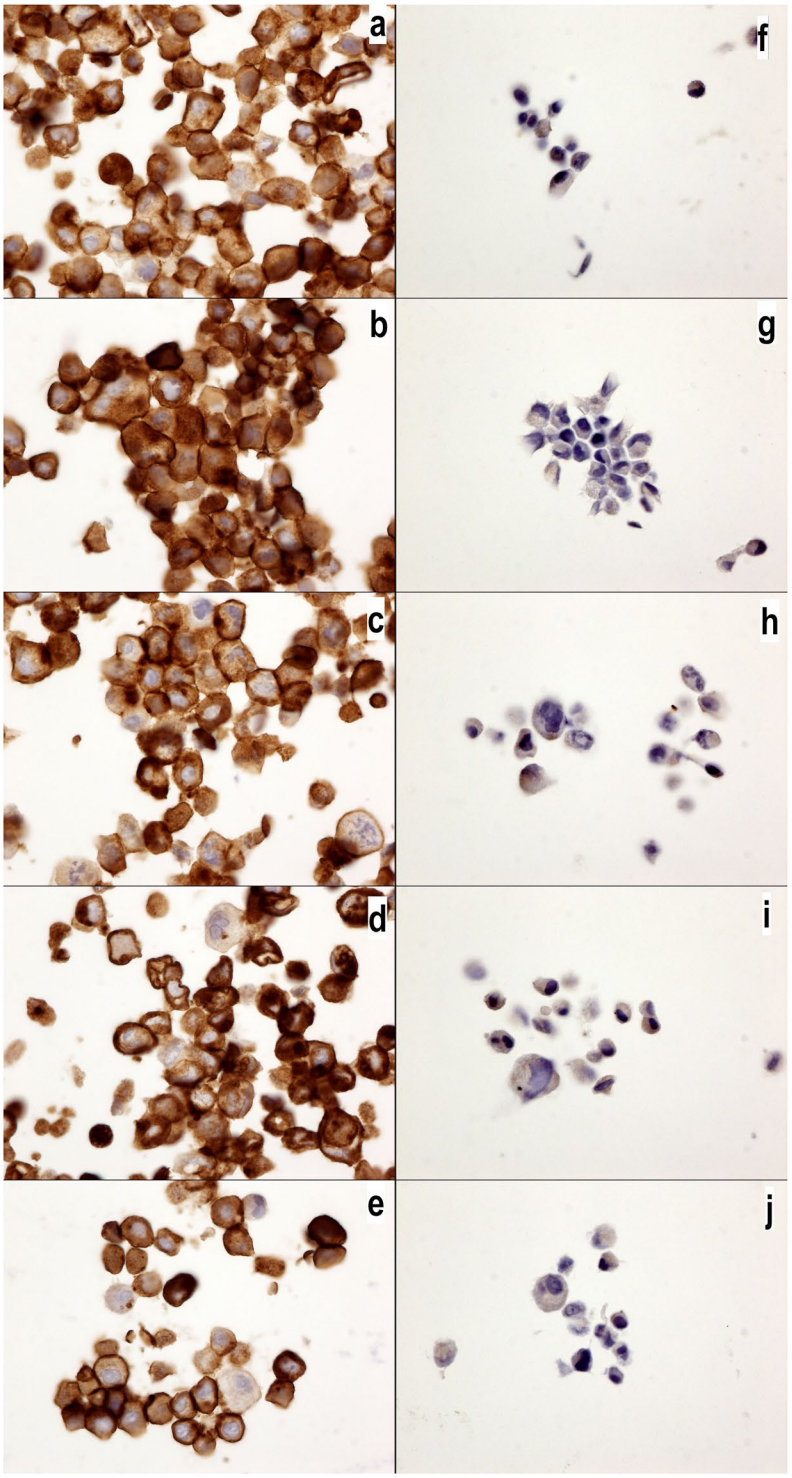

Figure 4. MUC1-C expression in MCF7 and MDA-MB231 cells. MUC1-C expression in MCF7 (**a**–**e**) and MDA-MB231 cells (**f**–**j**) without drugs or (**a**,**f**) with cyclophosphamide (**b**,**g**), doxorubicin (**c**,**h**), epirubicin (**d**,**i**) or 5-fluorouracil (**e**,**j**). Note the higher expression of MUC1-C in the MCF7 cells than that in the MDA-MB231 cells, but no changes were observed with the chemotherapy drug treatments. The MUC1-C antibody was diluted 1/400 (40x magnification).

Materials and Methods

Cell cultures and reagents. The MCF7 and MDA-MB231 cell lines were obtained from England Type Culture Collection (Salisbury). The cells were cultured in DMEM medium (VWR International SAS, Fontenay-sous-bois, France) supplemented with 10% Fetal Calf Serum (FCS), 2% glutamine and 1% penicillin/streptomycin

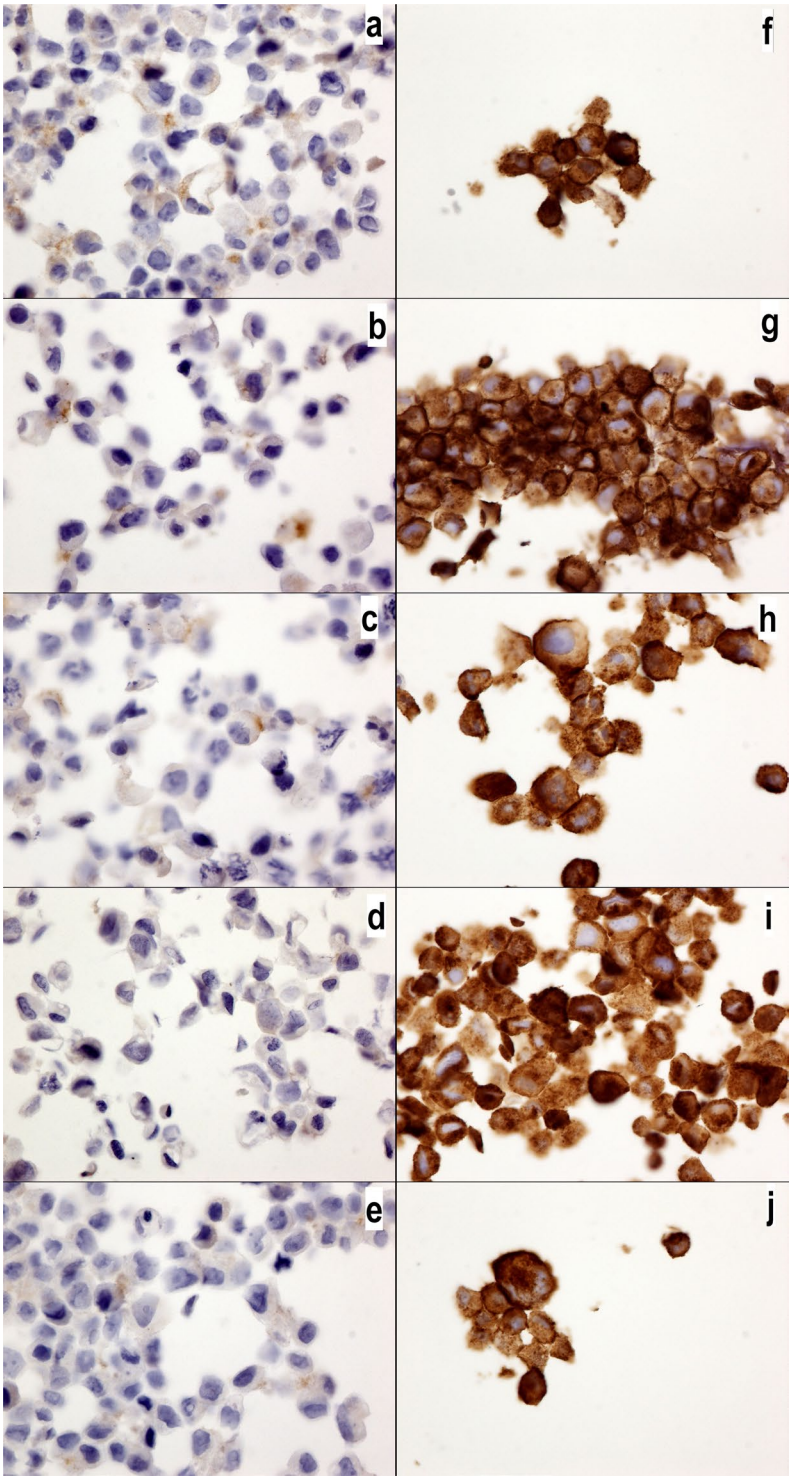

Figure 5. EGFR expression in MCF7 and MDA-MB231 cells. EGFR expression in MCF7 (**a**–**e**) and MDA-MB231 cells (**f**–**j**) without drugs or (**a**,**f**) with cyclophosphamide (**b**,**g**), doxorubicin (**c**,**h**), epirubicin (**d**,**i**) or 5-fluorouracil (**e**,**j**). Note the higher expression of EGFR in the MDA-MB231 cells than that in the MCF7 cells, but no changes were observed with the chemotherapy drug treatment. The EGFR antibody was diluted 1/200 (40x magnification).

antibiotics (Dutscher SAS, Brumath, France). All cells were kept at 37 °C in a 5% CO2 atmosphere incubator. Then, each cell line was incubated with a sub-lethal chemotherapy drug concentration calculated according to the mean of the metabolic activity as measured by Rotitest Vital® (Carl Roth EURL, Lauterbourg, France) and a spectrophotometer (iMark TM, Bio-Rad, France) as follows: the final concentrations consisted of only

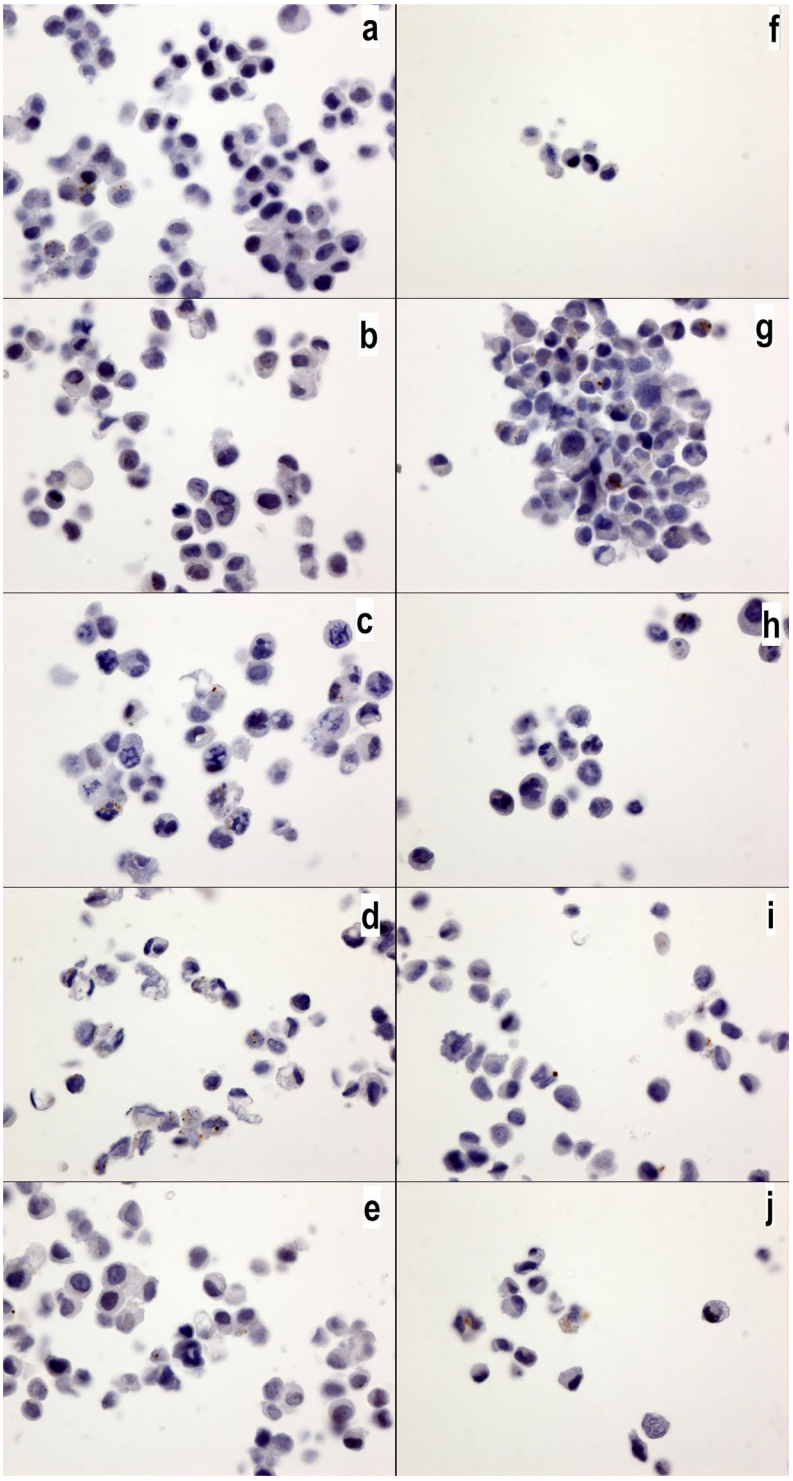

Figure 6. IL17A expression in MCF7 and MDA-MB231 cells. IL17A expression in MCF7 (**a**–**e**) and MDA-MB231 cells (**f**–**j**) without drugs or (**a**,**f**) with cyclophosphamide (**b**,**g**), doxorubicin (**c**,**h**), epirubicin (**d**,**i**) or 5-fluorouracil (**e**,**j**). No significantly positive signals were observed in any of the cultures. The IL17a antibody was diluted 1/800 (40x magnification).

DMEM in the control culture, 5 µg/ml in the epirubicin culture, 10 µg/ml in the docetaxel culture, 10 µg/ml in the 5-fluorouracil culture and 10 µg/ml in the cyclophosphamide culture. The chemotherapy drugs were added, and cell blocks were performed the following day. Each cell culture was replicated 3 times for the cell blocks and immunohistochemistry.

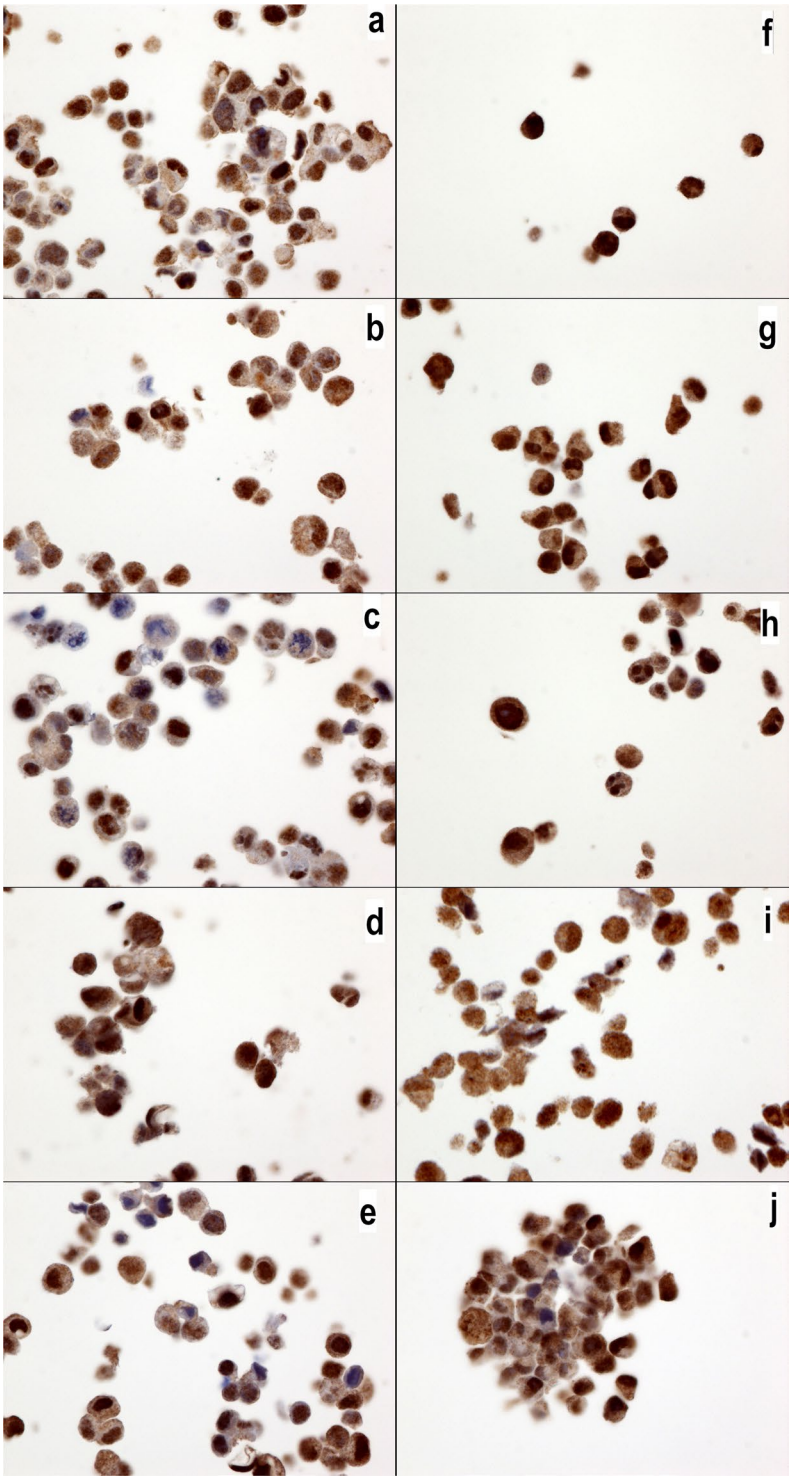

Figure 7. IL17RA expression in MCF7 and MDA-MB231 cells. IL17RA expression in MCF7 (**a**–**e**) and MDA-MB231 cells (**f**–**j**) without drugs or (**a**,**f**) with cyclophosphamide (**b**,**g**), doxorubicin (**c**,**h**), epirubicin (**d**,**i**) or 5-fluorouracil (**e**,**j**). All cell cultures show a positive cytoplasmic signal, but no changes were observed with the chemotherapy drug treatments. The IL17RA antibody was diluted 1/800 (40x magnification).

Cell block. After washing with PBS and treating with trypsin, the cell cultures were centrifuged at 1300 RPM for 8 min. Then, the cell pellets were fixed in 5 ml of 4% buffered formaldehyde solution for 8 to 48 hours. The cells were centrifuged at 1000 RPM for 5 min. The pellets were prepared using a Cytoblock® kit (Thermo Fisher Scientific, Brebieres, France) and then embedded in paraffin. The paraffin-embedded cell blocks were cut into 4 µm thick sections for the immunohistochemistry.

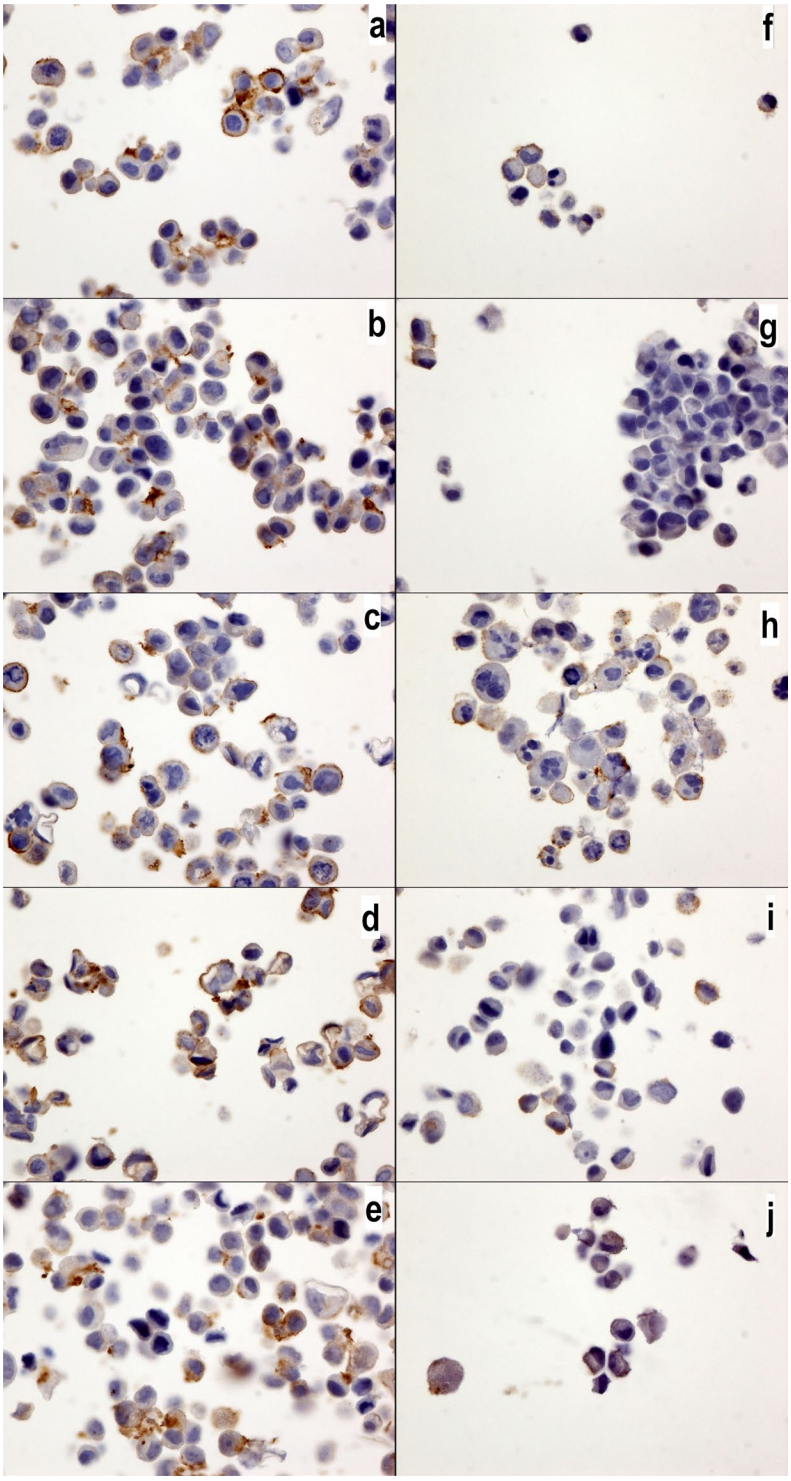

Figure 8. IL17RB expression in MCF7 and MDA-MB231 cells. IL17RB expression in MCF7 (**a**–**e**) and MDA-MB231 cells (**f**–**j**) without drugs or (**a**,**f**) with cyclophosphamide (**b**,**g**), doxorubicin (**c**,**h**), epirubicin (**d**,**i**) or 5-fluorouracil (**e**,**j**). All cells cultures exhibited a positive membrane signal, but no changes were observed with the chemotherapy drug treatments. Note that the MCF7 cells show a higher expression than the MBA-MB231 cells. The IL17RB antibody was diluted 1/40 (40x magnification).

Immunohistochemical Methods. Immunohistological staining was performed using a Dako Autostainer Link 48® immunostaining system (Dako Glostrub, Denmark). After dewaxing, the antigenic retrieval was performed using citrate buffered (pH 6) or EDTA buffered (pH 9) antigenic retrieval solution at 99 °C in a warm bath (EnVision Flex Target Retrieval solutions with a high and low pH, Dako). Endogenous peroxidase was inhibited

Antibodies	Clone	Abbreviation	Manufacture	Dilution	Retrievial	Incubation (minutes)
EGFR wild-type	DAK-H1-WT	EGFR	Dako	1: 200	pH9	30
MUC1-ter C	ARP41446	MUC1-CT	Aviva Syst. Biology	1: 400	pH9	60
α- Estrogen receptor	SP1	ER	Dako	RTU	pH9	20
Pregesteron receptor	PgR636	PR	Dako	RTU	pH9	20
HER2	c-ErB2	HER2	Dako	1: 800	pH6	30
LC3b	poly	LC3b	Abcam	1: 400	pH6	60
IL17a	poly	IL17A	Abcam	1: 800	pH6	60
IL17RA	49M4D2	IL17RA	Clniscience	1: 800	pH6	60
IL17RB	97C691	IL17RB	Cliniscience	1: 40	pH6	60

Table 1. Primary antibodies, dilution, antigenic retrieval, incubation times and abbreviations used in this study.

with a hydrogen peroxide phosphate buffered solution (EnVision Flex Peroxidase Blocking Reagent, Dako). After incubating with the primary antibodies, the immunological reaction was revealed by a polymer dextran coupled with the secondary antibody and peroxidase for 15 min (EnVision Flex HRP, Dako) and diaminobenzidine for 10 minutes (EnVision DAB+ chromogen, Dako). Counterstaining was performed with hematoxylin for 10 min (EnVision Flex hematoxylin, Dako). Negative controls were obtained using mouse or rabbit IgG1 (Universal Negative Control Mouse or Universal Negative Control Rabbit, Dako) instead of the primary antibodies for each culture. No specific signal was observed. The primary antibodies, dilutions and antigenic retrieval are described in Table 1 (Table 1).

Immunostaining quantification. The staining results were evaluated by C.G. and C.M. Only LCB3 was quantified and is expressed as the mean and SD of the cytoplasmic dots signals (autophagosomes) in 100 cells at 100x magnification (Fig. 1). Other immunohistochemical staining was evaluated as positive or negative.

Statistics. The results are expressed as the means and standard error. Mann-Whitney tests were performed. A p-value <0.05 was considered significant. The WinSTAT® version 2012 (Fitch Software, Bad Krozinger, Germany) and Excel 2013 (Microsoft Corp., Redmond, Washington U.S.A.) programs were used for the statistical analysis.

References

1. Perou, C. M. Molecular stratification of triple-negative breast cancers. *Oncologist.* **16**, 61–70 (2011).
2. Goldhirsch, A. *et al*. Panel embers. Personalizing the treatment of women with early breast cancer: highlights of the St Gallen International Expert Consensus on the Primary Therapy of Early Breast Cancer 2013. *Ann Oncol.* **24**, 2206–23 (2013).
3. Baselga, J. *et al*. Randomized phase II study of the anti-epidermal growth factor receptor monoclonal antibody cetuximab with cisplatin versus cisplatin alone in patients with metastatic triple-negative breast cancer. *J Clin Oncol.* **31**, 2586–92 (2013).
4. Lehmann, B. D. & Pietenpol, J. A. Identification and use of biomarkers in treatment strategies for triple-negative breast cancer subtypes. *J Pathol.* **232**, 142–50 (2014).
5. Joensuu H. *et al*. Adjuvent Capecitabine in combinaison with Docetaxel, Epirubicin, and cyclophosphamide for early breast cancer: the randomized clinical finXX trial. *JAMA Oncol*. (2017).
6. He, C. & Klionsky, D. J. Regulation mechanisms and signaling pathways of autophagy. *Annu Rev Genet.* **43**, 67–93 (2009).
7. Sui, X. *et al*. Autophagy and chemotherapy resistance: a promising therapeutic target for cancer treatment. *Cell Death Dis.* **10**(4), e838 (2013).
8. Baruch, A. *et al*. Preferential expression of novel MUC1 tumor antigen isoforms in human epithelial tumors and their tumor-potentiating function. *Int J Cancer.* **71**, 741–9 (1997).
9. Joshi, M. D. *et al*. MUC1 oncoprotein is a druggable target in human prostate cancer cells. *Mol Cancer Ther.* **8**, 3056–65 (2009).
10. Rubinstein, D. B. *et al*. MUC1/X protein immunization enhances cDNA immunization in generating anti-MUC1 alpha/beta junction antibodies that target malignant cells. *Cancer Res.* **66**, 11247–53 (2006).
11. Bafna, S., Kaur, S. & Batra, S. K. Membrane-bound mucins: the mechanistic basis for alterations in the growth and survival of cancer cells. *Oncogene.* **29**, 2893–904 (2010).
12. Raina, D., Kharbanda, S. & Kufe, D. The MUC1 oncoprotein activates the anti-apoptotic phosphoinositide 3-kinase/Akt and Bcl-xL pathways in rat 3Y1 fibroblasts. *J Biol Chem.* **279**, 20607–12 (2004).
13. Yin, L., Kharbanda, S. & Kufe, D. MUC1 oncoprotein promotes autophagy in a survival response to glucose deprivation. *Int J Oncol.* **34**, 1691–9 (2009).
14. Bitler., B. G., Goverdhan, A. & Schroeder, J. A. MUC1 regulates nuclear localization and function of the epidermal growth factor receptor. *J Cell Sci.* **123**, 1716–23 (2010).
15. Kufe, D. W. MUC1-C oncoprotein as a target in breast cancer: activation of signaling pathways and therapeutic approaches. *Oncogene.* **32**, 1073–81 (2013).
16. Dharmaraj, N., Engel, B. J. & Carson, D. D. Activated EGFR stimulates MUC1 expression in human uterine and pancreatic cancer cell lines. *J Cell Biochem.* **114**, 2314–22 (2013).
17. Lau, S. K. *et al*. EGFR-mediated carcinoma cell metastasis mediated by integrin αvβ5 depends on activation of c-Src and cleavage of MUC1. *PLoS One.* **7**, e36753 (2012).
18. Cochaud, S. *et al*. IL-17A is produced by breast cancer TILs and promotes chemoresistance and proliferation through ERK1/2. *Sci Rep.* **3**, 3456 (2013).
19. Mombelli, S. *et al*. IL-17A and its homologs IL-25/IL-17E recruit the c-RAF/S6 kinase pathway and the generation of pro-oncogenic LMW-E in breast cancer cells. *Sci Rep.* **5**, 11874 (2015).
20. Merrouche, Y. *et al*. IL-17E synergizes with EGF and confers *in vitro* resistance to EGFR-targeted therapies in TNBC cells. *Oncotarget.* **7**, 53350–61 (2016).
21. Garbar, C. *et al*. Autophagy is decreased in triple-negative breast carcinoma involving likely the MUC1-EGFR-NEU1 signalling pathway. *Int J Clin Exp Pathol.* **8**, 4344–55 (2015).

22. Zhou, Y., Wu, P. W., Yuan, X. W., Li, J. & Shi, X. L. Interleukin-17A inhibits cell autophagy under starvation and promotes cell migration via TAB2/TAB3-p38 mitogen-activated protein kinase pathways in hepatocellular carcinoma. *Eur Rev Med Pharmacol Sci.* **20**, 250–63 (2016).
23. Lefort, S. *et al.* Inhibition of autophagy as a new means of improving chemotherapy efficiency in high-LC3B triple-negative breast cancers. *Autophagy.* **10**, 2122–42 (2014).
24. Sivaprasad, U. & Basu, A. Inhibition of ERK attenuates autophagy and potentiates tumour necrosis factor-alpha-induced cell death in MCF-7 cells. *J Cell Mol Med.* **12**, 1265–71 (2008).
25. Shen P. *et al.* Inhibition of ERα/ERK/P62 cascades induces "autophagic switch" in the estrogen receptor-positive breast cancer cells exposed to gemcitabine. *Oncotarget*. **7**, 01–48516 (2016).
26. Chen, M. *et al.* The cytoprotective role of gemcitabine-induced autophagy associated with apoptosis inhibition in triple-negative MDA-MB-231 breast cancer cells. *Int J Mol Med.* **34**, 6–82 (2014).
27. Yin, L., Kharbanda, S. & Kufe, D. MUC1 oncoprotein promotes autophagy in a survival response to glucose deprivation. *Int J Oncol.* **34**, 1691–9 (2009).
28. Hiraki, M. *et al.* MUC1-C Stabilizes MCL-1 in the Oxidative Stress Response of Triple-Negative Breast Cancer Cells to BCL-2 Inhibitors. *Sci Rep.* **6**, 26643 (2016).
29. Uchida, Y., Raina, D., Kharbanda, S. & Kufe, D. Inhibition of the MUC1-C oncoprotein is synergistic with cytotoxic agents in the treatment of breast cancer cells. *Cancer Biol Ther.* **14**, 127–34 (2013).
30. Raina, D., Kharbanda, S. & Kufe, D. The MUC1 oncoprotein activates the anti-apoptotic phosphoinositide 3-kinase/Akt and Bcl-xL pathways in rat 3Y1 fibroblasts. *J Biol Chem.* **279**, 20607–12 (2004).

Author Contributions

C.G. and A.B. designed and supervised the study and wrote the manuscript text and figures. C.M. and C.G. performed the experiments. All authors reviewed the manuscript (C.G., A.B., Y.M., J.G.).

Additional Information

Competing Interests: The authors declare that they have no competing interests.

Publisher's note: Springer Nature remains neutral with regard to jurisdictional claims in published maps and institutional affiliations.

iv. Les altérations de la sialylation de MUC1 et EGFR et les cellules T cytotoxiques.

But du travail :

Dans le cancer, l'activation, quasi spécifique, des enzymes de sialylisation modifie ces glycoprotéines de surface qui deviennent hypoglycosylées par l'ajout de résidus d'acide sialique. La ST6GalNac-I est spécifique de MUC1-N (sTn), ST6Gal-I et II ont des substrats moins spécifiques, dont l'EGFR.

La présence d'acide sialique en surface des cellules est connue pour interagir avec les cellules T cytotoxiques (CTL), par le biais des siglecs et des interleukines.

Question posée : **« quelle est la relation entre les CTL et la sialylation des macromolécules membranaires ? »**

Matériel et Méthode :

Un TMA est utilisé sur du matériel FFPE de 39 LUM, 13 HER2 et 47 TN.

Des examens immunohistochimiques sont réalisés : ST6GalNac-I, ST6Gal-I, ST6Gal-II, CD4, CD8 et Granzyme-B (NK).

Résultats :

On confirme que les CTL sont significativement plus fréquents dans les TN et HER2 par rapport aux LUM.

Concernant les sialyltransférases, les TN expriment moins ST6Gal-I que les LUM ou les HER2 ($p<0.001$). STGalNac-I est moins secrété dans les LUM que dans les TN ou HER2 ($p=0.002$ et $p=0.02$). (figures 21 à 23)

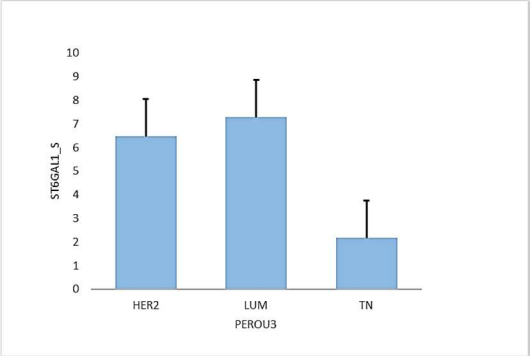

FIGURE 21 : Expression de ST6Gal1 dans les trois groupes de tumeur de sein. P est significatif entre TN et LUM ou HER2

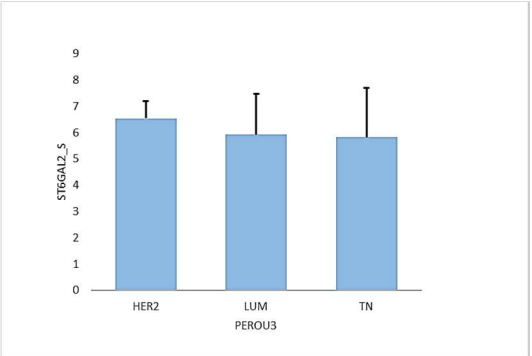

FIGURE 22 : Expression de ST6Gal2 dans les trois groupes de tumeur de sein. Absence de différence significative.

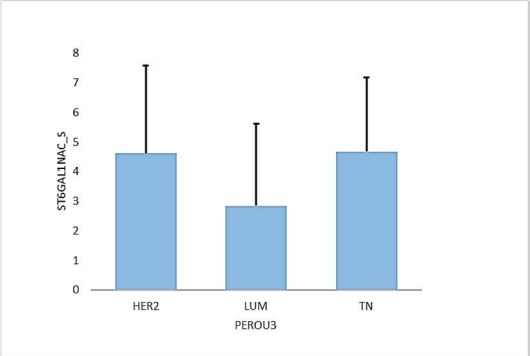

FIGURE 23: Expression de ST6GalNac1 dans les trois groupes de tumeur de sein. P est significatif entre TN et HER2 ou LUM.

Concernant la relation entre les sialyltransférases et les CTL, dans les HER2, on observe une association inverse entre ST6Gal-I et la présence de CTL. (figure 24)

Dans les TN, on observe une corrélation positive enter ST6Gal-II ou ST6GalNac-I et la présence de CTL. (figure 26) Aucune corrélation n'est observée dans les LUM.

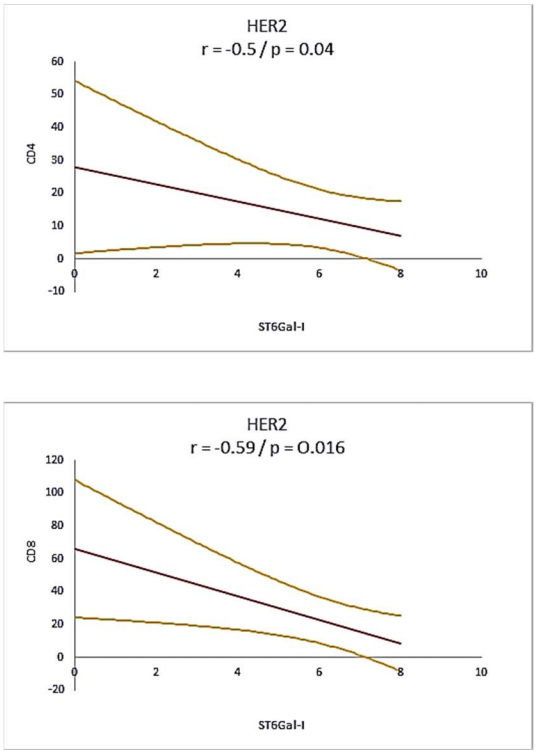

FIGURE 24 : Corrélation inverse entre ST6Gal-I et les CTL dans les HER2

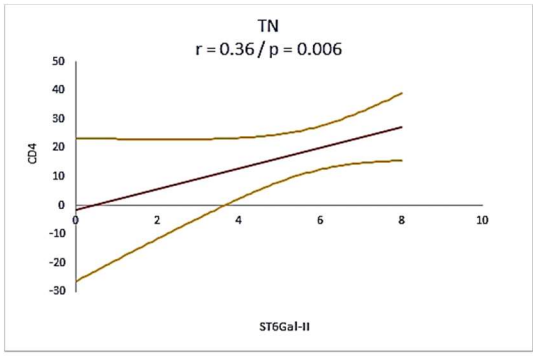

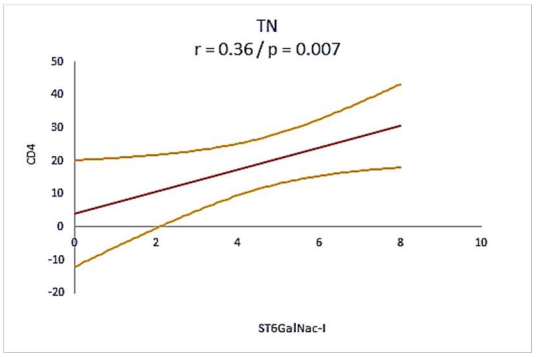

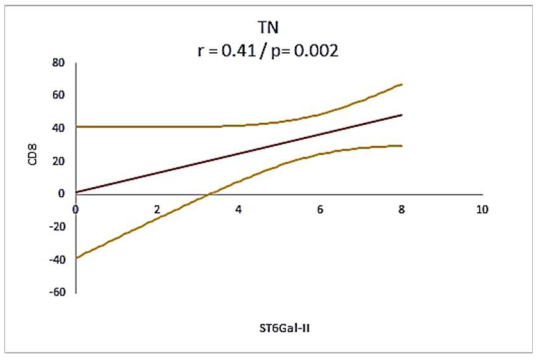

FIGURE 251 : Corrélation positive entre ST6Gal-II ou ST6GalNac-I et les CTL dans les TN

Conclusion :

Nos résultats illustrent que l'infiltrat immunitaire varie d'un type de tumeur à l'autre. Aussi, il est probable que la stratégie de défense est dirigée par la cellule tumorale elle-même. L'un des mécanismes possibles serait la modification de la charge d'acide sialique présente à la surface des glycoprotéines ou des glycolipides de membrane cellulaire.

En effet, comme le montre nos résultats, l'augmentation des lymphocytes intratumoraux pourrait être modulée par la sialylation principalement dans les HER2 surexprimés et les TN (EGFR positifs), suggérant que la charge d'acide sialique des récepteurs de croissance épithélial (ErbB) peut influencer la réponse lymphocytaire T intratumorale. L'intermédiaire serait les récepteurs spécifiques de reconnaissance de l'acide sialique présent sur les cellules immunes (SIGLECs).

Plusieurs travaux de la littérature illustrent une relation entre les sialyltransférases, et la résistance aux agents de chimiothérapie. Curieusement, les

lymphocytes intratumoraux sont également connus comme l'un des facteurs prédictifs de la réponse à la chimiothérapie, appuyant notre hypothèse de l'association de la charge des acides sialiques et des lymphocytes intratumoraux.

Notons que pour la première fois, nous avons décrit l'expression de ST6gal-II dans les cancers du sein provenant de matériel humain. Cette enzyme a démontré des effets associés aux cytokines pro-inflammatoires dans des cellules en culture, suggérant son implication sur la modulation du microenvironnement.

Enfin, des traitements basés sur des inhibiteurs des enzymes de sialylation sont déjà en étude et pourront être utilisés, dans un avenir proche comme cibles thérapeutiques.

Cancer Management and Research

Dovepress
open access to scientific and medical research

Open Access Full Text Article

ORIGINAL RESEARCH

Triple-negative and HER2-overexpressing breast cancer cell sialylation impacts tumor microenvironment T-lymphocyte subset recruitment: a possible mechanism of tumor escape

Christian Garbar[1,2]
Corinne Mascaux[1,2]
Yacine Merrouche[1,2]
Armand Bensussan[3]

[1]Biopathology Department, Institut Jean Godinot – Unicancer, Reims, France; [2]DERM-I-C EA7319, Université de Reims Champagne – Ardenne, Reims, France; [3]INSERM U976; Université Paris Diderot, Sorbonne Paris Cité, Laboratory of Immunology, Dermatology & Oncology, Paris, France

Introduction: Breast cancers develop different patterns of sialylation to modulate their tumor-infiltrating lymphocyte (TIL) environment. We studied the relationship between α-2,6 sialyltransferases and the TIL in different breast cancer molecular subgroups.

Materials and methods: Immunohistochemical preparations were made from 39 luminal (LUM), 13 human epidermal growth factor receptor 2-overexpressing (HER2) and 47 triple-negative (TN) breast carcinomas. Targeted proteins included ST6Gal-I, ST6Gal-II, ST6GalNac-I, CD8, CD4 and granzyme-B in both cytotoxic T lymphocytes and NK lymphocytes (CTL/NK).

Results: CTL/NK populations were significantly more frequent in TN than LUM (P <0.001). TN showed a lower level of ST6Gal-I expression than LUM or HER2 (both P > 0.001). ST6GalNac-I expression was lower in LUM than in TN or HER2 (P = 0.002 and P = 0.02, respectively). In HER2, a significant association was found between a low level of ST6Gal-I expression and a high TIL level. In TN, a significant association was observed between a high level of ST6Gal-II expression and a high TIL level.

Conclusion: An increase in infiltrating lymphocytes could be influenced by low expression of ST6Gal-I in HER2 and by high expression of ST6Gal-II in TN breast cancers. Thus, targeting these sialylation pathways could modulate the levels of TIL.

Keywords: breast, carcinoma, sialyltransferase, triple-negative, HER2

Introduction

To date, the molecular classification of breast cancers (BCs) proposed by Perou et al has been categorized according to the targeted therapy against these tumors. These authors have described three main molecular subtypes: luminal (LUM) BCs that express hormonal estrogen and progesterone receptors (ER+ and PR+) but no human epidermal growth factor receptor 2 (HER2), overexpressed HER2 BC (HER2; phenotype: ER±PR±HER2+) and triple-negative (TN; phenotype: ER /PR /HER2).[1]

It is now well established that tumor-infiltrating lymphocytes (TILs) play an important role in chemotherapy and that their stimulation or inhibition can influence the tumor therapeutic response and patient prognosis.[2,3] However, cell interactions between cancer cells and the TIL are complex, and our present knowledge represents only the tip of the iceberg. One of these intercellular communication mechanisms

Correspondence: Christian Garbar; Armand Bensussan
Biopathology Department, Institut Jean Godinot – Unicancer, 1 rue du Général Koenig CS80014, 51726 Reims, France.
Tel: +33 326504267
Email: christian.garbar@reims.unicancer.fr; corinne.garbar-mascaux@reims.unicancer.fr

submit your manuscript | www.dovepress.com
Dovepress
http://dx.doi.org/10.2147/CMAR.S162932

likely consists of changes to the cytoplasmic membrane, particularly in glycoproteins. In cancer cells, the most important glycoprotein alteration is sialylation.[4]

Sialylation consists of adding sialic acids (Sia) on an *N*- or *O*-linked glycoprotein. Sialylation is regulated by a balance of two enzyme families: the sialyltransferases, which add Sia, and the sialidases (or the neuraminidases, Neu), which remove Sia. Sialyltransferases are a family of ~20 different enzymes linking Sia to a galactose (Gal) in an α-2,3 position (ST3Gal)or an α-2,6 position (ST6Gal) or to an *N*-acetylgalactosamine (ST6GalNac). The third sialyltransferase family (ST8) promotes α-2,8 linkage. Four sialidases remove Sia residues: Neu1, localized in lysosomes and the cell surface; Neu2 or Neu4, located in the cytosol and Neu3, located in the cell membrane.[5]

Alpha-2,6 sialylation is the most commonly observed sialylation mechanism in tumor cells and is associated with an upregulation of both ST6Gal-I and ST6GalNac-I sialyltransferases.[6] Two of the most well-characterized substrates of these sialyltransferases are MUC1 and EGFR. Moreover, Wreschner et al demonstrated an association between MUC1 and EGFR.[7] Interestingly, Lillehoj et al suggested that both glycoproteins could be associated with Neu, one of the desialylation enzymes.[8] These authors suggested that Neu1 could regulate EGFR and MUC1 signaling.[7,8] We recently demonstrated that Neu1 and MUC1 have reduced expression in TN compared to LUM tumors, and that EGFR is more expressed in TN than LUM tumors, suggesting that the EGFR-MUC1-Neu1 molecular pathway is complex.[9] Intriguingly, in breast cancer, EGFR has been observed to be highly sialylated, and these changes have been shown to influence its metabolic activities and induce chemoresistance.[10]

Here, we investigated whether TILs and malignant cell sialylation were associated, and we discussed the possibility that this plays a role in the development of resistance to chemotherapy or targeted therapy.

To understand the α-2,6-sialylation pathway and its relationship with TIL, we determined the expression of three α-2,6-sialylidases (ST6Gal-I, ST6Gal-II and ST6GalNac-I), as well as their relationship with different TIL subsets, including CD4, CD8 and CTL/NK cells (granzyme B-positive cells; cytotoxic T/natural killer lymphocytes, respectively), in different molecular breast cancer groups.

Materials and methods

Patient population

Archival paraffin-embedded surgical material and clinical data from 99 women presenting with breast cancer were available for this study. All cases were classified according to immunohistochemical classification by means of a preliminary immunohistochemical study and subsequent confirmation by tissue microarray (TMA). Our data set included 39 luminal carcinomas (LUM, age = 59.3 ± 12.9 years), 13 HER2 over-expressing carcinomas (HER2, age = 58.1 ± 13.1 years) and 47 TN carcinomas (age = 61.7 ± 14.5 years, P = ns). No neo-adjuvant chemotherapy was performed.

This study was performed with the approval of the local ethics committee (Centre de Resources Biologiques de l'Intitut Jean Godinot) and conformed to the Declaration of Helsinki. Written informed consent was provided by all participants and all patients were informed and agreed to contribute to this study.

Histological procedures and Tissue Micro Array (TMA) construction

All surgical specimens were initially fixed in 4% buffered formaldehyde solution for 8–48 h, then embedded in paraffin and cut into 4-µm-thick sections. From these archival formaldehyde/paraffin blocks, we built a TMA to receive a paraffin block to perform all immunohistochemical studies. We used an automated TMA device, Minicore2 (Excilone, Elancourt, France) associated with a needle core 0.6 mm in diameter. We chose 3 distant core needle samples of each donor tumor paraffin block.

Immunohistochemical methods

Immunohistological staining was performed with a Dako Autostainer Link 48® immunostaining system (Dako Denmark A/S, Glostrup, Denmark). After dewaxing, antigenic retrieval was performed using citrate-buffered (pH 6) or EDTA-buffered (pH 9) antigenic retrieval solution at 99°C in a warm bath (EnVision Flex Target Retrieval solutions, high and low pH, Dako). Endogenous peroxidase was inhibited with a hydrogen peroxide phosphate-buffered solution (EnVision Flex Peroxidase Blocking Reagent, Dako). After incubation with the primary antibodies (ST6Gal-I – rabbit polyclonal, dilution 1:400, pH 6, Cliniscience®; ST6Gal-II – rabbit polyclonal, dilution 1:300, pH 6, Cliniscience®; ST6GalNac-I – rabbit polyclonal, dilution 1:500, pH 6, Novus®; CD4 – 4B12 clone, RTU, pH 9, Dako®; CD8 – C8/144B clone, RTU, pH 9, Dako®, and Granzyme B – GrB-7 clone, dilution 1:20, pH 9, Dako®), the immunological reaction was detected with a polymer dextran coupled with secondary antibody and peroxidase for 15 min (EnVision Flex HRP, Dako) and diaminobenzidine for 10

min (EnVision DAB + chromogen, Dako). Counterstaining was performed with hematoxylin for 10 min (EnVision Flex hematoxylin, Dako). Negative controls were obtained using mouse or rabbit IgG1 (Universal Negative Control Mouse or Universal Negative Control Rabbit, Dako) diluted 1:100, in place of the primary antibodies. MDA-MB231 and MCF7 breast cancer culture cells were known to express ST6Gal-I, ST6Gal-II and ST6GalNac-I.[11] From MDA-MB231 and MCF7 cells, we performed cell blocks as positive controls. Methods were previously described.[12]

Immunostaining quantification

The staining results were evaluated by CG and CM based on the intensity and percentage of staining tumor cells, and agreement was reached.

The parametric results were edited as a score by the addition of intensity (0 = none, 1 = weak, 2 = intermediated, 3 = strong) and the percentage of tumor cells (0 = none, 1 = 1%, 2 = 2% to 10%, 3 = 11% to 33%, 4 = 34% to 66% and 5 > 66% to 100%). The range of scores was 0 to 8. Nonparametric results were calculated as positive for a score >5.

Lymphocytes were counted in one hot spot of lymphocytes close to the tumor cells in a high-power field (HPF) and expressed as the number per HPF (400 magnification).

Statistics

The results were expressed as means and standard error. Mann–Whitney and Spearman's correlation rank tests were performed. A *P*-value <0.05 was considered significant. WinSTAT® version 2012 (Fitch Software, Bad Krozinger, Germany) and Excel 2013 (Microsoft Corporation, Redmond, WA, USA) programs were used for statistical analysis.

Results

TIL subsets in BCs

We first determined the molecular subtypes of BC TIL subsets, including CD4, CD8 and CTL/NK (granzyme B-positive) (Figure 1). The results reveal that cytotoxic lymphocytes were significantly increased in TN compared to LUM (LUM = 1.5 ± 2.2; HER2 = 4.8 ± 7.5 and TN = 9.6 ± 9.9 lymphocytes/HPF; *P* <0.0001 only for LUM versus TN). Although no statistically significant increase in CD4 (LUM = 18.4 ± 9.5; HER2 = 11.1 ± 15.0 and TN = 14.4 ± 16.6 lymphocytes/HPF) or CD8 (LUM = 22.5 ± 23.1; HER2 = 19.5 ± 27.6 and TN = 28.7 ± 28.5 lymphocytes/HPF) was observed in all molecular BC subgroups, we noted that CD8 was the predominant T-cell population.

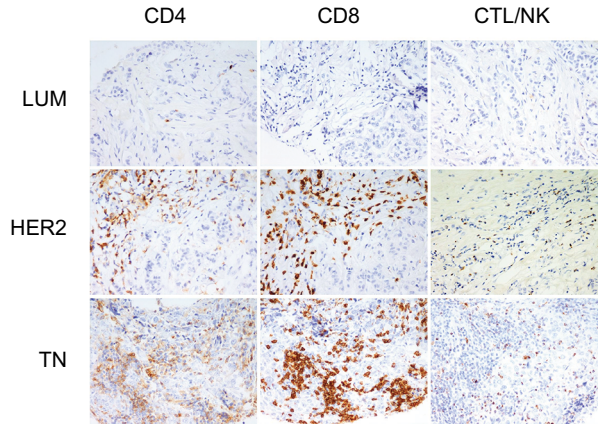

Figure 1 Tumor-infiltrating lymphocyte (TIL) subsets in different breast cancer groups.
Notes: CD4, CD8 and granzyme-B peroxidase-positive immunohistochemical staining in LUM, HER2 and TN breast cancers: LUM shows a low TIL level in comparison with HER2 or TN. CD8 is the predominant T-cell population. LUM, HER2 and TN are the same case of Figure 2. (200 magnification).
Abbreviations: LUM, luminal; HER2, human epidermal growth factor receptor 2; TN, triple negative; CTL/NK; cytotoxic T lymphocytes/natural killer lymphocytes.

Correlation between TIL and ST6Gal-I

We next evaluated whether ST6Gal-I influenced the TILs in different BCs (Figures 2 and 3). We found that ST6Gal-I expression was significantly lower in TN than in LUM or HER2 (TN: 2.1 ± 3.0 versus LUM: 7.2 ± 0.99, *P* <0.0001 and TN versus HER2: 6.4 ± 2.3, *P* <0.0001). Concerning TILs, low levels of ST6Gal-I were correlated with an increase in all lymphocytes subsets only for HER2, with no changes observed in LUM or TN. Only in HER2, Spearman's correlations were statistically positive and inverse between ST6Gal-I and CD4 ($r = -0.5$; $P = 0.04$) or CD8 ($r = 0.59$; $P = 0.016$). We conclude that ST6Gal-I plays an important role in HER2 and negatively influences the TIL. Consequently, overexpression of ST6Gal-I in HER2 led to reduced TILs.

Correlation between TILs and ST6Gal-II

We next characterized ST6Gal-II and found that its expression was similar in all 3 BC groups (LUM: 5.9 ± 1.5; HER2: 6.6 ± 0.6; TN: 5.8 ± 1.8; *P* = ns) (Figures 2 and 4). Concerning the amount of TILs, we noted that a low expression level of ST6Gal-II was significantly correlated with a decrease in TILs, mainly in the TN group. Only in TN, Spearman's correlations were statistically positive between ST6Gal-II and CD4 ($r = 0.36$; $P = 0.006$) or CD8 ($r = 0.41$; $P = 0.0026$) or CTL ($r = 0.28$; $P = 0.02$).

To our knowledge, this is the first time that ST6Gal-II has been described, in situ, in BC.

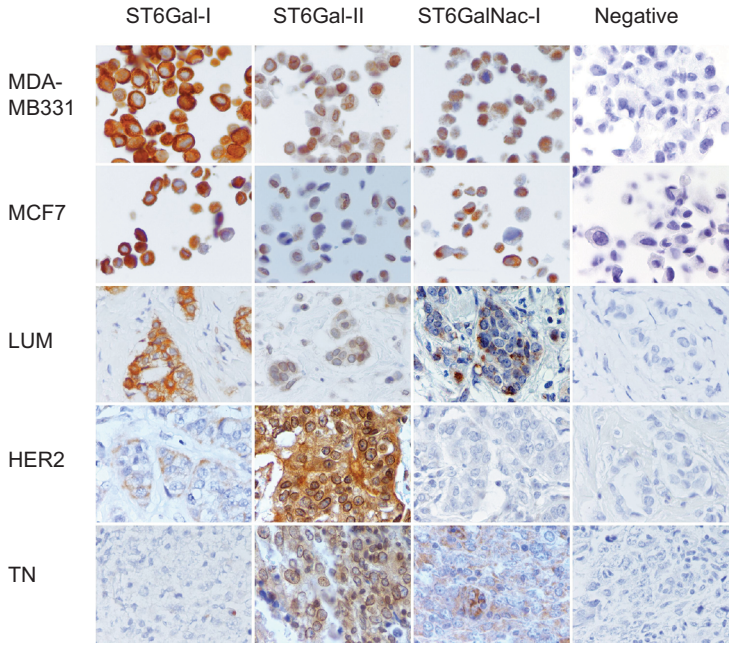

Figure 2 Immunohistochemical expression of ST6Gal-I, ST6Gal-II and ST6GalNac-I.
Notes: Peroxidase-positive immunohistochemical staining in breast carcinomas: MDA-MB231 and MCF7 controls are positive for ST6Gal-I, ST6Gal-II and ST6GalNac-I. ST6Gal-I presents a high expression level in LUM. ST6Gal-II and shows a high expression in TN and HER2. ST6GalNac-I is expressed more in TN. ST6Gal-I shows diffuse cytoplasmic expression, ST6Gal-II shows diffuse cytoplasmic and perinuclear expression and ST6GalNac-I shows granular cytoplasmic positivity. LUM, HER2 and TN are the same case of Figure 1. Negative controls were performed with IgG1 negative control mouse or rabbit (Dako®) (400 magnification).
Abbreviations: LUM, luminal; HER2, human epidermal growth factor receptor 2; TN, triple negative; IgG1, immunoglobulin G1.

Correlation between TILs and ST6GalNac-I

ST6GalNac-I is the enzyme associated with the sialylation of Thomsen-nouvelle antigen (Tn), which is localized on the external glycosylated region of MUC1-VNTR (Figures 2 and 5).[13] In our previous study, we demonstrated increased expression of MUC1 in LUM compared to TN.[9] Here, we observed a difference in expression between LUM and HER2 BCs (2.8 ± 2.7 versus 4.6 ± 2.9, respectively; $P = 0.02$) and TN (4.6 ± 2.5 respectively; $P = 0.002$). However, we found only a Spearman's correlation between ST6GalNac-I and CD4 for TN ($r = 0.36$; $P = 0.007$), suggesting that modulation of this sialylation pathway of MUC1 is not sufficient to have influence on TILs.

Discussion

Sialylation of tumor cells is complex, involving numerous enzymes that play a major role in oncogenesis and associated processes, such as adhesion, migration, apoptosis and receptor regulation. However, this mechanism of sialylation is not well studied, likely due to the absence of sufficient laboratory tools or complicated investigation techniques. To date, immunohistochemistry, which is used in the present study, is still the primary investigational method of choice.[5]

Here, we evaluated the relationship between α-2,6 sialylation and intratumoral T-cell lymphocytes. We found that sialylation could modulate the TILs and that this cell signaling pattern was altered depending on the molecular signature of the BC. Our observations appear particularly relevant in TN for ST6Gal-II and in HER2 for ST6Gal-I.

Moreover, clinical practice has previously described the importance of TILs in the prognosis or therapeutic response of breast cancers. TILs are heterogeneous lymphocyte subsets that are highly variable in different BC subgroups. Previously, TN and HER2 were found to exhibit increased TILs, which were correlated with better overall survival and better chemotherapeutic responses.[2,14,15]. Interestingly, we also observed that ST6Gal-I and ST6Gal-II influenced TILs only in HER2 and TN tumors.

Therefore, we propose that the sialyl charge of the membrane glycoproteins could regulate the immune response. First, ST6Gal-I and ST6Gal-II are involved in the α-2,6 sialylation of numerous cell membrane glycoproteins, including EGFR, CD45, β1 integrin, PECAM, Fas and immunoglobulin.[16] Second, it has been shown in B16 murine melanoma cell cultures that hypersialylation influences tumor growth and immune escape by alteration of T-cell activity, particularly NK cells, by inhibition of

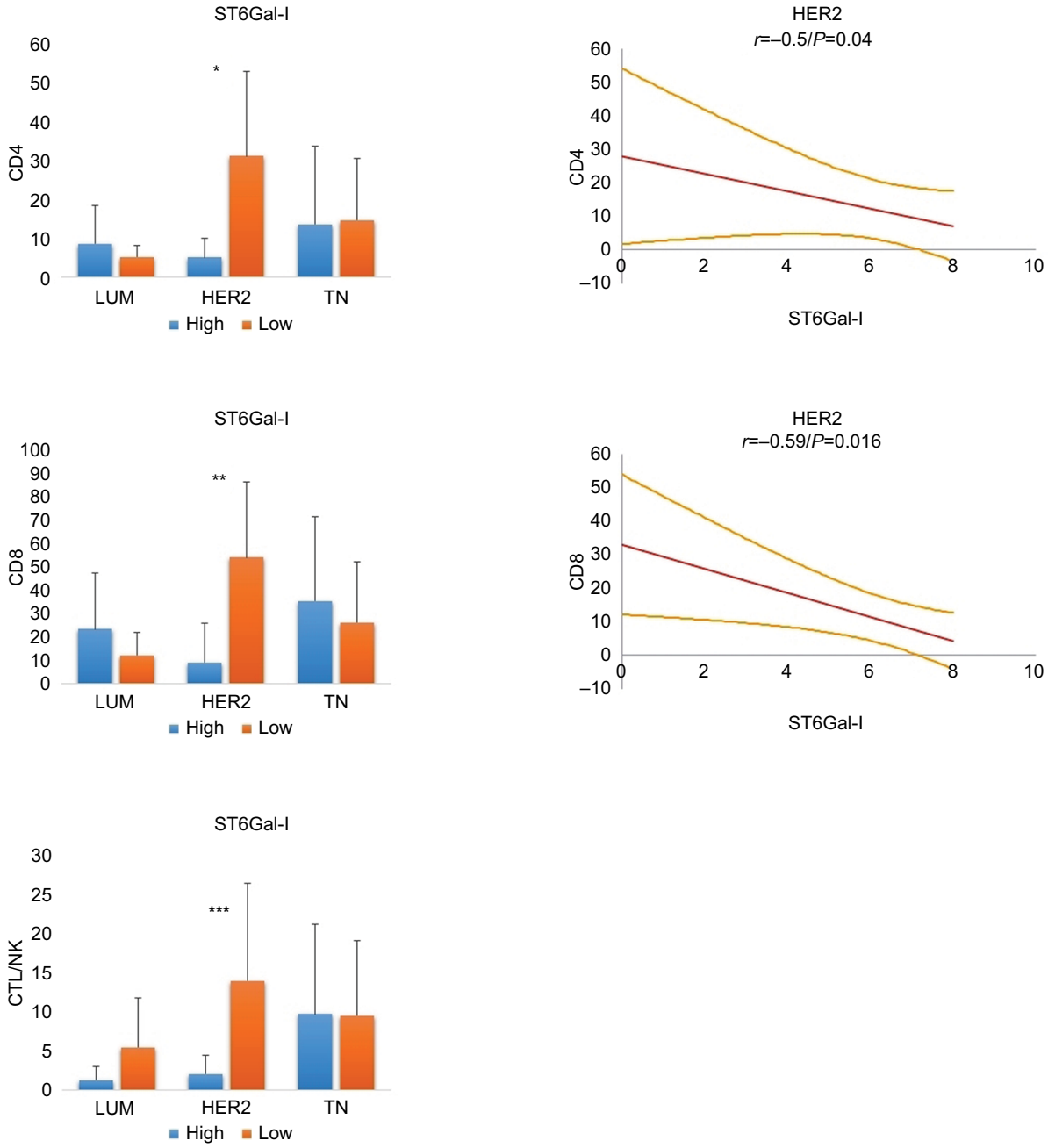

Figure 3 Relationship between ST6Gal-I and TILs in different breast cancer subtypes.

Notes: In HER2 tumors, low levels of ST6Gal-I are correlated with an increase in all lymphocyte subsets (*CD4: $P = 0.01$; **CD8: $P = 0.02$; ***CTL/NK: P = ns). On the right, statistical negative Spearmen's correlations are documented for CD4 and CD8 positive T lymphocytes in HER2 breast carcinoma (regression line and 95% CI). For LUM and TN, we found no significant correlation. We conclude that high expression of ST6Gal-I in HER2 leads to reduced TILs.

Abbreviations: TILs, tumor-infiltrating lymphocytes; HER2, human epidermal growth factor receptor 2; CTL/NK; cytotoxic T lymphocytes/natural killer lymphocytes; LUM, luminal; TN, triple negative; ns, not significant.

DC maturation.[17] Sialylation has also been associated with other immune mechanisms, such as the sialic acid-binding immunoglobulin-like lectins (siglecs), which are a family of receptors linking cancers cells to immune cells. Moreover, Hudak et al[16] demonstrated that increasing global sialylated glycans on cancer cells inhibit human NK activation through the recruitment of siglec.[6,18]

Finally, ST6GalNac-I is an enzyme associated with the sialylation of Tn antigen localized on the external glycosylated region of MUC1-VNTR.[13] Moreover, sialyl-Tn is known

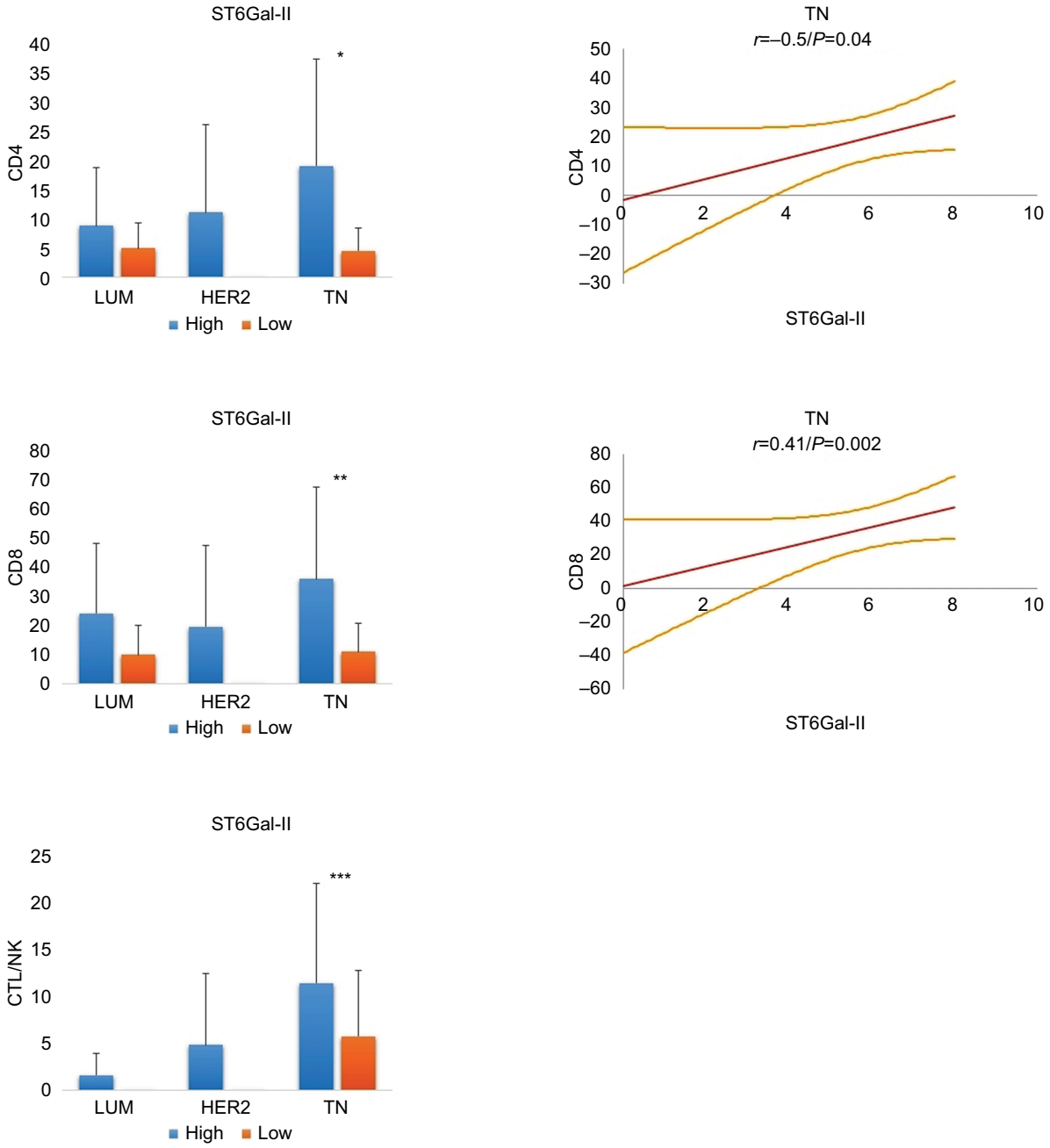

Figure 4 Relationship between ST6Gal-II and TILs in different breast cancer subtypes.

Notes: In TN, low levels of ST6Gal-II are significantly correlated with a decrease in lymphocyte subsets (*CD4: $P = 0.01$; **CD8: $P = 0.004$; ***CTL/NK: P = ns). On the right, statistical positive Spearmen's correlations are documented for CD4 and CD8 positive T lymphocytes in TN breast carcinoma (regression line and 95% CI). For LUM and HER2, we found no significant correlation. We conclude that a loss of expression of ST6Gal-II in TN leads to reduced TILs.

Abbreviations: TILs, tumor-infiltrating lymphocytes; TN, triple negative; CTL/NK; cytotoxic T lymphocytes/natural killer lymphocytes; LUM, luminal; HER2, human epidermal growth factor receptor 2; ns, not significant.

to play a role in the cellular immunologic regulation of tumor cells.[18] It has also been reported that aberrant glycosylation of MUC1 modulates the immunologic environment through the sialic acid and sialic acid-binding immunoglobulin-like lectin (siglec) pathway.[19,20] In our study, the relationship between ST6GalNac-I and TIL was not obvious, but the low levels of CTL/NKs in LUM or HER2, which broadly express MUC1 compared to TN (no significant difference between LUM and HER2, data not shown), suggest the loss of ST6GalNac-I sialylation activity due to the absence of MUC1 as a substrate. Similarly, EGFR, which is a substrate of ST6Gal-I and ST6Gal-II, is less expressed in LUM or HER2 tumors than

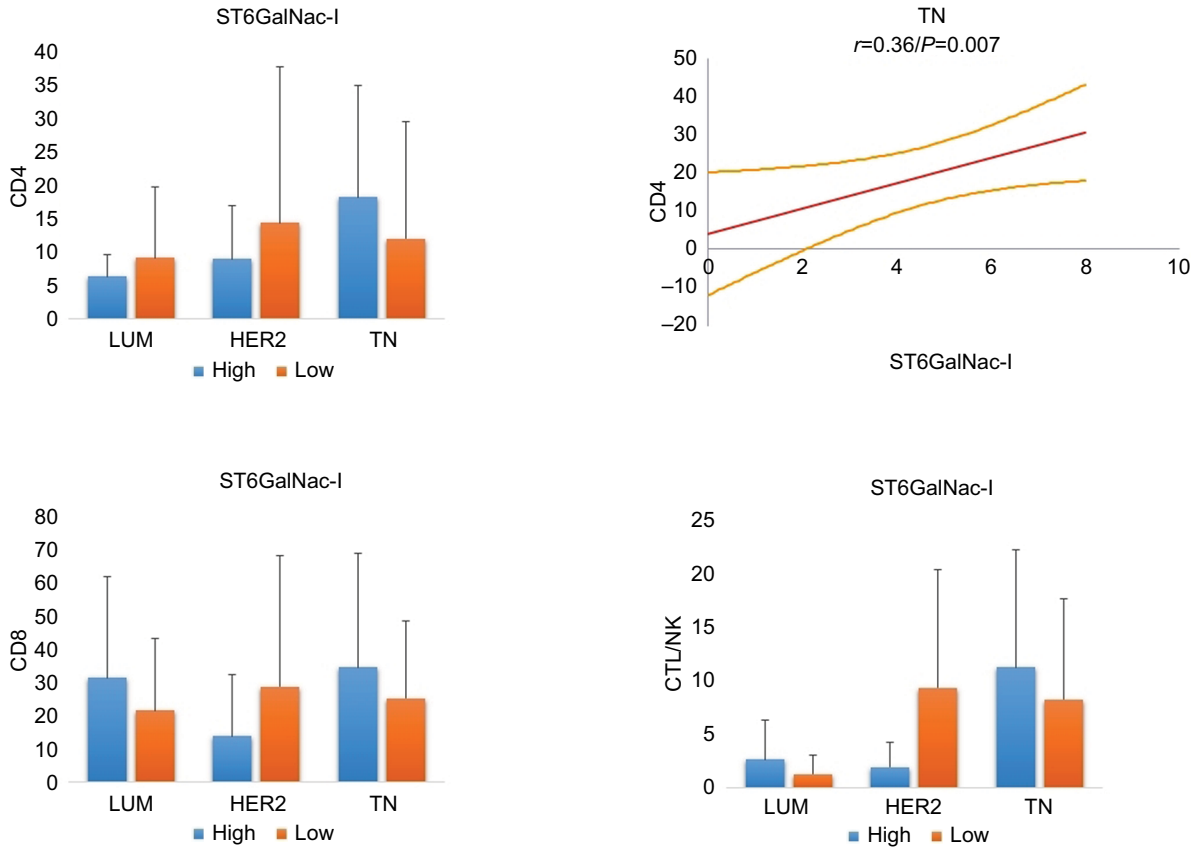

Figure 5 Relationship between ST6GalNac-I and TILs in different breast cancer subtypes.
Notes: On the right, statistical positive Spearmen's correlation is only documented for CD4 positive T lymphocytes in TN breast carcinoma (regression line and 95% CI). For ST6GalNac-I, no other significant correlation was observed, suggesting that ST6GalNac-I does not have a major effect on TILs.
Abbreviations: TN, triple negative; TILs, tumor-infiltrating lymphocytes; CTL/NK; cytotoxic T lymphocytes/natural killer lymphocytes.

in TN tumors (no significant difference between LUM and HER2, data not shown), which likely explains the different influences of these enzymes on TILs following molecular BC classification.[9,12] Other sialylated membrane glycoproteins or others sialylation enzymes could also be involved, such as ST3Gal or ST6GalNac-II, which also use MUC1 as a substrate.[21,22]

Concerning the relationship between therapeutic resistance or prognosis and sialyltransferases, the most studied enzyme in the literature is ST6Gal-I. Interestingly, in our series, we observed that the loss of ST6Gal-I was associated with a poor prognosis in TN (5-year disease-free survival: 91% for high expression versus 76% for low expression, $P = 0.04$; data no shown). Park et al demonstrated that loss of ST6Gal-I enhanced EGFR phosphorylation, which was also correlated with the sialylation of EGFR. These authors also showed that the overexpression of ST6Gal-I decreased the effects of gefitinib (an EGFR inhibitor).[10] Additionally, several authors have demonstrated the colocalization of MUC1 and EGFR at both the cell membrane and in the nucleus, involving internalization of EGFR and its activation.[23,24] Moreover, it is known that both MUC1 and EGFR show severe alterations of their glycosylation patterns, which are correlated with the tumor's capacity for metastasis.[25] It has been demonstrated that ST6Gal-I is associated with chemoresistance to docetaxel in hepatocarcinoma and to gemcitabine in pancreatic ductal adenocarcinoma.[26,27] Curiously, EGFR is also described as highly glycosylated, and its sialylation confers resistance to tyrosine kinase inhibitors in lung carcinoma cell lines.[28,29] To our knowledge, we report, for the first time, an inverse relationship between TILs and ST6Gal-I in HER2 tumors. As discussed, the high levels of TILs in HER2 tumors are associated with a good prognosis. However, MUC4, a highly glycosylated glycoprotein that can also be sialylated, is also associated with trastuzumab (an HER2 inhibitor) resistance.[30,31] Considering these observations, we hypothesize that the sialylation patterns of MUC1, EGFR and likely other membrane glycoproteins could serve as a

regulatory signal between TILs and the tumor cells and could be one of the pathways underlying therapeutic resistance.

To date, this is the first study to describe ST6Gal-II expression in human BC in situ. We demonstrated that ST6Gal-II is correlated with TILs in TN tumors. Only one additional report, in bovine breast epithelial cell cultures, has found that ST6Gal-II stimulates pro-inflammatory cytokines, particularly IL-6, known to be active in BCs, therefore suggesting that sialyltransferases could play an important role in the tumor immune microenvironnment.[32] In human bronchial mucosa and pancreatic cancer cell lines, IL-6 has been shown to increase the expression of ST6Gal-I and ST6Gal-II respectively, suggesting regulation by the immune system.[33]

Conclusion

Sialylation, mediated by different sialyltransferases, is one of the most important and complex mechanisms involving cell surface receptors and the relationship between the immune microenvironment and the tumor cells. It is not surprising that sialyltransferases are associated with therapeutic resistance, likely by inhibition of the immune response.

Disclosure

The authors report no conflicts of interest in this work.

References

1. Perou CM. Molecular stratification of triple-negative breast cancers. *Oncologist.* 2011;16(Suppl 1):61–70.
2. Miyan M, Schmidt-Mende J, Kiessling R, Poschke I, de Boniface J. Differential tumor infiltration by T-cells characterizes intrinsic molecular subtypes in breast cancer. *J Transl Med.* 2016;14:227.
3. Mao Y, Qu Q, Chen X, Huang O, Wu J, Shen K. The prognostic value of tumor-infiltrating lymphocytes in breast cancer: A systematic review and meta-analysis. *PLoS One.* 2016;11(4):e0152500.
4. Vajaria BN, Patel PS. Glycosylation: A hallmark of cancer? *Glycoconj J.* 2017;34(2):147–156
5. Schultz MJ, Swindall AF, Bellis SL. Regulation of the metastatic cell phenotype by sialylated glycans. *Cancer Metastasis Rev.* 2012;31(3–4): 501–518.
6. Lu J, Gu J. Significance of β-galactoside α2,6 sialyltranferase 1 in cancers. *Molecules.* 2015;20(5):7509–7527.
7. Wreschner DH, McGuckin MA, Williams SJ, et al. Generation of ligand-receptor alliances by "SEA" module-mediated cleavage of membrane-associated mucin proteins. *Protein Sci.* 2002;11(3): 698–706.
8. Lillehoj EP, Hyun SW, Feng C, et al. NEU1 sialidase expressed in human airway epithelia regulates epidermal growth factor receptor (EGFR) and MUC1 protein signaling. *J Biol Chem.* 2012;287(11):8214–8231.
9. Garbar C, Mascaux C, Giustiniani J, et al. Autophagy is decreased in triple-negative breast carcinoma involving likely the MUC1-EGFR-NEU1 signalling pathway. *Int J Clin Exp Pathol.* 2015;8(5):4344–4355.
10. Park JJ, Yi JY, Jin YB, et al. Sialylation of epidermal growth factor receptor regulates receptor activity and chemosensitivity to gefitinib in colon cancer cells. *Biochem Pharmacol*. 2012;83(7):849–857.
11. Ma X, Dong W, Su Z, et al. Functional roles of sialylation in breast cancer progression through miR-26a/26b targeting ST8SIA4. *Cell Death Dis*. 2016;7(12):e2561.
12. Garbar C, Mascaux C, Giustiniani J, Merrouche Y, Bensussan A. Chemotherapy treatment induces an increase of autophagy in the luminal breast cancer cell MCF7, but not in the triple-negative MDA-MB231. *Sci Rep.* 2017;7(1):7201.
13. Madsen CB, Lavrsen K, Steentoft C, Vester-Christensen MB, Clausen H, Wandall HH, Pedersen AE. Glycan elongation beyond the mucin associated Tn antigen protects tumor cells from immune-mediated killing. *PLoS One*. 2013;8(9):e72413.
14. Loi S, Sirtaine N, Piette F, et al. Prognostic and predictive value of tumor-infiltrating lymphocytes in a Phase III randomized adjuvant breast cancer trial in node-positive breast cancer comparing the addition of docetaxel to doxorubicin with doxorubicin-based chemotherapy: BIG 02-98. *J Clin Oncol.* 2013;31(7):860–867.
15. Luen SJ, Salgado R, Fox S, et al. Tumour-infiltrating lymphocytes in advanced HER2-positive breast cancer treated with pertuzumab or placebo in addition to trastuzumab and docetaxel: A retrospective analysis of the CLEOPATRA study. *Lancet Oncol.* 2017;18(1):52–62.
16. Hudak JE, Canham SM, Bertozzi CR. Glycocalyx engineering reveals a siglec-based mechanism for NK cell immunoevasion. *Nat Chem Biol.* 2014;10(1):69–75.
17. Perdicchio M, Cornelissen LA, Streng-Ouwehand I, et al. Tumor sialylation impedes T cell mediated anti-tumor responses while promoting tumor associated-regulatory T cells. *Oncotarget.* 2016;7(8): 8771–8782.
18. Ogata S, Maimonis PJ, Itzkowitz SH. Mucins bearing the cancer-associated sialosyl-Tn antigen mediate inhibition of natural killer cell cytotoxicity. *Cancer Res.* 1992;52(17):4741–4746.
19. Beatson R, Tajadura-Ortega V, Achkova D, et al. The mucin MUC1 modulates the tumor immunological microenvironment through engagement of the lectin Siglec-9. *Nat Immunol*. 2016;17(11): 1273–1281.
20. Tanida S, Akita K, Ishida A, et al. Binding of the sialic acid-binding lectin, Siglec-9, to the membrane mucin, MUC1, induces recruitment of β-catenin and subsequent cell growth. *J Biol Chem.* 2013;288(44): 31842–31852.
21. Marcos NT, Pinho S, Grandela C, et al. Role of the human ST6GalNAc-I and ST6GalNAc-II in the synthesis of the cancer-associated sialyl-Tn antigen. *Cancer Res.* 2004;64(19):7050–7057.
22. Solatycka A, Owczarek T, Piller F, et al. MUC1 in human and murine mammary carcinoma cells decreases the expression of core 2 β1,6-N-acetylglucosaminyltransferase and β-galactoside α2,3-sialyltransferase. *Glycobiology.* 2012;22(8):1042–1054.
23. Bitler BG, Goverdhan A, Schroeder JA. MUC1 regulates nuclear localization and function of the epidermal growth factor receptor. *J Cell Sci*. 2010;123(Pt 10):1716–1723.
24. Neeraja Dharmaraj, Engel BJ, Carson DD. Activated EGFR stimulates MUC1 expression in human uterine and pancreatic cancer cell lines. *J Cell Biochem*. 2013;114(10):2314–2322.
25. Senapati S, Das S, Batra SK. Mucin-interacting proteins: from function to therapeutics. Trends Biochem Sci. 2010 Apr;35(4):236-45.
26. Chen X, Wang L, Zhao Y, et al. ST6Gal-I modulates docetaxel sensitivity in human hepatocarcinoma cells via the p38 MAPK/caspase pathway. *Oncotarget.* 2016;7(32):51955–51964.
27. Chakraborty A, Dorsett KA, Trummell HQ, et al. ST6Gal-I sialyltransferase promotes chemoresistance in pancreatic ductal adenocarcinoma by abrogating gemcitabine-mediated DNA damage. *J Biol Chem*. 2018;293(3)984–994.
28. Yen HY, Liu YC, Chen NY, et al. Effect of sialylation on EGFR phosphorylation and resistance to tyrosine kinase inhibition. *Proc Natl Acad Sci USA*. 2015;112(22):6955–6960.
29. Peiris D, Spector AF, Lomax-Browne H, et al. Cellular glycosylation affects Herceptin binding and sensitivity of breast cancer cells to doxorubicin and growth factors. *Sci Rep*. 2017;7:43006.

30. Wimana Z, Gebhart G, Guiot T, et al. N-acetylcysteine breaks resistance to trastuzumab caused by MUC4 overexpression in human HER2 positive BC-bearing nude mice monitored by ^{89}Zr-Trastuzumab and ^{18}F-FDG PET imaging. *Oncotarget.* 2017;8(34):56185–56198.
31. Laporte B, Gonzalez-Hilarion S, Maftah A, Petit JM. The second bovine β-galactoside-α2,6-sialyltransferase (ST6Gal II): Genomic organization and stimulation of its in vitro expression by IL-6 in bovine mammary epithelial cells. *Glycobiology.* 2009;19(10):1082–1093.
32. Groux-Degroote S, Krzewinski-Recchi MA, Cazet A, et al. IL-6 and IL-8 increase the expression of glycosyltransferases and sulfotransferases involved in the biosynthesis of sialylated and/or sulfated Lewis^X epitopes in the human bronchial mucosa. *Biochem J.* 2008;410(1):213–223.
33. Bassagañas S, Allende H, Cobler L, Ortiz MR, Llop E, de Bolós C, Peracaula R. Inflammatory cytokines regulate the expression of glycosyltransferases involved in the biosynthesis of tumor-associated sialylated glycans in pancreatic cancer cell lines. *Cytokine.* 2015;75(1):197–206.

e. Perspectives

Dans ce chapitre, nous illustrons nos dernières mises au point en immunohistochimie par fluorescence sur prélèvement en FFPE.

Je tiens particulièrement à souligner que, contrairement au technique sur matériel frais, la mise au point d'immuno-marquages en fluorescence sur FFPE est particulièrement difficile.

Les buts de ces techniques seront de faire une relation par co-expression de plusieurs protéines avec deux ou trois antigènes différents et en particulier entre l'autophagie, MUC1 ou EGFR.

Nous mettons également au point, sur notre modèle de culture sous chimiothérapie, des essais avec inhibition de MUC1-C (GO-203, apigénine) et de l'autophagie (hydrochloroquine, apigénine), avec comme perspectives de lever la chimiorésistance des cancers TN mais aussi d'illustrer par nos techniques morphologiques, les relations entre MUC1, EGFR et/ou IL17RA/RB.

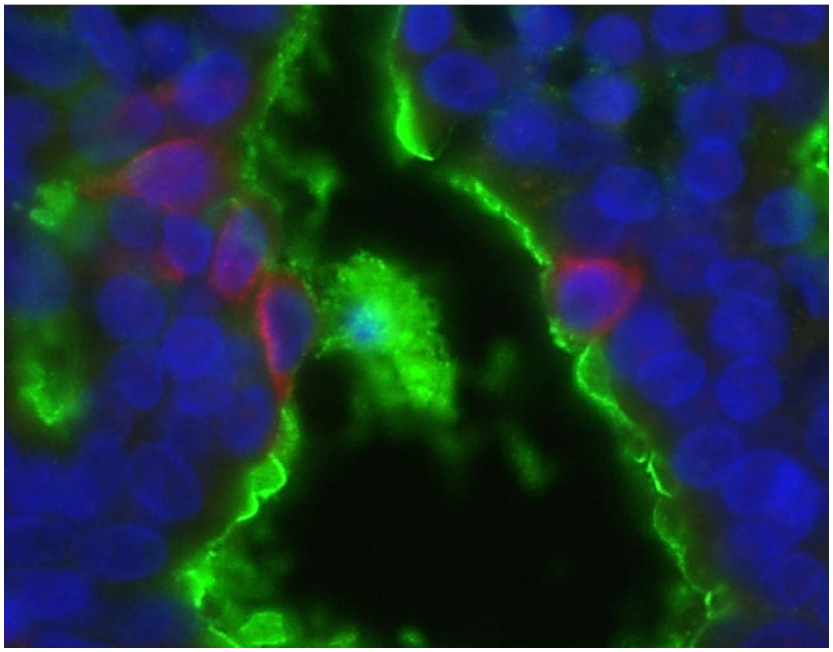

FIGURE 26 : Fluorescence de MUC-N (vert) et EGFR (rouge) dans une glande de sein normal. MUC1 est exprimé sur le pôle apical de la cellule et EGFR en baso-latéral.

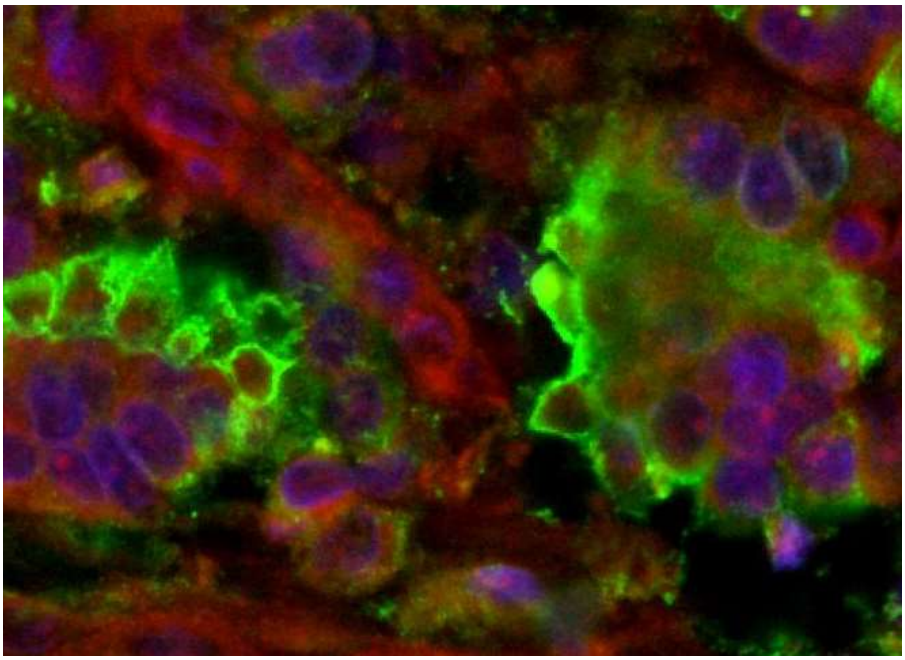

Figure 27 : Fluorescence de MUC1-C (vert) et de l'EGFR phosphorylé (rouge) dans le cancer du sein LUM. Expression de MUC1 dans le cytoplasme. Notez, le signal intranucléaire parfois observé pour EGFR.

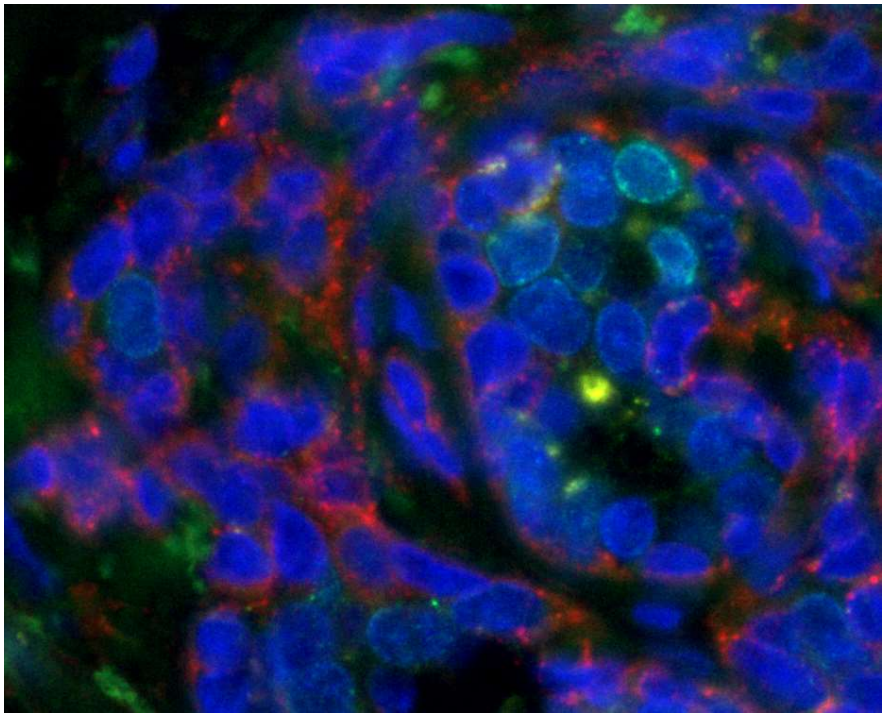

Figure 28 : Fluorescence de MUC1-ARF (vert) et de l'EGFR (rouge) dans le cancer du sein TN. On observe une fable expression de MUC1-ARF et une forte de l'EGFR. Notez la possible colocalisation parfois observée (en jaune) et le marquage périnucléaire de MUC1-ARF.

4. DISCUSSION

Les TN représentent environ 15 à 20 % des cancers du sein. Ils sont caractérisés par un pronostic clinique plus péjoratif par rapport aux autres sous-types de cancers du sein. De plus, en l'absence de cible thérapeutique hormonale ou HER2, la seule option est la chimiothérapie. Même si celle-ci est relativement efficace, les tumeurs TN deviennent souvent résistantes aux traitements et, par conséquent, incurables.(50) Le développement de nouvelles stratégies thérapeutiques est donc primordial pour lutter contre ces tumeurs.

Les TN expriment fortement EGFR

Comme dans le cancer des poumons, ou du côlon, la majorité des TN exprime l'EGFR. Par ailleurs, l'EGFR est reconnu comme un facteur de mauvais pronostic de ces tumeurs. Dans ces pathologies extramammaires, les traitements anti-EGFR, incluant les inhibiteurs de la tyrosine kinase (gefitinib, erlotinib, osimertinib…) ou les anticorps monoclonaux (cetuximab, panitumab, necitumumab…) ont montré leurs efficacités.(70)

Les traitements anti-EGFR dans le TN sont cependant assez décevants. Par exemple, les essais en phases II en monothérapie de gefitinib ou erlotinib sur des cancers TN métastatiques ont montré une réponse partielle seulement à 0 à 3 %. D'autres études sur les cancers TN métastatiques ont associé le cetuximab seul ou cetuximab + carboplatine vs cisplastine, avec un taux de réponse médiocre variant de 6 at 16 %. Enfin, le taux de réponse au traitement standard FEC (5-fluorouracil, epidoxorubicine, cyclophosphamide) comparé au docetaxel + panitumumab (anti-EGFR), n'a pas non plus été concluant.(70)

Si les TN expriment l'EGFR, pourquoi sont-ils résistants aux anti-EGFR ?

Dans les TN, la surexpression de la protéine d'EGFR n'est associée qu'à une faible évidence de son ARNm et/ou une quasi-absence d'amplification de gène de L'EGFR, suggérant une altération la régulation post-transcriptionnelle comme, par exemple, une stabilisation de la protéine ou une inhibition de son trafique interne. (63) Ces études vont dans le sens de nos observations : en effet, contrairement à l'EGFR, MUC1 est faiblement exprimé dans les TN et MUC1 participe intimement à la régulation, l'internalisation et les fonctions de EGFR. Par conséquent, on comprend aisément

pourquoi l'EGFR s'accumule à la membrane et qu'il est probablement inactif, quand MUC1 est déficient.

Une autre explication plausible de cette faible réponse aux anti-EGFR dans les TN est que ces tumeurs ne sont pas exclusivement tributaires de la voie de signalisation de l'EGFR. On sait que dans le poumon, les inhibiteurs des tyrosines kinases sont efficaces si elles possèdent une mutation activatrice de la voie de signalisation de l'EGFR. Malheureusement, ces mutations activatrices sont rares dans les TN et des voies alternatives doivent être aussi activées dans les TN, annihilant les effets des anti-EGFR. (41) En effet, on sait que dans le poumon, les mutants de la voie RAS sont capables d'activer la voie alternative de l'EGFR et d'induire une résistance aux anti-EGFR. (70) Rappelons que RAS peut être activé par la phosphorylation de MUC1-C par l'EGFR et qu'elle est aussi la voie d'activation de l'autophagie. De manière intéressante, sur cultures de cellule TN, certains ont montré une efficacité des anti-EGFR (lapatinb) associé à des inhibiteurs de RAF et MEK (MAPK kinase ou voie de signalisation RAS/RAF/MEK/ERK), suggérant l'importance de cette voie. La rareté des mutations de RAS dans les cancers TN, exclu cette voie comme facteur de résistance aux anti-EGFR. D'autres voies de signalisations sont donc impliquées comme celles associées à MUC1, l'autophagie (PI3K, AMKT…) et IL17, sujet de cette thèse.

MUC1 et la chimiorésistance ?

De nombreux travaux ont démontré les associations entre MUC-C et la chimiorésistance. Par exemple, MUC1-C est corrélé à la résistance au tamoxifène (anti-estrogènes) ou aux agents de chimiothérapie, dont la doxorubicine ou le taxol. (10, 20, 45, 58, 80, 86)

MUC1-C dimérisé est aussi connu comme le transporteur nucléaire de l'EGFR, par l'intermédiaire de la β-importine. Curieusement, dans le cancer du sein TN, la forme nucléaire de l'EGFR a été décrite comme promotrice de résistance au cétuximab (anti-EGFR). (7) Certaines études *in vitro*, ont déjà démontré l'efficacité des inhibiteurs de cette dimérisation de MUC1 (GO-201 et GO-203). Bien que soit séduisants, les applications cliniques pour lever les chimiorésistances et les effets secondaires de ces inhibiteurs de MUC1-C, restent encore floues.

Autophagie et chimiorésistance ?

Une autre approche intéressante pouvant lever la résistance des anti-EGFR dans les TN, est celle de l'autophagie. Comme nous l'avons précédemment décrit, on sait qu'elle est régulée par deux voies de signalisation majeures : PI3K/AKT/mTOR et RAF/MEK/ERK, toutes deux également liées à MUC1 et EGFR. De plus, la p110β (PI3K ce classe 1) est impliquée dans la chimiorésistance au paxitaxel dans le cancer des ovaires. (31). La voie de ERK est aussi connue être très active dans les TN et cette activité est corrélée avec la résistance à l'épirubicine, connu comme inhibiteur de l'autophagie.

De même, sur un modèle murin de cancer du sein TN, des études préliminaires ont démontré que l'inhibition de l'autophagie par la chloroquine augment les effets de l'adriamycine ou le cyclophosphamide. (47)

D'autres observations ont décrit que chez des patients ayant un cancer du côlon avec un niveau d'autophagie faible, le taux de réponse et de survie sont meilleures avec une association de cétuximab, un anti EGFR. (36, 99)

Quelques études cliniques en phase I et II associant des agents de chimiothérapie et des inhibiteurs de l'autophagie sont en cours sur des cancers avancés. Leurs résultats sont encore en attente.

IL17 et chimiorésistance ?

La dernière approche thérapeutique pour lever la résistance des anti-EGFR est celle des récepteurs de l'IL17 et en particulier de l'IL17RB. Comme nous l'avons discuté largement, la voie des MAPK (RAF/MEK/ERG) est une voie importante dans la résistance à la chimiothérapie. Notre équipe à précédemment démontré, in vivo et in vitro, que la cytokine pro-inflammatoire IL17A était produite intensément par les cellules du microenvironnement tumoral (lymphocytes Th17) des cancers du sein, les TN. IL17A est capable, dans les cellules cancéreuses TN, d'activer la voie des MAPK (pour rappel, aussi associée à MUC1/EGFR et l'autophagie) et de phosphoryler ERK, favorisant ainsi la prolifération, la migration et la résistance aux agents de

chimiothérapie conventionnelle comme le docétaxel. Cette résistance peut être levée, *in vitro*, par des anticorps bloquant anti-IL17A. (13)

Ensuite, nous avons également démontré que l'IL17E est impliqué dans des mécanismes similaires de chimiorésistance, en particulier en bloquant l'apoptose, mécanisme opposé à l'autophagie. Dans cette étude, nous avons montré que l'IL17A n'était pas produite par les cellules tumorales TN, mais que, par contre, ces cellules exprimaient au niveau de membranes les récepteurs IL17RA, IL17RB et IL17RC. (66) Dans nos travaux personnels, nous avons par une technique différente illustrée ces mêmes données.

Plus récemment encore, nous avons prouvé que l'IL17E activait la voie de l'EGFR des cellules tumorales TN, résistantes aux anti-EGFR, par l'intermédiaire de l'activation des récepteurs IL17RA et IL17RB et les cascades de phosphorylations associées de Src et STAT3 (deux intervenants associés également à MUC1-C) Cette voie d'activation favoriserait le transfert de l'EGFR phosphorylé vers le noyau. (62)

On comprend aisément l'intérêt d'inhiber cette voie de l'IL17 dans le cancer du sein. (19) En effet, les possibilités thérapeutiques sont existantes Les anti-IL17 (ixekizumab, brodalumab, guselkumab, tildrakizumab) sont déjà bien connus dans les pathologies inflammatoires dermatologiques comme le psoriasis ou dans les pathologies inflammatoires du colon. Malheureusement et de manière intrigante, à ce jour aucune publication ne développe les anti-IL17 dans les cancers. (38)

5. CONCLUSION GENERALE

Cette thèse est le fruit d'une convergence commune entre l'oncologue, l'immunologiste et le pathologiste afin de comprendre la résistance thérapeutique et l'agressivité des cancers du sein triple-négatif. Les solutions sont nombreuses et s'articulent souvent sur la voie des MAPK, activateur de l'autophagie, unissant à la fois EGFR, MUC1 et IL17. Les possibilités thérapeutiques sont connues, mais encore souvent aux stades expérimentales comme le GO-203 pour MUC1, la chloroquine ou l'hydroxychloroquine pour l'autophagie, ou encore, les anticorps bloquant anti-IL17. Des études cliniques aux stades II/III ont déjà été réalisées avec un traitement contre

mTOR (rapamycine, everolimus), mais s'associent à des résultats mitigés, principalement à cause des effets secondaires. (33)

Finalement, ce travail a été la résultante d'une synergie entre le clinicien et le chercheur expérimental. Le pathologiste jouant le rôle d'intermédiaire. Ce travail d'équipe permettra certainement, dans un avenir proche, de cristalliser des solutions aux traitements des cancers du sein triple négatif.

BIBLIOGRAPHIE

1. Ahmad R, Alam M, Rajabi H, Kufe D. The MUC1-C oncoprotein binds to the BH3 domain of the pro-apoptotic BAX protein and blocks BAX function. J Biol Chem. 2012 Jun 15;287(25):20866-75.
2. Albrecht H, Carraway KL 3rd. MUC1 and MUC4: switching the emphasis from large to small. Cancer Biother Radiopharm. 2011 Jun;26(3):261-71
3. Altschuler Y, Kinlough CL, Poland PA, Bruns JB, Apodaca G, Weisz OA, Hughey RP. Clathrin-mediated endocytosis of MUC1 is modulated by its glycosylation state. Mol Biol Cell. 2000 Mar;11(3):819-31.
4. Bafna S, Kaur S, Batra SK. Membrane-bound mucins: the mechanistic basis for alterations in the growth and survival of cancer cells. Oncogene. 2010 May
5. Bitler BG, Goverdhan A, Schroeder JA. MUC1 regulates nuclear localization and function of the epidermal growth factor receptor. J Cell Sci. 2010 May 15;123(Pt 10):1716-23.
6. Boshell M, Lalani EN, Pemberton L, Burchell J, Gendler S, Taylor-Papadimitriou J. The product of the human MUC1 gene when secreted by mouse cells transfected with the full-length cDNA lacks the cytoplasmic tail. Biochem Biophys Res Commun. 1992 May 29;185(1):1-8.
7. Brand TM, Iida M, Dunn EF, Luthar N, Kostopoulos KT, Corrigan KL, Wleklinski MJ, Yang D, Wisinski KB, Salgia R, Wheeler DL. Nuclear epidermal growth factor receptor is a functional molecular target in triple-negative breast cancer. Mol Cancer Ther. 2014 May;13(5):1356-68.
8. Brockhausen I. Biosynthesis and functions of O-glycans and regulation of mucin antigen expression in cancer. Biochem Soc Trans. 1997 Aug;25(3):871-4. Review.
9. Burchell J, Poulsom R, Hanby A, Whitehouse C, Cooper L, Clausen H, Miles D, Taylor-Papadimitriou J. An alpha2,3 sialyltransferase (ST3Gal I) is elevated in primary breast carcinomas. Glycobiology. 1999 Dec;9 (12):1307-11.

10. Cantley LC. The phosphoinositide 3-kinase pathway. Science. 2002 May 31;296(5573):1655-7. Review.
11. Carlos CA, Dong HF, Howard OM, Oppenheim JJ, Hanisch FG, Finn OJ. Human tumor antigen MUC1 is chemotactic for immature dendritic cells and elicits maturation but does not promote Th1 type immunity. J Immunol. 2005 Aug 1;175(3):1628-35.
12. Chalick M, Jacobi O, Pichinuk E, Garbar C, Bensussan A, Meeker A, Ziv R, Zehavi T, Smorodinsky NI, Hilkens J, Hanisch FG, Rubinstein DB, Wreschner DH.MUC1-ARF-A Novel MUC1 Protein That Resides in the Nucleus and Is Expressed by Alternate Reading Frame Translation of MUC1 mRNA. PLoS One. 2016 Oct21;11(10)
13. Cochaud S, Giustiniani J, Thomas C, Laprevotte E, Garbar C, Savoye AM, Curé H, Mascaux C, Alberici G, Bonnefoy N, Eliaou JF, Bensussan A, Bastid J. IL-17A is produced by breast cancer TILs and promotes chemoresistance and proliferation through ERK1/2. Sci Rep. 2013 Dec 9;3:3456.
14. Codogno P. Shining light on autophagy. Nat Rev Mol Cell Biol. 2014 Mar;15(3):153.
15. Dalby KN, Tekedereli I, Lopez-Berestein G, Ozpolat B. Targeting the prodeath and prosurvival functions of autophagy as novel therapeutic strategies in cancer. Autophagy. 2010 Apr;6(3):322-9.
16. Debailleul V, Laine A, Huet G, Mathon P, d'Hooghe MC, Aubert JP, Porchet N.Human mucin genes MUC2, MUC3, MUC4, MUC5AC, MUC5B, and MUC6 express stable and extremely large mRNAs and exhibit a variable length polymorphism. An improved method to analyze large mRNAs. J Biol Chem. 1998 Jan 9;273(2):881-90.
17. Dou Z, Chattopadhyay M, Pan JA, Guerriero JL, Jiang YP, Ballou LM, Yue Z, Lin RZ, Zong WX. The class IA phosphatidylinositol 3-kinase p110-beta subunit is a positive regulator of autophagy. J Cell Biol. 2010 Nov 15;191(4):827-43.
18. Dou Z, Pan JA, Dbouk HA, Ballou LM, DeLeon JL, Fan Y, Chen JS, Liang Z, Li G, Backer JM, Lin RZ, Zong WX. Class IA PI3K p110β subunit promotes autophagy through Rab5 small GTPase in response to growth factor limitation. Mol Cell. 2013 Apr 11;50(1):29-42.

19. Fabre J, Giustiniani J, Garbar C, Antonicelli F, Merrouche Y, Bensussan A, Bagot M, Al-Dacak R. Targeting the Tumor Microenvironment: The Protumor Effects of IL-17 Related to Cancer Type. Int J Mol Sci. 2016 Aug 30;17(9).
20. Fessler SP, Wotkowicz MT, Mahanta SK, Bamdad C. MUC1* is a determinant of trastuzumab (Herceptin) resistance in breast cancer cells. Breast Cancer Res Treat. 2009 Nov;118(1):113-24.
21. Garbar C, Mascaux C, Wespes E. Expression of MUC1 and sialyl-Tn in benign prostatic glands, high-grade prostate intraepithelial neoplasia and malignant prostatic glands: a preliminary study. Anal Quant Cytol Histol. 2008
22. Garbar C, Mascaux C. Expression of MUC1 (Ma695) in noninvasive papillary urothelial neoplasm according to the 2004 World Health Organization classification of the noninvasive urothelial neoplasm. An immunologic tool for the pathologist? Anal Quant Cytol Histol. 2011 Oct;33(5):277-82.
23. Hahn-Windgassen A, Nogueira V, Chen CC, Skeen JE, Sonenberg N, Hay N. Akt activates the mammalian target of rapamycin by regulating cellular ATP level and AMPK activity. J Biol Chem. 2005 Sep 16;280(37):32081-9.
24. Hohenberger M, Cardwell LA, Oussedik E, Feldman SR. Interleukin-17 inhibition: role in psoriasis and inflammatory bowel disease. J dermatolog Treat. 2018 Feb;29(1):13-18.
25. Horn G, Gaziel A, Wreschner DH, Smorodinsky NI, Ehrlich M. ERK and PI3K regulate different aspects of the epithelial to mesenchymal transition of mammary tumor cells induced by truncated MUC1. Exp Cell Res. 2009 May 1;315(8):1490-504.
26. Hossain MK, Wall KA. Immunological Evaluation of Recent MUC1 Glycopeptide Cancer Vaccines. Vaccines (Basel). 2016 Jul 26;4(3).
27. Hu X, Zhang K, Chen Z, Jiang H, Xu W. The HMGB1‐IL‐17A axis contributes to hypoxia/reoxygenation injury via regulation of cardiomyocyte apoptosis and autophagy. Mol Med Rep. 2018 Jan;17(1):336-341.

28. Hudak JE, Canham SM, Bertozzi CR. Glycocalyx engineering reveals a Siglec-based mechanism for NK cell immunoevasion. Nat Chem Biol. 2014 Jan;10(1):69-75.
29. Inoki K, Kim J, Guan KL. AMPK and mTOR in cellular energy homeostasis and drug targets. Annu Rev Pharmacol Toxicol. 2012;52:381-400.
30. Itzkowitz SH, Bloom EJ, Kokal WA, Modin G, Hakomori S, Kim YS. Sialosyl-Tn. A novel mucin antigen associated with prognosis in colorectal cancer patients.Cancer. 1990 Nov 1;66(9):1960-6.
31. Ju-yeon JY, Kim KS, Moon JS, Song JA, Choi SH, Kim KI, Kim TH, An HJ. Targeted inhibition of phosphatidyl inositol-3-kinase p110β, but not p110α, enhances apoptosis and sensitivity to paclitaxel in chemoresistant ovarian cancers.Apoptosis. 2013 Apr;18(4):509-20.
32. Jia S, Roberts TM, Zhao JJ. Should individual PI3 kinase isoforms be targeted in cancer? Curr Opin Cell Biol. 2009 Apr;21(2):199-208.
33. Jovanović B, Mayer IA, Mayer EL, Abramson VG, Bardia A, Sanders ME, Kuba MG,Estrada MV, Beeler JS, Shaver TM, Johnson KC, Sanchez V, Rosenbluth JM, Dillon PM, Forero-Torres A, Chang JC, Meszoely IM, Grau AM, Lehmann BD, Shyr Y, Sheng Q,Chen SC, Arteaga CL, Pietenpol JA. A Randomized Phase II Neoadjuvant Study of Cisplatin, Paclitaxel With or Without Everolimus in Patients with Stage II/III Triple-Negative Breast Cancer (TNBC): Responses and Long-term Outcome Correlated with Increased Frequency of DNA Damage Response Gene Mutations, TNBC Subtype, AR Status, and Ki67. Clin Cancer Res. 2017 Aug 1;23(15):4035-4045.
34. Julien S, Adriaenssens E, Ottenberg K, Furlan A, Courtand G,Vercoutter-Edouart AS, Hanisch FG, Delannoy P, Le Bourhis X. ST6GalNAc I expression in MDA-MB-231 breast cancer cells greatly modifies their O-glycosylation pattern and enhances their tumourigenicity. Glycobiology. 2006 Jan;16(1):54-64.
35. Julien S, Lagadec C, Krzewinski-Recchi MA, Courtand G, Le Bourhis X, Delannoy P. Stable expression of sialyl-Tn antigen in T47-D cells induces a decrease of cell adhesion and an increase of cell migration. Breast Cancer Res Treat. 2005 Mar;90(1):77-84.

36. Jutten B, Rouschop KM. EGFR signaling and autophagy dependence for growth,survival, and therapy resistance. Cell Cycle. 2014;13(1):42-51.
37. Kaewkangsadan V, Verma C, Eremin JM, Cowley G, Ilyas M, Eremin O. Crucial Contributions by T Lymphocytes (Effector, Regulatory, and Checkpoint Inhibitor) and Cytokines (TH1, TH2, and TH17) to a Pathological Complete Response Induced by Neoadjuvant Chemotherapy in Women with Breast Cancer. J Immunol Res.2016;2016:4757405.
38. Kaplon H, Reichert JM. Antibodies to watch in 2018. MAbs. 2018 Jan 4:1-21.
39. Kato K, Lu W, Kai H, Kim KC. Phosphoinositide 3-kinase is activated by MUC1 but not responsible for MUC1-induced suppression of Toll-like receptor 5 signaling. Am J Physiol Lung Cell Mol Physiol. 2007 Sep;293(3):L686-92.
40. Kharbanda A, Rajabi H, Jin C, Raina D, Kufe D. Oncogenic MUC1-C promotes tamoxifen resistance in human breast cancer. Mol Cancer Res. 2013Jul;11(7):714-23.
41. Kim A, Jang MH, Lee SJ, Bae YK. Mutations of the Epidermal Growth Factor Receptor Gene in Triple-Negative Breast Cancer. J Breast Cancer. 2017 Jun;20(2):150-159.
42. Kinlough CL, McMahan RJ, Poland PA, Bruns JB, Harkleroad KL, Stremple RJ,Kashlan OB, Weixel KM, Weisz OA, Hughey RP. Recycling of MUC1 is dependent on its palmitoylation. J Biol Chem. 2006 Apr 28;281(17):12112-22
43. Kinlough CL, Poland PA, Bruns JB, Harkleroad KL, Hughey RP. MUC1 membrane trafficking is modulated by multiple interactions. J Biol Chem. 2004 Dec 17;279(51):53071-7.
44. Kufe D, Inghirami G, Abe M, Hayes D, Justi-Wheeler H, Schlom J. Differential reactivity of a novel monoclonal antibody (DF3) with human malignant versus benign breast tumors. Hybridoma. 1984 Fall;3(3):223-32
45. Kufe DW. MUC1-C oncoprotein as a target in breast cancer: activation of signaling pathways and therapeutic approaches. Oncogene. 2013 Feb 28;32(9):1073-81.

46. Kufe DW. Mucins in cancer: function, prognosis and therapy. Nat Rev Cancer. 2009 Dec;9(12):874-85.
47. Lefort S, Joffre C, Kieffer Y, Givel AM, Bourachot B, Zago G, Bieche I, Dubois T, Meseure D, Vincent-Salomon A, Camonis J, Mechta-Grigoriou F. Inhibition of autophagy as a new means of improving chemotherapy efficiency in high-LC3B triple-negative breast cancers. Autophagy. 2014;10(12):2122-42.
48. Li Y, Ren J, Yu W, Li Q, Kuwahara H, Yin L, Carraway KL 3rd, Kufe D. The epidermal growth factor receptor regulates interaction of the human DF3/MUC1 carcinoma antigen with c-Src and beta-catenin. J Biol Chem. 2001 Sep 21;276(38):35239-42.
49. Li Y, Yu WH, Ren J, Chen W, Huang L, Kharbanda S, Loda M, Kufe D. Heregulin targets gamma-catenin to the nucleolus by a mechanism dependent on the DF3/MUC1 oncoprotein. Mol Cancer Res. 2003 Aug;1(10):765-75.
50. Liedtke C, Mazouni C, Hess KR, André F, Tordai A, Mejia JA, Symmans WF,Gonzalez-Angulo AM, Hennessy B, Green M, Cristofanilli M, Hortobagyi GN, Pusztai L. Response to neoadjuvant therapy and long-term survival in patients with triple-negative breast cancer. J Clin Oncol. 2008 Mar 10;26(8):1275-81.
51. Ligtenberg MJ, Kruijshaar L, Buijs F, van Meijer M, Litvinov SV, Hilkens J.Cell-associated episialin is a complex containing two proteins derived from a common precursor. J Biol Chem. 1992 Mar 25;267(9):6171-7.
52. Lillehoj EP, Han F, Kim KC. Mutagenesis of a Gly-Ser cleavage site in MUC1 inhibits ectodomain shedding. Biochem Biophys Res Commun. 2003 Aug 1;307(3):743-9.
53. Lin S, Kemmner W, Grigull S, Schlag PM. Cell surface alpha 2,6 sialylation affects adhesion of breast carcinoma cells. Exp Cell Res. 2002 May 15;276(1):101-10.
54. Litvinov SV, Hilkens J. The epithelial sialomucin, episialin, is sialylated during recycling. J Biol Chem. 1993 Oct 5;268(28):21364-71.
55. Liu H, Mi S, Li Z, Hua F, Hu ZW. Interleukin 17A inhibits autophagy through activation of PIK3CA to interrupt the GSK3B-mediated

degradation of BCL2 in lung epithelial cells. Autophagy. 2013 May;9(5):730-42.

56. Macao B, Johansson DG, Hansson GC, Härd T. Autoproteolysis coupled to protein folding in the SEA domain of the membrane-bound MUC1 mucin. Nat truct Mol Biol. 2006 Jan;13(1):71-6.
57. Mavrakis M, Lippincott-Schwartz J, Stratakis CA, Bossis I. Depletion of type IA regulatory subunit (RIalpha) of protein kinase A (PKA) in mammalian cells and tissues activates mTOR and causes autophagic deficiency. Hum Mol Genet. 2006 Oct 1;15(19):2962-71.
58. McCubrey JA, Steelman LS, Abrams SL, Lee JT, Chang F, Bertrand FE, Navolanic PM, Terrian DM, Franklin RA, D'Assoro AB, Salisbury JL, Mazzarino MC, Stivala F, Libra M. Roles of the RAF/MEK/ERK and PI3K/PTEN/AKT pathways in malignant transformation and drug resistance. Adv Enzyme Regul. 2006;46:249-79.
59. Mehla K, Singh PK. MUC1: a novel metabolic master regulator. Biochim Biophys Acta. 2014 Apr;1845(2):126-35.
60. Merlin J, Stechly L, de Beaucé S, Monté D, Leteurtre E, van Seuningen I, Huet G, Pigny P. Galectin-3 regulates MUC1 and EGFR cellular distribution and EGFR downstream pathways in pancreatic cancer cells. Oncogene. 2011 Jun 2;30(22):2514-25.
61. Merlo GR, Siddiqui J, Cropp CS, Liscia DS, Lidereau R, Callahan R, Kufe DW.Frequent alteration of the DF3 tumor-associated antigen gene in primary human breast carcinomas. Cancer Res. 1989 Dec 15;49(24 Pt):6966-71.
62. Merrouche Y, Fabre J, Cure H, Garbar C, Fuselier C, Bastid J, Antonicelli F, Al-Daccak R, Bensussan A, Giustiniani J. IL-17E synergizes with EGF and confers in vitro resistance to EGFR-targeted therapies in TNBC cells. Oncotarget. 2016 Aug 16;7(33):53350-53361.
63. Meseure D, Vacher S, Drak Alsibai K, Trassard M, Susini A, Le Ray C, Lerebours F, Le Scodan R, Spyratos F, Marc Guinebretiere J, Lidereau R, Bieche I. Profiling of EGFR mRNA and protein expression in 471 breast cancers compared with 10 normal tissues: a candidate biomarker to predict EGFR inhibitor effectiveness. Int J Cancer. 2012 Aug 15;131(4):1009-10.

64. Mizushima N, Yoshimori T, Ohsumi Y. The role of Atg proteins in autophagosome formation. Annu Rev Cell Dev Biol. 2011;27:107-32.
65. Modi S, D'Andrea G, Norton L, Yao TJ, Caravelli J, Rosen PP, Hudis C, Seidman AD. A phase I study of cetuximab/paclitaxel in patients with advanced-stage breast cancer. Clin Breast Cancer. 2006 Aug;7(3):270-7.
66. Mombelli S, Cochaud S, Merrouche Y, Garbar C, Antonicelli F, Laprevotte E, Alberici G, Bonnefoy N, Eliaou JF, Bastid J, Bensussan A, Giustiniani J. IL-17A and its homologs IL-25/IL-17E recruit the c-RAF/S6 kinase pathway and the generation of pro-oncogenic LMW-E in breast cancer cells. Sci Rep. 2015 Jul 8;5:11874.
67. Moniaux N, Escande F, Porchet N, Aubert JP, Batra SK. Structural organization and classification of the human mucin genes. Front Biosci. 2001 Oct 1;6:D1192-206. Review.
68. Munkley J, Elliott DJ. Hallmarks of glycosylation in cancer. Oncotarget. 2016 Jun 7;7(23):35478-89.
69. Nagaria TS, Shi C, Leduc C, Hoskin V, Sikdar S, Sangrar W, Greer PA. Combined targeting of Raf and Mek synergistically inhibits tumorigenesis in triple negative breast cancer model systems. Oncotarget. 2017 Aug 24;8(46):80804-80819.
70. Nakai K, Hung MC, Yamaguchi H. A perspective on anti-EGFR therapies targeting triple-negative breast cancer. Am J Cancer Res. 2016 Aug 1;6(8):1609-23.
71. Netea-Maier RT, Plantinga TS, van de Veerdonk FL, Smit JW, Netea MG. Modulation of inflammation by autophagy: Consequences for human disease. Autophagy. 2016;12(2):245-60
72. Netea-Maier RT, Klück V, Plantinga TS, Smit JW. Autophagy in thyroid cancer: present knowledge and future perspectives. Front Endocrinol (Lausanne). 2015 Feb 18;6:22.
73. Ozpolat B, Benbrook DM. Targeting autophagy in cancer management - strategies and developments. Cancer Manag Res. 2015 Sep 11;7:291-9.

74. Parry S, Hanisch FG, Leir SH, Sutton-Smith M, Morris HR, Dell A, Harris A.N-Glycosylation of the MUC1 mucin in epithelial cells and secretions.Glycobiology. 2006 Jul;16(7):623-34
75. Perou CM, Børresen-Dale AL. Systems biology and genomics of breast cancer.Cold Spring Harb Perspect Biol. 2011 Feb 1;3(2). pii: a003293.
76. Perou CM. Molecular stratification of triple-negative breast cancers. Oncologist. 2010;15 Suppl 5:39-48.
77. Pochampalli MR, Bitler BG, Schroeder JA. Transforming growth factor alpha dependent cancer progression is modulated by Muc1. Cancer Res. 2007 Jul15;67(14):6591-8.
78. Pochampalli MR, el Bejjani RM, Schroeder JA. MUC1 is a novel regulator of ErbB1 receptor trafficking. Oncogene. 2007 Mar 15;26(12):1693-701.
79. Pruneri G, Gray KP, Vingiani A, Viale G, Curigliano G, Criscitiello C, Láng I,Ruhstaller T, Gianni L, Goldhirsch A, Kammler R, Price KN, Cancello G, Munzone E,Gelber RD, Regan MM, Colleoni M. Tumor-infiltrating lymphocytes (TILs) are a powerful prognostic marker in patients with triple-negative breast cancer enrolled in the IBCSG phase III randomized clinical trial 22-00. Breast Cancer Res Treat. 2016 Jul;158(2):323-31.
80. Raina D, Agarwal P, Lee J, Bharti A, McKnight CJ, Sharma P, Kharbanda S, Kufe D. Characterization of the MUC1-C Cytoplasmic Domain as a Cancer Target. PLoS One. 2015 Aug 12;10(8):e0135156.
81. Raina D, Ahmad R, Rajabi H, Panchamoorthy G, Kharbanda S, Kufe D. Targeting cysteine-mediated dimerization of the MUC1-C oncoprotein in human cancer cells. Int J Oncol. 2012 May;40(5):1643-9.
82. Raina D, Kharbanda S, Kufe D. The MUC1 oncoprotein activates the anti-apoptotic phosphoinositide 3-kinase/Akt and Bcl-xL pathways in rat 3Y1 fibroblasts. J Biol Chem. 2004 May 14;279(20):20607-12.
83. Raina D, Kosugi M, Ahmad R, Panchamoorthy G, Rajabi H, Alam M, Shimamura T,Shapiro GI, Supko J, Kharbanda S, Kufe D. Dependence on the MUC1-C oncoprotein in non-small cell lung cancer cells. Mol Cancer Ther. 2011 May;10(5):806-16.
84. Rajabi H, Ahmad R, Jin C, Kosugi M, Alam M, Joshi MD, Kufe D. MUC1-C oncoprotein induces TCF7L2 transcription factor activation and

promotes cyclin D1 expression in human breast cancer cells. J Biol Chem. 2012 Mar 23;287(13):10703-13.

85. Ramasamy S, Duraisamy S, Barbashov S, Kawano T, Kharbanda S, Kufe D. The MUC1 and galectin-3 oncoproteins function in a microRNA-dependent regulatory loop. Mol Cell. 2007 Sep 21;27(6):992-1004.
86. Ren J, Agata N, Chen D, Li Y, Yu WH, Huang L, Raina D, Chen W, Kharbanda S,Kufe D. Human MUC1 carcinoma-associated protein confers resistance to genotoxic anticancer agents. Cancer Cell. 2004 Feb;5(2):163-75.
87. Ren J, Raina D, Chen W, Li G, Huang L, Kufe D. MUC1 oncoprotein functions in activation of fibroblast growth factor receptor signaling. Mol Cancer Res. 2006 Nov;4(11):873-83.
88. Rubinstein DB, Karmely M, Pichinuk E, Ziv R, Benhar I, Feng N, Smorodinsky NI,Wreschner DH. The MUC1 oncoprotein as a functional target: immunotoxin binding to alpha/beta junction mediates cell killing. Int J Cancer. 2009 Jan 1;124(1):46-54.
89. Schroeder JA, Thompson MC, Gardner MM, Gendler SJ. Transgenic MUC1 interacts with epidermal growth factor receptor and correlates with mitogen-activated protein kinase activation in the mouse mammary gland. J Biol Chem. 2001 Apr 20;276(16):13057-64.
90. Sewell R, Bäckström M, Dalziel M, Gschmeissner S, Karlsson H, Noll T, Gätgens J, Clausen H, Hansson GC, Burchell J, Taylor-Papadimitriou J. The ST6GalNAc-I sialyltransferase localizes throughout the Golgi and is responsible for the synthesis of the tumor-associated sialyl-Tn O-glycan in human breast cancer. J Biol Chem. 2006 Feb 10;281(6):3586-94.
91. Singh PK, Hollingsworth MA. Cell surface-associated mucins in signal transduction. Trends Cell Biol. 2006 Sep;16(9):467-76.
92. Spicer AP, Parry G, Patton S, Gendler SJ. Molecular cloning and analysis of the mouse homologue of the tumor-associated mucin, MUC1, reveals conservation of potential O-glycosylation sites, transmembrane, and cytoplasmic domains and a loss of minisatellite-like polymorphism. J Biol Chem. 1991 Aug 15;266(23):15099-109.
93. Stowell SR, Ju T, Cummings RD. Protein glycosylation in cancer. Annu Rev Pathol. 2015;10:473-510.

94. Taylor-Papadimitriou J, Burchell JM, Plunkett T, Graham R, Correa I, Miles D, Smith M. MUC1 and the immunobiology of cancer. J Mammary Gland Biol Neoplasia. 2002 Apr;7(2):209-21. Review.
95. Theodoropoulos G, Carraway KL. Molecular signaling in the regulation of mucins. J Cell Biochem. 2007 Dec 1;102(5):1103-16. Review.
96. Uchida Y, Raina D, Kharbanda S, Kufe D. Inhibition of the MUC1-C oncoprotein is synergistic with cytotoxic agents in the treatment of breast cancer cells. Cancer Biol Ther. 2013 Feb;14(2):127-34.
97. Utermark T, Rao T, Cheng H, Wang Q, Lee SH, Wang ZC, Iglehart JD, Roberts TM, Muller WJ, Zhao JJ. The p110α and p110β isoforms of PI3K play divergent roles in mammary gland development and tumorigenesis. Genes Dev. 2012 Jul 15;26(14):1573-86.
98. Wang Y, Ju T, Ding X, Xia B, Wang W, Xia L, He M, Cummings RD. Cosmc is an essential chaperone for correct protein O-glycosylation. Proc Natl Acad Sci U S A. 2010 May 18;107(20):9228-33.
99. Wei X, Xu H, Kufe D. MUC1 oncoprotein stabilizes and activates estrogen receptor alpha. Mol Cell. 2006 Jan 20;21(2):295-305.
100. Wreschner DH, Hareuveni M, Tsarfaty I, Smorodinsky N, Horev J, Zaretsky J, Kotkes P, Weiss M, Lathe R, Dion A, et al. Human epithelial tumor antigen cDNA sequences. Differential splicing may generate multiple protein forms. Eur J Biochem. 1990 May 20;189(3):463-73.
101. Yao M, Shang YY, Zhou ZW, Yang YX, Wu YS, Guan LF, Wang XY, Zhou SF, Wei X.The research on lapatinib in autophagy, cell cycle arrest and epithelial to mesenchymal transition via Wnt/ErK/PI3K-AKT signaling pathway in human cutaneous squamous cell carcinoma. J Cancer. 2017 Jan 15;8(2):220-226.
102. Ye M, Wang S, Wan T, Jiang R, Qiu Y, Pei L, Pang N, Huang Y, Huang Y, Zhang Z,Yang L. Combined Inhibitions of Glycolysis and AKT/autophagy Can Overcome Resistance to EGFR-targeted Therapy of Lung Cancer. J Cancer. 2017 Oct 17;8(18):3774-3784.
103. Yin L, Kharbanda S, Kufe D. MUC1 oncoprotein promotes autophagy in a survival response to glucose deprivation. Int J Oncol. 2009 Jun;34 (6):1691-9.

104. Yoon WH, Park HD, Lim K, Hwang BD. Effect of O-glycosylated mucin on invasion and metastasis of HM7 human colon cancer cells. Biochem Biophys Res Commun. 1996 May 24;222(3):694-9.

105. Zhou Y, Wu PW, Yuan XW, Li J, Shi XL. Interleukin-17A inhibits cell autophagy under starvation and promotes cell migration via TAB2/TAB3-p38 mitogen-activated protein kinase pathways in hepatocellular carcinoma. Eur Rev Med Pharmacol Sci.2016;20(2):250-63.

106. Zrihan-Licht S, Baruch A, Elroy-Stein O, Keydar I, Wreschner DH. Tyrosine phosphorylation of the MUC1 breast cancer membrane proteins. Cytokine receptor-like molecules. FEBS Lett. 1994 Dec 12;356(1):130-6.

ANNEXES

Les annexes regroupent nos travaux associés et/ou de collaboration liée à cette thèse :

1. article personnel sur les cancers du sein TN et leur hétérogénéité.
2. Article de collaboration sur MUC1-ARF dont nous avons mis au point l'immunohistochimie.
3. Quatre articles de notre équipe sur IL17/EGFR et cancer du sein TN.

Journal of Multidisciplinary Pathology

Open Access Research Article

Claudin-4 Immunohistochemical Expression Is an Independent Prognosis Factor in Triple-negative Breast Cancers

Christian Garbar,[1*] Oriane Dudez,[1] Sarah Mombelli,[2] Corinne Mascaux,[1] Aude-Marie Savoye,[2] and Hervé Curé[2]

[1] *Department of Biopathology and Oncology, Institut Jean Godinot – Unicancer, France*

[2] *Department of Oncology, Institut Jean Godinot – Unicancer, France*

***Corresponding author :**

Christian Garbar
Department of Biopathology and Oncology
Institut Jean Godinot-Unicancer
1 rue du Général Koenig CS80014
51726 Reims Cedex, France
E-mail: christian.garbar@reims.unicancer.fr

Received: 13 Aug 2014
Accepted: 04 Oct 2014
Published: 07 Oct 2014

Competing interests: The authors declare that no competing interests exist.

Access This Article

Abstract

Background: Evaluation of the clinical value of claudin-4 immunohistochemical staining for triple negative breast cancers.

Material and methodology: Histological material and clinical data of 70 patients with triple-negative breast cancers were available for this study. Thirteen patients died from breast carcinoma. Immunohistochemical analyses were performed using antibodies against estrogen receptors, progesterone receptors, androgen receptors HER2, EGFR, cytokeratin 5/6, cytokeratin14 and claudin-4. The mean of follow-up was 32.7 +/- 20.2 months. Statistical analysis was based on Kaplan-Meier survival probability curves.

Results: The survival curves of negative-claudin-4 and positive-claudin-4 breast tumours patients were significantly different (p = 0.01) confirming previous observations that loss of claudin-4 expression is associated with poor prognosis in triple-negative breast cancer. Although all non-basal triple-negative breast cancers (TnB) were stained by an anti- claudin-4 antibodies (n=12), distinct patterns of claudin-4 expression were observed among the basal-like TN (TB). We found that positive-claudin-4 TB(0.59 +/- 0.24 months) presented a better prognosis than negative-claudin-4 TB(0.40 +/- 0.17 months, p=0.004), as observed for the TnB (0.43 +/- 0.22 months, p = 0.02). We also demonstrated that negative-claudin-4 TB or TnB presented the same prognosis (p = 0.65).

Conclusions: Independently of AR expression results, negative-claudin-4 TB present the same poor prognosis than positive-claudin-4 TnB. Negative-claudin-4 TB could constitute a special type of TB presenting a poor clinical outcome.

Keywords: Biomarker, Triple negative, Breast cancer, Cancer therapy, Cancer prognosis, Targeted therapy, Immunohistochemistry

Introduction

Breast cancer is the most common cause of female cancer mortality despite a wide range of actual treatment regimens chosen according to the estrogens receptors (ER), progesterone receptors (PR), epidermal growth factor receptor type 2 (HER2) expression profiles of the patient.

A genetic classification proposed by Perou et al.[1-3] has recently been adopted by the St Gallen International Expert Consensus.[4] Briefly, this classification proposes five molecular subtypes: luminal A (ER+PR+HER2-, low Ki67 <14%), luminal B Her2 negative (ER+PR+HER-, high ki67 > 14%), luminal B Her2 positive (ER+PR+HER2+), HER2 surexpressed (ER-PR-HER2+) and triple negative carcinoma (ER-PR-HER2-). The patient outcome is particularly difficult to determinate within the heterogeneous triple-negative carcinoma category. Usually, 2 subgroups are classically described. The basal-like breast cancer (TB) stained with antibodies recognizing the epidermal growth factor receptor type 1 (EGFR), cytokeratin 5/6 or cytokeratin 14 and the non-basal-like triple negative breast carcinoma (TnB) in which none of these markers are detected.[5-9] The androgen receptors (AR) have been proposed as favourable prognostic factors in some cases of triple-negative breast cancers. Moreover, some authors suggest treating AR positive breast tumors with an anti-androgenic drug, usually given to treat prostate cancer.[10] Finally, as suggested by Perou et al., claudin proteins expression has been proposed as an important prognostic factor, in tumour called claudins low coming from progenitor cells.[11] Claudins are tight junction proteins contributing to cytoplasmatic membrane permeability (Figure. 01).

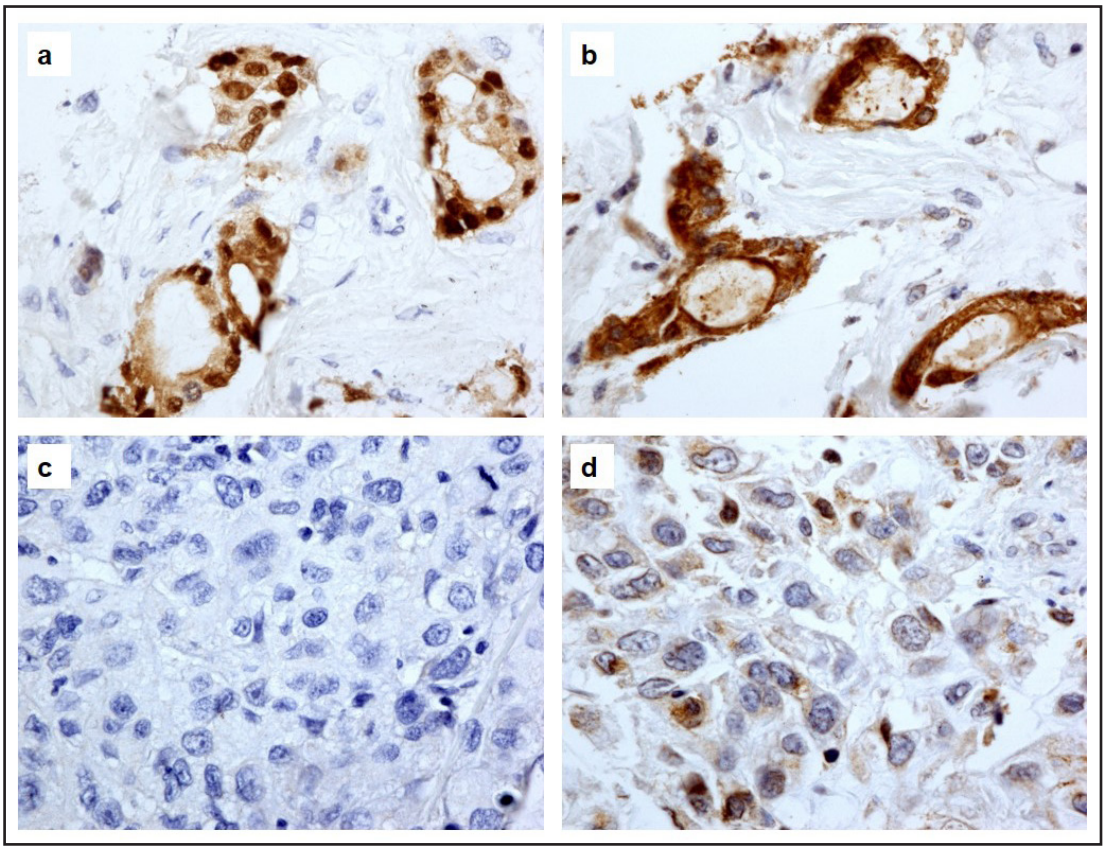

Figure. 01. *Anti-Androgen Receptors (AR) and anti-Claudin-4 immunohistochemistry on triple-negative basal-like carcinomas (TB).*

a and b : same case positive-AR(a) and positive-Claudin-4(b). AR is positive in nuclei and Claudin is positive in cytoplasm.

Cite as: Garbar C, Dudez O, Mombelli S, et al. Claudin-4 Immunohistochemical Expression Is an Independent Prognosis Factor in Triple-negative Breast Cancers. J Multidiscip Pathol. 2014;1(1):1-10.

c and d : same case negative-AR(c) and negative-Claudin-4 (d).
(Objective 40x)

In this study, we described the the expression of claudin-4 in TnB and TB and discussed its relevance for clinical prognosis.

Materials and methodology

Patient population

Between 2010 and 2012, archival paraffin embedded surgical materials and clinical data of 70 women (age: 60.9 +/- 13.7 years) presenting a triple negative breast cancer were available for this study. All cases were classified following the Perou's classification using a preliminary immunohistochemical study further confirmed by a tissue microarray (TMA). Finally the data included 58 TB, and 12 TnB.[1-3] Briefly, TB were negative for ER, PR, HER2 and positive for EGFR (52/58) or cytokeratin 5/6 (22/58) or cytokeratin 14 (28/58). The TnB were negative for EGFR, cytokeratin 5/6 and cytokeratin 14. All cases were also tested by in situ hybridization (FISH) with an HER2 probe in order to confirm the negative HER2 immunohistochemistry. Moreover, 16 patients (22.8%) presented lymph node metastasis and 12 (17.1%) had haematogenous metastasis (lung, liver and brain). Tumoral relapse was described for 16 (22.8%) patients. Thirteen patients died of breast cancer (18.5%). Twelve patients (17.1%) had neo-adjuvant chemotherapy and 56 patients (80.0%) received classical chemotherapy. Hormonotherapy or trastuzumab were not used. The mean of follow-up was 32.7+/- 20.2 months. Table. 01 presents the mains clinical and histological data of the patients and their tumours, respectively.

Luminal A (LumA), luminal B (LumB), and Her2 surexpressed (HER2) breast cancers were excluded from this study.

	TB	TnB	
N of case	58	12	p
Age (years)	61.5 +/- 13.9	58.1+/- 13.1	ns
Follow-up (months)	32.7 +/-20.7	33.7 +/- 18.4	ns
Tumor ize (mm)	25.7 +/- 13.9	18.2 +/- 7.2	ns
Tumoral relapse (%)	12 (20.7%)	4 (33.3%)	ns
Dead (%)	10 (17.2%)	3 (25.0%)	ns
T1	23 (39.7%)	8 (66.7%)	ns
T2	29 (50.1%)	4 (33.3%)	ns
T3 or more	6 (10.2%)	0 (0%)	ns
N1 or more	16 (27.8%)	1 (8.3%)	ns
M1	9 (16.1%)	3 (25.0%)	ns
SBR 1	0 (0%)	3 (25.0%)	0.01
SBR 2	6 (10.3%)	1 (14.3%)	ns
SBR 3	52 (89.7%)	3 (25.0%)	ns

Table. 01 *Clinical and immunohistological characteristics of each groups of Perou's classification.*

Cite as: Garbar C, Dudez O, Mombelli S, et al. Claudin-4 Immunohistochemical Expression Is an Independent Prognosis Factor in Triple-negative Breast Cancers. J Multidiscip Pathol. 2014;1(1):1-10.

TB = triple negative basal-like, TnB = triple negative non basal-like. TNM = 2009 UICC classification of malignant tumors, SBR = modified histological classification of Scarff-Bloom-Richardson. N of cases = number of cases, Age, follow-up and tumor size in mean +/-SD.

Histological procedures and tissue microarray (TMA) construction

All surgical specimens were initially fixed in 4% buffered formaldehyde solution between 8 to 48 hours, then imbedded in paraffin and sliced to 4 µm. The slides were stained with a classical hematoxylin-eosin stain to perform the initial diagnosis. A TMA paraffin receive-bloc was realized from these archival formol/paraffin blocs by an automated TMA device (Minicore2, Mitogen UK). Three distant core needle samples (needle core of 0.6 mm diameter) were chosen for each tumour paraffin donor-bloc. The TMA paraffin recipient bloc was cut in serial slides of 4 µm. The slides were consecutively stained by a classical hematoxylin-eosin stain and by different immunostainings.

Immunohistochemical methods

Immunohistological staining was performed using the Dako Autostainer Link 48® immunostaing system (Dako DK-2600 Glostrup, Denmark). After dewaxing, antigenic retrieval was performed using citrate buffered (pH 6) or EDTA buffered (pH 9) antigenic retrieval solution (EnVision Flex Target Retrieval solutions high and low pH, Dako) at 99°C. Endogen peroxydase was inhibited using a hydrogen peroxide phosphate buffered solution (EnVision Flex Peroxydase Blocking Reagent, Dako). After the incubation with primary antibodies, the immunological reaction was revealed by the peroxidase activity (EnVision DAB + chromogen, Dako) coupled to secondary antibodies (EnVision Flex HRP, Dako) Counterstain was realized using hematoxylin (EnVision Flex hematoxylin, Dako). Negative controls were obtained using mouse IgG1 (Negative Control Mouse IgG1, Dako) diluted at 1:100, in place of primary antibodies. Primary antibodies, dilutions and antigenic retrievals are described in Table. 02.

Immunohistochemistry classification

HER2 immunostaining were interpreted as positive according to the Guidelines of the College of American Pathologists.[12] Estrogens receptors (ER), progesterone receptors (PR) and androgen receptors (AR) were subsequently scored according the Allred score taking into account the intensity and proportion of the nuclear immunostaining.[13] Claudin-4 was identically scored but analysed in the cytoplasm. For negative results, a cut-off inferior or equal to 2 was considered as negative. According the St Gallien guideline,[4] all cases were classified following the Perou's classification.[1-2]

Fluorescent in situ Hybridisation (FISH)

HER2 positivity from TMA analysis was confirmed by a FISH technique using a HER2/C17 probe (Her2 FISH pharm DXTM, Dako), according the manufacture's instructions. In short, specimen was first denatured at 82°C for 5 minutes. The hybridisation was performed overnight at 45°C simultaneously for HER2/Texas Red labelled DNA probe and CEN-17/ FITC labelled DNA probe using a hybridizer device (Dako). Slides were washed in a stringent solution at 65°C for 10 minutes. We used a fluorescence microscope with appropriate filters (NIKON, Japan) to calculate the HER2/CEN-17 ratio according the Guidelines of the College of American Pathologists.[12]

Statistics

ANOVAs tests were performed for parametric results and Fisher's exact for non parametric data. Kaplan-Meier curves and Wilcoxon statistical tests were builded to evaluate the probability of breast cancer-specific survival curves. A p value <0.05 was considered significant. The WinSTAT 2012.1 (Fitch, Robert K®, Bad Krozingen, Germany) and Excel 2014 (Microsoft Corp., Redmond, Washington U.S.A.) programs were used

for statistical analysis.

This study was performed according the approval of an ethic committee and patients were informed and agreed to participate in this study.

Antibodies	Clone	Abbreviation	Manufacture	Dilution	Retrievial	Incubation (minutes)
Androgen Receptor	AR441	AR	Dako	1:20	EDTA, pH9	20
Claudine 4	N/A	Cl4	Spring	1:100	Citrate, pH6	20
Cytokeratin 14	LL002	Ck14	BioCare	1:50	EDTA, pH9	20
Cytokeratin 5/6	D5/16 B4	CK5/6	Dako	RTU	EDTA, pH9	20
EGFR wild-type	DAK-H1-WT	EGFR	Dako	1:200	EDTA, pH9	30
Estrogen Receptor alpha	SP1	ER	Dako	RTU	EDTA, pH9	20
HER2	c-erB-2	HER2	Dako	1:800	Citrate, pH6	30
Progesteron Receptor	PgR636	PR	Dako	RTU	EDTA, pH9	20

Table. 02 *Primary antibodies, dilution, antigenic retrieval, incubation times and abbreviations used in this study.*

Results

The Table. 01 and the Figure. 02 illustrated that TB and TnB were not positively correlated with the breast cancer-specific survival, nor the presence of lymph node, nor haematogenous metastasis.

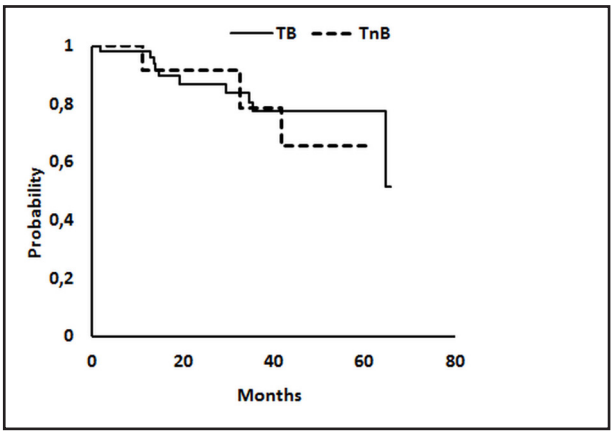

Figure. 02 *Comparison of specific breast cancer survival curves between TB and TnB following the Perou's classification of triple-negative breast cancers.*

No statistical significant difference was observed (p = ns)

Ten patients showed AR tumoral staining. As illustrated of the Figure. 03, the 5 years survival probability tends to be better for positive AR patients. Unfortunately this was not statistically significant (p = 0.61) : 0.48 +/- 0.20 for negative-AR (n=58/68) vs. 0.80 +/- 0.10 for positive-AR (n=10/68). Also, AR-positive TnB (n=3/12) seems to have a better prognosis than AR-negative TnB (n=8/12) : 5 years probability of survival respectively of 1.0 vs. 0.43 +/- 0.22 (p = ns). Moreover, the 5 years probability of survival of positive-AR TB (n=7/58) seems better than negative-AR TB (n=50/58), respectively, 0.66 +/- 0.27 vs 0.51 +/- 0.21 months (p=0.61). The number of positive-AR tumor was unfortunately too small to draw any conclusion.

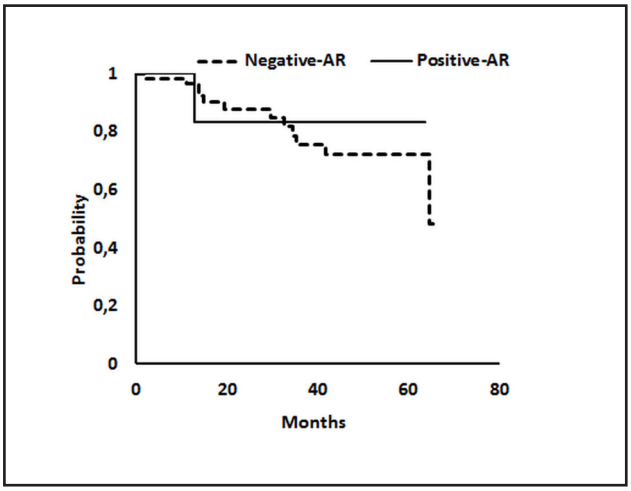

Figure. 03 *Comparison of specific breast cancer survival curves between positive-AR and negative-AR triple-negative breast tumours.*

No statistical significant difference was observed (p = ns)

Another biomarker studied in this study is claudin-4. In the all cases (n =70), negative-claudin-4 patients presented a significantly worse prognosis with a 5 years survival probability of 0.40 +/- 0.17 months for negative-claudin-4 (n=9) vs. 0.54 +/- 0.22 months for positive-claudin-4 (n=61), p = 0.01. This is illustrated in Figure. 04. All AR-positive TB (n=7/58) and all TnB (n =12/12) were also positive for claudin-4. Consequently, to avoid the bias of AR-positive tumour on the survival, TB (n=7) and AR-positive TnB (n=3) were discarded.

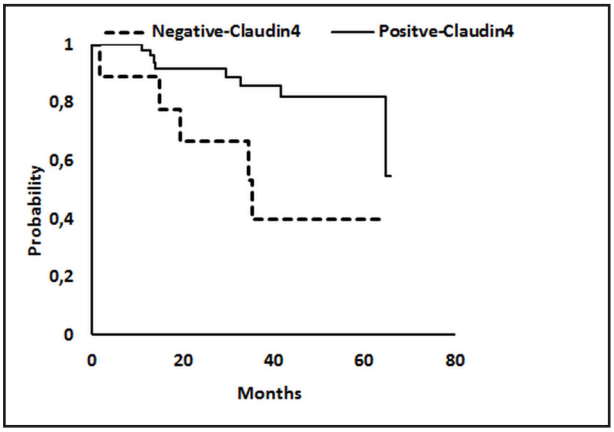

Figure. 04 *Comparison of specific breast cancer survival curves between positive-Claudin-4 and negative-Clau-*

din-4 triple-negative breast tumours.

There is a positive statistical difference (p = 0.01)

In Figure. 05, we found that positive-claudin-4 TB (n = 41/58) presented a better prognosis than negative-claudin-4 TB (n = 9/58, p=0.004) or TnB (n=8/58, p = 0.02), with a 5 years survival probability respectively of 0.59 +/- 0.24 vs 0.40 +/- 0.17 vs. 0.43 +/- 0.22 months (p = 0.005). We also demonstrated that negative-claudin-4 TB (n = 9/58, p=0.004) or TnB (n=8/58) presented the same prognosis (p = 0.65).

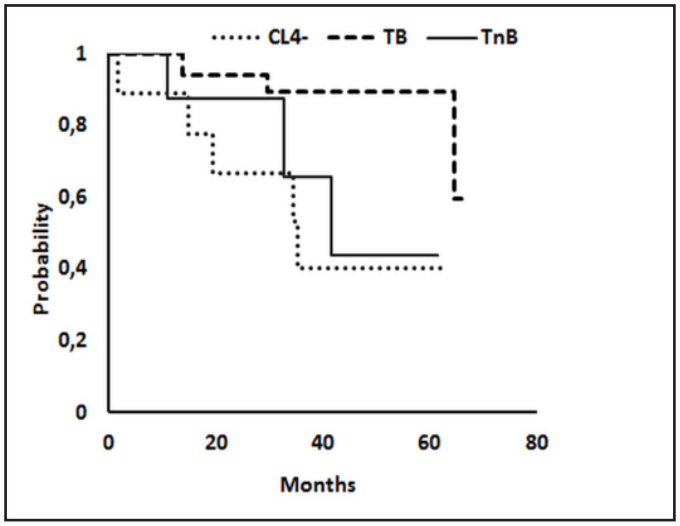

Figure. 05 *Comparison of specific breast cancer survival curves between negative-Claudin-4 TB and positive-Claudin-4 or TnB when positive-AR triple-negative breast cancers were discarded (see text).*

There is no statistical difference (p=ns) between negative-Claudin-4 TB (CL4-) and TnB (TnB) and a positive statistical difference between positive-Claudin-4 TB (TB) and negative-Claudin-4 TB (CL4-) (p = 0.005).

Discussion

Breast cancers are heterogeneous aggressive tumors implicating a difficult challenge to treat these patients. In the last past years, new biomarkers were developed in order to facilitate the choice of an appropriate drugs regimen. The expression of estrogens and progesterone receptors can, for example, indicates a potential effect of the corresponding hormonal inhibitors and the expression of HER2, on the other side, can be blocked by specific monoclonal antibodies. These three biomarkers are the basis of actual breast cancer classification described by Perou et al., wildly used in the clinical practice.[1-3] Unfortunately, about 20% of all breast tumours, called triple-negative breast carcinoma, don't express these molecules, leading to numerous difficulties to treat these patients.[14-17]

In routine practice, triple-negative breast cancers are divided into 2 groups, basal-like and non-basal-like, in agreement with the immunohistological detection of cytokeratin 5/6/14 or EGFR.[18] This classification does not allow identifying the patient with aggressive clinical outcome. Consequently, several authors suggested to change the Perou's classification of triple negative breast tumours in 5 or 7 different classes.[5,19-21] However, the clinical application of these new classifications is not obvious yet.

Herein, we demonstrated the clinically value of claudin-4 immunohistochemistry to discriminate a group of TB presenting a poor prognosis, independently of its AR hormonal status.

The favourable prognosis of tumour expressing AR is largely discussed in the literature. It is well-known that

AR is expressed simultaneously with ER in luminal breast cancers or in triple negative breast cancer with apocrine pattern.[10,22-24] Interestingly, Mc Ghan et al. suggested also that AR could be a potential therapeutic target.[25] This important role of AR in triple-negative breast carcinoma and its potential targeted treatment were largely debated in the literature.[25-31] Thike et al. showed a significantly better disease-free survival in positive-AR triple-negative tumors on a large series of 699 triple-negative invasive breast cancers.[26] Although this was not observed in our smaller series, both positive-AR TB and TnB tend to be of better prognosis than the negative-AR tumors.

Claudins are interesting makers originally described in the Perou's classification when considering the claudin low molecular pattern.[1,11] These proteins are major components of the tight junctions and the loss of their expression has been associated with malignancies.[31] Some authors reported the interest to perform immunohistochemistry to detect the claudin-low triple negative breast cancers.[32-33] Nevertheless, immunohistochemical studies over claudin-4 as a clinical prognosis factor in triple-negative breast cancers are still scarcely ever reported. Szasz et al. were the first to demonstrate the relationship between loss of claudin-4 and the poor prognosis of breast cancer. These authors showed that negative-claudin-4 breast cancer had more lymph node metastasis and a poor prognosis than positive-claudin-4 tumours.[34-38] These observations were confirmed by other studies illustrating that the claudin-low group of basal-like triple-negative breast cancer was strongly associated with tumour relapse.[20,31] More recently, Kolokytha et al. demonstrated the favourable prognosis of triple-negative carcinomas expressing claudin-4.[39] Our study confirms also these observations and suggests, in addition, that negative-claudin-4-negative TB show a poor breast cancer-specific survival curves. Those could constitute a new poor prognosis group of TB. A larger prospective series will be necessary to confirm our hypothesis and the clinical usefulness of this potential group. More recently, a subgroup of triple-negative breast carcinoma, negative for ER, PR, HER2, EGFR and cytokeratin 5/6, called quintuple-negative breast cancers, was also reported to present a poor prognosis.[40] In fact, this subgroup of triple-negative breast cancers corresponds to the triple-negative non basal-like cancers described in the Perou's classification (TnB). We demonstrated that despite the positive expression of claudin-4, all TnB patients showed a poor 5 years survival prognosis, independently of their AR hormonal status. This prognosis is quite similar than those of the negative-claudin-4 TB.

In conclusion, negative-Claudin-4 TB present the same poor prognosis than positive-claudin-4 TnB. Future studies will be necessary to confirm that negative-claudin-4 TB could be considered as a special type of TB, presenting a poor clinical outcome.

References

1. Perou CM. Molecular stratification of triple-negative breast cancers. Oncologist. 2010;16:39-48.
2. Strehl J, Wachter D, Fasching P, et al. Invasive breast cancer: recognition of molecular subtypes. Breast Care. 2011;6(4):256-264.
3. Won JR, Gao D, Chow C, et al. A survey of immunohistochemical biomarkers for basal-like breast cancer against a gene expression profile gold standard. Mod Pathol. 2013;26(11):1438-1450.
4. Goldhirsch A, Winer E, Coates A, et al. Personalizing the treatment of women with early breast cancer: highlights of the St Gallen Internalional Expert Consensus on the primary therapy of early breast cancer 2013. Ann Oncol. 2013;24(9):2206-2223.
5. Masuda H, Zhang D, Bartholomeusz C, et al. Role of epidermal growth factor receptor in breast cancer. Breast Cancer Res Treat. 2012;136(2):331-345.

Cite as: Garbar C, Dudez O, Mombelli S, et al. Claudin-4 Immunohistochemical Expression Is an Independent Prognosis Factor in Triple-negative Breast Cancers. J Multidiscip Pathol. 2014;1(1):1-10.

6. Rakha E, El-Sayed M, Reis-Filho J, et al. Patho-biological aspects of basal-like breast cancer. Breast Cancer Res Treat. 2009;113(3):411-422.
7. Ishikawa Y, Horiguchi J, Toya H, et al. Triple-negative breast cancer: histological subtypes and immunohistochemical and clinicopathological features. Cancer Sci 2011;102(3):656-662.
8. Sousa B, Paredes J, Milanezi F, et al. P-cadherin, vimentin and CK14 for identification of basal-like phenotype in breast carcinomas: an immunohistochemical study. Histol Histopathol. 2010;25(8):963-974.
9. Nassar A, Sussman ZM, Lawson D, et al. Inference of the Basal epithelial phenotype in breast carcinoma from differential marker expression, using tissue microarrays in triple negative breast cancer and women younger than 35. Breast J. 2012;18(5):399-405
10. Niemeier LA, Dabbs DJ, Beriwal S, et al. Androgen receptor in breast cancer: expression in estrogen receptor-positive tumors and in estrogen receptor-negative tumors with apocrine differentiation. Mod Pathol. 2010;23(2):205-212.
11. Harrell JC, Pfefferie AD, Zalles N, et al. Endothelial-like properties of claudin-low breast cancer cells promote tumor vascular permeability and metastasis. Clin Exp Metastasis. 2014;31(1):33-45.
12. Wolff AC, Hammond ME, Schwartz JN, et al. American Society of Clinical Oncology/College of American Pathologists guideline recommendations for human epidermal growth factor receptor 2 testing in breast cancer. J Clin Oncol. 2007;131(1):18-43.
13. Allred DC, Havey JM, Berardo M, et al. Prognostic and predictive factors in breast cancer by immunohistochemical analysis. Mod Pathol. 1998;11(2):155-68.
14. Lehmann BD, Bauer JA, Chen X, et al. Identification of human triple-negative breast cancer subtypes and preclinical models for selection of targeted therapies. J Clin Invest. 2011;121(7):2750-2767.
15. Burstein HJ. Patients with triple negative breast cancer: Is there an optimal adjuvant treatment? The breast. 2013;22S2:S147-S148.
16. Boisserie-Lacroix M, Macgrogan G, Debled M, et al. Triple-negative breast cancers: associations between imaging and pathological findings for triple-negative tumors compared with hormone receptor-positive/human epidermal growth factor receptor-2-negative breast cancer. Oncologist. 2013;18(7):802-811.
17. Rakha E, Reis-Filho J. Basal-like breast carcinoma. Arch Pathol Lab Med. 2009;133:860-868.
18. Cheang MC, Voduc D, Bajdik C, et al. Basal-like breast cancer defined by five biomarkers has superior prognostic value than triple-negative phenotype. Clin Cancer Res. 2008;14(5):1368-1376.
19. Miyashita M, Ishida T, Ishida K, et al. Histopathological subclassification of triple negative breast cancer using prognostic scoring system: five variables as candidates. Virschows Arch. 2011;458(1):65-72.
20. Choi J, Jung WH, Koo JS. Clinicopathologic features of molecular subtypes of triple negative breast cancer based on immunohistochemical markers. Histol Histopathol. 2012;27(11):1481-1493.
21. Masuda H, Baggerly KA, Wang Y, et al. Differential Response to Neoadjuvant Chemotherapy Among 7 Triple-Negative Breast Cancer Molecular Subtypes. Clin Cancer Res. 2013;19(19):5533-5540.
22. Park S, Koo J, Park HS, et al. Expression of androgen receptors in primary breast cancer. Ann Oncol. 2010;21(3):488-492.
23. Alshenawy HA. Prevalence of androgen receptors in invasive breast carcinoma and its relation with estro-

gen receptor, progesterone receptor and Her2/neu expression. J Egypt Natl Canc Inst. 2012;24(2):77-83.

24. McNamara KM, Yoda T, Miki Y, et al. Androgenic pathway in triple negative invasive ductal tumors: its correlation with tumor cell proliferation. Cancer Sci. 2013;104(5):639-646.

25. McGhan LJ, McCullough AE, Protheroe CA, et al. Androgen Receptor-Positive Triple Negative Breast Cancer: A Unique Breast Cancer Subtype. Ann Surg Oncol. 2014;21(2):361-367.

26. Thike AA, Yong-Zheng Chong L, Cheok PY, et al. Loss of androgen receptor expression predicts early recurrence in triple-negative and basal-like breast cancer. Mod Pathol. 2014;27:352-60

27. Masuda H, Baggerly KA, Wang Y, et al. Differential Response to Neoadjuvant Chemotherapy Among 7 Triple-Negative Breast Cancer Molecular Subtypes. Clin Cancer Res. 2013;19(19):5533-5540.

28. Guarneri V, Dieci MV, Conte P. Relapsed triple-negative breast cancer: challenges and treatment strategies. Drugs. 2013;73(12):1257-1265.

29. Sutton LM, Cao D, Sarode V, et al. Decreased androgen receptor expression is associated with distant metastases in patients with androgen receptor-expressing triple-negative breast carcinoma. Am J Clin Pathol. 2012;138(4):511-516.

30. McNamara KM, Yoda T, Takagi K, et al. Androgen receptor in triple negative breast cancer. J Steroid Biochem Mol Biol. 2013;133:66-76.

31. Lu S, Singh K, Mangray S, et al. Claudin expression in high-grade invasive ductal carcinoma of the breast: correlation with the molecular subtype. Mod Pathol. 2013;26(4):485-495.

32. Ricardo S, Gerhard R, Cameselle-Teijeiro JF, et al. Claudin expression in breast cancer: high or low, what to expect? Histol Histopathol. 2012;27:1283-1295.

33. Gerhard R, Ricardo S, Albergaria A, et al. Immunohistochemical features of claudin-low intrinsic subtype in metaplastic breast carcinomas. Breast 2012;21(3):354-360.

34. Szász MA. Claudins as prognostic factors of breast cancer. Magy Onkol. 2012;56(3):209-212.

35. Szasz AM, Nemeth Z, Gyorffy B, et al. Identification of a claudin-4 and E-cadherin score to predict prognosis in breast cancer. Cancer Sci. 2011;102(12):2248-2254.

36. Szasz AM, Tokes AM, Micsinai M, et al. Prognostic significance of claudin expression changes in breast cancer with regional lymph node metastasis. Clin Exp Metastasis. 2011;28(1):55-63.

37. Blanchard AA, Skliris GP, Watson PH, et al. Claudins 1, 3, and 4 protein expression in ER negative breast cancer correlates with markers of the basal phenotype. Virchows Arch. 2009;454(6):647-656.

38. Kulka J, Szász AM, Németh Z, et al. Expression of tight junction protein claudin-4 in basal-like breast carcinomas. Pathol Oncol Res. 2009;15(1):59-64.

39. Kolokytha P, Yiannou P, Keramopoulos D, et al. Claudin-3 and Claudin-4 : distinct prognostic significance in triple-negative and luminal breast cancer. Appl Immunohistochem Mol Morphol. 2014;22(2):125-131.

40. Choi YL, Oh E, Park S, et al. Triple-negative, basal-like, and quintuple-negative breast cancers: better prediction model for survival. BMC Cancer. 2010;23:507.

Cite as: Garbar C, Dudez O, Mombelli S, et al. Claudin-4 Immunohistochemical Expression Is an Independent Prognosis Factor in Triple-negative Breast Cancers. J Multidiscip Pathol. 2014;1(1):1-10.

PLOS ONE

RESEARCH ARTICLE

MUC1-ARF—A Novel MUC1 Protein That Resides in the Nucleus and Is Expressed by Alternate Reading Frame Translation of MUC1 mRNA

Michael Chalick[1☯], Oded Jacobi[1☯], Edward Pichinuk[1], Christian Garbar[2], Armand Bensussan[3], Alan Meeker[4], Ravit Ziv[1], Tania Zehavi[5], Nechama I. Smorodinsky[1], John Hilkens[6], Franz-Georg Hanisch[7], Daniel B. Rubinstein[8], Daniel H. Wreschner[1]*

1 Department of Cell Research and Immunology, Tel Aviv University, Ramat Aviv, Israel, **2** Department of Biopathology, Institut Jean-Godinot, Reims Cedex, France, **3** INSERM U976, Hôpital Saint Louis, Paris, France, **4** The Johns Hopkins University School of Medicine, Baltimore, Maryland, United States of America, **5** Department of Pathology, Meir Medical Center, Kfar Saba, Israel, **6** Division of Molecular Genetics, The Netherlands Cancer Institute, Amsterdam, The Netherlands, **7** Institute of Biochemistry II, Medical Faculty, University of Cologne, Köln, Germany, **8** BioModifying LLC, Silver Spring, Maryland, United States of America

☯ These authors contributed equally to this work.
* danielhw@post.tau.ac.il

Citation: Chalick M, Jacobi O, Pichinuk E, Garbar C, Bensussan A, Meeker A, et al. (2016) MUC1-ARF—A Novel MUC1 Protein That Resides in the Nucleus and Is Expressed by Alternate Reading Frame Translation of MUC1 mRNA. PLoS ONE 11 (10): e0165031. doi:10.1371/journal.pone.0165031

Editor: Surinder K. Batra, University of Nebraska Medical Center, UNITED STATES

Received: December 20, 2015

Accepted: October 5, 2016

Published: October 21, 2016

Data Availability Statement: All relevant data are within the paper.

Funding: This work was supported by Israel Science Foundation Grant 1167/10, http://www.isf.org.il/english/; and Israel Cancer Association 20112024, http://en.cancer.org.il/. The funders had no role in study design, data collection and analysis, decision to publish, or preparation of the manuscript. The author Dr. Daniel B. Rubinstein (DBR) is affiliated with BioModifying LLC, Silver Spring, Maryland, who provided partial support in

Abstract

Translation of mRNA in alternate reading frames (ARF) is a naturally occurring process heretofore underappreciated as a generator of protein diversity. The *MUC1* gene encodes MUC1-TM, a signal-transducing trans-membrane protein highly expressed in human malignancies. Here we show that an AUG codon downstream to the MUC1-TM initiation codon initiates an alternate reading frame thereby generating a novel protein, MUC1-ARF. MUC1-ARF, like its MUC1-TM 'parent' protein, contains a tandem repeat (VNTR) domain. However, the amino acid sequence of the MUC1-ARF tandem repeat as well as N- and C-sequences flanking it differ entirely from those of MUC1-TM. In vitro protein synthesis assays and extensive immunohistochemical as well as western blot analyses with MUC1-ARF specific monoclonal antibodies confirmed MUC1-ARF expression. Rather than being expressed at the cell membrane like MUC1-TM, immunostaining showed that MUC1-ARF protein localizes mainly in the nucleus: Immunohistochemical analyses of MUC1-expressing tissues demonstrated MUC1-ARF expression in the nuclei of secretory luminal epithelial cells. MUC1-ARF expression varies in different malignancies. While the malignant epithelial cells of pancreatic cancer show limited expression, in breast cancer tissue MUC1-ARF demonstrates strong nuclear expression. Proinflammatory cytokines upregulate expression of MUC1-ARF protein and co-immunoprecipitation analyses demonstrate association of MUC1-ARF with SH3 domain-containing proteins. Mass spectrometry performed on proteins coprecipitating with MUC1-ARF demonstrated Glucose-6-phosphate 1-dehydrogenase (G6PD) and Dynamin 2 (DNM2). These studies not only reveal that the *MUC1* gene generates a previously unidentified MUC1-ARF protein, they also show that

the form of funds for research materials only. BioModifying did not have any additional role in the study design, data collection and analysis, decision to publish, or preparation of the manuscript.

Competing Interests: The commercial affiliation of DBR does not alter our adherence to all PLOS ONE policies on sharing data and materials.

just like its 'parent' MUC1-TM protein, MUC1-ARF is apparently linked to signaling and malignancy, yet a definitive link to these processes and the roles it plays awaits a precise identification of its molecular functions. Comprising at least 524 amino acids, MUC1-ARF is, furthermore, the longest ARF protein heretofore described.

Introduction

Any AUG codon within a given mRNA sequence may potentially function as an initiation site for translation, provided that it is located within an appropriate extended nucleotide sequence context that can support translational initiation. Specifically, an in-frame N-terminally extended protein can be generated by translation initiated by an in-frame AUG start codon located 5' to a downstream start codon. Accordingly, deep proteome analyses have identified at least sixteen novel AUG start sites that give rise to N-terminally extended protein variants, in addition to four translated upstream ORFs [1]. Alternatively, start codons appearing at additional sites within the mRNA sequence can initiate mRNA translation in alternate reading frames (ARFs) yielding a peptide sequence differing entirely from the 'parent' protein product [2].

In viruses, utilization of alternate reading frames contributes to diversification of the protein repertoire that can be generated from the viral genome, whilst at the same time keeping it compact[3]. In contrast to viruses, in eukaryotic organisms and in humans in particular there have been relatively few definitive reports of translation in alternate reading frames yielding proteins differing from their 'parent' proteins [4–7]. The best-defined eukaryotic ARF protein studied thus far derives from the INK4-ARF locus, which generates two alternative transcripts that use different alternate frames of a constitutive exon to encode the tumor suppressor proteins $p16^{INK4a}$ and $p19^{ARF}$ [8]. These proteins inhibit cyclin dependent kinases (CDK4 and CDK6), thereby preventing phosphorylation and allowing the non-phosphorylated RB proteins to act as suppressors of cell growth [9]. Interestingly, the corresponding 'parent' protein $p16^{INK4A}$ and the alternatively translated $p19^{ARF}$ both act in shared pathways of tumor suppression.

Additional examples of well-defined ARF proteins include those derived from the mRNAs coding for the stimulatory G-protein specific to neuroendocrine cells (termed ALEX) [10, 11] and MASK-BP3 [12]. Despite their completely different amino acid sequences, functions mediated by these pairs of 'parent' and ARF proteins are intimately intertwined and also involve physical interaction between the 'parental' and the ARF proteins. In contrast to the limited number of well-characterized ARF proteins generated from the mammalian genome as described above, a recent publication suggests that translation in an alternate reading frame may, to the contrary, be much more prevalent than previously anticipated [2].

MUC1, a gene recognized for more than two decades, is clearly related to a malignant cell phenotype [13–15]. Its major protein product, the transmembrane MUC1-TM protein, is highly expressed over the entire cell surface of tumor cells from a variety of epithelial malignancies, whereas in normal epithelial cells its expression is not only considerably lower but is also restricted solely to the apical surface of epithelial cells that form luminal structures [16]. We demonstrate here for the first time that translation in an alternative reading frame of mRNA coding for MUC1-TM yields a novel protein, here designated MUC1-ARF. MUC1-ARF comprises an amino acid sequence entirely different from that of MUC1-TM and represents the largest eukaryotic protein derived from translation of an mRNA in an alternate reading frame reported to date. In contrast to localization of MUC1-TM on the cell surface, MUC1-ARF

locates primarily to the cell nucleus. Luminal epithelial cells of tissues such as pancreas and kidney, which normally express significant levels of MUC1-TM also express MUC1-ARF, while tissues that express low levels of MUC1-TM such as breast luminal-forming epithelial cells express very low levels of MUC1-ARF. In contrast, many breast cancers express MUC1-TM at high levels and of these, a discrete subset shows high MUC1-ARF expression. We show here that functionally, MUC1-ARF interacts with signaling proteins, including those comprising SH3 domains and mass spectrometry showed coprecipitation of MUC1-ARF with G6PD and Dynamin 2. While suggestive of a link between MUC1-ARF, signaling, and malignancy, definitive demonstration of such a link awaits identification of MUC1-ARF's precise function. In summary, the studies presented here demonstrate that the *MUC1* gene generates the novel MUC1-ARF protein by translation of MUC1 mRNA in an alternate reading frame. Moreover, MUC1-ARF is, to our knowledge, the longest ARF protein heretofore described.

Materials and Methods

Cell lines and cell culture

DA3-TM mouse mammary tumor cells transfected with, and expressing cDNA coding for full-length MUC1-TM [17], DA3-PAR non-transfected parental DA3 cells [17], human breast carcinoma cell lines T47D and ZR75 [17], and human pancreatic carcinoma cell line Colo357 [17] were grown in Dulbecco's Modified Eagle's Medium (DMEM), RPMI and DMEM: F12 (1:1) culture media. Human cell lines were authenticated by Short Tandem Repeat (STR) analysis (PowerPlexW 1.2 System, Promega, WI, US) and the STR profiles were matched to the German Collection of Microorganisms and Cell Cultures (DSMZ) database. Prior to treatment with cytokine, Colo357 cells were incubated in serum-free medium for 24 hrs. Cells were then treated at the following concentrations: IL-1beta (20ng/ml), IL-6 (40 ng/ml), TNF-alpha (20 ng/ml), or Interferon-gamma (10 ng/ml).

Whole cell lysates

Cells were washed with PBS, scraped from culture flasks and pelleted. Two volumes of cold lysis buffer [50mM Tris, 100mM NaCl, 1% Triton X-100 + protease inhibitor cocktail (Sigma)] were added to the cell pellet followed by incubation on ice for 30 minutes and centrifuged for 20 minutes at 12000 RPM. Concentration of protein samples were determined by BCA assay.

Nuclear and cytoplasmic lysates

Cell pellets were resuspended in extraction buffer [0.3M sucrose, 50mM Tris pH7.4 +protease inhibitor cocktail (Sigma)] and disrupted by 10 freeze and thaw cycles on dry ice. This was followed by centrifugation 20 minutes at 14000 rpm, and the supernatant collected as the cytoplasmic protein solution. The pellet was suspended in nuclear extraction buffer ([50mM Tris, 100 mM NaCl, 1% Triton X-100 + protease inhibitor cocktail (Sigma)] and sonicated for 30 seconds with a 1 minute rest 10 times at power setting 5. This was followed by centrifugation at 14,000 rpm for 20 minutes at 4°C, with the supernatant representing the nuclear protein solution.

Immunization of mice and generation of hybridomas

Mice were immunized with MUC1-ARF peptide conjugated to KLH. The MUC1-ARF peptide used for immunization comprised 1.3 repeats of the MUC1-ARF repeat unit, PQPTVSPRPRTPGRPRAPPP-PQPTVS- (one 20 amino acid long repeat is underlined and six amino acids of the following repeat is double-underlined). Use of animals was performed

under the supervision of Tel Aviv University Institutional Animal Care and Use Committee (TAU-IACUC), License number L-08-026. Animal welfare and steps taken to ameliorate suffering including methods of sacrifice were all performed in accordance with regulations stipulated by TAU-IACUC. Following immunization, samples of polyclonal sera were taken and antibody titers assessed using an ELISA assay wherein BSA-MUC1-ARF peptide was coated onto the well surface of 96 well plates. Spleen cells from immunized mice were fused with mouse myeloma NS0 and selected in HAT medium according to the standard protocol.

Three-tiered screening for selection of anti-MUC1-ARF monoclonal antibodies

The primary screen of the hybridomas was performed by assessing antibody present in hybridoma supernatants binding to MUC1-ARF peptide. Positive hybridomas were then submitted to a secondary screen wherein hybridoma supernatants were assessed for binding by western blot analysis using lysates from MUC1 transfected cells. Hybridomas that were positive on both the primary and secondary screens were finally assessed using immunofluorescence assay on DA3 mouse cells that do not express human MUC1 (as negative control), and on stable DA3 transfectants expressing human MUC1. Hybridomas secreting antibody that scored positive in all three screens were subsequently cloned by repeated limiting dilution until a stable clone was obtained.

Immunofluorescence—Cells (50,000 cells per well) were seeded on glass cover-slips in 24-well culture plates. The next day, cells were rinsed with ice-cold PBS and fixed with 100% methanol for 5 min at -20°C followed by permeabilization with methanol/acetone (1:1). The cells were subjected to immunofluorescence staining with primary antibody for 1h at room temperature, then washed and incubated with fluorescently-labeled secondary antibody at room temperature for an additional 1 h. The cells were examined by fluorescence confocal microscopy.

Immunohistochemistry

Tissue microarrays were purchased from US Biomax, Inc. URL- http://biomax.us. Tissue sections (paraffin embedded, 5 microns in thickness) were deparaffinized followed by rehydration. Automated Immunological stains were performed with the Dako Autostainer Link 48 (Dako) according to the manufacturer's instructions. Antigen retrieval was done using citrate buffer for 30 minutes at room temperature, or at alkaline pH (Tris-EDTA, pH9.0) for the anti-MUC1-ARF antibodies. Endogenous peroxidase activity was blocked with EnVision Flex Peroxidase Blocking Reagent (Dako) for 30 minutes, followed by incubation with primary antibody (5microgram/ml) for 120 minutes. The immunological reaction was revealed by means of polymer dextran coupled with peroxidase molecule and secondary antibodies for 15 minutes (EnVision-Flex /HRP, Dako) and diaminobenzidine for 10 minutes (DakoCytomation). Counterstain was carried out with hematoxylin for 10 minutes.

Immunoprecipitation and mass spectrometry analyses

Cell lysates prepared from MCF7 breast cancer cells that endogenously express MUC1-ARF were subjected to immunoprecipitation using ProteinA/ProteinG agarose beads (Santa Cruz Biotechnology, catalog number sc-2002) to which the monoclonal antibody MPR2G10 had been prebound. Following extensive washing of the beads, bound proteins underwent trypsin digestion. Liquid chromatography–tandem mass spectrometry (LC–MS/MS) was performed using a 15 cm reversed-phase fused-silica capillary column (inner diameter, 75 um) made in-house and packed with 3 um ReproSil-Pur C18AQ media (Dr. Maisch HPLC GmbH).The LC

system, an UltiMate 3000 (Dionex) was used in conjunction with an LTQ Orbitrap XL (Thermo Fisher Scientific) operated in the positive ion mode and equipped with a nanoelectrospray ion source. Peptides were separated with a four hour gradient from 5 to 65% acetonitrile (buffer A, 5% acetonitrile, 0.1% formic acid and 0.005% TFA; buffer B, 90% acetonitrile, 0.2% formic acid and 0.005%TFA). The voltage applied to the union to produce an electrospray was 1.2 kV. The mass spectrometer was operated in the data-dependent mode. Survey mass spectrometry scans were acquired in the Orbitrap with the resolution set to a value of 60,000. The seven most intense ions per scan were fragmented and analyzed in the linear ion trap. Raw data files were searched with MASCOT (Matrix Science) against a Swissprot database. Search parameters included a fixed modification of 57.02146 Da (carboxyamidomethylation) on Cys, and variable modifications 15.99491 Da (oxidation) on Met, and 0.984016 Da (deamidation) on Asn and Gln. The search parameters also included: maximum 2 missed cleavages, initial precursor ion mass tolerance 10 ppm, fragment ion mass tolerance 0.6 Da. Samples were further analyzed in Scaffold (Proteome software).

Flow cytometry

After trypsinization, cells were washed, and mouse 2G10 antibody, with or without competitor peptide was added for 1 hour at 4°C. Following washing with flow cytometry (FACS) buffer, fluorescein labeled goat anti-mouse IgG antibody was added for 45 minutes at 4°C. Detection of bound IgG was by flow cytometry on a FACSCalibur™ (Becton Dickinson).

Sandwich ELISA for determining MUC1-ARF/MUC1-TM levels

Elisa Immunoassay plates (CoStar) were coated with either MPR-2G10 mAb or with H23 mAb for detection of MUC1-ARF or MUC1-TM respectively, followed by blocking. Cell lysates at 1mg/ml protein concentration were then applied to the wells followed by adding anti-MUC1-ARF monoclonal antibody MPR-4B3, or anti-MUC1-TM monoclonal antibody H23, both conjugated to biotin. Detection of MUC1-ARF binding was performed by horseradish peroxidase (HRP)-conjugated to streptavidin. The results were calculated as an average of 3 experiments, performed in triplicates.

In vitro transcription and translation

In vitro transcription and translation reactions were performed as previously described [18] and in vitro translation products were analyzed on standard SDS-polyacrylamide gels.

Results

Translation of MUC1-TM mRNA results in synthesis of both MUC1-TM 'parent' protein and an alternately-read MUC1-ARF protein

Translation of mRNA transcribed from MUC1 cDNA comprising one 60 nucleotide repeat unit revealed the expected MUC1-TM protein products, namely uncleaved MUC1 alpha-beta indicated by unfilled arrow-head, the MUC1-TM alpha-subunit indicated by [alpha, black diamond], and the C-terminal MUC1-TM beta-subunit indicated by [beta, unfilled arrow] (Fig 1A, lanes 1–3, and Fig 1B, lanes 1 and 2). The MUC1 mRNA used here for the in vitro translation assays contained only a single 60 nucleotide repeat unit, as compared to the 15–125 tandem repeat units present in naturally occurring MUC1 mRNA, thus explaining the relatively low molecular masses observed in the in-vitro translation assays both for the MUC1 alpha-beta parental protein and the MUC1-TM alpha-subunit. That the band labeled by [alpha, black diamond] is in fact the N-terminal MUC1-TM alpha-subunit has been previously unequivocally

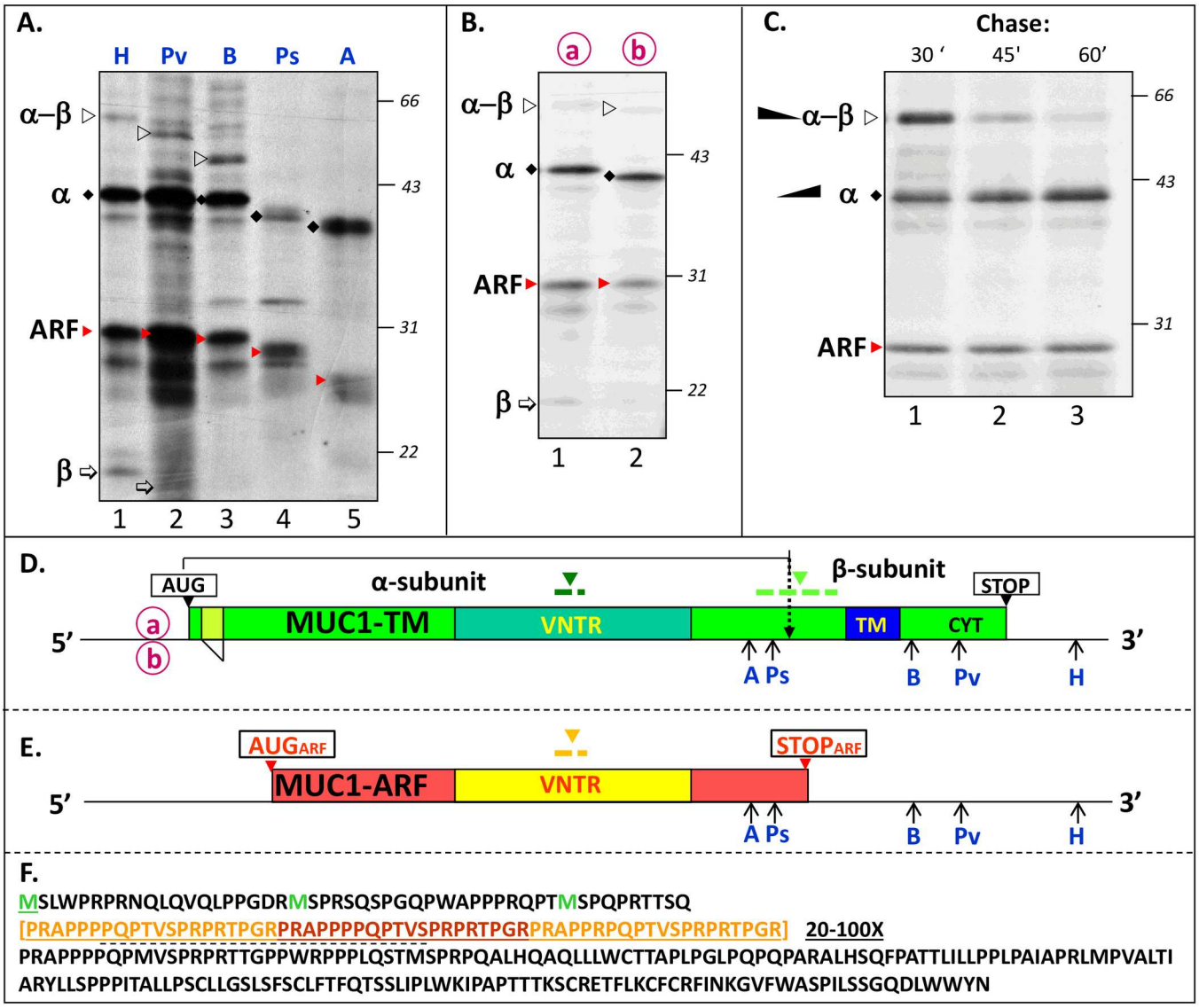

Fig 1. In vitro translation of MUC1 mRNA yields both MUC1-TM protein and MUC1-ARF protein. (A) RNAs transcribed from MUC1 cDNA [comprising a single 60 nucleotide (20 amino acid) repeat unit] cut with HindIII, PvuII, BalI, PstI or AccI (H, Pv, B, Ps and A, lanes 1–5 respectively, see Fig 1D and E) were translated in vitro with [^{35}S]-methionine and [^{35}S] cysteine and the products resolved by SDS-PAGE. Molecular masses of protein markers run in a parallel gel are indicated to the right of the autoradiogram, and are also shown in (B) and (C). (B) MUC1 mRNAs circled in red lettering a and b, that differ from each other by 27 nucleotides downstream from the MUC1-TM initiation codon (Fig 1D, a and b) were translated in vitro with [^{35}S]-methionine and [^{35}S]-cysteine and the products resolved by SDS-PAGE. (C) MUC1 mRNA containing a single 20 amino acid repeat was translated for 30 minutes in an in vitro reticulocyte protein translation system with [^{35}S]-methionine and [^{35}S]-cysteine and labelled proteins chased with an excess of unlabeled methionine and cysteine. Samples were removed (times indicated) and resolved by SDS-PAGE. (D) Locations of the initiating (AUG) and terminating (STOP) codons in the MUC1 mRNA driving translation of MUC1-TM are as indicated. The TransMembrane (TM) and cytoplasmic (CYT) domains, Variable Number of Tandem Repeats (VNTR) of MUC1-TM are as indicated. (E) MUC1-ARF, lacking these domains, is shown by VNTR (yellow color) flanked by 5' and 3' domains (red color). The initiation and stop codons (AUGARF and STOPARF) are shown (boxed). Regions bound by anti-MUC1-TM tandem repeats antibodies, anti-MUC1-ARF tandem repeats antibodies and anti-MUC1-SEA module antibodies (in MUC1-TM) are indicated by downward facing dark green, orange and light green arrowheads, respectively. (F) Amino acid sequence of MUC1-ARF. The MUC1-ARF twenty amino-acid-long repeat sequence is shown as three repeats (light and dark brown fonts) whereas in the actual MUC1-ARF protein the number of repeats may vary between fifteen and one hundred twenty five. The peptide sequence used for generating anti-MUC1-ARF monoclonal antibodies is underlined (dashed).

doi:10.1371/journal.pone.0165031.g001

demonstrated [18]. Specifically, (i) it is *not* radioactively labeled when cysteine is used as the sole radioactive amino acid in the in-vitro translation reaction [see Fig 1 in [18]], in accord with the absence of cysteine residues in the MUC1-TM alpha-subunit and (ii) as expected for the MUC1-TM alpha-subunit formed by the ongoing cleavage within the MUC1 SEA module, in a pulse chase experiment the intensity of the [alpha, black diamond] band increases with the efflux of time [Fig 1C, and see Fig 1 in [18]]. The band migrating with a molecular mass of about 20kDa and here indicated by [beta, unfilled arrow] (Fig 1A, lanes 1 and 2, and Fig 1B, lanes 1 and 2) has been previously unambiguously identified as the MUC1-TM beta-subunit [18] and reconfirmed here, because (i) the 20kDa band is absent following translation of a MUC1 mRNA truncated at both the Pst1 and Acc1 sites that are located upstream to the N-terminus of the region coding for the MUC1-TM beta-subunit [compare Fig 1A, lanes 4 and 5 with Fig 1A lane 1, and see Fig 1 in [18]], and (ii) during the chase period of a pulse-chase experiment the levels of this protein also increase with time as does the MUC1-TM alpha-subunit [see Fig 1 in [18]]. Note that translation of MUC1 mRNA truncated at the PvuII site (see Fig 1D for the location of the PvuII site within the region coding for the cytoplasmic domain of the MUC1-TM beta-subunit) leads to a faster migrating band representing the curtailed MUC1-TM beta-subunit (Fig 1A, compare lane 2 with lane 1), whereas no alternative fragment was observed following translation of MUC1 mRNA truncated at the BalI site (Fig 1A, lane 3). This is because the fragment of the MUC1-TM beta-subunit derived from translation of MUC1 mRNA truncated at the BalI site is much shortened and therefore likely comigrates with the globin present in great amounts in the reticulocyte lysate. In order to allow for better resolution of the MUC1 alpha-beta parental protein, the MUC1-TM alpha-subunit and the MUC1-ARF protein (see below), electrophoresis in Fig 1C was performed for an extended period of time leading to elution from the gel of the small MUC1-TM beta-subunit.

Unexpectedly, following in-vitro translation of MUC1 mRNA an additional prominently labeled band designated MUC1-ARF (indicated by [red arrow-head], Fig 1A, lanes 1–3, Fig 1B and 1C) was observed. It migrated with a molecular mass in the region of 30kDa, and as described above (and see below for a more detailed analysis), it represents neither the MUC1-TM alpha-subunit nor the MUC1-TM beta-subunit. The fact that in-vitro translation of MUC1 mRNA truncated at sites *upstream* to the C-terminal end of the MUC1-TM alpha-subunit [for location of restriction sites see Fig 1D and 1E, AccI (A) and PstI (Ps),] leads to synthesis of truncated forms of the MUC1-ARF protein (Fig 1A, lanes 4 and 5, indicated by red arrow heads)) clearly indicates two points: (i) MUC1-ARF cannot possibly represent the MUC1-TM beta-subunit, because the MUC1 mRNAs truncated either at the AccI or at the Pst1 sites do not comprise information coding for MUC1-TM beta-subunit, and (ii) MUC1-ARF must be coded for by the MUC1 mRNA. Comparison of the two protein products, MUC1-ARF and the MUC1-TM alpha-subunit (compare ARF protein [red arrow-head] with that of the MUC1-TM alpha-subunit designated by [black diamond], Fig 1A, 1B and 1C), shows that in vitro synthesis results in MUC1-ARF protein levels that are only slightly less than those of the MUC1-TM alpha-subunit, indicating that translation of MUC1 mRNA yields significant amounts of MUC1-ARF protein. Translation of mRNAs generated from MUC1 cDNAs digested by restriction enzymes cleaving at sites upstream to the C-terminal end of the MUC1-TM alpha-subunit [Fig 1D and 1E, AccI (A) and PstI (Ps)] lead as expected to synthesis of C-terminally truncated MUC1-TM alpha-subunits (Fig 1A, bands designated by [black diamond]; compare lanes 4 and 5 with lanes 1, 2 and 3). Translation of the same truncated MUC1 mRNAs yielded MUC1-ARF proteins that are similarly diminished in size (Fig 1A, bands designated by [red arrow-head]; compare lanes 4 and 5 with lanes 1, 2 and 3) confirming that MUC1-ARF proteins do in fact derive from translation of MUC1 mRNA, as described above. As expected, translation of mRNAs generated from MUC1 cDNAs digested by PvuII (Pv) and

BalI (B) that cut sites located upstream to the stop codon of *full-length* MUC1 yet downstream to the C-terminal end of the MUC1-TM alpha-subunit (see Fig 1D and 1E, for restriction sites), lead to the generation of truncated uncleaved MUC1 alpha-beta (Fig 1A, lanes 2 and 3, indicated by [unfilled arrowhead]), and intact MUC1-TM alpha-subunit and MUC1-ARF protein (Fig 1A, lanes 2 and 3, indicated by [black diamond] and [red arrow-head], respectively).

These results support the following conclusions: [1] The comparable decrease in molecular mass of the MUC1-TM alpha-subunit protein and of the MUC1-ARF protein arising from 3' truncation in the MUC1-TM mRNAs (Fig 1A, bands designated by [black diamond] and [red arrow-head], compare lanes 4 and 5 with lanes 1, 2 and 3) indicates that both proteins are translated from the same mRNA and terminate in proximity to each other. [2] Because the MUC1-TM mRNA in these experiments contained only a single tandem repeat sequence, the MUC1-ARF protein cannot represent polymorphic MUC-TM proteins varying in the numbers of tandem repeats, but in fact represents a distinct MUC1 protein entity. [3] The size difference between the MUC1-TM alpha-subunit proteins and the MUC1-ARF proteins (Fig 1A, 1B and 1C bands designated by [black diamond], and [red arrow-head] respectively) suggest that the two proteins are different.

Translation of two naturally occurring isoforms of MUC1-TM mRNA ('a' and 'b' in Fig 1, panel D), yields uncleaved full-length MUC1-TM protein and N-cleavage proteins that differ by about 1000 Daltons [alpha-beta (unfilled arrow-head) and alpha (black diamond), respectively Fig 1B, lanes 1 and 2). This is because variant 'a' differs from variant 'b' in that it comprises an additional 27 nucleotides coding for nine amino acids downstream to the AUG initiation codon of MUC1-TM. In contrast, because the two differently sized MUC1-TM mRNAs, 'a' and 'b', yield identically sized MUC1-ARF proteins [Fig 1B, lanes 1 and 2, compare MUC1-ARF proteins indicated by (red arrow-head)], we conclude that the initiation codon directing MUC1-ARF synthesis is located downstream to that initiating the MUC1-TM protein. Finally, because of the autoproteolytic cleavage of the precursor MUC1-TM protein within its SEA module into cleaved alpha- and beta-subunits, a pulse-chase experiment demonstrated a time-dependent decrease in levels of the full-length MUC1-TM protein (alpha-beta and designated by open arrow-head, Fig 1C, lanes 1–3), accompanied by an associated increase in MUC1-TM alpha-subunit (designated by alpha, black diamond, Fig 1C, lanes 1–3). In contrast, MUC1-ARF levels remained constant throughout the chase (indicated by ARF, red arrow-head, Fig 1C, lanes 1–3), demonstrating that MUC1-ARF clearly does not contain a cleavable SEA module and must represent a protein distinct from MUC1-TM.

Analysis of the MUC1 mRNA reveals an AUG codon located 265 nucleotides downstream to the MUC1-TM initiation codon that (i) initiates a long +1 frameshifted open reading frame, (ii) contains an upstream Kozak consensus sequences (ccaccacc/t), and (iii) has the potential to initiate translation of a frameshifted alternate reading frame (ARF) protein (Fig 2). As shown above, in vitro translation of MUC1 mRNA yields proteins consistent with translation of the MUC1-TM mRNA in an alternative reading frame directed by an initiation codon downstream to that initiating MUC1-TM synthesis. Like MUC1-TM, MUC1-ARF harbors a tandem repeat (VNTR) domain, but because of the +1 frameshift, the amino acid sequence of both the MUC1-ARF tandem repeat as well as the N- and C- sequences flanking it differ entirely from those of the MUC1-TM protein (Fig 1F). Because MUC1 mRNA comprising only *one* tandem repeat was used for the in vitro translation assays described above, the MUC1-ARF protein product (with one 20 amino acid repeat sequence) is predicted to contain 245 amino acids and the molecular mass for MUC1-ARF observed here (in the region of 30kDa) corresponds well with that expected for the in-vitro translated MUC1-ARF protein.

Remarkably, the alternate reading frame codes for 49 amino acids upstream to the VNTR and 175 amino acids downstream to the VNTR. Assuming a minimum of about 15 tandem

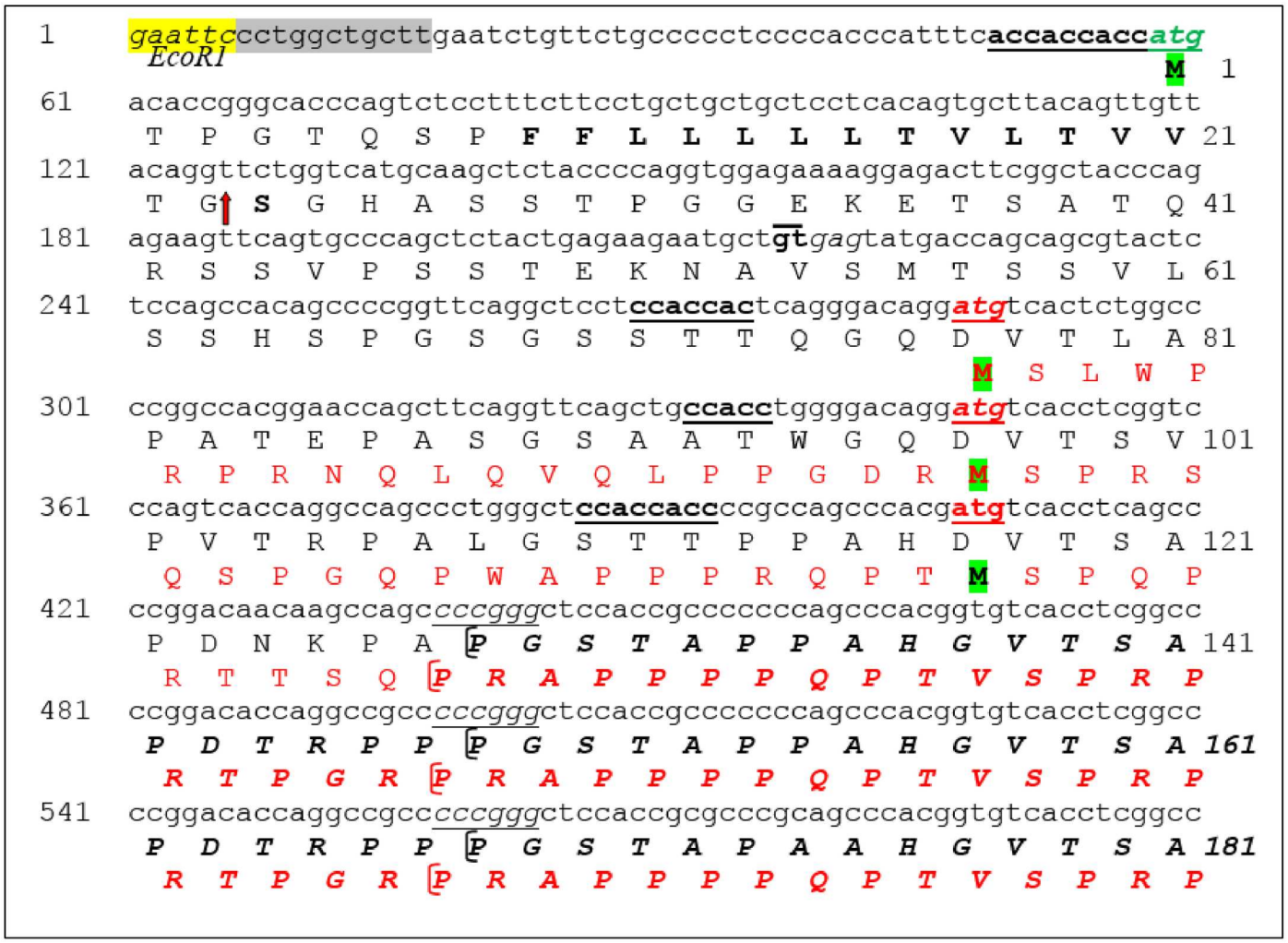

Fig 2. Nucleotide and amino acid sequence of MUC1-TM and MUC1-ARF. MUC1-TM initiation codon is shown in black font and green highlight. Downstream to this initiation codon, three potential MUC1-ARF initiation codons in a +1 frame are shown in red font and green highlight. Amino acid sequences are in black and red beneath the nucleotide sequence, represent MUC1-TM protein and MUC1-ARF protein, respectively. The red arrow indicates the signal peptide cleavage site of the MUC1-TM protein. Kozak sequences upstream to the initiation codons of both proteins are in bold fonts and underlined. The sequences shown for both MUC1-TM and MUC1-ARF extend from their respective initiation codons to their tandem repeat domains; three such repeats are shown indicated by square brackets. The EcoR1 site and grey highlighted regions are not part of the actual MUC1 cDNA sequence.

doi:10.1371/journal.pone.0165031.g002

repeats for a naturally occurring MUC1 mRNA, each comprising twenty amino acids [19], the VNTR of MUC1-ARF alone contains at least 300 amino acids, and the complete MUC1-ARF protein would then comprise at least 524 amino acids.

MUC1-ARF protein in MUC1 transfected cells

We investigated MUC1-ARF expression with anti-MUC1-ARF monoclonal antibodies (mAbs) generated by immunizing mice with a peptide representing 1.3 repeat units of the MUC1-ARF tandem repeat (PQPTVSPRPRTPGRPRAPPP-PQPTVS- one 20 amino acid repeat is underlined and six amino acids of the following repeat is double-underlined (Fig 1, panel F). Screening against the MUC1-ARF repeat peptide yielded three independent hybridomas secreting monoclonal antibodies MPR2G10, MPR4B3 and MPR5C9. Following reaction of each of the

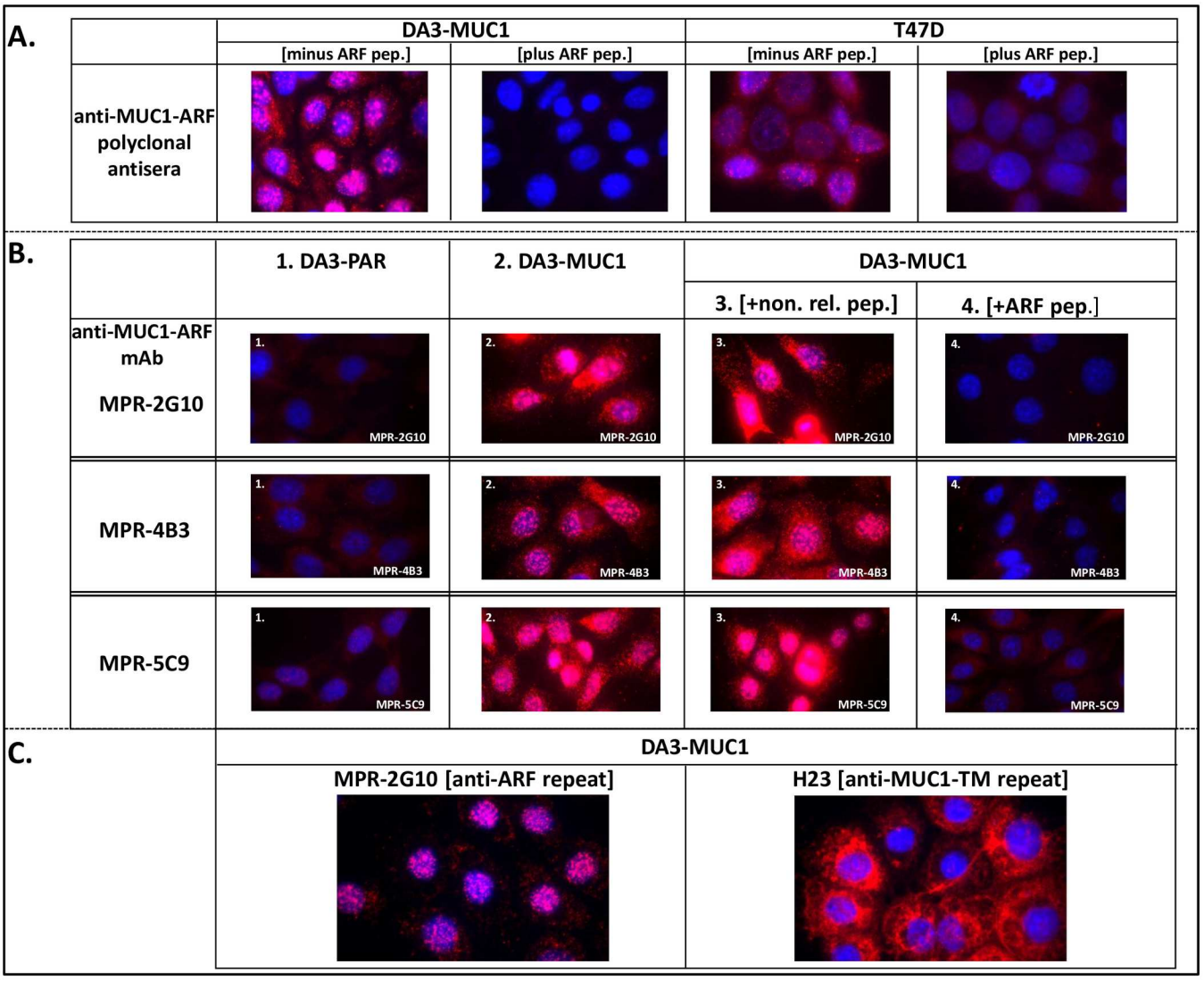

Fig 3. Detection of nuclear MUC1-ARF protein with polyclonal anti-MUC1-ARF antibodies and with three distinct anti-MUC1-ARF monoclonal antibodies, MPR2G10, MPR4B3 and MPR5C9. (A) Polyclonal anti-MUC1-ARF antibodies and (B) three independently isolated anti-MUC1-ARF monoclonal antibodies, MPR2G10, MPR4B3 and MPR5C9, were reacted in the presence of competing ARF peptide (B, panels 4), in its absence (B, panels 2), or with a non-relevant peptide (B, panels 3) with mouse DA3 cells stably transfected with and expressing human MUC1 DNA (DA3-MUC1) and with T47D human breast cancer cells that endogenously express MUC1. Parental DA3 cells (DA3-PAR) which do not express human MUC1 are shown in B, panels 1. Immunofluorescence of secondary antibody (red), DAPI staining of nuclei (blue) are shown in the merged images. (C) Mouse DA3 cells expressing human MUC1 reacted with anti-MUC1-ARF repeat monoclonal antibody MPR2G10 (left panel), compared with anti-MUC1-TM tandem repeat monoclonal antibody H23 (right panel), both followed by red-labelled secondary antibody.

doi:10.1371/journal.pone.0165031.g003

three antibodies with mouse mammary tumor cells stably transfected with and expressing human MUC1 DNA (DA3-MUC1) a strong nuclear signal was seen, as well as a lower level signal in the cell cytoplasm (Fig 3B Panels 2, DA3-MUC1). Parental mouse DA3 cells not expressing the human MUC1 protein, were uniformly non-reactive with the anti-MUC1-ARF monoclonal antibodies (Fig 3B Panels 1, DA3-PAR). Furthermore, addition of MUC1-ARF peptide abrogated the immunoreactivity of the antibodies, whereas addition of a non-relevant peptide had no effect (Fig 3B, DA3-MUC1, compare panels 4 and 3). Similar results were obtained with anti-MUC1-ARF polyclonal antisera, reacted with both DA3-MUC1 cells as well

as with T47D breast cancer cells (Fig 3A). As previously reported [16, 20–22], cells transfected with human MUC1 DNA express high levels of the human MUC-TM protein as assessed with anti-MUC1-TM tandem repeat mAbs that localized exclusively to the cell membrane and cytoplasm (Fig 3C, right-hand panel). Reacting the same cells in parallel with anti-ARF-repeat mAb MPR2G10 demonstrated predominantly nuclear localization (Fig 3C, left-hand panel), consistent with the pattern shown above. A sandwich ELISA assay consisting of capture mAb MPR2G10 and detecting biotinylated mAb MPR4B3 could readily detect the MUC1-ARF protein (see below section "**Endogenous MUC1-ARF protein is detected in human cancer cell lines**"), and although the anti-MUC1-ARF mAbs recognize discrete epitopes in the MUC1-ARF repeat sequence, they all bind to the MUC1-ARF protein. Immunoreactivity of anti-MUC1-ARF mAb MPR2G10 with DA3 cells transfected with both human MUC1 cDNA and human genomic MUC1 DNA was the most robust (Fig 4, panels A and B). It was therefore chosen for subsequent studies. Probing immunoblots of lysates from cells transfected with human MUC1 DNA demonstrated MUC1-ARF that migrated with a molecular mass of about 80kDa (Fig 4E, lane DA3-G). MUC1-ARF protein was seen neither in non-transfected cells (Fig 4E, lane DA3-P), nor following addition of competing ARF peptide.

Two distinct murine 3T3 transfectants, each receiving human MUC1 cDNA comprising a different number of tandem repeats provided further confirmation of MUC1-ARF expression in MUC1-transfected cells. Variation in the number of tandem repeats provides an inherent size-signature 'barcode' to MUC1 proteins translated by each of the two transfectants. Accordingly, when western blots were probed with anti-[MUC1-TM tandem repeat] antibodies, each of the two stable 3T3 transfectants showed differently sized high molecular mass MUC1-TM proteins (Fig 4F3, filled green arrows), reflecting the size of the tandem repeat domain contained within each of the MUC1 cDNAs used for transfection. MUC1-TM glycoprotein is heavily post-translationally modified by both N- and O-linked glycosylations [14, 23, 24]. Probing similar blots with anti-MUC1-ARF revealed that the two transfectants produced distinctly sized MUC1-ARF proteins (Fig 4F1, filled red arrowheads). Cells transfected with MUC1-I or MUC1-II cDNA expressed MUC1-ARF proteins of approximately 60kDa and 90kDa respectively, corresponding to the tandem repeat polymorphisms of the transfected MUC1 DNAs. The calculated mass of the MUC1-ARF protein with a single repeat unit is 27,253 Daltons. Each additional MUC1-ARF repeat unit adds on an additional calculated mass of 2,161.5 Daltons. We therefore estimate that the MUC1-I and MUC1-II cDNAs comprise about 17 and 28 MUC1-ARF repeat units, respectively. Addition of competing MUC1-ARF peptide ablated immunoreactivity, confirming the specificity of the anti-MUC1-ARF antibodies (Fig 4F2, lanes 2 and 3) as does the absence of reactivity in lysates from non-transfected cells (Fig 4F1, lane 1, designated PAR).

Since the molecular mass of MUC1-ARF protein correlates with the number of tandem repeat sequences contained within the *MUC1* gene, which varies between different individuals and cell lines, the size of MUC1-ARF proteins will correspondingly vary. This means that differently sized MUC1-ARF proteins will be detected in different cell lines.

To see whether MUC1-ARF has the potential to be post-translationally modified, the MUC1-ARF amino acid sequence was interrogated using the MotifScan analysis (http://scansit.mit.edu). In order to improve our level of confidence in the analysis, the scan was performed *only at the **highest** level* of stringency and we purposely did not opt for the medium and low stringency levels of scanning. This MotifScan analysis predicted, with very high levels of confidence, multiple sites for post-translational modifications within the MUC1-ARF protein. Sites for phosphorylation on serine or/and threonine (***S/T***) residues mediated by calmodulin dependent kinase 2 (CAMGK2G) were predicted in the following sequences: RQP***T***MSP located just upstream to the tandem repeats, RPR***T***PGR and PTV***S***PRP both sites located

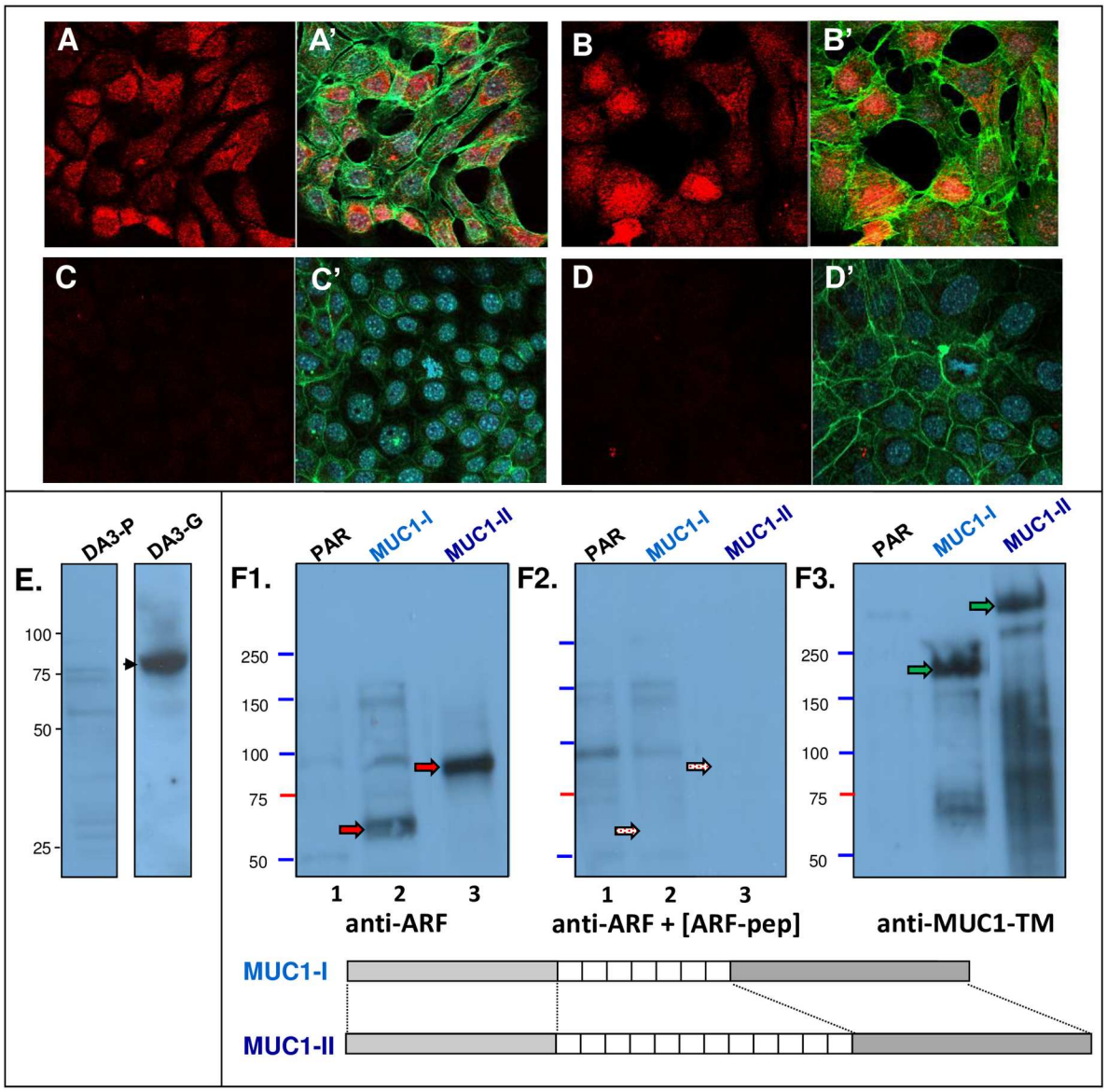

Fig 4. Mouse cell lines transfected with human MUC1 DNA express MUC1-ARF. (A, and C) DA3 cells transfected with MUC1 cDNA; (B) DA3 cells transfected with human MUC1 genomic DNA, and (D) non-transfected mouse parental DA3 cells were immunostained with anti MUC1-ARF monoclonal antibody MPR2G10 followed by red-labeled secondary antibody. DAPI (blue) and green-labeled phalloidin are shown as merged images. In (C), anti-MUC1-ARF monoclonal antibody was added together with competing ARF peptide. (E) Immunoblots with anti-MUC1-ARF antibodies of cell lysates prepared from either untransfected DA3 mouse cells (DA3-P) or from cells transfected with MUC1 genomic DNA (DA3-G). MUC1-ARF is indicated by the arrowhead. (F) Mouse 3T3 cells transfected with human MUC1 DNA containing differently sized VNTRs (diagrams designated MUC1-I, MUC1-II) express differently sized MUC1-ARF proteins: Cell lysates from either parental 3T3 cells or 3T3 transfectants stably expressing human MUC1 DNA (lanes 1, 2 and 3, designated PAR, MUC1-I and MUC1-II, respectively) were resolved by SDS-PAGE and immunoblots probed with anti-MUC1-ARF alone (F1) or together with competing ARF peptide (F2). Following probing, the immunoblot was stripped, reprobed with an antibody recognizing an epitope within the MUC1-TM tandem repeat sequence, and redeveloped with ECL (F3). Filled red arrows indicate MUC1-ARF proteins and filled green arrows indicate MUC1-TM proteins (F1 and F3, respectively). Stippled red arrows designate the positions of the MUC1-ARF proteins that have been specifically competed out. Protein loading with anti-actin antibodies confirmed that equal amounts of protein were present in each lane. MUC1-I and MUC1-II cDNAs used for transfections contains approximately 17 and 28 repeats respectively. The two cartoons at the bottom of the Figure designating the MUC1-I and MUC1-II cDNAs are intended for illustrative purposes only. They demonstrate the fact that the two cDNAs differ one from the other in the number of repeats each contains.

doi:10.1371/journal.pone.0165031.g004

within the tandem repeats, and PMV***S***PRP and YLL***S***PPP, sites located C-terminal to the tandem repeats (***T*** or ***S*** phosphorylation sites are in bold and italics).

The molecular masses of the two MUC1-ARF proteins (Fig 4F1, lanes 2 and 3) are considerably less than those of the corresponding MUC1-TM proteins (Fig 4F3, filled green arrows), suggesting that although the MUC1-ARF proteins are likely post-translationally modified, as described above, these are not as extensive as those of MUC1-TM.

Endogenous MUC1-ARF protein is detected in human cancer cell lines

We extended our analyses to human cancer cells which natively express high levels of the MUC1-TM protein. Immunofluorescent analyses done with anti-MUC1-ARF mAb 2G10 showed expression of endogenous MUC1-ARF protein that localized primarily to the cell nucleus. This was seen in T47D breast cancer cells (Fig 5, panels A and C), COLO357 pancreatic cancer cells (Fig 5, panels B) and ZR75 breast cancer cells (Fig 5, panels E and F). The prominent nuclear staining seen in T47D breast cancer cells with the anti-MUC1ARF mAb 2G10 was abrogated by addition of competing MUC1-ARF peptide (compare Fig 5, panels C and D), showing antibody specificity. Simultaneous costaining of breast cancer ZR75 cells (Fig 5, panels E) with anti-MUC1-TM mAbs [DMB5F3 [17], directly labeled with a green fluorescent dye] together with anti-MUC1-ARF mAb 2G10 (labeled red), clearly showed that the two MUC1 proteins did not colocalize: MUC1-TM localized at the cell membrane as expected, whereas MUC1-ARF protein was predominantly nuclear (Fig 5, see panels Ei, Eii and Eiii). Furthermore addition of competing MUC1-TM-junction protein abrogated the cell membrane signal of MUC1-TM, and was of no effect on the nuclear MUC1-ARF (Fig 5, compare panels E and panels F). Probing blots with anti-MUC1-ARF antibody 2G10 further demonstrated that endogenous MUC1-ARF protein migrated with a molecular mass of slightly more than 55kDa (Fig 5G, left lane), and that its reactivity was abolished by MUC1-ARF peptide (Fig 5G, open red arrow, right lane). The molecular mass of the protein seen in Colo357 cells corresponds to a MUC1-ARF protein containing about 14 MUC1-ARF repeat units.

Human cancer cell lines A431, MCF7 and KB known to express MUC1-TM protein were assessed for MUC1-ARF expression by western blot analyses. Results indicate that cells which express MUC1 mRNA also expressed MUC1-ARF proteins with molecular masses ranging from about 48kDa to 55kDa (Fig 6, panels A, B and C, MUC1-ARF protein indicated by lower red arrowhead). These correspond to MUC1-ARF proteins containing about 11 to 17 MUC1-ARF tandem repeat units expressed by the relatively smaller MUC1 allele present in the these cell lines. A larger MUC1-ARF protein, expressed from the larger MUC1 allele detected in MCF7 cells migrated with a molecular mass of about 130kDa, corresponding to a MUC1-ARF protein containing about 47 ARF tandem repeat units (Fig 6B, upper red arrowhead). Its intensity was significantly less as compared to that of the small allele gene product (Fig 6B, lane 1, compare upper and lower red arrowheads), consistent with the previously reported reduced expression of the larger MUC1 alleles gene products [25]. In fact in the absence of added cytokines, only the smaller MUC1-ARF allele could be detected in KB cells (Fig 6C, lane 1 red arrowhead). However, addition of IL1-beta and interferon-gamma to KB cells, a combination known to increase MUC1 gene expression [26], led to the appearance of the larger MUC1-ARF protein (Fig 6C lane 2, indicated by upper red arrowhead with a mass of about 120kDa) corresponding to the larger MUC1 allele present in these cells. The size difference of the two MUC1-ARF proteins observed in KB cells tallies remarkably well with that published for the two MUC1 alleles of KB cells as determined by Northern blotting analyses [26].

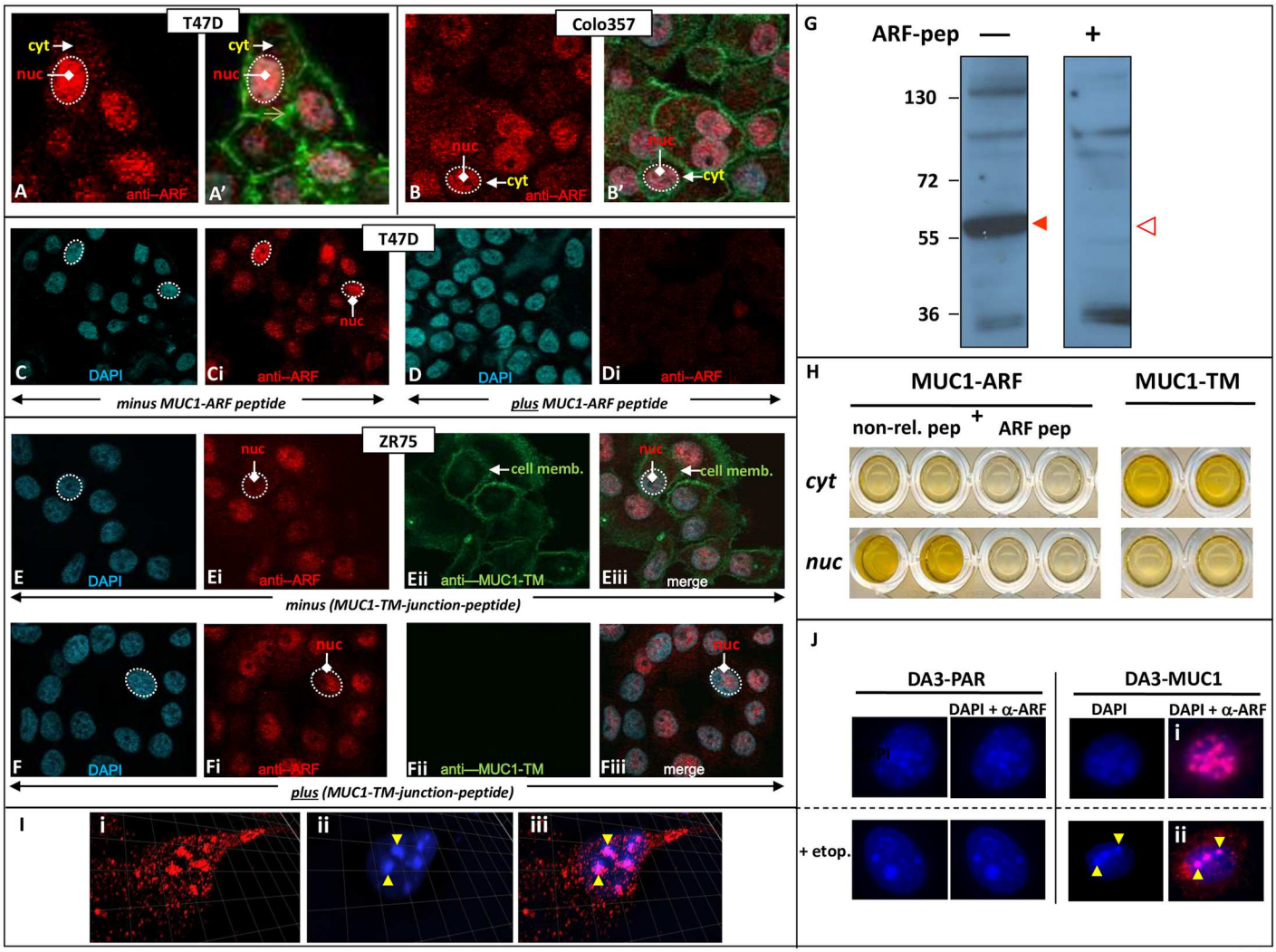

Fig 5. Human cancer cells express MUC1-ARF in both the nucleus and cytoplasm. T47D breast cancer cells (Panels A and C) and COLO357 pancreatic cancer cells (Panels B) were immunostained with anti-MUC1-ARF mAb MPR2G10 followed by red-labeled secondary antibody. DAPI (blue, demonstrating nuclei: white stippled ovals) and green-labeled phalloidin (labeling actin filaments) are shown in the merged images (Panels A' and B'). Immunostaining of T47D cells with anti-MUC1-ARF mAb MPR2G10 is abrogated when done in the presence of competing MUC1-ARF peptide (compare Panels C with Panels D). Simultaneous immunostaining of ZR75 breast cancer cells with anti-MUC1-TM antibodies (DMB5F3 mAbs directly green labeled) and anti-MUC1-ARF antibodies (MPR2G10, red labeled) in the absence of MUC1-TM-junction peptide is shown in Panels E, while the effect of adding MUC1-TM-junction peptide to an identical immunostaining of ZR75 breast cancer cells is shown in Panels F. (Panel G) Lysates of human COLO357 cancer cells were resolved on SDS-PAGE, western blotted, and probed with anti-MUC1-ARF MPR2G10. MUC1-ARF protein is indicated by the filled red arrow head (left panel). Immunoreactivity is abrogated by addition of competing free MUC1-ARF peptide (right panel). (Panel H, left side, labeled MUC1-ARF) Equivalent amounts of protein from either cytoplasmic or nuclear (cyt or nuc) T47D cell extracts were analyzed by a sandwich ELISA that detects MUC1-ARF. Competing MUC1-ARF peptide (ARF pep) added to the detecting biotinylated anti-MUC1-ARF MPR4B3, abolished signal in both cytoplasmic and nuclear samples, whereas non-relevant peptide (non-rel. pep) had no effect. (Panel H, right side, labeled MUC1-TM)-analysis of nuclear and cytoplasmic T47D cell extracts with a sandwich ELISA detecting MUC1-TM protein. (Panel I) Mouse DA3 mammary tumor cells expressing human MUC1 cDNA were immunostained with anti MUC1-ARF antibody MPR2G10 and red-labeled secondary antibody followed by DAPI staining. High magnification images of orthogonal projections of confocal laser microscopy are shown for anti-MUC1-ARF (Panel I-i), DAPI (Panel I-ii) and merged images (Panel I-iii). (Panel J) Untransfected mouse DA3 mammary tumor cells (DA3-PAR, left panels) or transfected with human MUC1 cDNA (DA3-MUC1, J, right panels) were stained with DAPI and immunostained with anti-MUC1-ARF monoclonal followed by red-labeled secondary antibody. DAPI staining alone (blue) and the merged images of DAPI plus red anti-ARF immunostaining (DAPI + anti-ARF) are shown. A parallel set of cells (Panel J, lower panels, plus etop.) were treated with Etoposide, a DNA topoisomerase II inhibitor.

doi:10.1371/journal.pone.0165031.g005

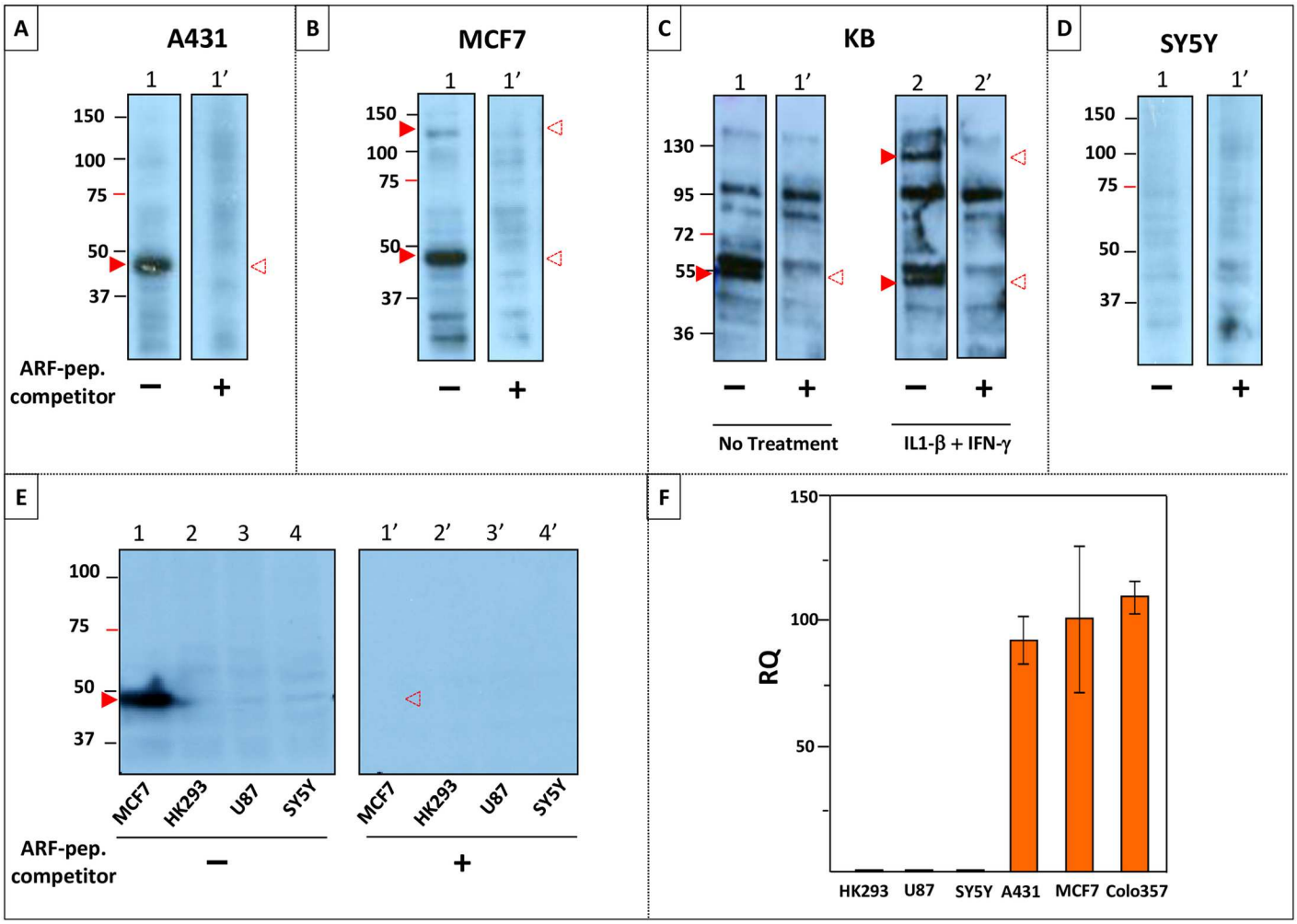

Fig 6. MUC1-ARF protein is observed only in those human cell lines that express the *MUC1* gene. Lysates prepared from human cell lines A431, MCF7, KB, SY5Y, HK293 and U87 (Panels 'A' to 'E') were resolved on SDS-PAGE, western blotted, and probed with anti-MUC1-ARF MPR2G10. MUC1-ARF protein is indicated by the filled red arrowheads. Addition of competing free MUC1-ARF peptide (indicated beneath the lanes by a 'plus' sign) competed out reactivity of the MUC1-ARF protein (white arrowheads with dotted red outline designate the positions of MUC1-ARF protein that has been competed out by added ARF peptide). (Panel F): Expression levels of the *MUC1* gene in the various cell lines were assessed in triplicate by quantitative PCR (qPCR). Expression in MCF7 cells was set to be 100. (Immunoblot analysis of Colo357 for MUC1-ARF expression appears in Fig 5G).

doi:10.1371/journal.pone.0165031.g006

The reactivity of the MUC1-ARF protein was in all cases abolished by the addition of competing MUC1-ARF peptide [Fig 6A, 6B and 6C, compare lanes 1 (minus competing MUC1-ARF peptide) with lanes 1' (plus competing MUC1-ARF peptide); Fig 6C, compare lanes 2 and 2'; red arrowheads indicate the MUC1-ARF proteins and white arrowheads with dotted red outline designate the position of MUC1-ARF protein competed out by added ARF peptide]. No MUC1-ARF protein was detected in the neuroblastoma cell line SY5Y consistent with the undetectable expression of the *MUC1* gene in these cells (Fig 6D and 6F). An additional two cell lines, HK293 and U87, which do not express the *MUC1* gene, also did not express the MUC1-ARF protein (Fig 6E).

Quantitative PCR analyses (qPCR) to assess expression of MUC1 mRNA validated that only those cells (A431, MCF7 and Colo357) that express MUC1 mRNA also displayed MUC1-ARF protein, whereas those cells that had low to undetectable levels of MUC1 expression (HK293, U87 and SY5Y) were likewise negative for MUC1-ARF protein (Fig 6A–6F).

Taken together, these analyses confirm endogenous MUC1-ARF protein in human cancer cell lines known to express the *MUC1* gene, and conversely the absence of MUC1-ARF protein in cells that do not express the *MUC1* gene.

Quantitation of MUC1-ARF protein in nuclear and cytoplasmic compartments demonstrated MUC1-ARF protein in nuclear extracts prepared from human T47D breast cancer cells while cytoplasmic extracts displayed much lower levels (Fig 5H, left panel). Analysis of MUC1-TM revealed an inverse picture: while high levels were observed in cytoplasmic extracts, nuclear MUC1-TM was almost undetectable (Fig 5H, right panel). Within the nucleus itself MUC1-ARF staining revealed a non-homogeneous distribution, with intense MUC1-ARF immunostaining observed in discrete subnuclear aggregates (red staining, Fig 5A, 5B, 5C-i, 5E-i and 5F-i). Additional analyses by confocal laser microscopy and orthogonal projections (Fig 5I, 5i, 5ii and 5iii) showed intense staining with both DAPI and with anti-MUC1-ARF antibodies, suggesting that MUC1-ARF localizes to subnuclear regions comprising condensed chromatin. This colocalization was further confirmed by etoposide treatment of MUC1 cDNA-transfected cells which induced large DAPI-positive condensed chromatin aggregates to which MUC1-ARF clearly colocalized (Fig 5J, compare panels i and ii). In contrast, immunostaining of non-transfected cells was negative (Fig 5J, DA3-PAR).

Expression of MUC1-ARF in normal human tissues correlates with MUC1-TM expression

MUC1-TM is detected on the apical surface of normal epithelial cells that form luminal structures (for example, [27]). To see whether MUC1-ARF protein is co-expressed with MUC1-TM in these cells, sequential serial sections of human tissues were reacted with monoclonal antibodies specific for either MUC1-TM or MUC1-ARF. To detect MUC1-TM we used the previously characterized mAb DMB5F3 [17] which binds specifically to the MUC1-TM SEA module with picomolar affinity. For MUC1-ARF detection, use was made of the mAb MPR2G10, here shown to bind the MUC1-ARF tandem repeat sequence (see Fig 1D and 1E for regions of MUC1-TM and MUC1-ARF recognized by the antibodies). In kidney tissue, MUC1-ARF expression was seen only in those cells that also expressed MUC1-TM [Fig 7, compare Panels A-i (MUC1-TM) with A-ii (MUC1-ARF)]. Larger fields and higher magnifications are shown in Fig 7; Panels C-i and C-i' (MUC1-TM) and Panels D-i and D-i' (MUC1-ARF)]. Similar results were seen with pancreatic sections (Fig 7, Panels B-i (MUC1-TM) with B-ii (MUC1-ARF)]. For larger fields and at higher magnifications see Fig 7, Panels E-i and E-i' (MUC1-TM) and Panels E-ii and E-ii' (MUC1-ARF). In contrast to MUC1-TM localization on the apical surfaces of normal luminal-forming epithelial cells, MUC1-ARF localized primarily to the nuclei of these same cells both in kidney and in pancreas. Addition of ARF peptide abrogated reactivity only of anti-MUC1-ARF antibody (Fig 7, compare Panel B-ii with B-ii''), whereas recombinant MUC1-SEA-module protein abrogated reactivity only of anti-MUC1-SEA antibody (Fig 7, compare Panels B-i with B-i''), confirming specificity of each antibody with its target protein.

Kidney tissue sections were particularly informative in that only luminal-forming cells of distal tubules (DT) stained positive for the MUC1-TM protein (Fig 7, Panels A-i, C-i and C-i') whereas cells of proximal tubules (PT), glomeruli (G), and Bowman's capsule were uniformly negative. Correspondingly MUC1-ARF is expressed only in cells forming the lumen of distal tubules where it localized to cell nuclei, directly correlating with MUC1-TM expression (compare MUC1-ARF expression in Fig 7, Panels A-ii, D-i and D-i' with MUC1-TM expression in Fig 7, Panels A-i, C-i and C-i'). In cells of the exocrine pancreas most cells demonstrated

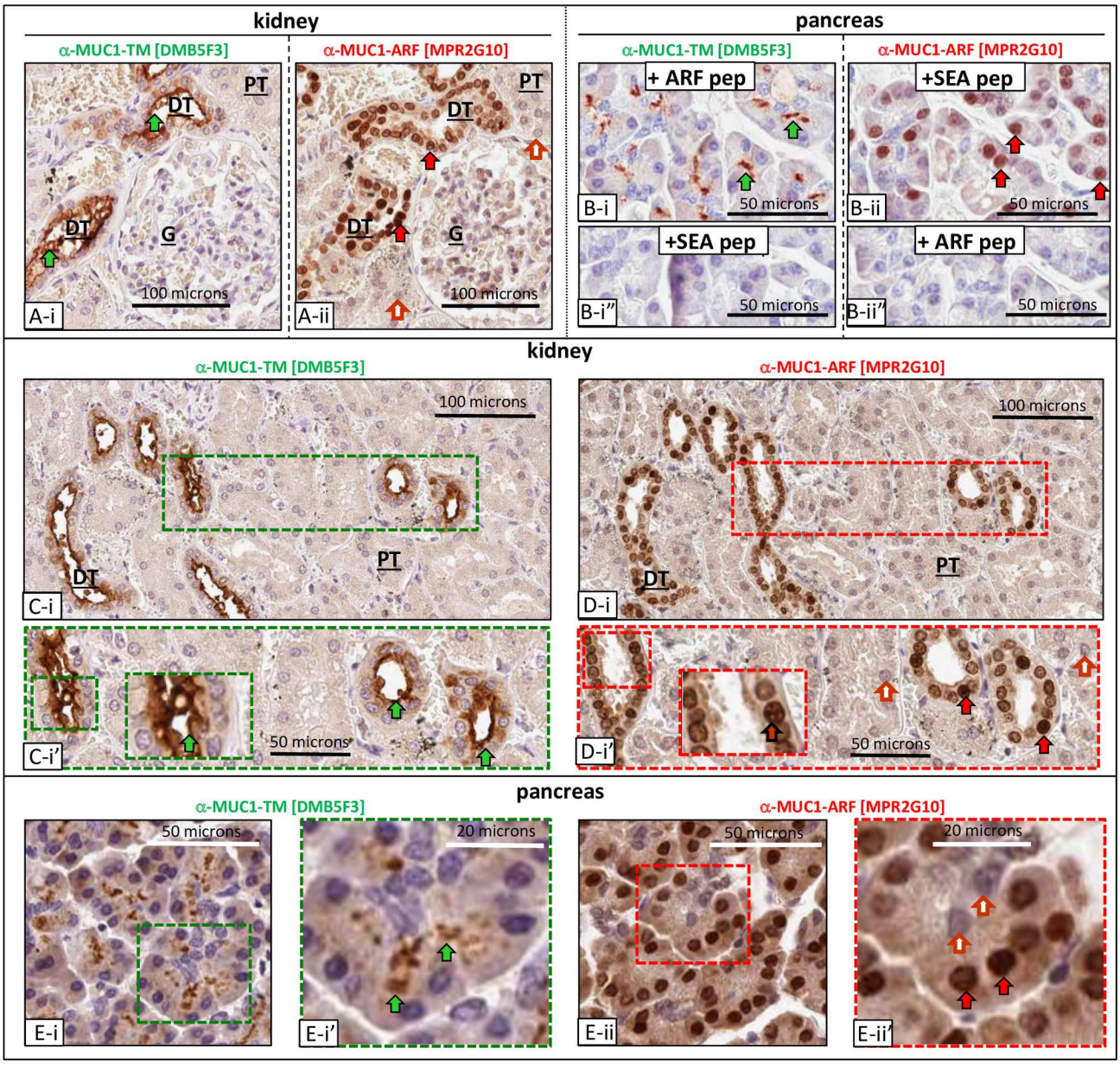

Fig 7. MUC1-TM and MUC1-ARF expression in normal human kidney and pancreas. Serial sections of paraffin-embedded human pancreatic and renal tissues were immunohistochemically stained with anti-MUC1-TM SEA module antibodies (anti-MUC1-TM [DMB5F3]) and anti-MUC1-ARF antibodies (anti-MUC1-ARF [MPR2G10]) as indicated. Normal kidney is shown in Panels A-i (MUC1-TM) and A-ii (MUC1-ARF); larger fields and higher magnifications are shown in Panels C-i, C-i' (MUC1-TM), and D-i, D-i' (MUC1-ARF)]. Glomerulus, proximal tubule, and distal tubule are designated by **G**, **PT** and **DT** respectively. Filled green arrows designate sites of MUC1-TM-SEA protein at the cell surface whereas filled red arrows designate MUC1-ARF protein; absence of anti-MUC1-ARF immunoreactivity is shown by filled red and white arrows. Normal pancreatic tissue reacted with anti-MUC1-TM in the presence of ARF peptide (plus ARF pep) or in the presence of MUC1-TM SEA peptide (plus SEA pep), are shown in Panels B-i and B-i", respectively. MUC1-TM protein on the cell surface of ductal epithelial cells is competed out by MUC1-TM SEA peptide (B-i") but not by MUC1-ARF peptide (B-i). Conversely MUC1-ARF protein in the nuclei of pancreatic epithelial cells is competed out by MUC1-ARF peptide (B-ii") but not by MUC1-SEA peptide (B-ii). Larger fields and higher magnifications of pancreatic tissue is shown in E-i, E-i' (MUC1-TM), and E-ii, E-ii' (MUC1-ARF).

doi:10.1371/journal.pone.0165031.g007

nuclear MUC1-ARF expression, whereas a subset showed neither nuclear nor cytoplasmic MUC1-ARF (Fig 7, Panels B-ii, E-ii and E-ii').

Expression of both MUC1-ARF and MUC1-TM expression is restricted to the exocrine pancreas and neither are expressed in the endocrine pancreas

Whereas MUC1-TM protein was readily observed at the apical surfaces of pancreatic ducts of the exocrine pancreas (Fig 8B and 8B'), no immunoreactivity for MUC1-TM was observed in the pancreatic islets forming the 'endocrine pancreas' (Fig 8B and 8B'- note the absence of MUC1-TM immunoreactivity in the Islets of Langerhans, demarcated by the blue dotted lines). This is in accord with the known expression of MUC1-TM solely within the exocrine pancreas, in cells lining the intercalated, intralobular and interlobular ducts. Cells of neuroendocrine origin forming the Islets of Langerhans are known not to express MUC1 [28–30]. MUC1-ARF protein was also exclusively expressed in cells of the exocrine pancreas where it localized primarily to cell nuclei (Fig 8A and 8A'). In contrast, and again in accord with MUC1-TM expression, all cells of the endocrine pancreas were uniformly negative for MUC1-ARF (Fig 8A and 8A'). These results demonstrate that (a) in the pancreas only those cells that express the MUC1-TM protein isoform also express MUC1-ARF, just as observed for kidney tissue, and (b) the nuclear staining for MUC1-ARF is specific because nuclei of cells comprising the Islets of Langerhans were uniformly negative for MUC1-ARF staining, whereas cells of the exocrine pancreas contained within the same section were MUC1-ARF positive.

Taken together, these studies show a tight correlation in normal tissues between MUC1-ARF expression and that of MUC1-TM. Certain cell types both in the kidney and pancreas that express MUC1-TM also express MUC1-ARF, whereas those kidney and pancreatic cells that do not express MUC1-TM, also do not express MUC1-ARF (Figs 7 and 8). Furthermore, normal tissues such as brain and liver that have no MUC1-TM expression are also devoid of MUC1-ARF protein.

MUC1-ARF expression in normal and malignant pancreatic and breast tissues

The patterns of MUC1-TM and MUC1-ARF expression in normal and malignant pancreatic and breast tissues displayed significant differences. High MUC1-TM expression was observed in pancreatic cancer tissues, accompanied by a loss of MUC1-ARF expression [compare expression of MUC1-TM and MUC1-ARF in normal pancreatic tissue (Fig 9C, left and right panels respectively), to that seen in pancreatic cancer tissue (Fig 9D, left and right panels respectively)]. In contrast to normal pancreatic tissues, both MUC1-TM and MUC1-ARF are expressed at very low levels in resting normal breast tissue. In breast cancer cells we found substantial MUC1-TM expression (Fig 9A, examples of expression in 3 breast cancer samples, left-hand panels), consistent with elevated MUC1-TM expression in breast tumors as described in the literature [14, 31]. Our analyses of a series of breast tumor tissues demonstrated that approximately 40% of the MUC1-TM positive sections (totaling 96 different samples) were MUC1-ARF positive. MUC1-ARF expressers (for examples see Fig 9A, middle panels, labeled anti-MUC1-ARF) could be roughly divided into three groups differing from each other in their patterns of MUC1-ARF expression: **[i]** high expression of both MUC1-TM and nuclear MUC1-ARF, **[ii]** high MUC1-TM expression and no MUC1-ARF expression, **[iii]** high MUC1-TM expression and focal MUC1-ARF expression in only a subset of cells. The significance of this MUC1-ARF expression in only some of the breast cancer samples is further considered in the Discussion section.

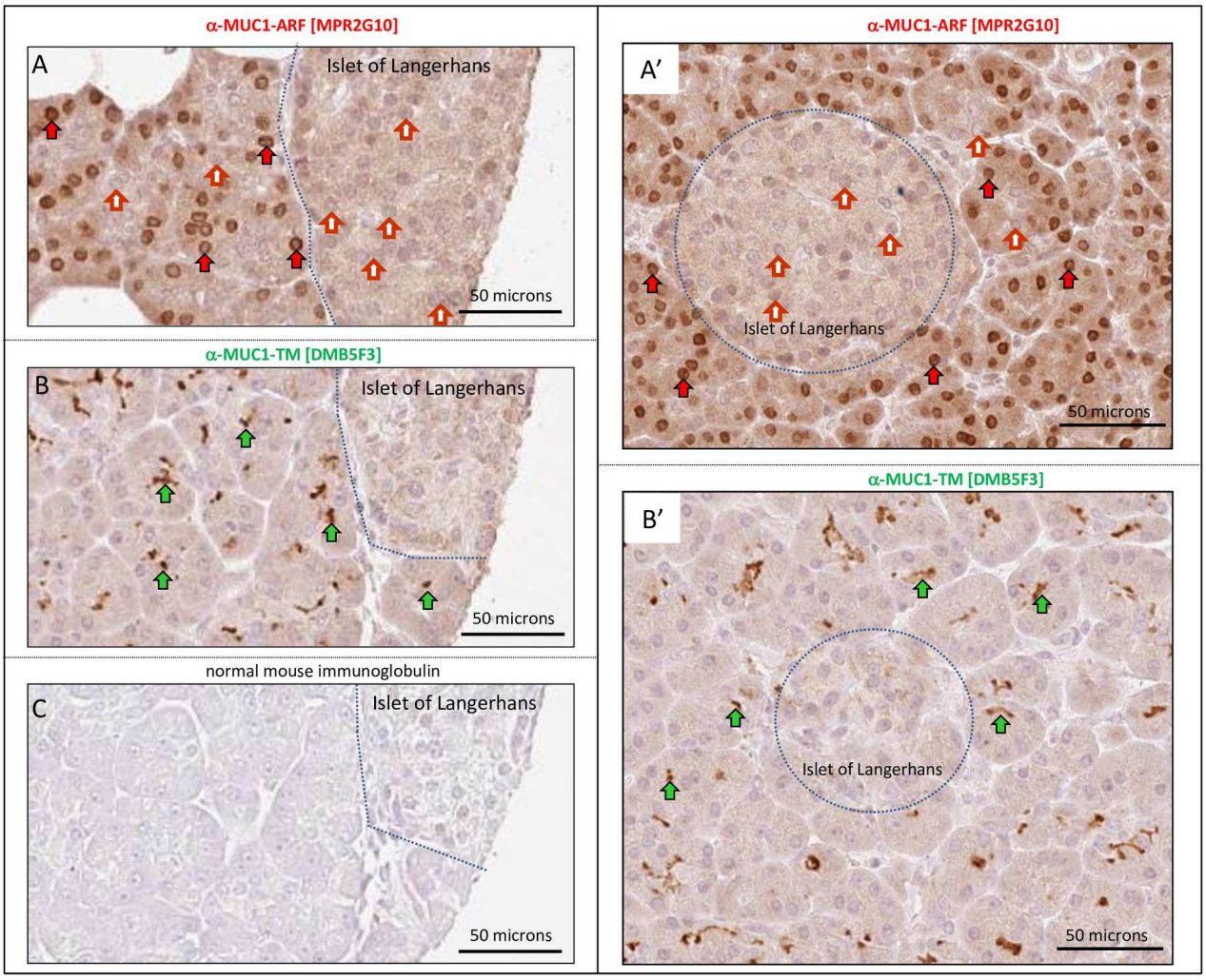

Fig 8. MUC1-TM and MUC1-ARF proteins are expressed solely in the exocrine pancreas and not in the endocrine pancreatic islets. Serial sections of paraffin-embedded human pancreatic tissues were immunohistochemically stained with anti-MUC1-TM SEA module antibodies (anti-MUC1-TM [DMB5F3]), anti-MUC1-ARF antibodies (anti-MUC1-ARF [MPR2G10]) and normal mouse immunoglobulin as indicated. Filled green arrows designate sites of MUC1-TM-SEA protein at the cell surface whereas filled red arrows designate MUC1-ARF protein; absence of anti-MUC1-ARF immunoreactivity is shown by filled red and white arrows. The pancreatic islets (Islets of Langerhans) are demarcated by the dotted blue lines.

doi:10.1371/journal.pone.0165031.g008

Proinflammatory cytokines upregulate expression of MUC1-ARF protein

Cytokines such as interferon-gamma, tumor necrosis factor-alpha (TNF), IL-1beta and IL-6, and combinations of these cytokines, have been shown to elicit marked increases in MUC1-TM expression [26, 32–38]. Although interferon-gamma by itself was shown to upregulate MUC1 expression in most cell lines, the addition of tumor necrosis factor-alpha to interferon-gamma elicited marked synergistic stimulation of MUC1 expression [26, 33]. Specifically, combinations of the cytokines [interferon-gamma and IL-1beta], [IL-6 together with TNFalpha] and [interferon-gamma and TNFalpha] have been shown to stimulate MUC1-TM expression to several-fold higher than by each cytokine alone [26]. We therefore looked at the effect of these combinations of cytokines on MUC1-ARF expression. Similarly to cytokine stimulation of MUC1-TM expression, MUC1-ARF showed both quantitative and qualitative changes

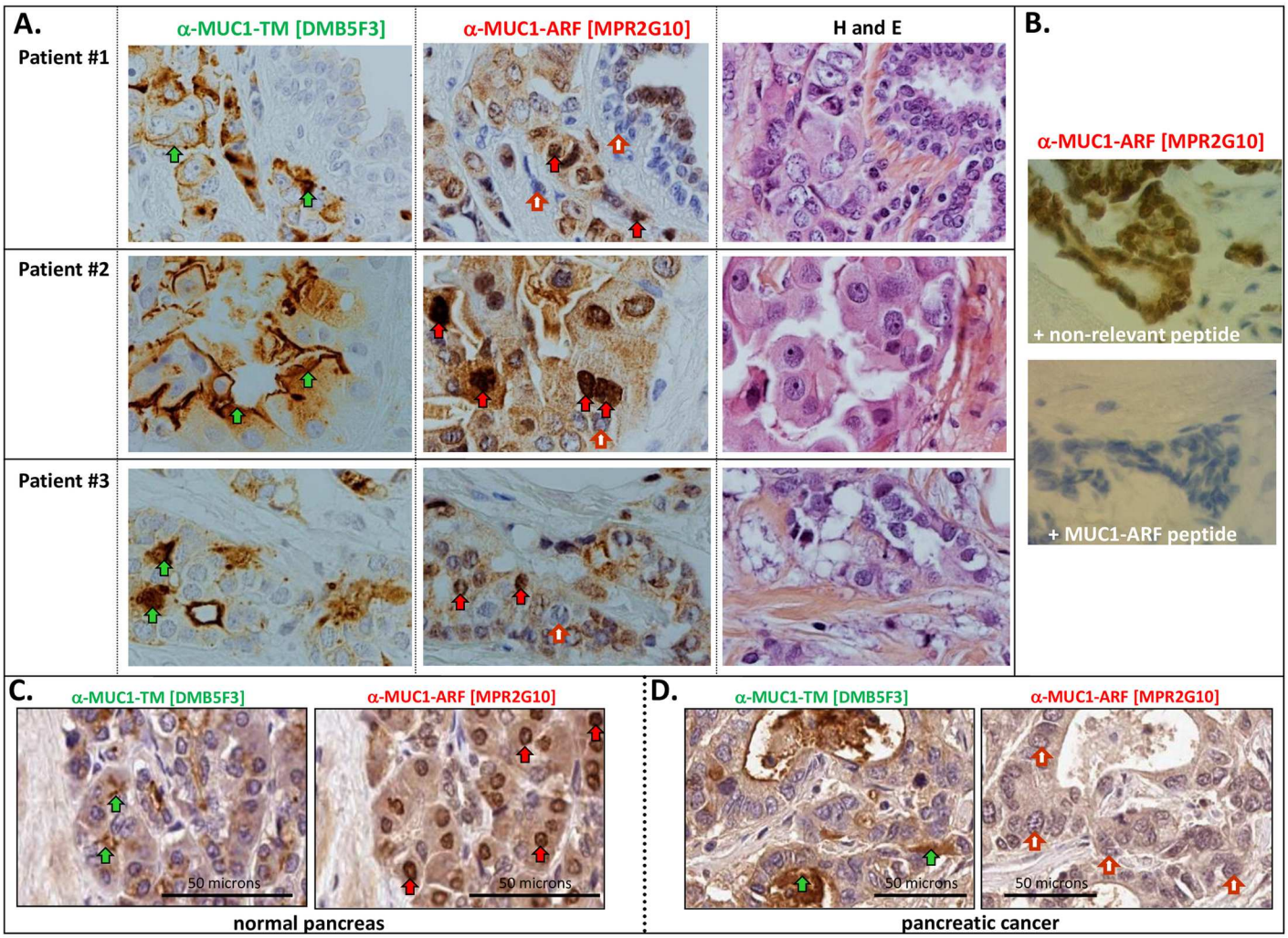

Fig 9. Immunohistochemical analyses of MUC1-TM and MUC1-ARF expression in breast and pancreatic cancer. (A) Serial sections of breast cancer tissues from three distinct individuals were immunohistochemically stained with anti-MUC1-TM antibodies (anti-MUC1-TM [DMB5F3]), anti-MUC1-ARF antibodies (anti-MUC1-ARF [MPR2G10]) and with hematoxylin/eosin (H and E). Green arrows indicate sites of MUC1-TM reactivity at the cell surface, and red arrows designate MUC1-ARF reactivity in the nuclei. Absence of anti-MUC1-ARF immunoreactivity is shown by filled red and white arrows. (B) Binding specificity of anti-MUC1-ARF [MPR2G10] antibody is demonstrated by addition of either MUC1-ARF peptide or a non-relevant peptide, as indicated. Only MUC1-ARF peptide abrogates immunoreactivity. Serial sections of normal pancreas (C) or pancreatic cancer tissue (D), were immunohistochemically stained with anti-MUC1-TM [DMB5F3] or anti-MUC1-ARF [MPR2G10]. Both MUC1-TM and MUC1-ARF are expressed in the normal pancreatic tissue (C). In contrast, cancer tissue expresses only MUC1-TM. MUC1-ARF was not detected (red and white arrows).

doi:10.1371/journal.pone.0165031.g009

following cytokine treatment (Fig 10). Immunofluorescence with mAb MPR2G10, combinations of interferon-gamma and IL-1beta, IL-6 together with TNFalpha, and of interferon-gamma and TNFalpha clearly led to increased MUC1-ARF expression (Fig 10A, compare Panels 'b', 'c' and 'd', with Panel 'a'). Flow cytometry analyses and quantitative ELISA assays using anti-MUC1-ARF monoclonal antibody MPR2G10 confirmed these findings (Fig 10B, Panels 'a', 'b' and 'c').

As expected, prolonged cytokine treatment with interferon-gamma and IL-1beta clearly induced MUC1-TM. Irrespective of cytokine addition, MUC1-TM remained tethered at the cell membrane (Fig 10C, compare panels a and b). In contrast, prolonged cytokine treatment elicited a disproportionate increase in cytoplasmic MUC1-ARF at the expense of nuclear

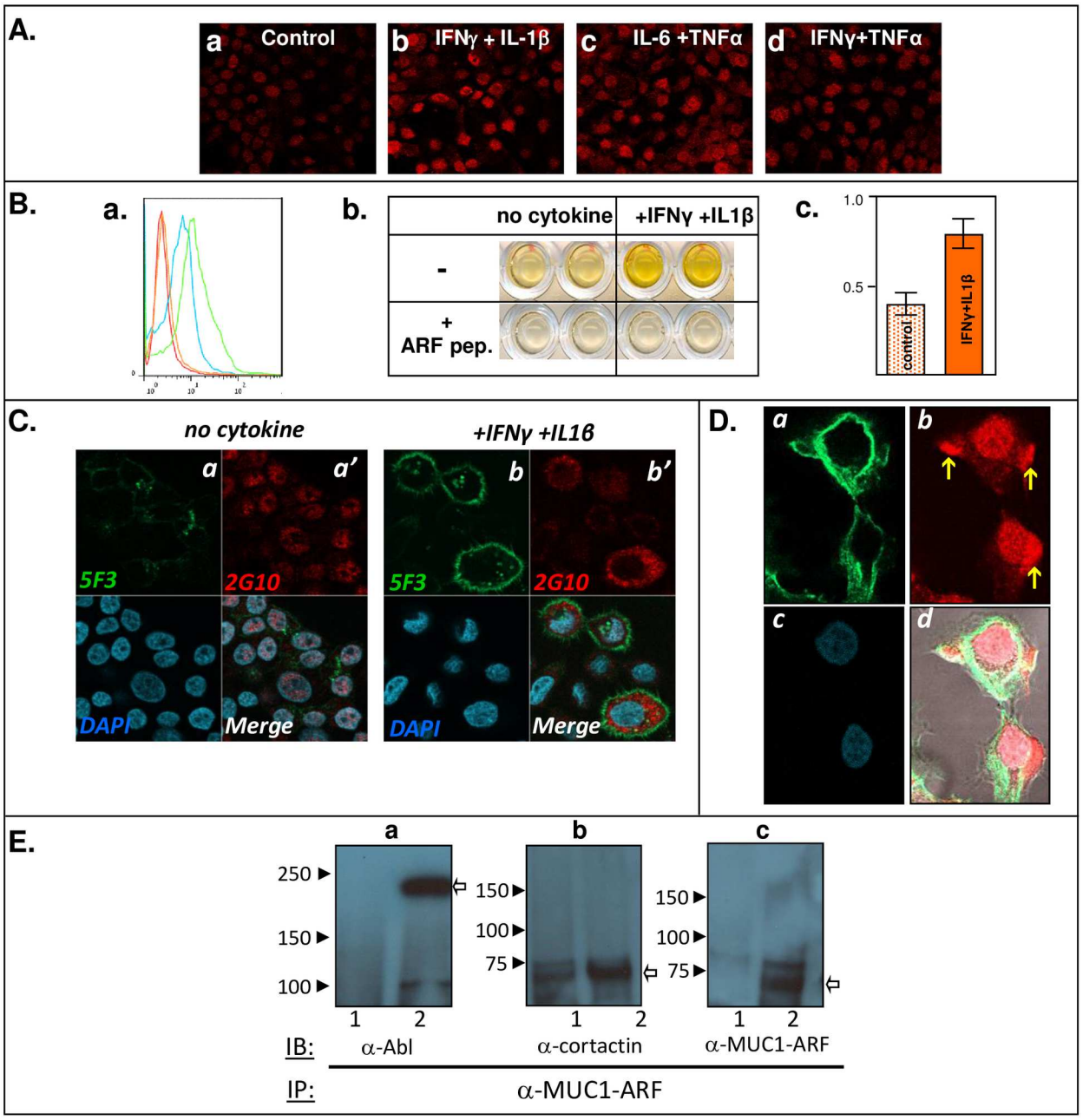

Fig 10. Cytokines upregulate MUC1-ARF expression and result in its relocalization. (A) COLO357 pancreatic cancer cells were either untreated (Control, Panel a), or incubated for 8 hours with interferon-gamma and interleukin1-beta (Panel b); interleukin 6 and TNFalpha (Panel c); interferon-gamma and TNFalpha (Panel d). This was followed by immunostaining with anti MUC1-ARF antibody MPR2G10 and red-labeled secondary detection. (B a.) COLO357 cells were either untreated or incubated for 8 hours with interferon-gamma and interleukin1-beta, (blue and green tracings, respectively), permeabilized, and analyzed by flow cytometry with anti-MUC1-ARF MPR-2G10, and detection with fluorescently labeled secondary anti-mouse antibody. Addition of secondary antibodies alone to untreated and cytokine-treated cells is shown by the orange and red tracings, respectively. (B b. c.) MUC1-ARF protein in untreated and cytokine-treated COLO357 cells was quantitatively assessed by sandwich ELISA (b), and shown in block graphs in (c). Specificity of antibody binding to MUC1-ARF protein was confirmed by addition of competing MUC1-ARF peptide (b. plus ARF peptide). (C) COLO357 cells were either untreated (Panels a, a', designated 'no cytokine') or incubated for 24 hours with interferon-gamma plus interleukin1-beta (Panels b, b', designated 'plus IFNgamma plus IL1beta'). Immunostaining with anti-MUC1-ARF MPR2G10 and detection by red-labeled secondary antibody (a' and b') was followed by green-labeled anti-MUC1-SEA module DMB5F3 (a and b). DAPI (blue) and merged images are presented in the lower left and right panels, respectively. (D) COLO357 cells were treated for forty-eight hours with IFNgamma and IL1beta, and actin filaments visualized by staining with green-labeled phalloidin (a), and MUC1-ARF protein immunostained with anti MUC1-ARF MPR2G10 followed by detection with red-labeled secondary antibody

(b). DAPI-stained nuclei and merged images are shown in (c) and (d), respectively. Following prolonged cytokine treatment, MUC1-ARF expression shifted in part to membrane protrusions, indicated by yellow arrows. (E) Cell lysates were prepared from HK293 cells transiently transfected with an expression vector driving expression of MUC1 cDNA (lanes 2) or with a control empty expression vector (lanes 1). Anti-MUC1-ARF immunprecipitates were resolved on SDS-PAGE, western blotted, and probed with antibodies as indicated.

doi:10.1371/journal.pone.0165031.g010

MUC1-ARF (Fig 10C, compare panels a' and b'), indicating that exposure to the cytokines leads not only to a quantitative increase in MUC1-ARF but also to cellular relocalization of MUC1-ARF. This shift was particularly prominent following extended cytokine treatment, and discrete compartments that stained intensely for MUC1-ARF appeared to be in the process of forming blebs at the cell surface (Fig 10D, indicated by yellow arrows).

MUC1-ARF function: The proline-rich tandem repeat domain of MUC1-ARF interacts with SH3-domain containing signaling proteins

In an attempt to define MUC1-ARF function, we used a bioinformatic MotifScan approach to search for proteins putatively interacting with MUC1-ARF. This yielded a set of signaling proteins such as Grb2, phospholipase C-gamma1, p85 subunit of PI-3'-kinase, and Abl tyrosine kinase which were predicted to bind via their SH3 domains with a high level of confidence ($>99.9^{th}$ percentile) to proline-rich regions of MUC1-ARF tandem repeat sequence GRPRAPP**P**PQPTVSP. To see whether MUC1-ARF in fact forms complexes with SH3-containing proteins as predicted, anti-MUC1-ARF immunoprecipitates (IP) were resolved by SDS-PAGE and probed by immunoblotting (IB) with an array of antibodies recognizing SH3–domain containing proteins. These assays demonstrated that in fact Abl tyrosine kinase and cortactin, both of which contain SH3 domains co-precipitated with MUC1-ARF from MUC1 cDNA transfected HK cells (Fig 10E, lanes 2, panels 'a' and 'b'). HK cells transfected with mock cDNA and therefore not expressing endogenous MUC1 did not show the coprecipitating proteins (Fig 10E, lanes 1).

To further our understanding of MUC1-ARF function, it would be highly informative to knockout MUC1-ARF expression in cells that naturally express MUC1-ARF protein and look at the resulting phenotype. However the entire MUC1-ARF protein coding region, including the initiation codons directing MUC1-ARF protein expression, is an integral component of the MUC1-TM reading frame (Fig 2). As a result, knocking out MUC1-ARF expression inevitably means that MUC1-TM protein produced in these cells will be truncated. Whatever phenotype is seen in such cells could not be unambiguously ascribed to the lack of MUC1-ARF; it could just as well be attributed to expression of a truncated MUC1-TM protein. Thus knocking out MUC1-ARF expression, for example by CRISPR technology, is not a feasible experimental approach to learn about MUC1-ARF function.

Much information on MUC1-TM function has been gained by identifying proteins that interact with MUC1-TM. In a similar manner, identification of proteins interacting with MUC1-ARF in cells that natively express MUC1-ARF could shed light on MUC1-ARF function. To identify such proteins, we prepared lysates from MCF7 cells (that express MUC1-ARF, see above Fig 6) and MUC1-ARF protein was immunoprecipitated using anti-MUC1-ARF monoclonal antibody MPR2G10 prebound to Protein A/G agarose beads. Proteins associated with the beads were then trypsin digested, followed by mass spectrometric analyses. Addition of MUC1-ARF repeat peptide consistently competed out MPR2G10 monoclonal antibody immunoreactivity in all modalities employed including immunofluorescence, immunohistochemistry, ELISA assays and western blotting, and in all cells expressing MUC1-ARF including cell transfectants expressing the human *MUC1* gene, cell lines endogenously expressing the

MUC1 gene, and in human tissues expressing the *MUC1* gene. To eliminate the possibility of non-specific antibody binding, MUC1-ARF protein was immunoprecipitated, either in the absence of competing MUC1-ARF peptide or in its presence. Only those proteins that showed a significant mass spectrometric signal in the absence of ARF peptide and a complete 'competing-out' of signal (a reading of "0") in the presence of ARF peptide were deemed to be true proteins that interact with MUC1-ARF. This analysis yielded two prominently interacting proteins, Glucose-6-phosphate dehydrogenase (G6PD) and Dynamin 2 (DNM2), whereas all other proteins gave substantially lower signals. Tryptic digestion releases Protein A and Protein G peptides from the affinity support matrix (Protein A/G agarose beads)- these peptides represent approximately 1.5% of total spectra. As an indication of their abundance, G6PD and DNM2 yielded percentage values of total spectra of 0.16% and 0.11%, respectively, and both proteins gave zero readings in the samples that had been immunoprecipitated in the presence of MUC1-ARF peptide demonstrating their binding specificity. When viewed in relation to the abundant Protein A and Protein G peptides, the values recorded for G6PD and DNM2 are exceptionally high.

Discussion

We demonstrate here that translation of MUC1 mRNA in an alternate reading frame generates MUC1-ARF protein, which differs in its entirety from the amino acid sequence of its tumor-associated 'parent' protein, MUC1-TM (Figs 1 and 2). MUC1-ARF is comprised of 49 amino acids N-terminal to the tandem repeat domain, followed by the tandem repeat domain and finally by a C-terminal domain of 175 amino acids. Since the MUC1-TM tandem repeat domain has a lower limit of about 300 amino acids (15 copies of a twenty amino acid repeat unit [19, 25, 39–41]), the complete MUC1-ARF protein must contain at least 524 amino acids making it as far as we are aware, the largest protein reported to date generated by an overlapping alternate reading frame.

The studies reported here demonstrate unequivocal expression of the frameshifted MUC1-ARF protein in MUC1 cell transfectants, in MUC1-expressing cancer cell lines, and in sections of normal and malignant human tissues. In normal tissues, expression of the MUC1-ARF and MUC1-TM proteins showed a tight correlation, such that epithelial cells forming ducts in the pancreas and kidney expressed not only MUC1-TM, but also clearly expressed MUC1-ARF (Figs 7 and 8). The contrary was also true: tissues such as brain and liver which do not express MUC1-TM do not express MUC1-ARF. Similarly, ductal epithelial cells of resting breast tissue showed very low MUC1-TM expression, accompanied by almost undetectable levels of MUC1-ARF.

Mass spectrometric analyses were ineffective in identifying peptides contained within the MUC1-ARF protein, and several possibilities could explain the inability of this modality to identify MUC1-ARF. It may well be that MUC1-ARF undergoes post-translational modifications on multiple amino acid residues (see above in Results for the MotifScan analysis), the type of which we do not presently know, rendering its identification by mass spectrometry intractable. Such post-translational modifications or combinations thereof appearing in the protein either stoichiometrically or/and substoichiometrically, could include, yet not be restricted to, methylation, phosphorylation and/or O-GlcNAcylation [42], the latter of which is known to be particularly prevalent on nuclear-resident proteins, such as MUC1-ARF. In this context it is pertinent to note that the latest review of a flurry of recent studies uncovering the unexplored alternative ORF proteome (AltORFs) [43], notes that mass spectrometry experiments often lack the sensitivity or technical details required for detection of all proteins, as appears to be the case for MUC1-ARF.

In contrast to this, the evidence presented here that MUC1-ARF is expressed as a protein is strikingly convincing: (i) its expression is seen only in cells that express the human *MUC1* gene (Figs 3, 4, 6, 7 and 8) (ii) mouse cells that do not express human MUC1 are negative for MUC1-ARF whereas the same cells transfected with and expressing human MUC1 DNA express MUC1-ARF, as observed by immunofluorescence, western blots, flow cytometry and ELISA assays (Figs 3 and 4), (iii) MUC1-ARF expression was detected not only with the anti-MUC1-ARF monoclonal antibody MPR2G10, but also with purified anti-MUC1-ARF polyclonal antisera as well as with an additional two independently isolated anti-MUC1-ARF monoclonal antibodies (Fig 3), and (iv) MUC1-ARF immunoreactivity was in all cases abrogated by the addition of MUC1-ARF specific peptide, and not by non-specific peptides. Constituting perhaps the most forceful piece of evidence, (v) the immunohistochemical analyses performed on unmanipulated normal human tissues clearly show MUC1-ARF protein that localizes to the cell nucleus (Figs 7, 8 and 9). Particularly compelling is the picture seen with normal kidney tissue (Fig 7) where MUC1-ARF localizes to the nuclei of only those epithelial cells lining the ducts of distal tubules. All other cells within the same section of kidney tissue are unequivocally negative for MUC1-ARF. In the kidney, this discrete expression of MUC1-ARF correlates precisely with the distribution of MUC1-TM expression, which is restricted solely to the identical ductal-forming epithelial cells of the distal tubules. Comparison of sequential kidney sections stained for either MUC1-TM or MUC1-ARF clearly reveals that those cells expressing MUC1-TM also express MUC1-ARF. Within the same section, epithelial cells other than those forming the lumen of distal tubules serve admirably both for antibody specificity and as negative controls. They are all negative not only for MUC1-TM but also for MUC1-ARF. Further bolstering this evidence for the in-vivo expression of MUC1-ARF are the analyses of MUC1 protein expression in the normal pancreas (Figs 7 and 8). In the pancreas, a similar situation pertains to that seen in the kidney, in that both MUC1-TM and MUC1-ARF are clearly expressed in acinar and ductal cells of the exocrine pancreas (Figs 7 and 8). In contrast to the pancreatic acinar and ductal cells, the pancreatic islets forming the endocrine pancreas do not express MUC1-TM as we demonstrate here (Fig 8) and as is known from the literature [28]. Consistent with this, MUC1-ARF is unambiguously absent from the pancreatic islet cells, just as is MUC1-TM (Fig 8).

Additional evidence for expression of MUC1-ARF protein was provided by (vi) Analyses of MUC1-ARF protein expression by western blots in cell lines that were in parallel analyzed for expression of MUC1 mRNA by qPCR analyses (Fig 6). Without exception, we observed an absolute correlation of MUC1-ARF protein expression to expression of MUC1 mRNA. The converse was also true in that all cell lines that did not show MUC1 mRNA expression, were likewise negative for MUC1-ARF protein (Fig 6). (vii) Polymorphic allelic forms of the MUC1-ARF protein were observed in those cell lines expressing the MUC1-ARF protein, consistent with the known allelic polymorphism of the *MUC1* gene itself (Fig 6). Finally, (viii) the smaller MUC1-ARF allele was always expressed at significantly higher levels as compared to expression of the larger allele consistent with previously published data on expression of MUC1 mRNA (25). Taken together, the experimental evidence detailed in the Results section (Figs 1, 3–10), and summarized above [items (i)–(viii)] compellingly favors MUC1-ARF protein expression and makes it highly unlikely, if not untenable, that the MUC1-ARF protein is an experimental artifact.

Among its multiple functions, cell-surface MUC1-TM acts to protect the cell from foreign organisms such as bacteria and viruses [44–47]. Consistent with this is our finding that *MUC1* gene expression, including that of MUC1-ARF, is markedly upregulated by interferons and other cytokines (Fig 10). Correspondingly, a single STAT responsive element has been identified within the MUC1 promoter, that when mutated both decreases MUC1 promoter activity

in breast cancer cells and also abolishes stimulation by interleukin-6 and interferon-gamma [35]. Expression of both MUC1-TM and MUC1-ARF may in fact be favored in environments that are conducive to the growth of foreign organisms, such as within the lumen of distal renal tubules, as we observed here (Fig 6). In keeping with this, resting normal breast comprising ductal tissue through which little if any fluid flows demonstrates low expression of both MUC1-TM and MUC1-ARF. This contrasts with lactating breast, where high levels of MUC1-TM protein are present on the apical surfaces of epithelial cells forming ducts involved in lactation [48].

It has been amply documented that MUC1-TM transduces signals from the extracellular space into the cell via tyrosine phosphorylation of its cytoplasmic domain [49] which then recruits second messenger signaling proteins such as Grb2 and beta catenin [49–54]. Following its binding to STAT3 and nuclear factor-kappa-b (NF-kappa-b), the cytoplasmic MUC1-TM domain re-localizes from the cell membrane to the cell nucleus, and can modulate the activity of the NF-kappa-b pathway by interacting with, and activating NF-kappa-b p65 and family members of IKK [55]. It is intriguing therefore that MUC1-ARF not only localizes primarily to the cell nucleus, but also binds the SH3-domain containing proteins Abl and cortactin. In fact, because of the tandem repeat of its proline-rich binding motif, MUC1-ARF protein likely contains multiple docking sites for signaling proteins, suggesting that MUC1-ARF may serve as a scaffold capable of binding multiple copies of [SH3-domain]-containing proteins. It is notable then that the cytoplasmic domain in the beta-subunit of the MUC1-TM protein undergoes phosphorylation on a series of tyrosine residues thereby complexing to SH2-domain-containing signaling proteins including the Abl tyrosine kinase [56]. Furthermore, like the Abl tyrosine kinase [57] MUC1-ARF localizes both to the cytoplasm and to the nucleus, suggesting that MUC1-ARF could serve to facilitate the shuttling of bound signaling proteins to and from the nucleus.

Following the initial discovery of MUC1-TM tyrosine phosphorylation [49] understanding MUC1-TM function has been considerably enhanced by identifying proteins interacting with the MUC1-TM protein. A similar approach was therefore used here to gain insight into MUC1-ARF function. By mass spectrometric analyses of proteins interacting with MUC1-ARF, we found that Glucose-6-phosphate 1-dehydrogenase (G6PD) and Dynamin 2 (DNM2) were the highest scoring proteins interacting with MUC1-ARF. Recent work has demonstrated that MUC1-TM acts as a novel metabolic master regulator by acting as a transcriptional coactivator thereby regulating expression of metabolic genes [reviewed in [58]]. Because of this, the interaction of MUC1-ARF with G6PD, an important metabolic regulator, is particularly intriguing. G6PD is a significant metabolic regulator that provides reducing power (NADPH) and pentose phosphates for fatty acid and nucleic acid synthesis. MUC1-ARF interaction with G6PD may act to modulate G6PD activity thereby acting similarly to MUC1-TM as a metabolic regulator (58).

MUC1-ARF interaction with dynamin 2, a GTPase that facilitates vesicle fission during synaptic vesicle endocytosis, is also of interest because the C-terminal domain of dynamin is a proline-rich domain (PRD) very similar in make-up to the proline-rich domain of the MUC1-ARF tandem repeats [59, 60]. Dynamin is recruited to sites of endocytosis by interacting with the SH3 domains of a variety of proteins, via dynamin PXXP motifs (where X represents any amino acid) that are flanked on either side by a basic residue such as arginine. Such PXXP motifs are particularly prevalent in the MUC1-ARF tandem repeats (see Results), and appear there as PRAP, PPPP, PPQP, PRTP and PGRP. It therefore may well be that protein(s) containing two or more SH3 domains bridge between dynamin 2 and MUC1-ARF. Significantly, dynamin interacts with cortactin, which comprises a well characterized SH3 domain [61, 62] and is an actin-binding protein shown to participate in receptor-mediated endocytosis.

Regulation of receptor-mediated endocytosis requires remodeling of actin filaments involving dynamin2 GTPase activity that is dependent on its interaction with the F-actin-binding protein cortactin [63]. Because it has been extensively documented that cell surface receptor regulation involves both dynamin and a number of SH3 domain-containing proteins such as cortactin (for example [64–67], the interaction of MUC1-ARF not only with dynamin 2 but also with cortactin (Fig 10, Panel E) suggests that MUC1-ARF may also be involved in the regulation of cell surface receptors. As compelling as the above evidence is, the definitive nature of MUC1-ARF function remains to be determined.

Parental and ARF proteins expressed from the same gene are often functionally linked. For example, the proteins p16INK4A and p19ARF proteins are both expressed from a common ARF/INK4A locus, and act as tumor suppressor proteins and function in similar pathways [8]. Interestingly, the protein ALEX derived by alternate frame reading of the mRNA coding for the G-protein alpha-subunit XLas physically interacts with the XL-domain of the 'parent' XLas gene product, such that both parent and ARF proteins act in concert [10, 68]. Such physical interaction between 'parent' and ARF proteins is also seen between Xbp1(S) protein, a transcription factor that participates in the unfolded protein response, and Xbp1(U)-ARF protein generated by alternate reading frame translation of an unspliced Xbp mRNA [69, 70]. Similarly, the overlapping reading frame in the ataxin-1 coding sequence encodes a novel protein that also interacts with the 'parental' ataxin-1 protein [71]. The pattern emerging from these findings is that despite very different amino acid sequences of expressed ARF proteins compared to their 'parent' proteins, ARF proteins can be functionally linked to their 'parent' proteins. We do not as yet know with any degree of certainty, whether the MUC1-TM and MUC1-ARF proteins are in fact functionally linked as is the case for parental and ARF proteins cited above.

MUC1-ARF is a very basic protein, rich in proline residues that comprise about 35% of the tandem repeat sequence. This structural make-up is in line with other ARF proteins that are basic and show a conspicuous bias for a high proline content suggesting an increase in the level of structural disorder. For example, the ALEX protein has a predicted pI of 11.8 with a 21% proline content [10] and the ARF protein derived from the INK4 locus is composed of approximately 20% arginine residues [8]. Because of its high proline content, MUC1-ARF appears to be natively unstructured, just as are ALEX and $p19^{ARF}$. Of note, both ALEX and $p19^{ARF}$ form specific and tight interactions with partner proteins, and $p19^{ARF}$ acquires activity and stability only when bound to targets [72].

In contrast to localization of MUC1-TM to the cell surface, MUC1-ARF localizes to the cell nucleus, as observed in normal kidney and pancreas as well as in breast cancer tissues (Figs 5–8). The cytoplasmic domain of MUC1-TM has been observed to also localize to the cell nucleus [50], thus highlighting the similarity of MUC1-ARF and MUC1-TM.

Proteins locating at and functioning in the nucleus frequently contain nuclear localization signals (NLS), required for translocation through the nuclear pore complex. These typically contain clusters of basic amino acids, usually flanked by proline residues, and many NLS motifs appear in pairs (bipartite NLS signals) or even as multiple signals within the one protein [73]. Although there is no canonical nuclear localization signal present in the MUC1-ARF protein, it is notable that the MUC1-ARF tandem repeat itself comprises the proline-arginine rich motifs *PRAPP*, *PRPR* and *GRPR*. In this context, various FGF2 and FGF3 protein isoforms, especially those initiating at upstream alternative initiation sites, localize to the cell nucleus [74–76] not because they contain a canonical nuclear localization signal, but because they also comprise motifs such as PRAAP, PRTR and GRGR very similar to those seen in the MUC1-ARF tandem repeat (compare FGF/*MUC1-ARF* motifs- PRAAP/*PRAPP*, PRTR/*PRPR* and GRGR/ *GRPR*). It is therefore possible that just as in the case of the FGF2 and FGF3

proteins, proline-arginine rich motifs within the MUC1-ARF tandem repeat direct nuclear localization of MUC1-ARF.

In contrast to the significant expression of both MUC1-TM and of MUC1-ARF on the apical surfaces of normal luminal epithelial cells present both in the kidney and those forming the exocrine pancreatic ducts and acini (Figs 7 and 8), the normal luminal epithelial cell of the resting non-lactating breast expresses very low levels if at all of these MUC1 proteins. Epithelial cells of breast cancer tissue, however, show in many instances very high MUC1-TM expression. The accepted consensus is that this increased expression in breast cancer cells in some way links MUC1-TM protein to a malignant phenotype [see review [15]].

Increased expression of MUC1-TM taken as the single parameter, however, without taking into account the tissue architecture of MUC1-expressing cells has been shown not to have prognostic significance [77]. In a study encompassing more than 1,300 cases of breast cancer it was clearly shown that the specific tissue architecture of MUC1-expressing cells has prognostic value: cytoplasmic expression with *circumferential* membranous MUC1-TM localization was unmistakably associated with a worse prognosis, whereas apical, luminal expression predicted a favorable outcome. Thus not only is tissue type (breast tissue versus kidney and/or pancreatic tissues) important in considering the relevance of MUC1 expression to malignant phenotype, but also the spatial organization of MUC1 expression on malignant epithelial cells can be determinant. Breast cancer cannot be considered to be one homogeneous disease. Indeed molecular expression signatures [78] have identified at least 5 major breast cancer types- luminal A, luminal B, basal, HER2-enriched and normal-like [[79] and references contained therein], and although this broad classification has prognostic implications, such prognostic forecasting is not at all times clear-cut. The luminal A subtype, with a better prognosis, and luminal B subtype with a worse prognosis are both considered to be derived from the breast luminal epithelial cell. Yet these two subtypes are particularly difficult to differentiate one from the other, and in this regard our studies on MUC1-ARF expression may help to discriminate the luminal A and luminal B subtypes. MUC1-ARF expression, as shown here, is seen only in a select subgroup (~40%) of those breast tumors that express MUC1-TM, and thus may designate a breast cancer subtype with a specific prognostic outcome for the following reasons. Because *normal* pancreatic and kidney cells coexpress both MUC1-TM and MUC1-ARF, thus typifying the MUC1 expression pattern of a normal epithelial cell (both MUC1-TM and MUC1-ARF), it would appear as if the subtype of breast cancers that also coexpress both MUC1-TM and MUC1-ARF, a signature MUC1-expression pattern reflecting the normal epithelial cell, may have a better prognosis than those tumors that express only MUC1-TM. The tissue architecture of MUC1-TM and MUC1-ARF expressing cells, as described above, might also be a factor. The unambiguous prognostic significance of MUC1-ARF expression (or the lack of its expression) together with MUC1-TM will require the further analysis of much larger population samples.

In cancer tissues, expression of MUC1-ARF protein was highly dependent on the tissue in question. Pancreatic cancers, known for their aggressive malignant phenotype, showed a loss of MUC1-ARF expression, as compared to high MUC1-ARF expression in epithelial cells from normal pancreatic tissue. In contrast, a number of human breast cancer samples showed preferential MUC1-ARF expression in the cancer cell population, with little to no expression in normal breast tissue, suggesting that just as the transmembrane MUC1 protein is preferentially overexpressed in transformed breast epithelial cells, so too is the MUC1-ARF protein. Although in these samples MUC1-ARF expression segregated with MUC1-TM expression, it did so in only a restricted subset of the MUC1-TM positive samples, implying that mechanisms other than the mere presence of MUC1 mRNA determine MUC1-ARF expression and that regulatory controls ultimately govern which reading frame(s) are translated, and to what

extent. Possible mechanisms include leaky scanning, ribosomal shunting and mechanisms promoting use of internal ribosomal entry sites. As demonstrated here, a diversity of cytokines induce MUC1-ARF expression, suggesting that a specific milieu of cytokines and growth factors present in the tumor microenvironment may govern its restricted expression. This in turn could define a cancer subtype, wherein MUC1-ARF positivity confers prognostic significance, as also discussed above. The intracellular distribution of MUC1-ARF protein, whether nuclear or/and cytoplasmic, may also be important, and extensive immunohistochemical studies will be required to see whether the quantitative and qualitative changes in MUC1-ARF expression in breast cancer tissue indeed have prognostic significance to disease outcome.

The expression of a given protein by normal non-malignant cells does not preclude linkage of that protein to a malignant phenotype. This linkage to malignancy may be seen as an altered pattern of expression of the protein, that could involve a quantitative alteration in its level of expression or/and in its cellular localization. A case in point, clearly pertinent to this report is that of MUC1-TM itself, which is universally accepted as linked in some way to breast cancer (see above and for a recent review [15]), despite the fact that MUC1-TM is extensively expressed on epithelial cells of, amongst others, the normal pancreas, kidney and normal, lactating breast. Further emphasizing this point are the well-known examples of the normal cellular proteins epidermal growth factor receptor (EGFR), HER2 (epidermal growth factor receptor 2) and estrogen receptor (ER). It is their *inappropriate* expression that inextricably links these proteins to a malignant phenotype, and it is universally accepted that EGFR, HER2 and ER are unambiguously linked to the breast cancer cell. Indeed cancer therapies such as antibodies targeting EGFR and HER2 [for example [80, 81]] as well as inhibitors of estrogen receptor activity are extensively used in the clinic. Yet notwithstanding their undisputed relevance to cancer, it is a well-known fact that EGFR, HER2 and ER are all expressed in normal cells, in which they play critical roles in normal cell growth and differentiation [82]. It is their inappropriate expression- quantitatively and qualitatively, spatially and temporally- just as we show here for MUC1-ARF, that links these proteins to the malignant cell.

The murine *MUC1* gene and its protein product [83] show major differences compared to those of primates and humans. In the mouse, the region spanning from the MUC1-TM initiation AUG codon to the tandem repeat domain encompasses only 41 amino acids, whereas in humans it comprises 125 amino acids. It is precisely within this segment that the human ARF initiation codon is located and it is likely that because of this difference between human and mouse, the mouse *MUC1* gene does not generate a MUC1-ARF protein. The mouse tandem repeat domain contains two additional crucial differences from that of primates: Whereas in primates the number of repeats can vary in any allele from ~15–125 repeats [19], the number of repeats is fixed in the mouse at an invariable 16 repeats [83]. Furthermore, the mouse repeat sequences themselves are far more divergent from each other as compared to the human and primate repeat sequences which are very similar one to the other [25, 84]. It thus appears that mammals higher up on the evolutionary ladder, such as primates and humans, have developed a more complex *MUC1* gene that is reflected in differences in the region from the MUC1-TM start codon until the tandem repeat domain as well as in the repeat domain itself. Although facilitating the synthesis of the MUC1-ARF protein in addition to MUC1-TM as shown here, this sophistication exacts a price from the cellular machineries that must cope with the non-trivial tasks of faithful replication and transcription of highly conserved GC-rich sequences, as found in the tandem repeat sequences and those immediately flanking it. That mistakes can occur here is amply demonstrated by the recent report on a mutation within the MUC1 tandem repeat which results in medullary cystic kidney disease 1 (MCKD1)[85].

The human *MUC1* gene has been previously shown to generate not only the transmembrane mucin-like protein that comprises a highly glycosylated tandem repeat domain, but additional alternative isoforms designated MUC1-X, MUC1-Y and MUC1-ZD [20–22, 86], that are generated by differential splicing events. Like MUC1-TM, both MUC1-X and MUC1-Y are transmembrane proteins. Yet in distinction to MUC1-TM they are both devoid of the central tandem repeat domain, that is spliced out using splice donor and acceptor sites located upstream and downstream to the tandem repeat array. Interestingly, the MUC1-ZD protein [86] utilizes the same splice donor site to that used by MUC1-X and MUC1-Y, yet the alternative MUC1-ZD splice acceptor site located downstream to the tandem repeat array leads to a downstream frameshifted sequence initiating with the amino acid sequence IPAPTTTKSCR. . . and terminating with GQDLWWYN. This C-terminal region of MUC1-ZD contains 43 amino acids, a region that is identical to the C-terminal portion of the MUC1-ARF protein reported here. Despite the identity of this C-terminal region, it is clear that these two MUC1 proteins localize to different cellular/extracellular compartments-MUC1-ZD is likely a secreted protein [86], whereas MUC1-ARF is a nuclear and cytoplasmic protein, as shown here. The overall scheme, that of a secreted protein and a nuclear/cytoplasmic protein both being derived from the same gene, is also observed with the FGF proteins. Some FGF protein isoforms are secreted proteins and others localize to the cytoplasmic/nuclear compartments, yet all derive from the same gene [for example [87, 88]].

Until very recently the scope of proteome diversity in eukaryotic organisms was thought to be determined primarily by canonical mechanisms such as utilization of alternative promoters, alternative splicing, usage of alternative adenylation sites and RNA editing. This canon is now being seriously challenged by the realization that enhancement of proteome diversity by non-canonical mechanisms, such as dual-coding mRNAs [43], wherein a single mRNA is decoded not only in the canonical reading frame, but also in alternative reading frames, is far more common than previously envisioned [2]. Here we have shown that the *MUC1* gene generates a MUC1 mRNA that yields more than a single protein, resulting not only in the well-characterized tumor-associated MUC1-TM protein, but also a novel MUC1-ARF protein. Furthermore MUC1-ARF represents the longest eukaryotic ARF protein heretofore reported. In addition to enhancing our understanding of *MUC1* gene involvement in the malignant transformation of cells, the discovery of MUC1-ARF furthers, at the more general level, our appreciation of dual-coding mechanisms in expanding proteome diversity.

Author Contributions

Conceptualization: DHW MC OJ EP JH F-GH AB.

Formal analysis: DHW OJ MC EP AB AM JH F-GH DBR.

Funding acquisition: DHW DBR.

Investigation: DHW MC OJ EP CG AM RZ TZ NIS JH.

Methodology: DHW MC OJ EP JH CG TZ NIS AM.

Project administration: DHW.

Supervision: DHW.

Writing – original draft: DHW DBR MC OJ.

Writing – review & editing: DHW DBR.

References

1. Menschaert G, Van Criekinge W, Notelaers T, Koch A, Crappe J, Gevaert K, et al. Deep proteome coverage based on ribosome profiling aids mass spectrometry-based protein and peptide discovery and provides evidence of alternative translation products and near-cognate translation initiation events. Mol Cell Proteomics. 2013; 12(7):1780–90. doi: 10.1074/mcp.M113.027540 PMID: 23429522; PubMed Central PMCID: PMCPMC3708165.
2. Vanderperre B, Lucier JF, Bissonnette C, Motard J, Tremblay G, Vanderperre S, et al. Direct detection of alternative open reading frames translation products in human significantly expands the proteome. PLoS One. 2013; 8(8):e70698. doi: 10.1371/journal.pone.0070698 PMID: 23950983; PubMed Central PMCID: PMCPMC3741303.
3. Normark S, Bergstrom S, Edlund T, Grundstrom T, Jaurin B, Lindberg FP, et al. Overlapping genes. Annu Rev Genet. 1983; 17:499–525. PMID: 6198955. doi: 10.1146/annurev.ge.17.120183.002435
4. Rosenberg SA, Tong-On P, Li Y, Riley JP, El-Gamil M, Parkhurst MR, et al. Identification of BING-4 cancer antigen translated from an alternative open reading frame of a gene in the extended MHC class II region using lymphocytes from a patient with a durable complete regression following immunotherapy. J Immunol. 2002; 168(5):2402–7. PMID: 11859131.
5. Oh S, Terabe M, Pendleton CD, Bhattacharyya A, Bera TK, Epel M, et al. Human CTLs to wild-type and enhanced epitopes of a novel prostate and breast tumor-associated protein, TARP, lyse human breast cancer cells. Cancer Res. 2004; 64(7):2610–8. PMID: 15059918.
6. Wang RF, Parkhurst MR, Kawakami Y, Robbins PF, Rosenberg SA. Utilization of an alternative open reading frame of a normal gene in generating a novel human cancer antigen. J Exp Med. 1996; 183 (3):1131–40. PMID: 8642255.
7. Ronsin C, Chung-Scott V, Poullion I, Aknouche N, Gaudin C, Triebel F. A non-AUG-defined alternative open reading frame of the intestinal carboxyl esterase mRNA generates an epitope recognized by renal cell carcinoma-reactive tumor-infiltrating lymphocytes in situ. J Immunol. 1999; 163(1):483–90. PMID: 10384152.
8. Quelle DE, Zindy F, Ashmun RA, Sherr CJ. Alternative reading frames of the INK4a tumor suppressor gene encode two unrelated proteins capable of inducing cell cycle arrest. Cell. 1995; 83(6):993–1000. PMID: 8521522.
9. Sherr CJ, Bertwistle D, DENB W, Kuo ML, Sugimoto M, Tago K, et al. p53-Dependent and -independent functions of the Arf tumor suppressor. Cold Spring Harb Symp Quant Biol. 2005; 70:129–37. PMID: 16869746. doi: 10.1101/sqb.2005.70.004
10. Klemke M, Kehlenbach RH, Huttner WB. Two overlapping reading frames in a single exon encode interacting proteins—a novel way of gene usage. Embo J. 2001; 20(14):3849–60. PMID: 11447126. doi: 10.1093/emboj/20.14.3849
11. Abramowitz J, Grenet D, Birnbaumer M, Torres HN, Birnbaumer L. XLalphas, the extra-long form of the alpha-subunit of the Gs G protein, is significantly longer than suspected, and so is its companion Alex. Proc Natl Acad Sci U S A. 2004; 101(22):8366–71. PMID: 15148396. doi: 10.1073/pnas.0308758101
12. Poulin F, Brueschke A, Sonenberg N. Gene fusion and overlapping reading frames in the mammalian genes for 4E-BP3 and MASK. J Biol Chem. 2003; 278(52):52290–7. PMID: 14557257. doi: 10.1074/jbc.M310761200
13. Gendler SJ. MUC1, the renaissance molecule. J Mammary Gland Biol Neoplasia. 2001; 6(3):339–53. PMID: 11547902.
14. Hattrup CL, Gendler SJ. Structure and function of the cell surface (tethered) mucins. Annu Rev Physiol. 2008; 70:431–57. Epub 2007/09/14. doi: 10.1146/annurev.physiol.70.113006.100659 PMID: 17850209.
15. Kimura T, Finn OJ. MUC1 immunotherapy is here to stay. Expert Opin Biol Ther. 2013; 13(1):35–49. doi: 10.1517/14712598.2012.725719 PMID: 22998452.
16. Rubinstein DB, Karmely M, Pichinuk E, Ziv R, Benhar I, Feng N, et al. The MUC1 oncoprotein as a functional target: Immunotoxin binding to alpha/beta junction mediates cell killing. Int J Cancer. 2008. PMID: 18821582. doi: 10.1002/ijc.23910
17. Pichinuk E, Benhar I, Jacobi O, Chalik M, Weiss L, Ziv R, et al. Antibody targeting of cell-bound MUC1 SEA domain kills tumor cells. Cancer Res. 2012; 72(13):3324–36. doi: 10.1158/0008-5472.CAN-12-0067 PMID: 22507854.
18. Ligtenberg MJ, Kruijshaar L, Buijs F, van Meijer M, Litvinov SV, Hilkens J. Cell-associated episialin is a complex containing two proteins derived from a common precursor. J Biol Chem. 1992; 267(9):6171–7. PMID: 1556125.

19. Silva F, Carvalho F, Peixoto A, Seixas M, Almeida R, Carneiro F, et al. MUC1 gene polymorphism in the gastric carcinogenesis pathway. Eur J Hum Genet. 2001; 9(7):548–52. doi: 10.1038/sj.ejhg.5200677 PMID: 11464247.

20. Baruch A, Hartmann M, Yoeli M, Adereth Y, Greenstein S, Stadler Y, et al. The breast cancer-associated MUC1 gene generates both a receptor and its cognate binding protein. Cancer Res. 1999; 59 (7):1552–61. PMID: 10197628.

21. Baruch A, Hartmann M, Zrihan-Licht S, Greenstein S, Burstein M, Keydar I, et al. Preferential expression of novel MUC1 tumor antigen isoforms in human epithelial tumors and their tumor-potentiating function. Int J Cancer. 1997; 71(5):741–9. PMID: 9180140.

22. Zrihan-Licht S, Vos HL, Baruch A, Elroy-Stein O, Sagiv D, Keydar I, et al. Characterization and molecular cloning of a novel MUC1 protein, devoid of tandem repeats, expressed in human breast cancer tissue. Eur J Biochem. 1994; 224(2):787–95. Epub 1994/09/01. PMID: 7925397.

23. Poland PA, Kinlough CL, Rokaw MD, Magarian-Blander J, Finn OJ, Hughey RP. Differential glycosylation of MUC1 in tumors and transfected epithelial and lymphoblastoid cell lines. Glycoconj J. 1997; 14 (1):89–96. PMID: 9076518.

24. Saeland E, Belo AI, Mongera S, van Die I, Meijer GA, van Kooyk Y. Differential glycosylation of MUC1 and CEACAM5 between normal mucosa and tumour tissue of colon cancer patients. Int J Cancer. 131 (1):117–28. PMID: 21823122. doi: 10.1002/ijc.26354

25. Wreschner DH, Hareuveni M, Tsarfaty I, Smorodinsky N, Horev J, Zaretsky J, et al. Human epithelial tumor antigen cDNA sequences. Differential splicing may generate multiple protein forms. Eur J Biochem. 1990; 189(3):463–73. PMID: 2351132.

26. Li X, Wang L, Nunes DP, Troxler RF, Offner GD. Pro-inflammatory cytokines up-regulate MUC1 gene expression in oral epithelial cells. J Dent Res. 2003; 82(11):883–7. PMID: 14578499.

27. Russo CL, Spurr-Michaud S, Tisdale A, Pudney J, Anderson D, Gipson IK. Mucin gene expression in human male urogenital tract epithelia. Hum Reprod. 2006; 21(11):2783–93. PMID: 16997931. doi: 10.1093/humrep/del164

28. Kopinke D, Murtaugh LC. Exocrine-to-endocrine differentiation is detectable only prior to birth in the uninjured mouse pancreas. BMC Dev Biol. 2010; 10:38. doi: 10.1186/1471-213X-10-38 PMID: 20377894; PubMed Central PMCID: PMCPMC2858732.

29. Pierreux CE, Poll AV, Kemp CR, Clotman F, Maestro MA, Cordi S, et al. The transcription factor hepatocyte nuclear factor-6 controls the development of pancreatic ducts in the mouse. Gastroenterology. 2006; 130(2):532–41. doi: 10.1053/j.gastro.2005.12.005 PMID: 16472605.

30. Cano DA, Murcia NS, Pazour GJ, Hebrok M. Orpk mouse model of polycystic kidney disease reveals essential role of primary cilia in pancreatic tissue organization. Development. 2004; 131(14):3457–67. doi: 10.1242/dev.01189 PMID: 15226261.

31. Singh PK, Hollingsworth MA. Cell surface-associated mucins in signal transduction. Trends Cell Biol. 2006; 16(9):467–76. PMID: 16904320. doi: 10.1016/j.tcb.2006.07.006

32. Koga T, Kuwahara I, Lillehoj EP, Lu W, Miyata T, Isohama Y, et al. TNF-alpha induces MUC1 gene transcription in lung epithelial cells: its signaling pathway and biological implication. Am J Physiol Lung Cell Mol Physiol. 2007; 293(3):L693–701. PMID: 17575006. doi: 10.1152/ajplung.00491.2006

33. Lagow EL, Carson DD. Synergistic stimulation of MUC1 expression in normal breast epithelia and breast cancer cells by interferon-gamma and tumor necrosis factor-alpha. J Cell Biochem. 2002; 86 (4):759–72. PMID: 12210742. doi: 10.1002/jcb.10261

34. Clark S, McGuckin MA, Hurst T, Ward BG. Effect of interferon-gamma and TNF-alpha on MUC1 mucin expression in ovarian carcinoma cell lines. Dis Markers. 1994; 12(1):43–50. PMID: 7842630.

35. Gaemers IC, Vos HL, Volders HH, van der Valk SW, Hilkens J. A stat-responsive element in the promoter of the episialin/MUC1 gene is involved in its overexpression in carcinoma cells. J Biol Chem. 2001; 276(9):6191–9. PMID: 11084045. doi: 10.1074/jbc.M009449200

36. Grohmann GP, Schirmacher P, Manzke O, Hanisch FG, Dienes HP, Baldus SE. Modulation of MUC1 and blood group antigen expression in gastric adenocarcinoma cells by cytokines. Cytokine. 2003; 23 (3):86–93. PMID: 12906871.

37. Reddy PK, Gold DV, Cardillo TM, Goldenberg DM, Li H, Burton JD. Interferon-gamma upregulates MUC1 expression in haematopoietic and epithelial cancer cell lines, an effect associated with MUC1 mRNA induction. Eur J Cancer. 2003; 39(3):397–404. PMID: 12565994.

38. Li YY, Hsieh LL, Tang RP, Liao SK, Yeh KY. Macrophage-derived interleukin-6 up-regulates MUC1, but down-regulates MUC2 expression in the human colon cancer HT-29 cell line. Cell Immunol. 2009; 256(1–2):19–26. doi: 10.1016/j.cellimm.2009.01.001 PMID: 19201396.

39. Gendler SJ, Lancaster CA, Taylor-Papadimitriou J, Duhig T, Peat N, Burchell J, et al. Molecular cloning and expression of human tumor-associated polymorphic epithelial mucin. J Biol Chem. 1990; 265 (25):15286–93. PMID: 1697589.

40. Lan MS, Batra SK, Qi WN, Metzgar RS, Hollingsworth MA. Cloning and sequencing of a human pancreatic tumor mucin cDNA. J Biol Chem. 1990; 265(25):15294–9. PMID: 2394722.

41. Ligtenberg MJ, Vos HL, Gennissen AM, Hilkens J. Episialin, a carcinoma-associated mucin, is generated by a polymorphic gene encoding splice variants with alternative amino termini. J Biol Chem. 1990; 265(10):5573–8. PMID: 2318825.

42. Hart GW. Minireview series on the thirtieth anniversary of research on O-GlcNAcylation of nuclear and cytoplasmic proteins: Nutrient regulation of cellular metabolism and physiology by O-GlcNAcylation. J Biol Chem. 289(50):34422–3. PMID: 25336646. doi: 10.1074/jbc.R114.609776

43. Landry CR, Zhong X, Nielly-Thibault L, Roucou X. Found in translation: functions and evolution of a recently discovered alternative proteome. Curr Opin Struct Biol. 2015; 32:74–80. doi: 10.1016/j.sbi.2015.02.017 PMID: 25795211.

44. McAuley JL, Linden SK, Png CW, King RM, Pennington HL, Gendler SJ, et al. MUC1 cell surface mucin is a critical element of the mucosal barrier to infection. J Clin Invest. 2007; 117(8):2313–24. PMID: 17641781. doi: 10.1172/JCI26705

45. Linden SK, Sheng YH, Every AL, Miles KM, Skoog EC, Florin TH, et al. MUC1 limits Helicobacter pylori infection both by steric hindrance and by acting as a releasable decoy. PLoS Pathog. 2009; 5(10): e1000617. PMID: 19816567. doi: 10.1371/journal.ppat.1000617

46. Linden SK, Florin TH, McGuckin MA. Mucin dynamics in intestinal bacterial infection. PLoS One. 2008; 3(12):e3952. PMID: 19088856. doi: 10.1371/journal.pone.0003952

47. Sando L, Pearson R, Gray C, Parker P, Hawken R, Thomson PC, et al. Bovine Muc1 is a highly polymorphic gene encoding an extensively glycosylated mucin that binds bacteria. J Dairy Sci. 2009; 92 (10):5276–91. PMID: 19762846. doi: 10.3168/jds.2009-2216

48. Mather IH, Jack LJ, Madara PJ, Johnson VG. The distribution of MUC1, an apical membrane glycoprotein, in mammary epithelial cells at the resolution of the electron microscope: implications for the mechanism of milk secretion. Cell Tissue Res. 2001; 304(1):91–101. PMID: 11383890.

49. Zrihan-Licht S, Baruch A, Elroy-Stein O, Keydar I, Wreschner DH. Tyrosine phosphorylation of the MUC1 breast cancer membrane proteins. Cytokine receptor-like molecules. FEBS Lett. 1994; 356 (1):130–6. Epub 1994/12/12. 0014-5793(94)01251-2 [pii]. PMID: 7988707.

50. Wen Y, Caffrey TC, Wheelock MJ, Johnson KR, Hollingsworth MA. Nuclear association of the cytoplasmic tail of MUC1 and beta-catenin. J Biol Chem. 2003; 278(39):38029–39. PMID: 12832415. doi: 10.1074/jbc.M304333200

51. Li Y, Bharti A, Chen D, Gong J, Kufe D. Interaction of glycogen synthase kinase 3beta with the DF3/MUC1 carcinoma-associated antigen and beta-catenin. Mol Cell Biol. 1998; 18(12):7216–24. PMID: 9819408.

52. Kinlough CL, Poland PA, Bruns JB, Harkleroad KL, Hughey RP. MUC1 membrane trafficking is modulated by multiple interactions. J Biol Chem. 2004; 279(51):53071–7. PMID: 15471854. doi: 10.1074/jbc.M409360200

53. Thompson EJ, Shanmugam K, Hattrup CL, Kotlarczyk KL, Gutierrez A, Bradley JM, et al. Tyrosines in the MUC1 cytoplasmic tail modulate transcription via the extracellular signal-regulated kinase 1/2 and nuclear factor-kappaB pathways. Mol Cancer Res. 2006; 4(7):489–97. PMID: 16849524. doi: 10.1158/1541-7786.MCR-06-0038

54. Hattrup CL, Gendler SJ. MUC1 alters oncogenic events and transcription in human breast cancer cells. Breast Cancer Res. 2006; 8(4):R37. PMID: 16846534. doi: 10.1186/bcr1515

55. Mori Y, Akita K, Tanida S, Ishida A, Toda M, Inoue M, et al. MUC1 protein induces urokinase-type plasminogen activator (uPA) by forming a complex with NF-kappaB p65 transcription factor and binding to the uPA promoter, leading to enhanced invasiveness of cancer cells. J Biol Chem. 289(51):35193–204. PMID: 25371209. doi: 10.1074/jbc.M114.586461

56. Raina D, Ahmad R, Kumar S, Ren J, Yoshida K, Kharbanda S, et al. MUC1 oncoprotein blocks nuclear targeting of c-Abl in the apoptotic response to DNA damage. Embo J. 2006; 25(16):3774–83. PMID: 16888623. doi: 10.1038/sj.emboj.7601263

57. Pendergast AM. Nuclear tyrosine kinases: from Abl to WEE1. Curr Opin Cell Biol. 1996; 8(2):174–81. PMID: 8791414.

58. Mehla K, Singh PK. MUC1: a novel metabolic master regulator. Biochim Biophys Acta. 2014; 1845 (2):126–35. doi: 10.1016/j.bbcan.2014.01.001 PMID: 24418575; PubMed Central PMCID: PMCPMC4045475.

59. Okamoto PM, Herskovits JS, Vallee RB. Role of the basic, proline-rich region of dynamin in Src homology 3 domain binding and endocytosis. J Biol Chem. 1997; 272(17):11629–35. PMID: 9111080.

60. Luo L, Xue J, Kwan A, Gamsjaeger R, Wielens J, von Kleist L, et al. The Binding of Syndapin SH3 Domain to Dynamin Proline-rich Domain Involves Short and Long Distance Elements. J Biol Chem. 2016; 291(18):9411–24. doi: 10.1074/jbc.M115.703108 PMID: 26893375; PubMed Central PMCID: PMCPMC4850282.

61. McNiven MA, Kim L, Krueger EW, Orth JD, Cao H, Wong TW. Regulated interactions between dynamin and the actin-binding protein cortactin modulate cell shape. J Cell Biol. 2000; 151(1):187–98. PMID: 11018064; PubMed Central PMCID: PMCPMC2189798.

62. Cao H, Orth JD, Chen J, Weller SG, Heuser JE, McNiven MA. Cortactin is a component of clathrin-coated pits and participates in receptor-mediated endocytosis. Mol Cell Biol. 2003; 23(6):2162–70. PMID: 12612086; PubMed Central PMCID: PMCPMC149460. doi: 10.1128/MCB.23.6.2162-2170.2003

63. Mooren OL, Kotova TI, Moore AJ, Schafer DA. Dynamin2 GTPase and cortactin remodel actin filaments. J Biol Chem. 2009; 284(36):23995–4005. doi: 10.1074/jbc.M109.024398 PMID: 19605363; PubMed Central PMCID: PMCPMC2781994.

64. Seugnet L, Simpson P, Haenlin M. Requirement for dynamin during Notch signaling in Drosophila neurogenesis. Dev Biol. 1997; 192(2):585–98. doi: 10.1006/dbio.1997.8723 PMID: 9441691.

65. Singleton PA, Salgia R, Moreno-Vinasco L, Moitra J, Sammani S, Mirzapoiazova T, et al. CD44 regulates hepatocyte growth factor-mediated vascular integrity. Role of c-Met, Tiam1/Rac1, dynamin 2, and cortactin. J Biol Chem. 2007; 282(42):30643–57. doi: 10.1074/jbc.M702573200 PMID: 17702746.

66. Lee MY, Skoura A, Park EJ, Landskroner-Eiger S, Jozsef L, Luciano AK, et al. Dynamin 2 regulation of integrin endocytosis, but not VEGF signaling, is crucial for developmental angiogenesis. Development. 2014; 141(7):1465–72. doi: 10.1242/dev.104539 PMID: 24598168; PubMed Central PMCID: PMCPMC3957370.

67. Wang Z, Moran MF. Requirement for the adapter protein GRB2 in EGF receptor endocytosis. Science. 1996; 272(5270):1935–9. PMID: 8658166.

68. Freson K, Jaeken J, Van Helvoirt M, de Zegher F, Wittevrongel C, Thys C, et al. Functional polymorphisms in the paternally expressed XLalphas and its cofactor ALEX decrease their mutual interaction and enhance receptor-mediated cAMP formation. Hum Mol Genet. 2003; 12(10):1121–30. PMID: 12719376.

69. Yoshida H, Oku M, Suzuki M, Mori K. pXBP1(U) encoded in XBP1 pre-mRNA negatively regulates unfolded protein response activator pXBP1(S) in mammalian ER stress response. J Cell Biol. 2006; 172(4):565–75. PMID: 16461360. doi: 10.1083/jcb.200508145

70. Nekrutenko A, He J. Functionality of unspliced XBP1 is required to explain evolution of overlapping reading frames. Trends Genet. 2006; 22(12):645–8. PMID: 17034899. doi: 10.1016/j.tig.2006.09.012

71. Bergeron D, Lapointe C, Bissonnette C, Tremblay G, Motard J, Roucou X. An out-of-frame overlapping reading frame in the ataxin-1 coding sequence encodes a novel ataxin-1 interacting protein. J Biol Chem. 288(30):21824–35. PMID: 23760502. doi: 10.1074/jbc.M113.472654

72. Pomerantz J, Schreiber-Agus N, Liegeois NJ, Silverman A, Alland L, Chin L, et al. The Ink4a tumor suppressor gene product, p19Arf, interacts with MDM2 and neutralizes MDM2's inhibition of p53. Cell. 1998; 92(6):713–23. PMID: 9529248.

73. Kiefer P, Acland P, Pappin D, Peters G, Dickson C. Competition between nuclear localization and secretory signals determines the subcellular fate of a single CUG-initiated form of FGF3. EMBO J. 1994; 13(17):4126–36. PMID: 8076608; PubMed Central PMCID: PMCPMC395335.

74. Antoine M, Reimers K, Dickson C, Kiefer P. Fibroblast growth factor 3, a protein with dual subcellular localization, is targeted to the nucleus and nucleolus by the concerted action of two nuclear localization signals and a nucleolar retention signal. J Biol Chem. 1997; 272(47):29475–81. PMID: 9368007.

75. Patry V, Arnaud E, Amalric F, Prats H. Involvement of basic fibroblast growth factor NH2 terminus in nuclear accumulation. Growth Factors. 1994; 11(3):163–74. PMID: 7734142.

76. Bugler B, Amalric F, Prats H. Alternative initiation of translation determines cytoplasmic or nuclear localization of basic fibroblast growth factor. Mol Cell Biol. 1991; 11(1):573–7. PMID: 1986249.

77. Rakha EA, Boyce RW, Abd El-Rehim D, Kurien T, Green AR, Paish EC, et al. Expression of mucins (MUC1, MUC2, MUC3, MUC4, MUC5AC and MUC6) and their prognostic significance in human breast cancer. Mod Pathol. 2005; 18(10):1295–304. doi: 10.1038/modpathol.3800445 PMID: 15976813.

78. Kittaneh M, Montero AJ, Gluck S. Molecular profiling for breast cancer: a comprehensive review. Biomark Cancer. 2013; 5:61–70. doi: 10.4137/BIC.S9455 PMID: 24250234; PubMed Central PMCID: PMCPMC3825646.

79. Perou CM, Borresen-Dale AL. Systems biology and genomics of breast cancer. Cold Spring Harb Perspect Biol. 2011; 3(2). doi: 10.1101/cshperspect.a003293 PMID: 21047916; PubMed Central PMCID: PMCPMC3039533.

80. Baselga J, Mendelsohn J. Receptor blockade with monoclonal antibodies as anti-cancer therapy. Pharmacol Ther. 1994; 64(1):127–54. PMID: 7846112.

81. Baselga J, Mendelsohn J. The epidermal growth factor receptor as a target for therapy in breast carcinoma. Breast Cancer Res Treat. 1994; 29(1):127–38. PMID: 8018961.

82. Tsutsumi Y, Naber SP, DeLellis RA, Wolfe HJ, Marks PJ, McKenzie SJ, et al. neu oncogene protein and epidermal growth factor receptor are independently expressed in benign and malignant breast tissues. Hum Pathol. 1990; 21(7):750–8. PMID: 1972932.

83. Spicer AP, Parry G, Patton S, Gendler SJ. Molecular cloning and analysis of the mouse homologue of the tumor-associated mucin, MUC1, reveals conservation of potential O-glycosylation sites, transmembrane, and cytoplasmic domains and a loss of minisatellite-like polymorphism. J Biol Chem. 1991; 266(23):15099–109. PMID: 1714452.

84. Hareuveni M, Tsarfaty I, Zaretsky J, Kotkes P, Horev J, Zrihan S, et al. A transcribed gene, containing a variable number of tandem repeats, codes for a human epithelial tumor antigen. cDNA cloning, expression of the transfected gene and over-expression in breast cancer tissue. Eur J Biochem. 1990; 189(3):475–86. 0002112460. PMID: 2112460

85. Kirby A, Gnirke A, Jaffe DB, Baresova V, Pochet N, Blumenstiel B, et al. Mutations causing medullary cystic kidney disease type 1 lie in a large VNTR in MUC1 missed by massively parallel sequencing. Nat Genet. 45(3):299–303. PMID: 23396133. doi: 10.1038/ng.2543

86. Levitin F, Baruch A, Weiss M, Stiegman K, Hartmann ML, Yoeli-Lerner M, et al. A novel protein derived from the MUC1 gene by alternative splicing and frameshifting. J Biol Chem. 2005; 280(11):10655–63. doi: 10.1074/jbc.M406943200 PMID: 15623537.

87. Acland P, Dixon M, Peters G, Dickson C. Subcellular fate of the int-2 oncoprotein is determined by choice of initiation codon. Nature. 1990; 343(6259):662–5. doi: 10.1038/343662a0 PMID: 2406607.

88. Florkiewicz RZ, Baird A, Gonzalez AM. Multiple forms of bFGF: differential nuclear and cell surface localization. Growth Factors. 1991; 4(4):265–75. PMID: 1764263.

SCIENTIFIC REPORTS

OPEN

SUBJECT AREAS:
BREAST CANCER
TUMOUR IMMUNOLOGY

Received
28 August 2013

Accepted
22 November 2013

Published
9 December 2013

Correspondence and requests for materials should be addressed to J.B. (jeremy.bastid@orega-biotech.com) or A.B. (armand.bensussan@inserm.fr)

* These authors contributed equally to this work.

IL-17A is produced by breast cancer TILs and promotes chemoresistance and proliferation through ERK1/2

Stéphanie Cochaud[1]*, Jérôme Giustiniani[2]*, Clémence Thomas[3], Emilie Laprevotte[4], Christian Garbar[2], Aude-Marie Savoye[2], Hervé Curé[2], Corinne Mascaux[2], Gilles Alberici[3], Nathalie Bonnefoy[4], Jean-François Eliaou[4,5], Armand Bensussan[1]* & Jeremy Bastid[3]*

[1]Institut National de la Santé et de la Recherche Médicale (INSERM) UMR-S 976; Université Paris Diderot, Sorbonne Paris Cité, Laboratoire Immunologie Dermatologie & Oncologie, F-75475, Paris, France, [2]Institut Jean Godinot, F- 51726 Reims, France, [3]OREGA Biotech, F-69130 Ecully, France, [4]IRCM, Institut de Recherche en Cancérologie de Montpellier; INSERM, U896; Université Montpellier 1; CRLC Val d'Aurelle Paul Lamarque, Montpellier, F-34298, France, [5]Département d'Immunologie, Centre Hospitalier Régional Universitaire de Montpellier et Faculté de Médecine Université Montpellier 1, F-34295 Montpellier, France.

The proinflammatory cytokine Interleukin 17A (hereafter named IL–17A) or IL-17A producing cells are elevated in breast tumors environment and correlate with poor prognosis. Increased IL-17A is associated with ER(−) or triple negative tumors and reduced Disease Free Survival. However, the pathophysiological role of IL-17A in breast cancer remains unclear although several studies suggested its involvement in cancer cell dissemination. Here we demonstrated that a subset of breast tumors is infiltrated with IL-17A-producing cells. Increased IL-17A seems mainly associated to ER(−) and triple negative/basal-like tumors. Isolation of tumor infiltrating T lymphocytes (TILs) from breast cancer biopsies revealed that these cells secreted significant amounts of IL-17A. We further established that recombinant IL-17A recruits the MAPK pathway by upregulating phosphorylated ERK1/2 in human breast cancer cell lines thereby promoting proliferation and resistance to conventional chemotherapeutic agents such as docetaxel. We also confirmed here that recombinant IL-17A stimulates migration and invasion of breast cancer cells as previously reported. Importantly, TILs also induced tumor cell proliferation, chemoresistance and migration and treatment with IL-17A-neutralizing antibodies abrogated these effects. Altogether these results demonstrated the pathophysiological role of IL-17A-producing cell infiltrate in a subset of breast cancers. Therefore, IL-17A appears as potential therapeutic target for breast cancer.

Inflammation often occurs in the microenvironment of tumors, and actively takes part to the tumor progression process by favoring tumor cell survival and growth, angiogenesis and metastasis[1]. Interleukin 17A (hereafter named IL-17A) is a pro-inflammatory cytokine that belongs to a family encompassing 6 interleukins (IL-17A to F)[2]. IL-17A binds to a receptor composed of IL-17RA and IL-17RC dimer whose expressions are ubiquitous. IL-17A is mainly produced by a subset of CD4+ lymphocytes called Th17 cells. However, other cell types were reported to produce IL-17A including macrophages, dendritic cells, γδ T cells, NK and NKT cells, CD8+ T cells and neutrophils[3,4]. In humans, increased IL-17A is associated with infections, chronic inflammatory diseases and autoimmunity[3]. IL-17A or IL-17A-producing cells are also increased in malignancies[5] including breast cancers[6–10]. In fact, the tumors cells and tumor-associated fibroblasts secrete factors and generate a pro-inflammatory cytokine milieu that leads to the recruitment of Th17 cells in the tumor microenvironment[8]. IL-17A producing cells thereby represent a subpopulation within the TILs from breast cancer[8] and infiltration with IL-17A-producing immune cells is a poor prognosis factor[10]. A recent study indicated that infiltration with IL-17A+ immune cells is mainly observed in estrogen receptor negative (ER(−)), progesterone receptor negative (PR(−)) and triple negative tumors and associated with high histological grade and reduced disease free survival (DFS)[10]. It is therefore important to elucidate the pathophysiological role of IL-17A in breast cancer. It was previously shown that IL-17A may favor breast tumor cell dissemination[6] and may be required for the growth of a murine breast tumor cell line *in vivo*[11]. Yet, the pro-oncogenic effect of IL-17A in breast cancer has not been thoroughly investigated and we thus decided to elucidate the functional role of IL-17A and IL-17A producing TILs in human breast cancers.

Results

IL-17A producing cells infiltrate human breast cancer biopsies. We first assessed expression of IL-17A by IHC in 40 breast cancer cases, 10 metastases and 10 matched controls. Whereas no or few IL-17A+ cells were observed in the normal tissues, 8 out of 40 (20%) of the cancer cases showed moderate to strong infiltration with IL-17A+ immune cells, mostly lymphocytes and macrophages, in the tumoral stroma (Figure 1, Supplementary Figure 1 and Table 1). There was a trend of association between the presence of IL-17A+ lymphocytes and tumors with ER(−) status (88% of IL-17A+ tumors were ER(−)). Conversely, the majority (92%) of ER(+) tumors were not infiltrated with IL-17A producing cells. Yet, the number of cases was too small to reach statistical significance. Among the 8 tumors that were infiltrated with IL-17A+ cells, 7 were ER(−), including 4 triple negative breast cancers and 1 Her2+ tumor. These observations are in line with the recent study from Chen and colleagues[10] who reported that 18% of the 207 breast cancer cases analyzed were infiltrated with IL-17A producing cells. The presence of IL-17A was significantly associated with ER(−)/PR(−) tumors ($P < 0.01$) and triple negative ($P < 0.05$) tumors.

In order to further demonstrate that IL-17A is released by lymphocytes infiltrating ER(−) breast cancers, we isolated and expanded tumor-infiltrating lymphocytes (TILs) from 6 ER(−) breast cancer biopsies. Biopsies were obtained following surgical procedures of breast cancer patients. 4 patients had a triple negative tumor and 2 patients had a Her2+ tumor. Tumor biopsies were collected and preserved in culture medium for subsequent isolation and separation of the different cell populations. The T lymphocytes were then expanded *ex vivo* as described in materials and methods section. Results revealed a phenotypic heterogeneous T lymphocyte population isolated from these biopsies. As illustrated in Figure 2, we could obtain significant IL-17A-secreting TILs in 4 out of the 6 TILs. Patient AL is a 29 year-old patient who presented with a triple negative, basal-like, pT2N0, SBR3 grade tumor. When isolated, the TILs from this patient were CD3+ lymphocytes, mostly (75%) CD4+, and secreted large amounts of IL-17A. Patient CP is a 40 year-old woman with a triple negative, basal-like, pT3N3a, SBR3 grade tumor. The tumor was infiltrated with a mixed population of CD3+ TILs that were CD4+, CD8+ or CD4+CD8+ and secreted IL-17A. Patient 432 is a 78 year-old woman with a relapsing triple negative, basal-like, pT4bNx, SBR3 grade breast cancer. The biopsy was infiltrated with TILs that secreted moderate amounts of IL-17A and were CD3+ (100%) and mostly CD8+ (90%) T cells. Patient 452 is a 52 year-old woman with and ER(−), PR(−) and Her2+, pT4bN1 and SBR3 grade breast cancer. The TIL population was mostly CD3+ (96%), CD4+ (70%) and secreted IL-17A. The expanded TILs of the 2 other patients, PR, a 66 year-old patient with a triple negative, apocrine, SBR3 grade, pT2N0 breast cancer and MAR, a 42 year-old woman with an ER(−), PR(−) and Her2+, SBR3 grade, pT3N1 tumor, did not secrete IL-17A *ex vivo*. It should be noted that in all cases, we could expand from the tumor biopsies between 1 to 3% of TCRγδ expressing lymphocytes. In aggregates, IHC and clinical data along with previous work published by others demonstrate that breast cancers are infiltrated with IL-17A producing immune cells. Such infiltration is particularly frequent in ER(−) tumors, and more specifically in triple negative/basal-like tumors.

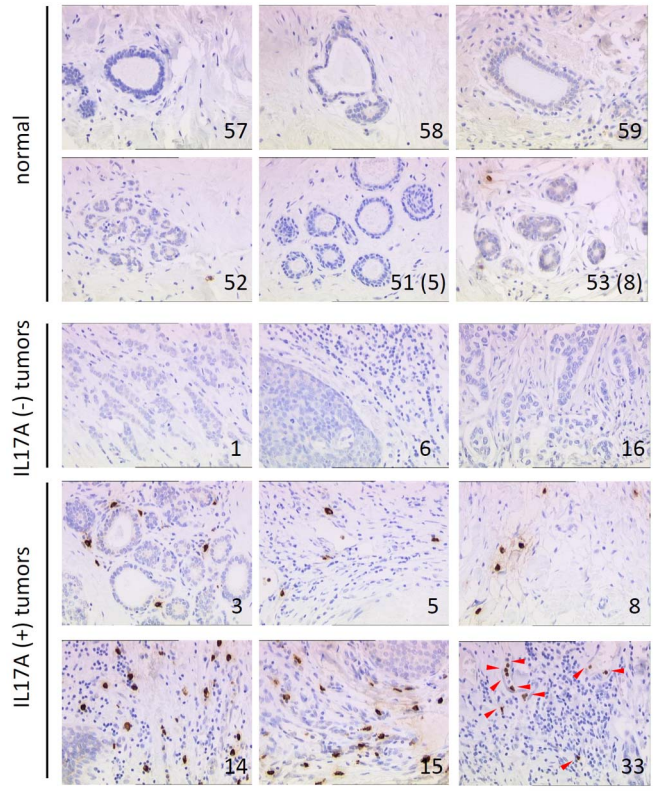

Figure 1 | Representative Immunohistochemical staining of IL-17A expression in normal and breast cancer human tissues. IL-17A stained sections of 40 invasive ductal breast carcinomas, 10 metastases and 10 matched normal counterparts. Brown staining indicates IL-17A protein. Arrows indicate IL-17A positive cells within the stroma, # refers to the corresponding sample in Supplementary Table 1.

IL-17A activates the ERK1/2 pathway in breast cancer cells. To address the functional role of IL-17A, we stimulated various human breast cancer cell lines with recombinant human IL-17A. Of note, all the human breast cancer cell lines tested expressed *IL17RA* and *IL17RC* (Supplementary Figure 2) the two monomers that form the functional receptor of IL-17A[2]. Therefore, all the breast cancer cell lines are able to respond to IL-17A stimulation. Putative signaling pathways activated by IL-17A were identified using anti-phospho tyrosine whole blot analysis. We identified several putative protein kinases recruited by IL-17A in the MCF7 and T47D breast cancer cell lines that could correspond to FAK, p70 S6 kinase, c-Raf and ERK1/2 according to their molecular weight (data not shown). However, when validated with specific antibodies, only ERK1/2 was consistently shown to be recruited by recombinant IL-17A in all the cell lines tested as illustrated in MCF7, T47D, MDA-MB468, MDA-MB157 and BT20 cells (Figure 3).

IL-17A promotes resistance to docetaxel *via* activation of ERK1/2 pathway. We demonstrated here that IL-17A recruited the ERK1/2 pathway in breast cancer cells. As ERK kinases are involved in resistance to taxane-based therapies[12], we tested whether IL-17A would mediate resistance to conventional chemotherapeutic agents such as docetaxel. To this end, human breast cancer cell lines were stimulated with recombinant human IL-17A and subsequently incubated with the drug. As illustrated in Figure 4, IL–17A decreased docetaxel-induced cell death in MCF7, T47D, BT20, MDA-MB468 and MDA-MB157 breast cancer cells in a dose-dependent manner. To delineate the role of ERK1/2 in IL-17A-mediated resistance to chemotherapeutic agents, we treated the cells with the MEK Inhibitor U0126. U0126 is a chemically synthesized organic compound that blocks the phosphorylation of ERK1/2 by inhibiting the kinase activity of MAP Kinase Kinase (MAPKK or MEK 1/2)[13]. U0126 inhibited IL-17A-induced phosphorylation of ERK1/2 (Figure 5B) and abrogated IL-17A-mediated protection from docetaxel-induced cell death in MCF7 (Figure 5A) whereas MEK inhibitor alone did not affect cytotoxicity (data not shown). U0126 also inhibited phosphorylation of ERK1/2 (Figure 5D) and abrogated resistance to docetaxel in BT20 cells stimulated with IL-17A (Figure 5C). Altogether these data demonstrate that IL–17A protects from docetaxel-induced cell death through activation of the ERK1/2

A)

code	TILs Phenotype				Diagnosis	Tumor caracteristics	Age
	CD3	*CD4*	*CD8*	*TCRγδ*			
AL	98%	75%	30%	1%	Triple negative basal like	pT2N0, SBR3	29
CP	100%	80%	70%	1%	Triple negative basal like	pT3N3a, SBR3	40
432	100%	10%	90%	2%	Triple negative basal like (r)	pT4bNx, SBR3	78
452	96%	70%	40%	1%	Her2 overexpressed	ER-PR-Her2+, SBR 3, pT4bN1	52
PR	98%	36%	62%	1%	Triple negative apocrine	SBR3, pT2N0	66
MAR	100%	91%	60%	3%	Her2 overexpressed	ER-PR-Her2+, SBR 3, pT3N1	42

B)

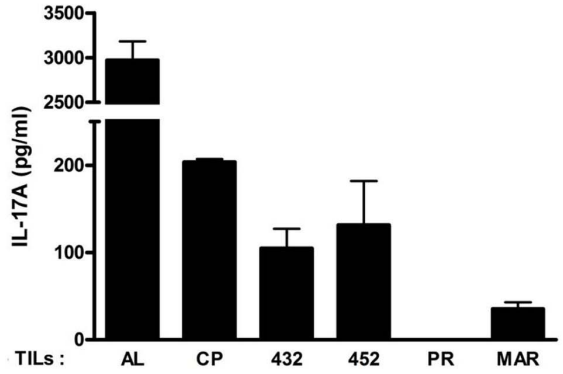

Figure 2 | Characterization of lymphocyte subpopulations isolated from ER(−) breast cancer biopsies. (A) Tumor infiltrating lymphocytes (TILs) were isolated from biopsies then short-term amplified *ex vivo*. Expression of CD3, CD4, CD8 and TCRγδ receptors were analyzed by flow cytometry. (B) Production of IL-17A by TILs was measured by ELISA in cell culture supernatants of 16 h cultures. Quantification was performed in duplicates.

kinases and may therefore participate to therapy-resistance in breast cancer.

IL-17A increases the proliferation of some breast cancer cell lines. IL-17A activated the ERK kinases in breast cancer cells and it was reported to stimulate the proliferation of human airway smooth muscle cells via this pathway[14]. We therefore investigated whether IL-17A could also enhance the proliferation of breast cancer cell lines. The proliferation of the T47D cells requires ERK recruitment (see Supplementary Figure 6 from ref[15]) and IL-17A indeed stimulated their proliferation in a dose-dependent manner (Figure 6). In contrast, the MCF7 cell line, which was found to be less sensitive to ERK-recruitment for prolactin-inducing proliferation[15], failed to respond to IL-17A. IL-17A did not enhance the proliferation of BT20 and MDA-MB468 cells. In conclusion, IL-17A can increase the proliferation of some breast cancer cells potentially through the ERK1/2 pathway.

IL-17A promotes breast cancer cell migration and invasion. In our attempt to unravel the oncogenic properties of IL-17A in breast cancer, we tested whether IL-17A would promote migration and invasion as reported by others. Previous work indeed demonstrated that IL-17A stimulates migration and invasion in several cancer types[16–18] including breast cancer[6], thereby favoring metastasis.

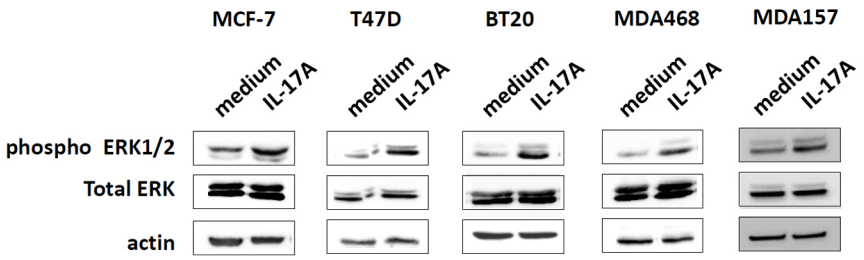

Figure 3 | IL-17A activates ERK1/2 pathway in breast cancer cells. Western blot analysis of phospho (pThr202/pTyr204) ERK1/2 and total ERK1/2 in several breast cancer cell lines untreated (medium) or treated with 10 ng/ml of recombinant IL-17A for 20 min (IL-17A). Data are representative of two independent experiments for each cell line.

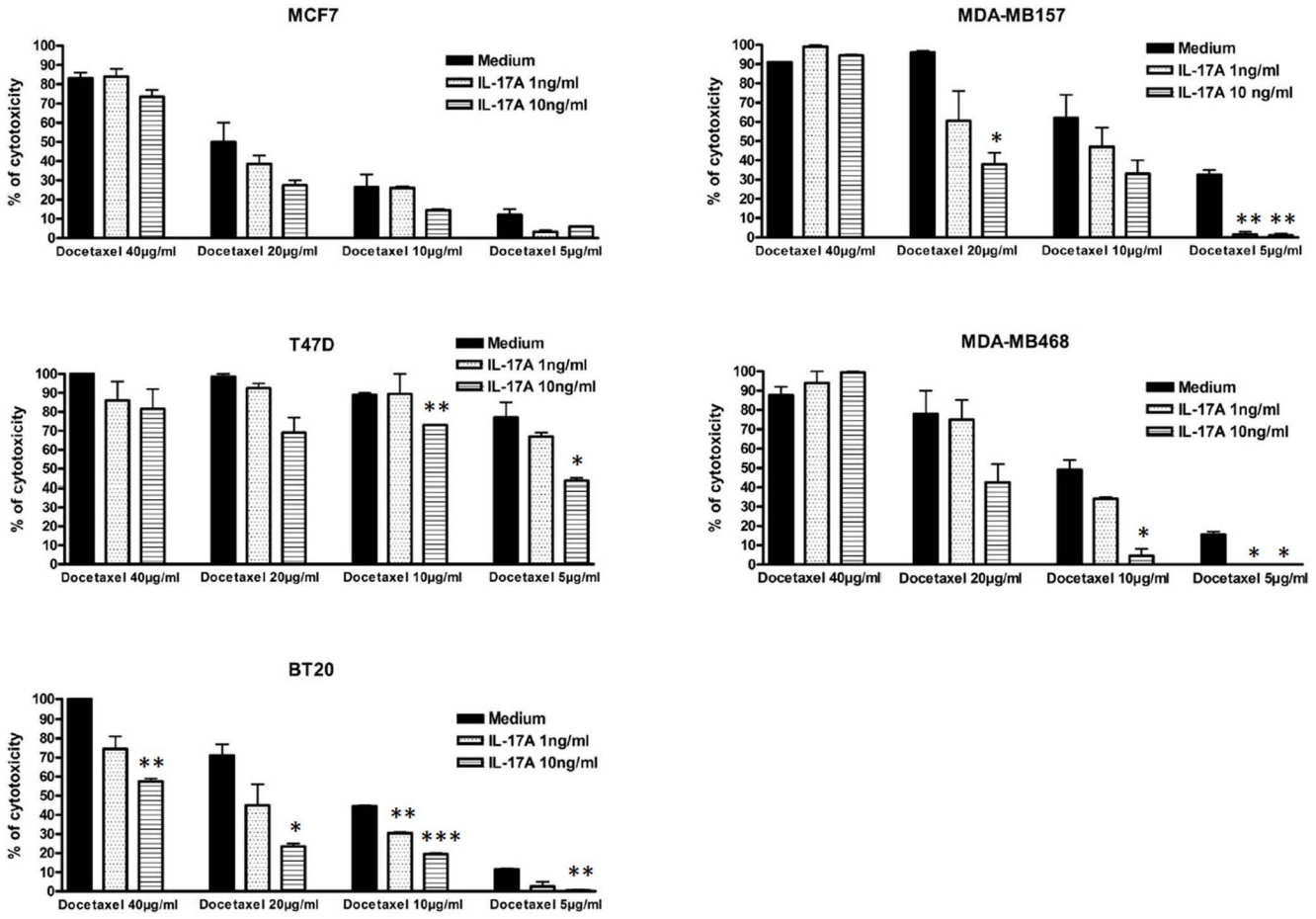

Figure 4 | IL-17A promotes resistance to docetaxel. MCF7, T47D, BT20, MDA-MB468 and MDA-MB157 cells were cultured for 48 h in complete medium alone (medium) or treated with recombinant human IL–17A at 1 or 10 ng/ml as indicated. Cells were then culture in FCS free medium supplemented with corresponding concentration of cytokine for 24 h and then further supplemented with docetaxel at 5, 10, 20 or 40 µg/ml as indicated for 7 h. The cytotoxicity was determined using the Cytotoxicity Detection Kit (Roche). For each cell line, data are representative of 3 independent experiments performed in duplicates (* $P < 0.05$; ** $P < 0.01$; *** $P < 0.001$).

As shown in Figure 7A, IL-17A increased the migration of the poorly motile and non-invasive MCF7 cell line in a dose-dependent manner. Although IL-17A also increased the invasive ability of MCF7 cells in Boyden chambers assays (data not shown), the majority of IL-17A-treated-MCF7 cells remained non-invasive. Therefore, to evaluate the ability of IL-17A to foster cell invasion of the surrounding extracellular matrix, we used the MDA-MB231 cell line which endows intrinsic invasion capacities. As shown in Figure 7B, IL-17A increased invasion of MDA-MB231 cells in Boyden chambers assays. Increased invasive ability of IL-17A-treated MDA-MB231 cells was then further demonstrated using 3D Clusters assays (Figure 7C). As expected, MDA-MB231 cells invaded the matrigel locally around the mass of the tumor cells (top left). However, when stimulated with IL-17A, MDA-MB231 exhibited increased local invasiveness (bottom left) with much more aggressive features (bottom right, highly invasive extensions indicated by arrows). Furthermore, invasion was not restricted to the cellular mass as the tumor cells were disseminated all around the matrigel and became organized like a network (top right) which is typical of high aggressiveness. In conclusion, IL-17A increases pro-migratory and pro-invasive properties of breast cancer cells and confers an aggressive and highly invasive phenotype in 3D cultures.

IL-17A released by TILs promotes tumor cell chemoresistance, proliferation and migration. We then asked whether infiltrating T lymphocytes that secrete IL-17A would mediate similar effects on tumor cells as the ones obtained with recombinant IL-17A, and whether the effects of TILs could be neutralized by IL-17A blocking monoclonal antibodies. To address this question, we cultured breast cancer cell lines with TIL-conditioned medium. We collected culture supernatant from IL-17A-producing TILs isolated from patient AL (TIL(AL)) and tested whether it could promote resistance to docetaxel, proliferation and migration in an IL-17A-dependent manner. As TILs secrete many soluble factors, the specific contribution of IL-17A was determined using anti-IL-17A neutralizing antibodies or their matched isotype control. Recombinant IL-17A was very potent at protecting BT20 cells from docetaxel-induced cell death (Figure 4) and TIL(AL)-conditioned medium also inhibited docetaxel-induced cytotoxicity (Figure 8A). Specific neutralization of IL-17A using OREG-203 monoclonal antibody markedly decreased the protection mediated by TIL(AL). TIL(AL) also increased the proliferation of T47D cells (which responded well to recombinant IL-17A, Figure 6). Again, this effect was diminished by neutralizing IL-17A with OREG-203 but not by the control antibody (Figure 8B). TIL(AL) also stimulated the migration of MCF7 cells (as observed with the recombinant cytokine, Figure 7A) which was abrogated by antibody-mediated neutralization of IL-17A (Figure 8C). Similar results were obtained with OREG-210, a distinct IL-17A neutralizing monoclonal antibody (data not shown). In aggregates, we found that IL-17A is released by breast cancer TILs and mediates proliferation, chemoresistance (at least in part through the ERK kinases) and migration/invasion. Treatment

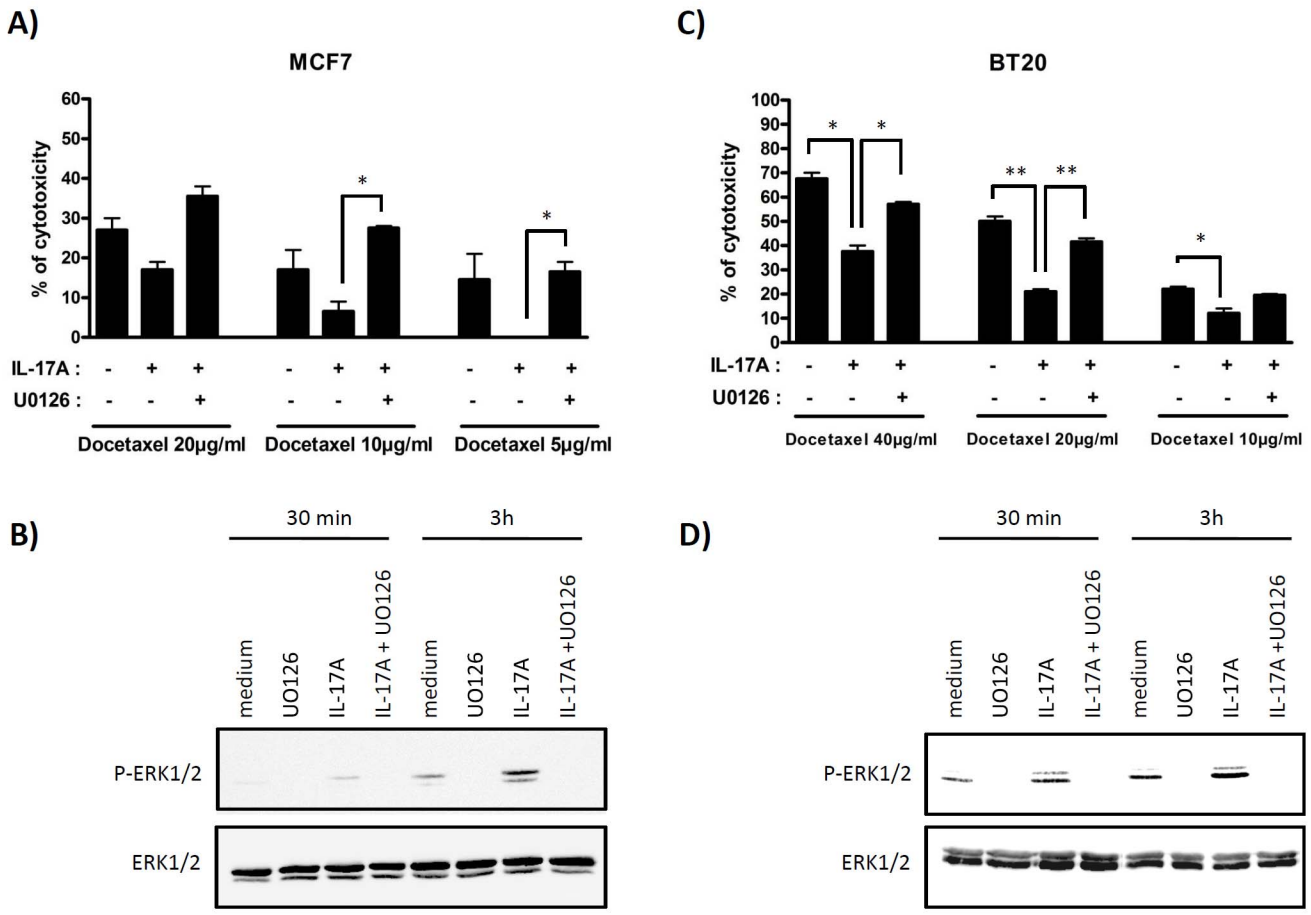

Figure 5 | IL-17A-induced resistance to docetaxel is dependent of ERK1/2 activation. (A and C) MCF7 and BT20 cells were stimulated as described in Figure 4. When indicated, the MEK inhibitor U0126 was added at 10 µM 24 h before docetaxel. The cytotoxicity was determined using the Cytotoxicity Detection Kit (Roche). For each cell line, data are representative of 3 independent experiments performed in duplicates (* $P < 0.05$; ** $P < 0.01$). (B and D) Western blot analysis of phospho (pThr202/pTyr204) ERK1/2 and total ERK1/2 in MCF7 and BT20 cell lines untreated (medium) or treated with 10 µM U0126 inhibitor alone (U0126), 10 ng/ml of recombinant IL-17A (IL-17A) or 10 ng/ml of recombinant IL-17A + 10 µM U0126 inhibitor (IL-17A + U0126) for 30 min and 3 h.

with IL-17A-neutralizing antibodies abrogated the pro-oncogenic effects of IL–17A released by TILs.

Discussion

We demonstrated here that IL-17A producing cells infiltrate breast cancer. Our results from human tissue microarrays and human biopsies confirmed previous observations[6,8–10] reporting upregulation of IL–17A or IL-17A producing cells in breast cancers. Some tumors were infiltrated with high number of IL–17A positive immune cells, whereas no or few IL-17A positive cells were observed in the stroma of healthy mammary tissues. We observed that most IL-17A+ immune cells were lymphocytes and macrophages, which is in accordance with previous reports[6]. *In silico* analyses of a published study from reference[19] using the ONCOMINE software sustain the conclusions that *IL17A* mRNA is increased in breast cancer stroma ($P < 10^{-6}$) compared to the stroma of normal breast. In this dataset, *IL17A* expression is higher in the tumors that recurred versus the non-recurrent diseases and higher in the poor prognosis group versus the good prognosis group.

In vitro experiments presented here, using cell lines and primary material from cancer patients, suggest that IL-17A may promote breast cancer cell proliferation, invasion as well as resistance to chemotherapy. Therefore, IL-17A is suspected to be a poor prognosis factor in breast cancer. Our breast cancer cohort (SUPER BIO CHIPS, slide CBA3) contains a small number of cancer cases with limited clinical information, which did not allow us to investigate the clinical relevance of IL-17A upregulation in breast cancer or perform statistical analyses. However, patients with IL-17A positive tumors tend to have a higher frequency of lymph node metastasis (75% of IL-17A+ tumors are N+ compared to 63% of IL-17A- tumors that are N+) which may reflect the fact that IL-17A produced by TILs stimulates breast cancer cell migration and invasion as reported by us (Figures 7 and 8C) and others[6]. We cannot conclude regarding its role in systemic metastases, resistance to therapy or its overall impact on survival.

To gain insight into the clinical relevance of IL-17A in breast cancer we would like to refer to the study published recently by Chen and colleagues[10]. To our knowledge, this is the only study assessing the expression of IL-17A by IHC in a large number of breast cancer patients (207 breast cancer cases) with extensive clinical parameters. In this cohort, infiltration of breast cancer by IL-17A producing cells significantly correlates with higher tumor grade ($P < 0.01$), ER and PR negative status ($P < 0.01$) and triple negative tumors ($P < 0.05$). Patients with IL-17A positive tumors have shorter DFS compared to IL-17A negative tumors (5-year DFS of 64% compared to 87.3%, respectively, $P < 0.01$). In univariate Cox analysis, elevated IL-17A is a significant prognostic factor influencing DFS ($P < 0.01$). Multivariate Cox proportional hazard analysis also showed that elevated IL-17A was a significant prognostic factors for DFS after controlling for age, histology, tumor grade, and nodal status and expression status of ER and PR ($P < 0.05$).

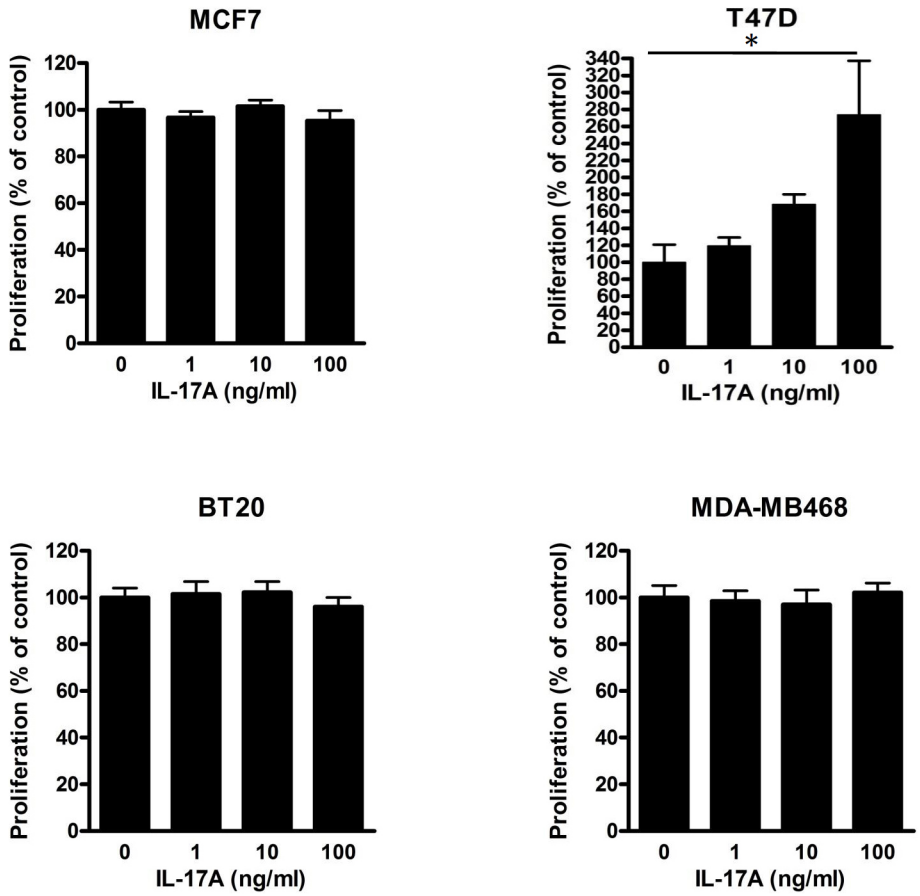

Figure 6 | **IL-17A increases proliferation of T47D cells.** MCF7, T47D, BT20 and MDA-MB468 breast cancer cell lines were cultured in complete medium supplemented with 0, 1, 10 or 100 ng/ml of recombinant human IL-17A as indicated. Cell proliferation was assessed at 72 h using tritiated thymidine ([3H]-TdR) incorporation protocol. Data are the mean ± SEM of two independent experiments, each performed in hexaplicates (* $P < 0.05$).

One of the main finding of our work is that IL-17A derived from breast cancer TILs may influence the response and outcome of chemotherapy treatment. Again, the above mentioned study seems to support our conclusion. Among their 207 breast cancer patients, 58 presented with locally advanced breast cancer and received neoadjuvante chemotherapy. Although IL-17A was not statistically associated with the response to chemotherapy, the presence or absence of IL-17A drastically influenced the DFS of patients receiving chemotherapy ($P < 0.01$) as 5-year DFS dropped from 81.5% for IL-17A- patients to 38.5% for IL-17A+ patients. Because the impact of IL-17A on DFS is much stronger in the context of chemotherapy (81.5% compared to 38.5%) than in the entire cohort (87% to 64%), we believe that this points out a particular impact of IL-17A within this subgroup of patients with locally advanced tumors receiving chemotherapy. In aggregate, the clinical data form the 207 breast cancer patient cohort of Chen et al. strongly supports the notion that IL-17A is a poor prognostic factor in breast cancer and is associated with ER- or triple negative, high grade tumors with shortened DFS.

Our and other[10] studies raise the conclusion that IL-17A is involved in ER(−) tumors, including triple negative tumors. The mechanisms underlying the association between IL-17A and ER deficiency remained unknown. However, it is interesting to mention that several studies reported a direct relation between estrogen status and IL-17A[20,21] and estrogen/ER signaling deficiency was shown to promote the differentiation of Th17 cells[21]. Therefore, one could speculate that ER deficiency in breast tumors may directly promote the expansion of IL-17A+ TILs, a possibility that would require further investigation. We believe that this speculation is a plausible scenario as we demonstrated here that ER(+) and ER(−) cell lines respond to IL-17A in a similar manner. Therefore, the association of ER deficiency and IL-17A expression may not reflect a functional synergy but rather an inter-regulation or co-regulation by a common pathway.

We showed here that IL-17A exerts several oncogenic effects on cancer cells including resistance to chemotherapy-induced cell death, proliferation, migration and invasion. The modulation of drug sensitivity of cancer cells by IL-17A is an important oncogenic property of IL-17A with clinical significance, and it has never been reported. However, it was found that IL-17A promotes survival of synoviocytes in rheumatoid arthritis through activation of STAT3-Bcl-2 axis[22] and confers broad chemoresistance to dendritic cells through the regulation of the Bcl-2 family member BCL2A1[23]. Using knockout (KO) mice, Yu and colleagues demonstrated that IL-17A controls tumor progression by regulating the STAT3- Bcl-2/Bcl-XL pathway in several cancer models[24,25]. Here we report that IL-17A activates the ERK pathway, an important survival pathway for cancer cells, and we demonstrated that this pathway is a crucial mediator of IL-17A-induced resistance to docetaxel. Altogether these results suggest that IL-17A present in the tumor microenvironment may be an important survival factor and source of therapy resistance for breast cancer cells. We also evidenced that IL-17A promotes the proliferation of some breast cancer cell lines. Although this had not been reported previously for cancer cells, it had been demonstrated that IL-17A promotes the proliferation of smooth muscle airway cells[14] and human mesenchymal stem cells[26] through the activation of the MEK-ERK pathway. However, IL-17A did not systematically increase the proliferation of breast cancer cell lines, at least *in vitro*. This may reflect the fact that the cell lines used have been kept in Fetal

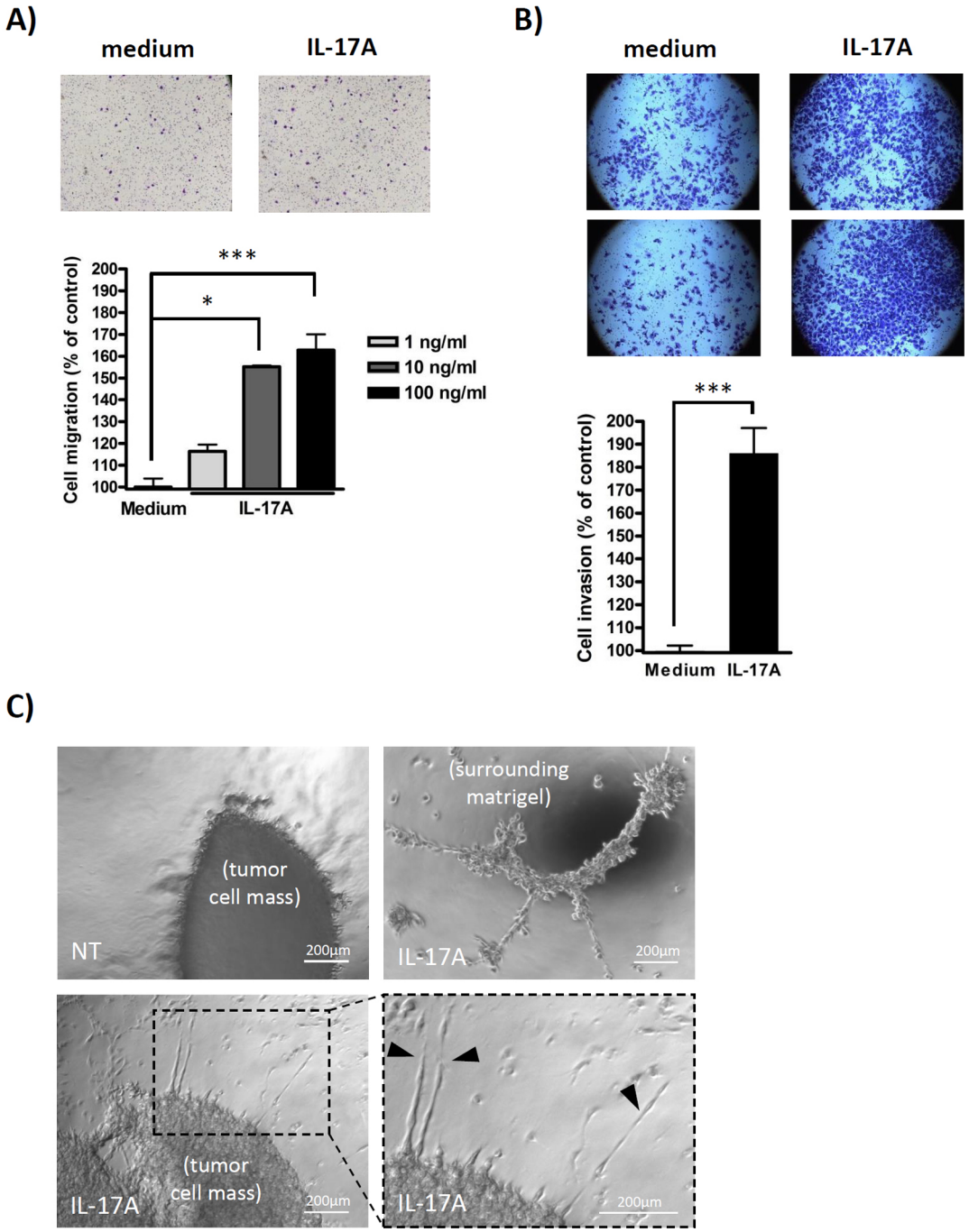

Figure 7 | IL-17A promotes breast cancer cell migration and invasion. (A) MCF7 cells were cultured in complete medium alone (medium) or supplemented with 1, 10 or 100 ng/ml of recombinant human IL-17A (IL-17A) as indicated. Cell migration was evaluated in transwell migration assay (upper panel, representative photomicrographs; lower panel, quantification: mean ± SEM of two independent experiments). (B and C) MDA-MB231 were cultured for 2 days in complete medium alone (medium) or supplemented with 100 ng/ml of recombinant human IL-17A as indicated. Cell invasiveness was then evaluated using Matrigel Invasion Chambers (B, upper panel, representative photomicrographs; lower panel, quantification: mean +− SEM of three independent experiments) and using 3D Clusters assays (C, upper left: invasive boarder of untreated cells; lower left and right: invasive boarder of IL-17A-treated cells; upper right: invasion of the surrounding ECM by IL-17A treated cells). (* $P < 0.05$; ** $P < 0.01$; *** $P < 0.001$).

Calf Serum (FCS) rich-medium for a long period and their proliferation is unlikely to rely on external factors. We are currently testing the effect of IL-17A on primary cells or freshly isolated tumor cells, models that may be more relevant to assess its impact on proliferation. To our knowledge, this is the first report that used primary material from cancer biopsies to assess in depth the role of IL-17A released by TILs from breast cancer patients. Importantly, these freshly isolated TILs exert similar pathophysiologic effects as described above mainly through IL-17A as specific neutralization of IL-17A largely abrogated their effects. These observations are critical to understand the role of IL-17A in breast carcinogenesis, as TILs secrete many soluble factors that could contribute to their pro-tumor effects.

Whereas IL-17A or IL-17A producing immune cells are unambiguously increased in numerous tumors including breast cancers, their pro- *versus* anti-tumor effects remains debated[27,28]. When sig-

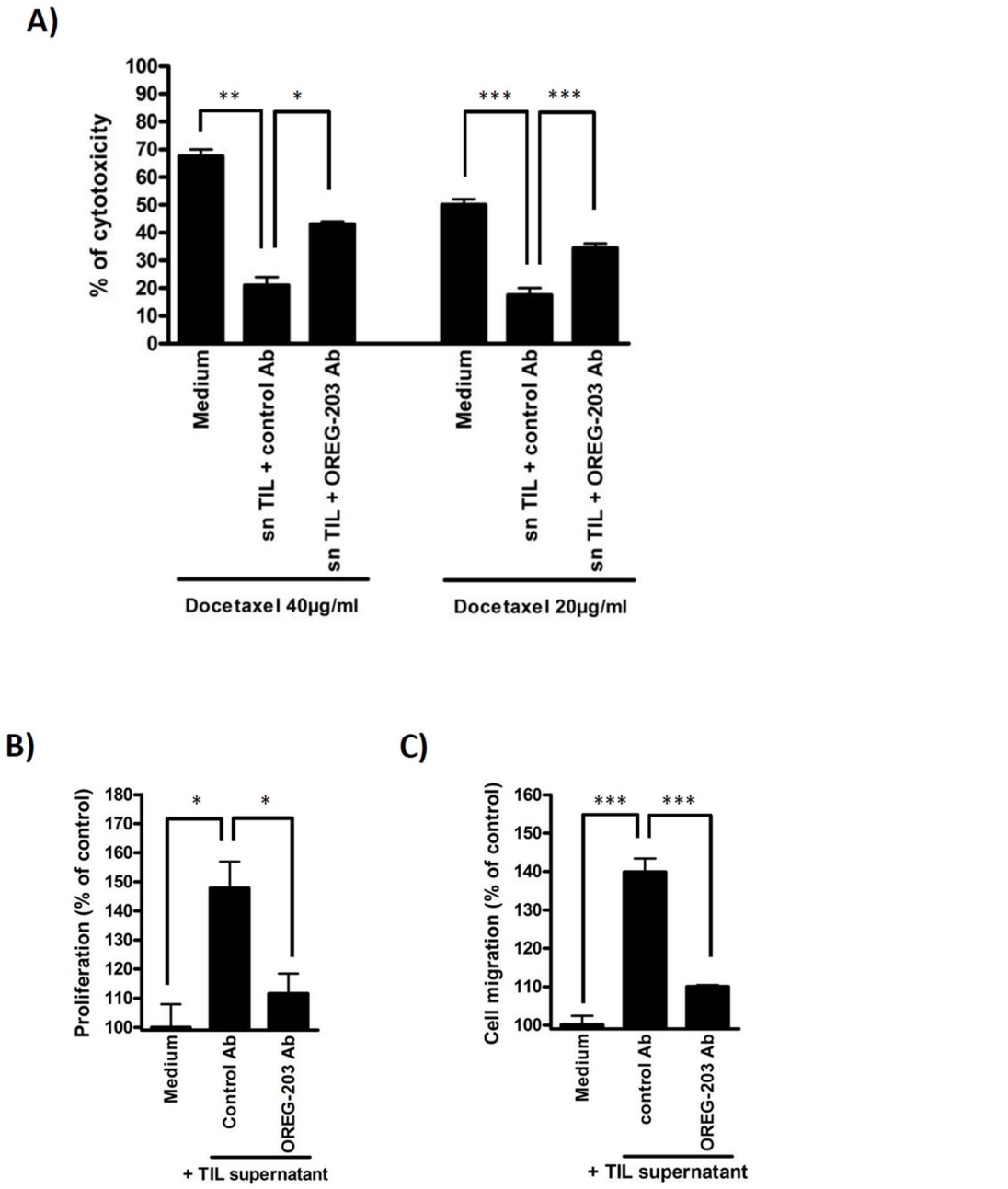

Figure 8 | Physiological IL-17A from TIL supernatants promotes tumor cell chemoresistance, proliferation and migration. (A) BT20 breast cancer cells were cultured in complete medium alone (medium) or supplemented with TIL(AL)-conditioned medium (1/10 vol/vol) and control antibody (control Ab) or IL-17A-neutralizing antibody (OREG-203) at 10 µg/ml as indicated for 48 h. Cells were then switched in FCS-free medium supplemented with TIL(AL)-conditioned medium (1/10 vol/vol) and antibodies as indicated for 24 h and then further treated with docetaxel at 20 or 40 µg/ml for 7 h. The cytotoxicity was determined using the Cytotoxicity Detection Kit (Roche). Data shown are representative of 3 independent experiments. (B) T47D cells were cultured in complete medium supplemented with TIL(AL)-conditioned medium (1/10 vol/vol) and control antibody (control Ab) or IL-17A-neutralizing antibody (OREG-203) at 10 µg/ml as indicated. Cell proliferation was assessed at 72 h using tritiated thymidine ([3H]-TdR) incorporation protocol. Data are representative of 3 independent experiments performed in triplicates. (C) MCF7 cells were cultured in complete medium alone (medium) or supplemented with TIL(AL)-conditioned medium (1/10 vol/vol) and control antibody (control Ab) or IL-17A-neutralizing antibody (OREG-203) at 10 µg/ml as indicated. Cell migration was evaluated in transwell migration assay. Data are the mean ± SEM of two independent experiments, each performed in triplicates. (* $P < 0.05$; ** $P < 0.01$; *** $P < 0.001$).

naling on the tumor cells or the tumor vasculature, IL-17A may favor tumor progression by promoting cell proliferation, survival, chemoresistance and dissemination as well as angiogenesis[29–31]. On the other hand Th17 were demonstrated to exert antitumor activity[32,33]. Interestingly, these two studies demonstrated that the antitumor response mediated by Th17 cells was independent of IL-17A and rather relied on IFN–γ secretion. Therefore, as previously suggested by Maniati and colleagues in their review[28], we believe that our work could indeed help to reconcile the pro and antitumor effects of IL-17A and Th17 cells as IL–17A may favor tumor progression whereas Th17 cells may exert antitumor effects mainly through IFN–γ production. In line with such speculation, the specific role of IL-17A, independently of the cells that produce it, can be addressed in *IL17A* KO mice. These mice consistently exhibit a tumor-resistant

phenotype. They have reduced development of TPA/DMBA-induced skin tumors[24], decreased colon tumor initiation in the $APC^{+/-}$ genetic background[34] and exhibited reduced growth of the B16 melanoma and MB49 bladder carcinoma cells[25]. *IL17A* KO mice also exhibited reduced growth, decreased metastasis and improved survival when challenged with lung cancer cell lines[17,35]. Along similar lines, blockade of IL-17A signaling in *IL17RC* KO mice revealed decreased tumor progression in a prostate cancer model[36]. Furthermore, anti-IL-17A antibody therapy decreased tumor growth and metastasis in colon cancer[31] and breast cancer[37,38] mouse models. Therefore, the role allotted to IL-17A itself seems to be tumor and metastasis-promoting. This suggests an interesting therapeutic opportunity where IL-17A neutralization could block pro-tumor and pro-metastatic effects of IL-17A while allowing Th17-mediated tumor eradication through IFN–γ production.

Methods

Cell culture and reagents. MCF7, T47D, BT20, MDA-MB468, MDA-MB157 and MDA-MB231 cell lines were obtained from the American Type Culture Collection. MCF7, T47D, BT20 and MDA-MB231 were cultured in RPMI medium (Invitrogen) supplemented with 10% Fetal Calf Serum (FCS), 2% glutamine and 1% antibiotics (Life technologies). MDA-MB468 cell line was cultured in DMEM/F12 medium (Life Technologies) supplemented as described above. MDA-MB157 cell line was cultured in L15/DMEM medium (Life Technologies) supplemented as described above. All cells were kept at 37°C in 5% CO_2 atmosphere incubator. Recombinant human IL-17A was purchased at Peprotech (Rocky Hill, NJ).

IL-17A immunohistochemistry. IL-17A staining on tissues arrays (SUPER BIO CHIPS, slide CBA3) was performed by a pathologist using a standard peroxidase method according to a protocol adapted from Coury *et al*[39]. and validated on renal allograft paraffin sections from patient with chronic active rejection. Goat polyclonal anti-human IL-17A antibody (dilution 1 : 40, R&D Systems, Minneapolis, MN) was employed as the primary antibody followed by anti-goat antibody (LSAB kit, DAKO). IL-17A expression was scored −, +, ++ and +++ for the absolute number of IL-17A positive immune cells within the stroma (see Supplementary Figure 1).

Clinical breast cancer biopsies. Human biopsy samples were obtained from the cancer center Institut Jean Godinot. This study was made according the approval of an ethic committee and all patients were informed and agreed the study.

Tumor-infiltrating lymphocyte (TIL) cultures. TILs from 6 ER(−) breast cancer biopsies were isolated and expanded according to the protocol adapted from Bagot M *et al*[40]. Briefly, TILs from patients were obtained from surgical tumor fragments mechanically dispersed into single-cell suspensions and cultured in 12-well plates with culture medium consisting of RPMI 1640, 2 mmol/L L-glutamine, penicillin (100 U/mL), streptomycin (100 μg/mL), 10% heat-inactivated human serum and 100 U/mL interleukin-2. Cultures were then fed every 3 days with IL-2–containing culture medium and the growing wells were expanded for 2 weeks. TILs were then washed and cultured in IL-2–containing medium with irradiated PBL (feeders) stimulated with PHA at 1 μg/ml. After 3 days the expanded TILs were extensively washed and fed with IL-2–containing medium for 6 days. Cells were harvested for IL-17A secretion and stained with anti-CD3, anti-CD4, anti-CD8, and anti-TCRγδ antibodies for flow cytometry analysis. Production of IL-17A by TILs was measured by ELISA in cell culture supernatants of 16 h cultures in PHA/IL-2 activation medium.

Quantification of IL-17A in cell culture supernatants. IL-17A from cell culture supernatants was quantified using commercial ELISA kit (R&D Systems) following instructions of the manufacturer.

Isolation of mRNA and quantitive RT-PCR. Total RNA was isolated using the GenElute™ Mammalian Total RNA kit (Sigma–Aldrich, St. Louis, MO) following the manufacturer's instructions. Total RNA (1 μg) was treated with 1 U/μg RNA of DNase I Amplification Grade (Invitrogen) according to the manufacturer's instructions, and in the presence of 10 U/μg RNA of RNaseOUT (Invitrogen). After DNase inactivation, RNA was reverse transcribed using random nonamers (Promega, Madison, WI) and M-MLV Reverse Transcriptase H Minus (Promega) according to the manufacturer's instruction.

The forward and reverse primers used in the PCR reaction were designed with Primer-BLAST software except for IL-17A (described in ref[41]) and GAPDH (described in ref[42]) and were as follow: GAPDH-forward 5′-GAAGGTGAAGGTCG GAGTCA-3′, GAPDH-reverse 5′-GACAAGCTTCCCGTTCTCAG-3′, IL-17A-forward 5′- ACTACAACCGATCCACCTCAC-3′, IL-17A-reverse 5′- ACTTTGC CTCCCAGATCACAG-3′, IL-17 RA-forward 5′-TGCCCCTGTGGGTGTACTG GT-3′, IL-17 RA-reverse 5′-GCAGGCAGGCCATCGGTGTA-3′, IL-17 RC-forward 5′-GGCTTGGTTTCACGCGCAGC-3′ and IL-17 RC-reverse 5′-CGGCCCTGCA AGAAGTCGGG-3′.

Real-time polymerase chain reaction quantification was carried out with the LightCycler 480 II System (Roche Diagnostics, Basel, Switzerland) using the SYBR Premix Ex Taq (Tli RNaseH Plus) kit (Ozyme, Saint-Quentin-en-Yvelines, France). The cycling conditions were as follows: 95°C for 1 min followed by 40 cycles of 95°C for 20 s, 60°C for 20 s and 72°C for 30 s. The sizes of the RT-PCR products were confirmed by agarose electrophoresis. At the end of the amplification, a melting temperature analysis of the amplified gene products was performed routinely for all cases. The PCR products were melted by gradually increasing the temperature from 60 to 95°C in 0.3°C steps, and the dissociation curves were generated with the Melting Curve analysis tool of the LightCycler 480 software (Roche Diagnostics). We confirmed that only one product was consistently amplified in all PCR reactions. The negative water control showed no amplification.

ERK1/2 immunoblotting. Cells were seeded at 3.10^6 cells per well in 6-well plates and cultured overnight in FCS-free medium. Cells were stimulated with IL-17A at 10 ng/ml and/or U0126 at 10 μM for 20, 30 min or 3 h as indicated. The medium was then removed, the cells were lysed in 1% Triton X100 lysis buffer, incubated for 1 h on ice and centrifuged at 4°C for 20 min at 10,000 g. The supernatants were collected and protein concentration was determined using the Bradford Assay (Bio-Rad, Hercules, CA). Proteins (70 μg) were resolved in 8% SDS–PAGE and transferred on nitrocellulose membrane. The membrane was blocked for 1 h at room temperature, by using 5% nonfat milk in tris-buffered saline (TBS) containing 0.1% Tween 20 (Sigma–Aldrich) and incubated overnight at 4°C with a monoclonal rabbit anti-phospho-p44/42 MAPK (Erk1/2) antibody (1 : 1,000), a monoclonal rabbit anti-p44/42 MAPK (Erk1/2) antibody (1/1,000) or with a monoclonal mouse anti-actin antibody (1 : 1,000) (Cell Signalling, Danvers, MA) used as a loading control, in blocking solution. After 3 washes, the membrane was incubated 1 h at room temperature with goat anti-rabbit or goat anti-mouse secondary antibodies (1 : 10,000) (Jackson Immunoresearch, West Grove, PA) conjugated to horseradish peroxydase.

Cytotoxicity assay. MCF7, T47D (1000 cells/well), BT20, MDA-MB468 and MDA-MB157 (3,000 cells/well) cells were seeded in a 96 wells plate in adequate complete medium alone or treated with recombinant human IL-17A (1 or 10 ng/ml) or TIL(AL)-conditioned medium (1/10 vol/vol) and/or antibodies (10 μg/ml) as indicated. After 48 h of culture, medium was changed to a FCS-free one supplemented with corresponding concentration of cytokines or TIL(AL)-conditioned medium and/or antibodies and further supplemented with U0126 inhibitor (10 μM) when indicated. After 24 h, culture medium is then further supplemented with docetaxel at 5, 10, 20 or 40 μg/ml as indicated. Untreated cells (control medium) and Triton X100 treated cells (100% cell death) were used as controls. Each condition was performed in duplicates. The cytotoxicity was determined using the Cytotoxicity Detection Kit (Roche) according to the manufacturer's instructions. To this aim, 50 μl of supernatant from each well were collected into a 96 wells plate and incubated with 50 μl of freshly prepared Reaction Mixture for 30 minutes at room temperature. Optical density was then read at 490 nm. The percentage of cytotoxicity is calculated as followed: % = 100 × (exp value - control medium value)/(Triton X100 treated cells value - control medium value).

Cell proliferation assay ([3H]-TdR). MCF7, T47D, MDA-MB468 (500 cells/well) and BT20 (1,000 cells/well) were plated on 96-well plates and maintained for 24 h in complete medium. Medium is then removed and replaced with complete medium supplemented with recombinant human IL-17A (0, 1, 10 or 100 ng/ml) or TIL(AL)-conditioned medium (1/10 vol/vol) and/or antibodies (10 μg/ml) as indicated. After 72 h of culture, cells were pulsed with 1 μCi of tritiated thymidine ([3H]-TdR) per well. [3H]-TdR uptake was measured using PerkinElmer PerkinElmer MicroBeta2 plate counter (PerkinElmer, Waltham, MA, USA). Each experiment was performed in hexaplicates.

Transwell migration assay. 2.10^4 cells were seeded on the upper compartment of transwell chambers (24-well insert; pore size, 8 μm; BD Biosciences) in 1% FCS medium alone (medium) supplemented with recombinant human IL-17A (1, 10 or 100 ng/ml) or TIL(AL)-conditioned medium (1/10 vol/vol) and/or antibodies (10μg/ml) for 22 hours at 37°C as indicated. Medium supplemented with 10% FCS is added to the lower compartment of the chambers. The cells on the transwell were stained with 0.5% crystal violet prior imaging and enumeration. Total number of migrating cells was calculated by analyzing 5 fields per well in at least two independent experiments performed in duplicates, that is 10 fields per condition.

Matrigel invasion assay. MDA-MB231 cells were cultured in complete medium supplemented with 100 ng/ml of recombinant IL-17A for 2 days. Matrigel Invasion Chambers (BD BioCoat™ BD Matrigel™ Invasion Chamber, 24-well Cell culture inserts) were then used to study the invasiveness of cancer cells. 2.10^4 cells are then added to the upper compartment of the chambers in 1% FCS medium alone or supplemented with 100 ng/ml of recombinant cytokines as indicated. Medium supplemented with 10% FCS is added to the lower compartment of the chambers. Plates are incubated for 22 hours at 37°C. Transwell filters are then fixed and stained in Giemsa solution following which non-invading cells are removed from the upper surface of the transwell membrane using a cotton swab. Images of cells from three representative fields are captured digitally and the number of cells present on the

transwell is counted. Data are mean of three independent experiments performed in triplicates.

3D Cluster assays. MDA-MB231 cells were cultured in complete medium supplemented with 100 ng/ml of recombinant IL-17A for 2 days. 275 µl of cold Basement Membrane Matrix (LDEV-Free, 354234, BD Biosciences) was added per refrigerated CultureSlides (8-wells, 354118, BD Biosciences). Inserts were then incubated for 20 min at 37°C to obtain a solid plug of Matrigel. 10^6 pretreated cells were centrifuged and 1 µl of the cell pellet was loaded directly into the plug of Matrigel. 10 µl of Matrigel was added on top of the plug and inserts were incubated at 37°C for 5 min. 250 µl of culture medium supplemented or not with the cytokines was added on top and inserts were kept at 37°C, 5% CO2 humidified incubator and invasive behavior was analyzed at 24 h.

Statistical analyses. All values are expressed as mean +/− SEM unless otherwise specified. Quantitative data were compared using student's *t* test. The dose-dependent effects on cell proliferation (Figure 6) and migration (Figure 7A) were analyzed using the Kruskal-Wallis test. $P < 0.05$ was considered significant.

1. Mantovani, A., Allavena, P., Sica, A. & Balkwill, F. Cancer-related inflammation. *Nature* **454**, 436–444, doi:10.1038/nature07205 (2008).
2. Gaffen, S. L. Structure and signalling in the IL-17 receptor family. *Nat Rev Immunol* **9**, 556–567, doi:10.1038/nri2586 (2009).
3. Onishi, R. M. & Gaffen, S. L. Interleukin-17 and its target genes: mechanisms of interleukin-17 function in disease. *Immunology* **129**, 311–321, doi:10.1111/j.1365-2567.2009.03240.x (2010).
4. Iwakura, Y., Ishigame, H., Saijo, S. & Nakae, S. Functional specialization of interleukin-17 family members. *Immunity* **34**, 149–162, doi:10.1016/j.immuni.2011.02.012 (2011).
5. Ji, Y. & Zhang, W. Th17 cells: positive or negative role in tumor? *Cancer Immunol Immunother* **59**, 979–987, doi:10.1007/s00262-010-0849-6 (2010).
6. Zhu, X. *et al.* IL-17 expression by breast-cancer-associated macrophages: IL-17 promotes invasiveness of breast cancer cell lines. *Breast Cancer Res* **10**, R95, doi:10.1186/bcr2195 (2008).
7. Jung, M. Y., Kim, S. H., Cho, D. & Kim, T. S. Analysis of the expression profiles of cytokines and cytokine-related genes during the progression of breast cancer growth in mice. *Oncol Rep* **22**, 1141–1147 (2009).
8. Su, X. *et al.* Tumor microenvironments direct the recruitment and expansion of human Th17 cells. *J Immunol* **184**, 1630–1641, doi:10.4049/jimmunol.0902813 (2010).
9. Benevides, L. *et al.* Enrichment of regulatory T cells in invasive breast tumor correlates with the upregulation of IL-17A expression and invasiveness of the tumor. *Eur J Immunol*, doi:10.1002/eji.201242951 (2013).
10. Chen, W. C. *et al.* Interleukin-17-producing cell infiltration in the breast cancer tumour microenvironment is a poor prognostic factor. *Histopathology*, doi:10.1111/his.12156 (2013).
11. Nam, J. S. *et al.* Transforming growth factor beta subverts the immune system into directly promoting tumor growth through interleukin-17. *Cancer Res* **68**, 3915–3923, doi:10.1158/0008-5472.CAN-08-0206 (2008).
12. MacKeigan, J. P., Collins, T. S. & Ting, J. P. MEK inhibition enhances paclitaxel-induced tumor apoptosis. *J Biol Chem* **275**, 38953–38956, doi:10.1074/jbc.C000684200 (2000).
13. Favata, M. F. *et al.* Identification of a novel inhibitor of mitogen-activated protein kinase kinase. *J Biol Chem* **273**, 18623–18632 (1998).
14. Chang, Y. *et al.* Th17-associated cytokines promote human airway smooth muscle cell proliferation. *Faseb J* **26**, 5152–5160, doi:10.1096/fj.12-208033 (2012).
15. Acosta, J. J. *et al.* Src mediates prolactin-dependent proliferation of T47D and MCF7 cells via the activation of focal adhesion kinase/Erk1/2 and phosphatidylinositol 3-kinase pathways. *Mol Endocrinol* **17**, 2268–2282, doi:10.1210/me.2002-0422 (2003).
16. Gu, F. M. *et al.* IL-17 induces AKT-dependent IL-6/JAK2/STAT3 activation and tumor progression in hepatocellular carcinoma. *Mol Cancer* **10**, 150, doi:10.1186/1476-4598-10-150 (2011).
17. Li, Q. *et al.* IL-17 promoted metastasis of non-small-cell lung cancer cells. *Immunol Lett* **148**, 144–150, doi:10.1016/j.imlet.2012.10.011 (2012).
18. Li, J. *et al.* Interleukin 17A promotes hepatocellular carcinoma metastasis via NF-kB induced matrix metalloproteinases 2 and 9 expression. *PLoS One* **6**, e21816, doi:10.1371/journal.pone.0021816 (2011).
19. Finak, G. *et al.* Stromal gene expression predicts clinical outcome in breast cancer. *Nat Med* **14**, 518–527, doi:10.1038/nm1764 (2008).
20. DeSelm, C. J. *et al.* IL-17 mediates estrogen-deficient osteoporosis in an Act1-dependent manner. *J Cell Biochem* **113**, 2895–2902, doi:10.1002/jcb.24165 (2012).
21. Tyagi, A. M. *et al.* Estrogen deficiency induces the differentiation of IL-17 secreting Th17 cells: a new candidate in the pathogenesis of osteoporosis. *PLoS One* **7**, e44552, doi:10.1371/journal.pone.0044552 (2012).
22. Lee, S. Y. *et al.* IL-17-mediated Bcl-2 expression regulates survival of fibroblast-like synoviocytes in rheumatoid arthritis through STAT3 activation. *Arthritis Res Ther* **15**, R31, doi:10.1186/ar4179 (2013).
23. Olsson Akefeldt, S. *et al.* Chemoresistance of human monocyte-derived dendritic cells is regulated by IL-17A. *PLoS One* **8**, e56865, doi:10.1371/journal.pone.0056865 (2013).
24. Wang, L., Yi, T., Zhang, W., Pardoll, D. M. & Yu, H. IL-17 enhances tumor development in carcinogen-induced skin cancer. *Cancer Res* **70**, 10112–10120, doi:10.1158/0008-5472.CAN-10-0775 (2010).
25. Wang, L. *et al.* IL-17 can promote tumor growth through an IL-6-Stat3 signaling pathway. *J Exp Med* **206**, 1457–1464, doi:10.1084/jem.20090207 (2009).
26. Huang, H. *et al.* IL-17 stimulates the proliferation and differentiation of human mesenchymal stem cells: implications for bone remodeling. *Cell Death Differ* **16**, 1332–1343, doi:10.1038/cdd.2009.74 (2009).
27. Hemdan, N. Y. Anti-cancer versus cancer-promoting effects of the interleukin-17-producing T helper cells. *Immunol Lett* **149**, 123–133, doi:10.1016/j.imlet.2012.11.002 (2013).
28. Maniati, E., Soper, R. & Hagemann, T. Up for Mischief? IL-17/Th17 in the tumour microenvironment. *Oncogene* **29**, 5653–5662, doi:10.1038/onc.2010.367 (2010).
29. Numasaki, M. *et al.* Interleukin-17 promotes angiogenesis and tumor growth. *Blood* **101**, 2620–2627, doi:10.1182/blood-2002-05-1461 (2003).
30. Numasaki, M. *et al.* IL-17 enhances the net angiogenic activity and in vivo growth of human non-small cell lung cancer in SCID mice through promoting CXCR-2-dependent angiogenesis. *J Immunol* **175**, 6177–6189 (2005).
31. Wu, S. *et al.* A human colonic commensal promotes colon tumorigenesis via activation of T helper type 17 T cell responses. *Nat Med* **15**, 1016–1022, doi:10.1038/nm.2015 (2009).
32. Muranski, P. *et al.* Tumor-specific Th17-polarized cells eradicate large established melanoma. *Blood* **112**, 362–373, doi:10.1182/blood-2007-11-120998 (2008).
33. Hinrichs, C. S. *et al.* Type 17 CD8+ T cells display enhanced antitumor immunity. *Blood* **114**, 596–599, doi:10.1182/blood-2009-02-203935 (2009).
34. Chae, W. J. *et al.* Ablation of IL-17A abrogates progression of spontaneous intestinal tumorigenesis. *Proc Natl Acad Sci U S A* **107**, 5540–5544, doi:10.1073/pnas.0912675107 (2010).
35. Carmi, Y. *et al.* Microenvironment-derived IL-1 and IL-17 interact in the control of lung metastasis. *J Immunol* **186**, 3462–3471, doi:10.4049/jimmunol.1002901 (2011).
36. Zhang, Q. *et al.* Interleukin-17 promotes formation and growth of prostate adenocarcinoma in mouse models. *Cancer Res* **72**, 2589–2599, doi:10.1158/0008-5472.CAN-11-3795 (2012).
37. Das Roy, L. *et al.* Breast-cancer-associated metastasis is significantly increased in a model of autoimmune arthritis. *Breast Cancer Res* **11**, R56, doi:10.1186/bcr2345 (2009).
38. Novitskiy, S. V. *et al.* TGF-beta receptor II loss promotes mammary carcinoma progression by Th17 dependent mechanisms. *Cancer Discov* **1**, 430–441, doi:10.1158/2159-8290.CD-11-0100 (2011).
39. Coury, F. *et al.* Langerhans cell histiocytosis reveals a new IL-17A-dependent pathway of dendritic cell fusion. *Nat Med* **14**, 81–87, doi:10.1038/nm1694 (2008).
40. Bagot, M. *et al.* Isolation of tumor-specific cytotoxic CD4+ and CD4+CD8dim+ T-cell clones infiltrating a cutaneous T-cell lymphoma. *Blood* **91**, 4331–4341 (1998).
41. Miyagaki, T. *et al.* IL-22, but not IL-17, dominant environment in cutaneous T-cell lymphoma. *Clin Cancer Res* **17**, 7529–7538, doi:10.1158/1078-0432.CCR-11-1192 (2011).
42. Mayer, C. *et al.* DNA repair capacity after gamma-irradiation and expression profiles of DNA repair genes in resting and proliferating human peripheral blood lymphocytes. *DNA Repair (Amst)* **1**, 237–250 (2002).

Acknowledgments

The authors wish to thank F. Dijoud for performing IHC on breast cancer TMA. This work is supported by grants from INSERM, Agence Nationale pour la Recherche and OREGA Biotech.

Author contributions

J.B. and A.B. designed and supervised the study and wrote the main manuscript text. S.C., J.G., C.T., E.L. performed experiments and prepared the figures. C.G., A.M.S., H.C., C.M. provided biopsies. G.A., N.B., J.F.E. contributed to the design and interpretation of experiments and to the editing of the manuscript. All authors reviewed the manuscript.

Additional information

Supplementary information accompanies this paper at http://www.nature.com/scientificreports

Competing financial interests: Drs Bonnefoy, Bensussan, Alberici and Eliaou are cofounders and shareholders of OREGA Biotech. Dr Bastid is an employee of OREGA Biotech. Drs Cochaud, Giustiniani, Thomas, Laprevotte, Garbar, Savoye, Curé and Mascaux declare no conflict of interest.

How to cite this article: Cochaud, S. *et al.* IL-17A is produced by breast cancer TILs and promotes chemoresistance and proliferation through ERK1/2. *Sci. Rep.* **3**, 3456; DOI:10.1038/srep03456 (2013).

SCIENTIFIC REPORTS

OPEN

IL-17A and its homologs IL-25/IL-17E recruit the c-RAF/S6 kinase pathway and the generation of pro-oncogenic LMW-E in breast cancer cells

Received: 03 February 2015
Accepted: 08 June 2015
Published: 08 July 2015

Sarah Mombelli[1,2,3,4], Stéphanie Cochaud[1,2,5], Yacine Merrouche[3,4], Christian Garbar[3], Frank Antonicelli[4], Emilie Laprevotte[5,6], Gilles Alberici[5], Nathalie Bonnefoy[6], Jean-François Eliaou[6,7], Jérémy Bastid[5], Armand Bensussan[1,2,*], & Jérôme Giustiniani[3,4,*]

Pro-inflammatory IL-17 cytokines were initially described for their pathogenic role in chronic inflammatory diseases and subsequent accumulating evidence indicated their involvement in carcinogenesis. In the present study we report that IL-17A and IL-17E receptors subunits mRNA expressions are upregulated in breast cancers versus normal samples. IL-17E, which is undetectable in most normal breast tissues tested, seems more expressed in some tumors. Investigation of the molecular signaling following stimulation of human breast cancer cell lines with IL-17A and IL-17E showed that both cytokines induced the phosphorylation of c-RAF, ERK1/2 and p70 S6 Kinase were involved in the proliferation and survival of tumor cells. Accordingly, IL-17A and IL-17E promoted resistance to Docetaxel and failed to induce apoptosis as previously reported for IL-17E. Interestingly, we also revealed that both cytokines induced the generation of tumorogenic low molecular weight forms of cyclin E (LMW-E), which high levels correlated strongly with a poor survival in breast cancer patients. These results show for the first time some of the molecular pathways activated by IL-17A and IL-17E that may participate to their pro-oncogenic activity in breast cancers.

The IL-17 cytokine family is composed of six members, IL-17A to IL-17F with IL-17A as the prototypic one[1]. A total of five receptors have been described, IL-17RA to IL-17RE. IL-17A binds and signals through the IL-17RA/IL-17RC receptor heterodimer, whereas IL-17E, also named IL-25, is a ligand for the IL-17RA/RB heterodimer[2]. IL-17A is mainly produced by T helper 17 (TH17) cell subset and by innate immunity lymphocytes including TCR-$\gamma\delta^+$ T cell, iNKT, lymphoid tissue inducer (LTi) cells, $CD3^-NKp46^+$ lymphocytes or neutrophils that are potentially responsible for initiating pathogenic TH17 cells proliferation[1,3–5]. A growing body of evidence indicated important roles for this cytokine and TH17

[1]Institut National de la Santé et de la Recherche Médicale (INSERM) U976, Hôpital Saint Louis, 75010 Paris, France. [2]Université Paris Diderot, Sorbonne Paris Cité, Laboratoire Immunologie Dermatologie & Oncologie, UMR-S 976, F-75475, Paris, France. [3]Institut Jean Godinot, Unicancer, F- 51726 Reims, France. [4]Université Reims-Champagne-Ardenne, DERM-I-C, EA7319, 51 rue Cognacq-Jay, 51095 Reims Cedex, France. [5]OREGA Biotech, F-69130 Ecully, France. [6]IRCM, Institut de Recherche en Cancérologie de Montpellier; INSERM, U896; Université Montpellier 1; CRLC Val d'Aurelle Paul Lamarque, Montpellier, F-34298, France. [7]Département d'Immunologie, Centre Hospitalier Régional Universitaire de Montpellier et Faculté de Médecine Université Montpellier 1, Montpellier, France. *These authors contributed equally to this work. Correspondence and requests for materials should be addressed to A.B. (email: armand.bensussan@inserm.fr)

cells in the development of allergic and autoimmune diseases as well as in protective mechanisms against bacterial and fungal infections[6] and gained prominence in cancer, particularly in breast carcinomas[7,8,9]. Mouse models of breast cancers revealed that IL-17A promotes tumor growth and angiogenesis[10,11]. Recently, we have shown that IL-17A produced by tumor infiltrating lymphocytes promotes breast cancer cell chemoresistance and proliferation through activation of ERK1/2 pathway[12,13] . Interestingly, it has been reported that IL-17B produced by malignant cells could also promote cancer cell survival through activation of NF-κB[14,15]. In contrast IL-17E was reported to be produced by normal mammary epithelial cells, and its binding to IL-17RA-IL-17RB complex induced breast cancer cell apoptosis[15]. Thus, it was suggested that IL-17E production by normal epithelium might prevent the emergence of transformed epithelial cells by inducing malignant cell apoptosis, while IL-17B produced by transformed cells promoted cancer cell survival by displacing IL-17E from its receptor.

In the present study, we aimed to identify in breast cancer cells the signaling pathways recruited following IL-17A and IL-17E cytokine stimulation. The results revealed that both cytokines activated similar oncogenic pathways in breast malignant cell lines leading to Docetaxel resistance and generation of LMW cyclin E. In contrast to previous report, we failed to found IL-17E expression by non-transformed epithelial cells and to reproduce its potential induction of breast cancer cell apoptosis. These results shed new light on the potential role of IL-17A and IL-17E in breast cancer and further studies should contribute to understand whether they could be potential therapeutic targets. Furthermore, these data question the role of IL-17E as a potential tumor suppressor.

Results

Expression of IL-17E and its receptor in breast cancer biopsies and cell lines. To elucidate the potential role of IL-17E in breast cancer, we first assessed the expression of this cytokine and the IL17-RA, RB and RC receptor subunits in human normal and cancer breast tissues, using RT-QPCR. As illustrated in Fig. 1 IL-17E mRNA, which is undetectable in most normal breast tissues tested, seems more expressed in some tumors. Furthermore, the three IL-17R subunits, corresponding to the IL-17E (IL17RA/RB) and IL-17A (IL17 RA/RC) receptors, were highly upregulated in tumor versus normal samples, suggesting that IL-17E as IL-17A signaling is potentially active in human breast cancer.

We then asked whether the cytokine and IL-17 receptor subunits are expressed by the tumor cells. To address this question, we assessed the expression of IL-17E, IL-17RA, IL-17RC and IL-17RB in various human breast cancer cell lines as well as in non-transformed mammary epithelial cells MCF10A, in primary tumor cells (IJG-1731) derived *ex vivo* from an ER-negative breast cancer biopsy. As illustrated in Fig. 2, the expression of the IL-17RA and IL-17RC receptor subunits was ubiquitous as all the primary cells and cell lines tested expressed high levels of IL-17RA and IL-17RC. In line with the results obtained from biopsies (Fig. 1), IL-17RB was undetectable in non-transformed MCF10A cells and significantly upregulated in most breast cancer cell lines tested; suggesting that increased expression of IL17RB could be a malignant trait.

Further, we found that cell lines and the primary tumor cells did not expressed IL-17E transcripts, indicating that the cytokines are likely to be produced by the tumor microenvironment. Although a previous report[15] indicated that non-transformed MCF10A mammary epithelial cells expressed IL-17E, we were unable to detect IL-17E transcript in this cell line (Fig. 2).

IL-17E fails to induce breast cancer cell apoptosis and promoted chemoresistance. Furuta *et al.* reported that non-transformed mammary epithelial cells express IL-17E and low levels of IL-17RB, and this cytokine induced apoptosis in transformed breast cells (with upregulated IL-17RB) but not in non-transformed cells, thereby serving as a tumor suppressor. Although we here confirmed that IL-17RB expression is much higher in tumor cells than in non-transformed cells, we were unable to detect IL-17E mRNA in MCF10A cells (Fig. 2). IL-17E was even express at higher levels in tumor biopsy specimens than in normal breast tissues (Fig. 1). These results raised questions about the potential role of IL-17E as a tumor suppressor.

We therefore decided to test the ability of IL-17E to induce apoptosis of breast cancer cell lines, and used IL-17A as negative control as we previously demonstrated that it fails to induce apoptosis by itself[12]. As illustrated in Fig. 3A, we analyzed cell apoptosis by evaluating PARP proteolysis in the representative T47D malignant cell line treated with IL-17E or IL-17A either at 100 ng/ml or 500 ng/ml. Treatment with Docetaxel at 10 μg/ml was used as a positive control for apoptosis. The results clearly show that, in contrast to Docetaxel, neither IL-17A nor IL-17E induced PARP cleavage at the indicated concentrations.

Next, to further confirm the lack of apoptosis induced by IL-17A and IL-17E, we measured the level of cell death of MCF7, T47D and MDA-MB468 cells cultured in presence of recombinant IL-17A or IL-17E used at concentrations from 20 ng to 500 ng/ml. Docetaxel at 10 μg/ml and 1% Triton × 100 were used as positive controls. Results presented in Fig. 3B revealed that IL17A and IL-17E did not induce the cell death of MCF-7, T47D or MDA-MB468 cells.

Although IL-17E did not induce apoptosis of IL-17RB expressing breast cancer cells, we tested whether it could modulate cell death induced by chemotherapy drugs. As we previously reported that 1 to 10 ng/ml of IL-17A was very potent at inhibiting Docetaxel induced cell death in various human breast cancer cell lines[12].The results shown in Fig. 4 indicated that pretreatment of MCF-7, T47D or primary

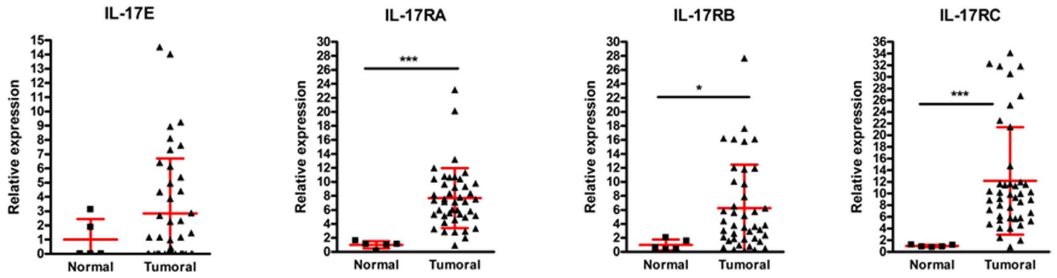

Figure 1. Expression of IL-17 cytokines and receptors in clinical samples. The TissueScan Breast Tissue qPCR array was used to determine transcript levels of the IL-17 cytokines (IL-17A and IL-17E) and their receptors (IL-17 RA, IL-17 RB and IL-17 RC). The breast tissue scan contains 48 tissues covering 4 diseases stages and normal tissues. The target transcript levels were normalized to β-Actin and calibrated to the mean mRNA level (arbitrary value of 1) in normal tissue. Data were compared using student's *t* test (*$P < 0.05$, **$P < 0.01$, ***$P < 0.001$).

tumor cells IJG-1731 with 1 to 10 ng/ml of IL-17E consistently results in decreased Docetaxel-induced cell death.

IL-17A and IL-17E promotes the phosphorylation of c-Raf, ERK and p70S6 kinase. In order to identify the kinases involved in chemoresistance induced by IL-17A and IL-17E pre-treatments, we explored the activation of signaling pathways involved in cancer progression. To this aim, MCF-7, T47D, and primary tumor cells IJG-1731 cells were starved overnight then treated with the cytokines. We analyzed their phosphorylation status for 20 min following the cytokine treatment. In cell lines tested, we observed an activation of the MAP kinases pathway through the phosphorylation of c-RAF on Serine 338 (p-cRAF) (Fig. 5) and p42/p44MAPK (suppl Figure 2A and 2B)[12]. In untreated IJG-1731 and MDA-MB468 cells p-cRAF was almost undetectable and was highly induced after addition of cytokines. 120% up to 1000% increased signal was obtained, depending on the IL-17 cytokine used.

It should be mentioned that c-RAF serine 338 is phosphorylated by the p21 activated kinase[16] and corresponded to similar phosphorylated sites in A-Raf (Ser299) and B-Raf (Ser445)[17].

Because the PI3K/mTOR/p70S6K axis is well known to play an important role in cell growth and survival, and is described to be involved in breast cancer cell proliferation and chemoresistance[18], we looked at the activation of the p70S6K ($p70^{S6K}$), which regulates cell cycle, inhibits the pro-apoptotic protein BAD and controls protein synthesis through the phosphorylation of the S6 protein of the 40S ribosomal subunit[19]. We measured the phosphorylation of Thr389, which closely correlates with p70 kinase activity *in vivo*[20]. The results showed in Fig. 5 indicated that incubation with IL-17A or Il-17E enhanced the phosphorylation of on Thr389 $p70^{S6K}$, in T47D, MDA-MB 468 and IJG-1731 cell lines (Fig. 5). We could not reproduce this result with MCF7 cell line due to the constitutive phosphorylation of the S6 kinase (data not shown).

As p70S6K may also be activated by the c-RAF/ERK pathway, we chemically blocked p42/p44MAPK with the U0126 MEK specific inhibitor to further demonstrate the contribution of the c-RAF, ERK, p70S6K pathway in IL-17-induced chemoresistance in breast cancer cell lines. The results in Supp Figure 1 show that lack of ERK1/2 activation in the BT20 breast cancer cell totally abolished the chemoresistant effect induced by IL-17E cell stimulation.

IL-17A or IL-17E treatment enhances the generation of low molecular weight forms of cyclin E (LMW-E) in breast tumor cell line. As we found that breast malignant cell proliferation was increased by IL-17A or IL-17E (suppl Fig. 2C), we next investigated the expression of the full length cyclin E, a regulatory subunit of Cdk2 that contributes to G_1/S transition, as well as the expression of LMW forms of cyclin E for which the regulatory domain is missing[21,22].

Interestingly, we found that IL-17A or IL-17E did not increase the expression of the full length cyclin E in MCF7, T47D and MCF10A cell lines, when compared to untreated cells. In contrast, we observed a consistent increase of cyclin E in the primary breast cancer cell line IJG-1731 when cultured with either IL-17A or IL-17E (Fig. 6). More importantly, we found that all breast cancer cell lines upregulated the generation of LMW-E forms. Although some of LMW-cyclin E forms could be weakly present at basal level, we detected almost all of the five published short forms[23], ranging from 34 to 49 kDa, after 72 h of treatment with each cytokines. Cyclin E proteolysis might be a tumor specific mechanism as IL-17A failed to up-regulate the generation of LMW-E forms in the non-transformed mammary epithelial MCF10A cells although these cells express significant levels of IL-17RA and IL-17RC (Fig. 1). Of note, MCF10A cells lack IL-17RB and did not respond to IL-17E.

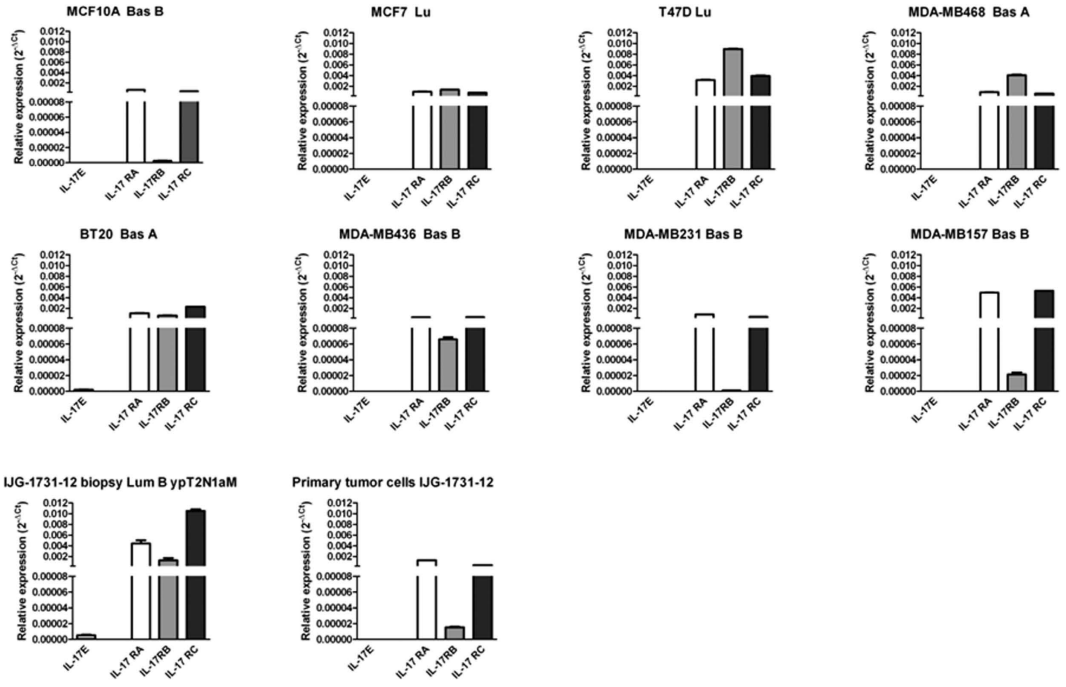

Figure 2. Expression of IL-17 cytokines and receptors in human breast cell lines. Real-Time RT-PCR analysis of the IL-17 cytokines mRNA (IL-17A and IL-17E) and their receptors (IL-17 RA, IL-17 RB and IL-17 RC) in different human beast cell lines. Expression was normalized to the GAPDH mRNA expression. Data are the mean +/− SEM of one experiment performed in duplicate.

Discussion

Interleukins are known to promote tumor growth and metastasis, and IL-17A could be a typical example. This cytokine produced by infiltrating lymphocytes has been shown to promote tumor proliferation[10,12] as well as migration, invasion and resistance to chemotherapy[12] and to anti-angiogenic treatment[24]. Recent works focused on IL-17B and IL-17E, which are found in breast tumor microenvironment, have reported opposite functions. Although they share the IL-17RB chain as co receptor, pro-oncogenic features were described for the breast tumor cell secreted IL-17B, whereas tumor suppressor role was associated to the normal breast epithelial cells secreted IL-17E. Here, we investigated the action of IL-17A and IL-17E on breast cancer cell lines and cell signaling events induced after recruitment of IL-17RA/IL-17RC or IL-17RA/IL-17RB receptors.

We found that IL-17E receptor mRNA was increased in malignant breast tissues and breast cell lines as compared to healthy tissues and that IL-17E mRNA seems expressed in some of tumors. Neither IL-17E nor IL-17A stimulation induced cell apoptosis. The absence of apoptosis was not due to the inability of the cytokine to signal through the IL-17E receptor as the E-coli-produced IL-17E, similarly to IL-17A[12], activated the ERK pathway in breast cancer cells (supp Figs 2A and 2B). Moreover, a potential cross reactivity between IL17A receptor (IL17RA/RC) and IL-17E is unlikely, since this cytokine, on the contrary to IL-17A, is not able to induce any signaling event on IL17RB^{neg} MDA-MB231 cells (data not shown). These findings are contradictory to published data[15,25] showing a pro-apoptotic effect of E-coli-derived IL-17E on breast cancer cell line expressing IL-17RB such as MDA-MB468. A potential explanation for these discrepancies is that all our assays were performed with physiological compatible IL-17E concentrations (1–10 ng/ml), while *In vitro* pro-apoptotic effects were observed with higher concentrations (250 up to 2000 ng/ml) in the study of Vahid Younesi *et al.*[25].

In our study, not only IL-17E did not display a pro-apoptotic role, but we also demonstrated that IL-17E pretreatment was capable to partially prevent drug sensitivity in association with the activation of the p70S6K, ERK and c-RAF pathway. Activation of b-RAF have been already described in tumor cells[26] and it is interesting to underline that c-RAF and b-RAF are interconnected and their heterodimerization increases the activity of both kinases[27,28]. Our results are in agreement with Huang *et al.* indicating that IL-17RB has an important role in breast tumorigenesis and that its high expression correlates with shorter survival. Of note, such activation was also observed when cells were pretreated with IL-17A. Furthermore, the chemoresistant phenomenon observed was not drug specific as IL-17E also protected breast cancer from doxorubicin-induced toxicity (data not shown). Thus, our results support the hypothesis that both IL-17A and IL-17E are involved in breast cancer progression by activating common signaling cascade end point despite the fact these cytokines trigger distinct receptors.

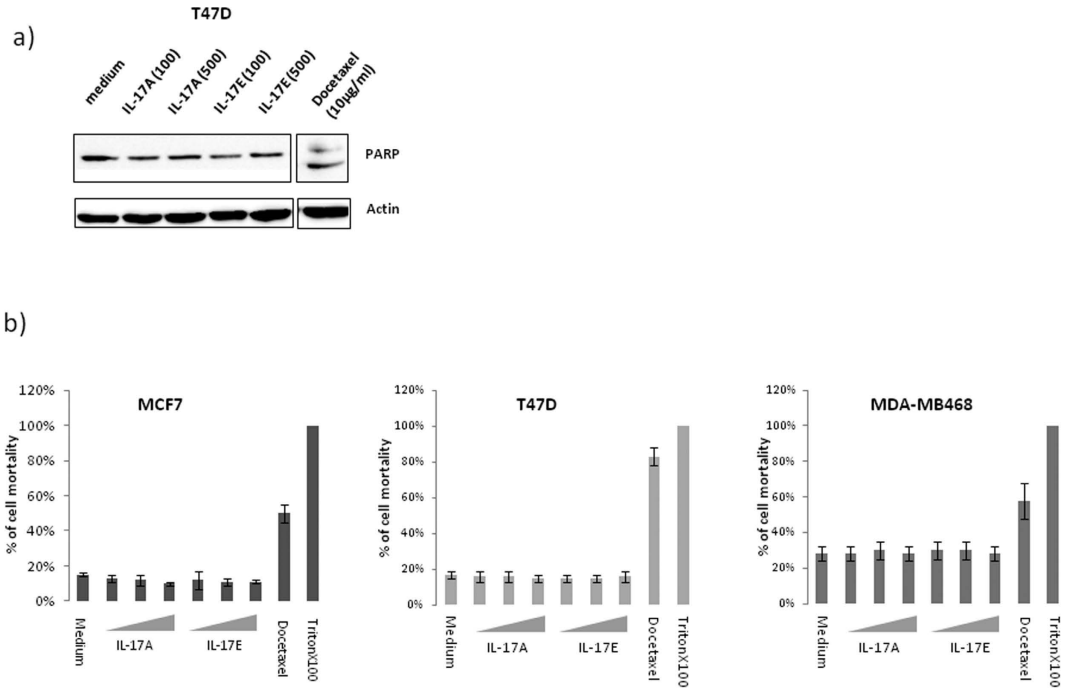

Figure 3. IL-17E do not induce apoptosis. Cell apoptosis was analyzed by detection of PARP proteolysis (**a**) or measurement of LDH released into cell supernatants (**b**) to this aim; cells were treated 24 h in a serum free medium with IL-17A or IL17-E at 20, 100 or 500 ng/ml. As positive control for PARP cleavage or LDH detection we used Docetaxel at 10 µg/ml.

Conversely to previous studies[15,25], we demonstrated that IL-17E displayed a protumoral role in breast cancer. Such discrepancies in the function of a single molecule are quite puzzling, and might rely on its environment. In this regard, it is worth to note that IL-17 was not secreted by tumoral but by infiltrating cells in breast human biopsy. Conversely, Furuta *et al.* demonstrated a potent anticancer activity of purified IL-17E in mouse cancer models[15]. Interestingly, previous work already demonstrated that IL-17E exhibits potent antitumor effects against various human cancer cell lines (including the MDA-MB-435 breast cancer cells) *in vivo*[29]. Although the mechanisms were not fully elucidated, antitumor activity was evidenced in nude mice (normal B cells) but lost in SCID mice (no B cells), suggesting that the anti-tumoral effects of IL-17E were B-cell dependent. Tumor infiltrating B cells were extensively studied in breast cancer, where they are present in ~25% of tumors and could represent up to 40% of the TIL population[30]. Moreover in node negative breast cancer, presence of TIL-B was positively associated with survival[31]. The recruitment of IL-17RB, expressed on B cells[32], could participate to the homing of such cells in the tumor microenvironment and positively regulates the response observed in nude mice. An IL-17E enhanced cytotoxicity of TIL-B cells could be discussed as well as it was already demonstrated that B cells stimulated with IL-21 can secrete granzyme B and could have a direct cytotoxicity against tumor cells[33]. Therefore, in breast cancer IL-17E could display antagonistic effects on tumour progression, a direct pro-tumoral effect on breast cancer cells and an indirect anti-tumoral effect via B-cell recruitment and activation.

Noteworthy, in our study the IL-17E protumoral effects were characterized by an enhanced proliferation capacity of breast cancer cells. During the last decade, it was shown that high expression of low molecular form of cyclin E (LMW-E) corresponded to a poor disease free survival factor in breast cancers[26]. LMW-E forms, generated by proteolysis from the full length cyclin E, highly enhance CDK2 activity and are not inhibited by p21 and p27 proteins[22]. Here, we report for the first time that both IL-17E and IL-17A triggered signaling cascades converging towards the generation of LMW-E forms. Such stimulation was only observed with tumor cell lines, opening the possibility that anti-IL-17 therapy could specifically target cancer cells. These active forms of cyclin-E are highly oncogenic as demonstrated by Duong. T *et al.*, in mice model, where ectopic LMW-E expression on hMEC cell line renders it tumorogenic and induces the development of mammary carcinoma and metastasis, whereas the full length expression of cyclin E do not[26]. Two enzymes have been involved in the LMW-E generation; calpain and an elastase like protease which is inhibited by endogenic Elafin a critical component of the epithelial barrier against neutrophil elastase[23,34]. We could thus hypothesize that IL-17A/E-induced signaling cascades could affect the protease/anti-protease balance both by up regulating the elastase like protease expression and down regulating Elafin expression in breast cancer cells compared to normal cells[35]. Such tumor

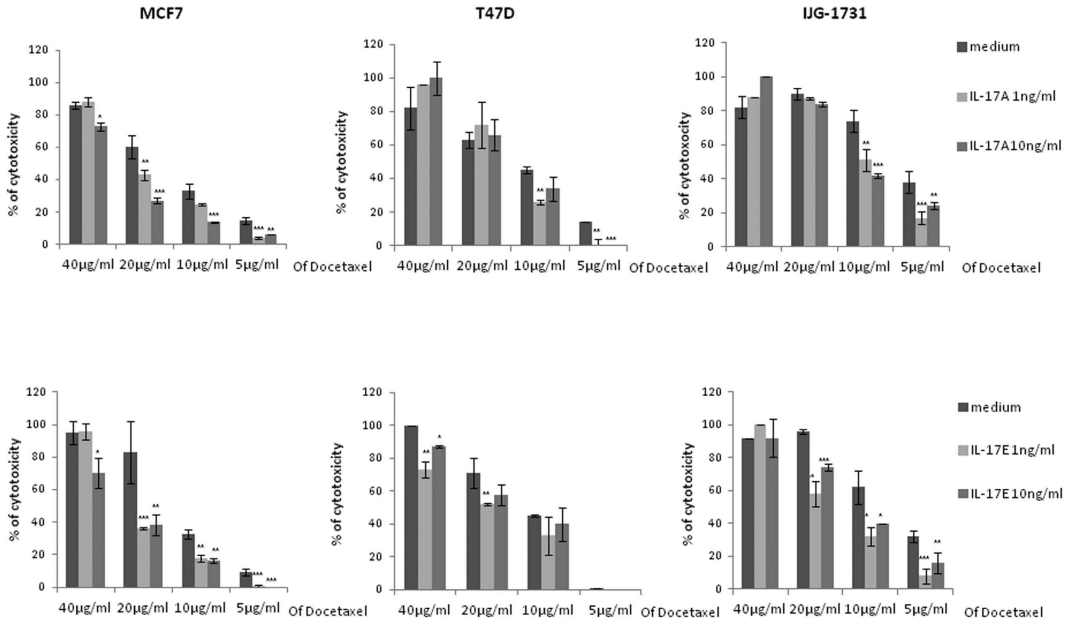

Figure 4. IL-17E induces cell chemoresistance to Docetaxel. Breast cancer cells were cultured in complete medium alone (medium) or supplemented with IL-17A or -E for 48 h. Cells were then switched in FCS-free medium supplemented with the respective cytokine for 24 h before adding Docetaxel at various concentration for 7 h at 37 °C. The cytotoxicity was determined using the Cytotoxicity Detection Kit (Roche). Data shown are representative of 3 independent experiments. (*$P < 0.05$; **$P < 0.01$; ***$P < 0.001$).

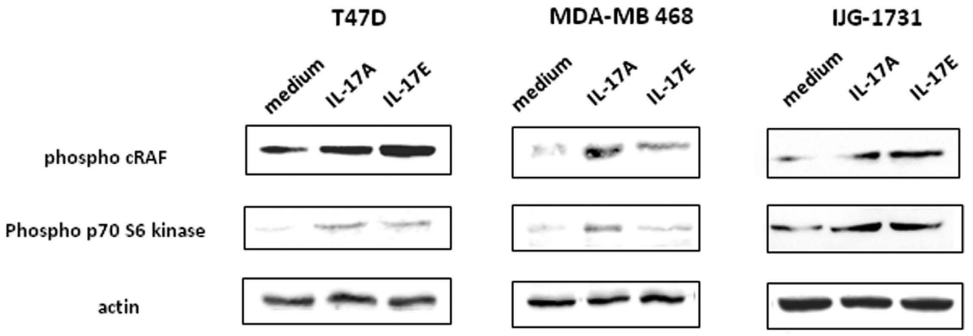

Figure 5. IL-17A and IL-17E activate c-Raf and p70S6 kinase. Activation of c-Raf (pSer338) and p70S6 kinase (pThr 389) was analyzed successively by Western Blot (WB) on T47D, MDA-MB468 and IJG-1731 cell lines. Cells were treated with either IL-17A or IL-17E at 20 ng/ml for 20 min before cell lysis. 70 µg of protein were loaded for each condition and loading control was done with an anti β-actin mAb. Data are representative of 3 independent experiments and all the lines were run on the same gel and under the same experimental procedure.

specific pro-oncogenic effects could involve direct and indirect mechanisms. LMW-E could both originate from the c-RAF/ERK pathway activation triggered by IL-17, but also from other signaling cascades that control the protease/antiprotease balance in the tumour microenvironment. Whether these latter regulations are direct or indirect through the release of other molecules that could interfere by autocrine/paracrine mechanisms still need to be determined. In this setting, our data suggest that several IL-17 family members, present in the tumor breast cancer microenvironment, may both act as survival factors and promote chemoresistance. It was reported that IL-17A and IL-17B neutralizing antibody treatments led to decreased breast cancer growth in mice. It would be interesting to test whether anti-IL-17A, IL-17B and/or IL-17E based therapies could affect tumor growth and sensitivity to chemotherapy and immunotherapy (anti-HER2) in animal models of cancer. To that matter, further work on the expression of IL-17 receptors from metastatic breast cancer cells compared to primary tumor could be informative, especially for liver and lung metastasis where IL-17E is expressed[36,37].

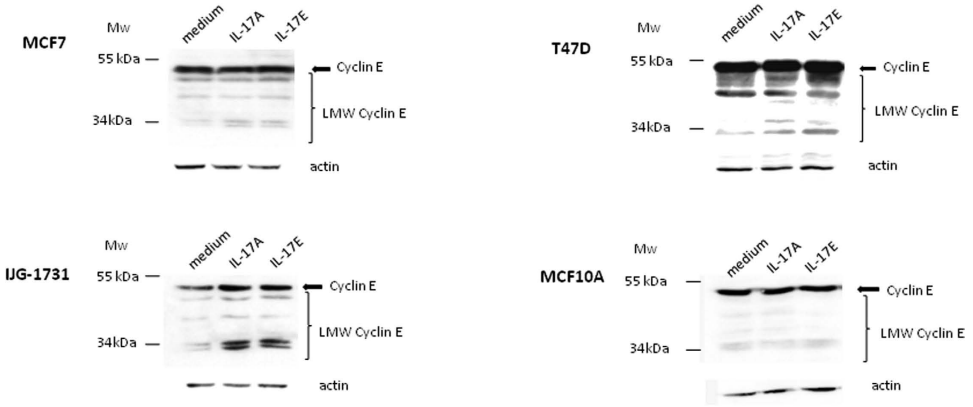

Figure 6. IL-17A or IL-17E enhance the generation of low molecular weight forms of cyclin E (LMW-E). LMW-E generation was analyzed by WB on MCF-7, T47D, IJG-1731 and MCF10A after 72 h of treatment with Il-17A or IL-17E at 20 ng/ml. 70 μg of protein were loaded for each condition and loading control was done with an anti β-actin mAb after stripping. Almost all of the five published short forms ranging from 34 to 49 kDa, were induced. No induction was found for the nonmalignant MCF10A cell line suggesting a specific feature of tumor cells. Data are representative of 3 independent experiments and all the lines were run on the same gel and under the same experimental procedure.

Taking together the findings reported here suggest that IL-17A and IL-17E are expressed and active in breast cancer and may participate to tumorogenesis.

Materials and Methods

Cell lines and culture conditions. T47D (ATCC No. HTB-133) cells and MCF7 (ATCC No. HTB-22), BT-20 (ATCC No HTB-19) and IJG-1731 cells were cultured in a complete RPMI-1640 media with L-glutamine, supplemented with 10% fetal calf serum (FCS) and penicillin–streptomycin solution (100 μg/ml each) (Life technology,Saint-Aubain, France). All cells were cultivated in a humidified 5% CO2 incubator at 37 °C. Cells were grown for 4–5 days until confluency. Cells were harvested with 0.25% Trypsin–EDTA solution (Life technology, Saint-Aubain, France) and then passed into new T-75 tissue culture flasks. Starvation medium did not contain FCS.

Generation of IJG-1731 cell line. IJG-1731 cell line was obtained from a LumB tumor characterized as a ypT2N1aM tumor. Briefly, biopsy was cut and trypsinized to liberate tumor cells. Cell preparation obtained was then cultured in complete RPMI1640 medium. After several weeks of cell culture stabilization, cells were phenotyped as negative for eostrogen, progesterone and HER2 receptors and positive for EGFR (HER1).

Antibodies. Rabbit Anti-phospho Ser388 c-RAF (clone 56A6), mouse anti-phospho Thr389 P70 S6 kinase (clone 1A5), rabbit phospho Erk1/2 (Thr202/Tyr204) (D13.14.4E), rabbit Erk1/2 (137F5), mouse anti-Cyclin E (clone HE12), polyclonal rabbit anti-PARP/cPARP and rabbit anti-Actin (clone 13E5) were obtained from Cell Signaling Technology (Leiden, Netherlands).

Proliferation assay (^{3}H). 400 cells per well (total volume of 200 μl) were seeded in a 96 wells plate with medium alone or completed with cytokines at 20 ng/ml during 72 hours at 37 °C, 5% CO2 After 72 h of culture, cells were pulsed for 16 h with 1 μCi of tritiated thymidine ([3H]-TdR) per well. [3H]-TdR uptake was measured using MicroBeta2 plate counter (PerkinElmer, Courtaboeuf, France). All conditions were done in triplicate.

Immunoblotting. *c-RAF and S6 kinase.* To detect phosphorylation of c-RAF, and p70S6 kinase 3.10^5 cells per well 6 wells plate are seeded in 2 ml of complete medium 24 h then cultured overnight in starvation medium. Medium is removed and cells are activated with cytokine at 20 ng/ml (1 ml) in free FCS RPMI. After an incubation of 20 min at 37 °C, the cells were lysed in 1% Triton × 100 lysis buffer, incubated for 1h on ice and centrifuged at 4 °C for 10 min at 10,000 g. The supernatants were collected and protein concentration was determined using the Bradford Assay (Bio-Rad, Marnes la Coquette, France). Proteins (70 μg) were resolved in 8% SDS–PAGE and transferred on nitrocellulose membrane. The membrane was blocked for 1 h at room temperature, by using 5% nonfat milk in Tris-buffered saline (TBS) containing 0.1% Tween20 (Sigma–Aldrich) and incubated overnight at 4 °C with a anti-phospho-c-RAF antibody (1:1,000), anti-phospho S6 kinase (1:1,000) or with an anti-Actin antibody (1:1,000) (Cell Signaling, Leiden, Netherlands) used as a loading control, in blocking solution. After 3 washes, the

membrane was incubated 1h at room temperature with goat anti-rabbit or goat anti-mouse secondary antibodies (1:10,000) (Jackson Immunoresearch, West Grove, USA) conjugated to horseradish peroxydase.

Cyclin E. To detect multiple forms of Cyclin E, cells were seeded in a 6 wells plate in 2 ml of starvation medium then cultured overnight. Cells are activated with cytokines diluted at 20 ng/ml in a 3% FCS medium for 72 hours. Cells are then treated as described above.

PARP/cleaved PARP. 3.10^5 cells per well 6 wells plate are seeded in 2 ml of complete medium 24 h then cultured overnight in starvation medium. Medium is removed and cells are activated with cytokine at 100 or 500 ng/ml (1 ml) in free FCS RPMI. A positive control was performed by treating cells with Docetaxel at 10 μg/ml. After 24 h of culture, the medium is removed and cells are immediately lysed as described previously.

For each sample, 70 μg of protein were subjected to 8% SDS-PAGE under reducing conditions. Resolved proteins were transferred onto nitrocellulose membrane which was blocked in 5% milk/TBS Tween20 0.1% (TBS-T) solution for 1 h at RT. Primary antibodies were added overnight at 4 °C in 5% Bovine Serum Albumin (BSA)/TBS-T solution and extensively washed with TBS-T. Corresponding horseradish peroxidase conjugated anti-mouse or anti-rabbit antibodies (Jackson Immuno Research) were used at dilution 1:10 000 for 1 h at RT before final wash with TBS-T and subsequent detection of protein bands using SuperSignal West Pico Chemoluminescent kit (Thermo Scientific, Rockford, USA). All experiments were performed in triplicates.

cDNA synthesis. Total RNA was isolated using the GenElute™ Mammalian Total RNA kit (Sigma–Aldrich, Saint-Quentin Fallavier, France) following the manufacturer's instructions. Total RNA (1 μg) was treated with 1 U/μg RNA of DNase I Amplification Grade (Life Technologies, Saint-Aubain, France) according to the manufacturer's instructions, and in the presence of 10 U/μg RNA of RNaseOUT (Life Technologies, Saint-Aubain, France). After DNase inactivation, RNA was reverse transcribed using random nonamers (Sigma–Aldrich, Saint-Quentin Fallavier, France) and M-MLV Reverse Transcriptase H Minus (Promega, Charbonnières, France) according to the manufacturer's instruction.

Polymerase chain reaction of reverse transcribed mRNA. The forward and reverse primers used in the PCR reaction were designed with Primer-BLAST software (http://www.ncbi.nlm.nih.gov/tools/primer-blast/), except for IL-17A[38] and GAPDH[39] and were listed in Table 1.

Real-time polymerase chain reaction quantification was carried out with the LightCycler 480 II System (Roche Diagnostics, Meylan, France) using the SYBR Premix Ex Taq (TliRNaseH Plus) kit (Ozyme, Saint Quentin, France). The cycling conditions were as follows: 95 °C for 1 min followed by 40 cycles of 95 °C for 20 s, 60 °C for 20 s and 72 °C for 30 s. The sizes of the RT-PCR products were confirmed by agarose electrophoresis. At the end of the amplification, a melting temperature analysis of the amplified gene products was performed routinely for all cases; the PCR products were melted by gradually increasing the temperature from 60 to 95 °C in 0.3 °C steps, and the dissociation curves were generated with the Melting Curve analysis tool of the LightCycler 480 software (Roche Diagnostics, Meylan, France). We confirmed that only one product was consistently amplified in all PCR reactions. The negative water control showed no amplification. The relative expression of the genes of interest normalized to GAPDH was determined by the delta Ct method.

Tissue qPCR array. The target genes expression was also analyzed in normal and tumoral breast tissues using the TissueScan Breast Tissue qPCR array (BCRT502, OriGene Technologies, Rockville, USA). This tissue scan is a panel of normalized cDNA from 5-normal and 42 different stages of breast cancer tissues. A description in depth pathology report (including histology sections) for all of the RNA used in the panel can be viewed on OriGene's Website.

For this study, the real-time PCR was carried out with the ABI Prism 7300 Real-Time PCR (Applied Biosystems/Life Technologies, Saint-Aubain, France) using the Power SYBR Green PCR Master Mix (Applied Biosystems/Life Technologies, Saint-Aubain, France). The cycling conditions were as follow according to the manufacturer's instruction: 50 °C for 2 min for the activation, 95 °C for 5 min for the pre-soak followed by 42 cycles of 95 °C for 15 s, 60 °C for 1 min and 72 °C for 30 s. As the LightCycler 480 II System, a melting temperature analysis of the amplified gene products was performed at the end of the amplification. The relative expression of the genes of interest normalized to β-Actin (provided by OriGene, Rockville, USA), was determined by the delta Ct method.

Cytotoxicity assay (LDH assay). *IL-17 induced apoptosis assay.* MCF7, T47D (1000 cells/well), and MDA-MB468 (3000 cells/well) were seeded in a 96 wells plate in adequate complete medium for 24 h. Then, medium was changed to a FCS-free one alone or treated with recombinant cytokines (20,100 or 500 ng/ml) for 24 h. Untreated cells (control medium), Docetaxel (10 μg/ml) and 1% Triton × 100 treated cells (100% cell death) were used as controls. The cytotoxicity was determined using the Cytotoxicity Detection Kit (Roche, Meylan, France) according to the manufacturer's instructions. To this aim, 50 μl

Gene and GenBank accession	Primer sequence	Product length
IL17-A # NM_002190.2	5'- ACTACAACCGATCCACCTCAC-3'	83 bp
	5'-ACTTTGCCTCCCAGATCACAG-3'	
IL-17E # NM_022789.3	5'-TCCCCCTGGAGATATGAGTTGGACA-3'	175 bp
	5'-GGCATGGCCGCCGGTAGAAG-3'	
IL17RA # NM_014339.5	5'-TGCCCCTGTGGGTGTACTGGT-3'	151 bp
	5'-GCAGGCAGGCCATCGGTGTA-3'	
IL17RB # NM_018725.3	5'-TACCCCGAGAGCCGACCGTT-3'	182 bp
	5'-GGCATCTGCCCGGAGTACCCA-3'	
IL17RC # NM_153460.3	5'-GGCTTGGTTTCACGCGCAGC-3'	192 bp
	5'-CGGCCCTGCAAGAAGTCGGG-3'	
GAPDH	5'-GAAGGTGAAGGTCGGAGTCA-3'	199 bp
	5'-GACAAGCTTCCCGTTCTCAG-3'	
B-Actin	5'-CAGCCATGTACGTTGCTATCCAGG-3'	151 bp
	5'-AGGTCCAGACGCAGGATGGCATG-3'	

Table 1. Primer sequence and product length.

of supernatant from each well were collected into a 96 wells plate and incubated with 50 μl of freshly prepared Reaction Mixture for 30 minutes at room temperature. Optical density was then read at 490 nm. The percentage of cytotoxicity is calculated as followed: % = 100 × (exp value - control medium value)/(Triton × 100 treated cells value - control medium value).

Docetaxel induced cell death. MCF7, T47D, BT20 and IJG-1731 cells (1000 cells/well) were seeded in a 96 wells plate in adequate complete medium alone or treated with recombinant cytokines (1 or 10 ng/ml). After 48 h of culture, medium was changed to a FCS-free one supplemented with corresponding concentration of cytokines. When needed, the U0126 MEK inhibitor was added at 10 μM 24 h before adding the drug. After 24 h, culture medium is then further supplemented with Docetaxel at 5, 10, 20 or 40 μg/ml as indicated. Untreated cells (control medium) and Triton × 100 treated cells (100% cell death) were used as controls. Each condition was performed in duplicates. The cytotoxicity was determined using the Cytotoxicity Detection Kit (Roche, Meylan, France) according to the manufacturer's instructions as described above.

References

1. Iwakura, Y., Ishigame, H., Saijo, S. & Nakae, S. Functional specialization of interleukin-17 family members. *Immunity*. **34**, 149–62.
2. Gaffen, S. L. Structure and signalling in the IL-17 receptor family. *Nat Rev Immunol.* **9,** 556–67 (2009).
3. Cua, D. J. & Tato, C. M. Innate IL-17-producing cells: the sentinels of the immune system. *Nat Rev Immunol*. **10**, 479-89.
4. Roark, C. L., Simonian, P. L., Fontenot, A. P., Born, W. K. & O'Brien, R. L. gammadelta T cells: an important source of IL-17. *Curr Opin Immunol.* **20,** 353–7 (2008).
5. Onishi, R. M. & Gaffen, S. L. Interleukin-17 and its target genes: mechanisms of interleukin-17 function in disease. *Immunology*. **129,** 311–21 (2010).
6. Ouyang, W., Kolls, J. K. & Zheng, Y. The biological functions of T helper 17 cell effector cytokines in inflammation. *Immunity*. **28,** 454–467 (2008).
7. Yang, B. *et al.* The role of interleukin 17 in tumour proliferation, angiogenesis, and metastasis. *Mediators Inflamm*. 623759; doi: 10.1155 (2014).
8. Zhu, X. *et al.* IL-17 expression by breast-cancer-associated macrophages: IL-17 promotes invasiveness of breast cancer cell lines. *Breast Cancer Res*. **10** doi: 10.1186/bcr2195 (2008).
9. Chen, W. C. *et al.* Interleukin-17-producing cell infiltration in the breast cancer tumour microenvironment is a poor prognostic factor. *Histopathology*. **63,** 225–33 (2013).
10. Numasaki, M. *et al.* Interleukin-17 promotes angiogenesis and tumor growth. *Blood*. **101,** 2620–7 (2003).
11. Nam, J. S. *et al.* Transforming growth factor beta subverts the immune system into directly promoting tumor growth through interleukin-17. *Cancer Res*. **10,** 3915–23 (2008).
12. Cochaud, S. *et al.* IL-17A is produced by breast cancer TILs and promotes chemoresistance and proliferation through ERK1/2. *Sci Rep*. **3,** 3456; doi: 10.1038/srep03456 (2013).
13. Bastid, J., Bonnefoy, N., Eliaou, J. F. & Bensussan, A. Lymphocyte-derived interleukin-17A adds another brick in the wall of inflammation-induced breast carcinogenesis. *Oncoimmunology*. **3,** 28273; e28273 (2014).
14. Huang, C. K. *et al.* Autocrine/paracrine mechanism of interleukin-17B receptor promotes breast tumorigenesis through NF-kappaB-mediated antiapoptotic pathway. *Oncogene*. **33,** 2968–77 (2014).
15. Furuta, S. *et al.* IL-25 causes apoptosis of IL-25R-expressing breast cancer cells without toxicity to nonmalignant cells. *Sci Transl Med*. **3,** 78ra3116; doi: 10.1126/scitranslmed (2011).
16. King, A. J. *et al.* The protein kinase Pak3 positively regulates Raf-1 activity through phosphorylation of serine 338. *Nature*. **396,** 180–3 (1998).
17. Mason, C. S. *et al.* Serine and tyrosine phosphorylations cooperate in Raf-1, but not B-Raf activation. *EMBO*. **18,** 2137–48 (1999).

18. Ghayad, S. E. & Cohen, P. A. Inhibitors of the PI3K/Akt/mTOR pathway: new hope for breast cancer patients. *Recent Pat Anticancer Drug Discov*. **1,** 29–57 (2010).
19. Pullen, N. & Thomas, G. The modular phosphorylation and activation of p70s6k. *FEBS Lett.* **410,** 78–82 (1997).
20. Weng, Q. P. *et al.* Regulation of the p70 S6 kinase by phosphorylation in vivo. Analysis using site-specific anti-phosphopeptide antibodies. *J Biol Chem*. **273,** 16621–9 (1998).
21. Porter, D. C. & Keyomarsi, K. Novel splice variants of cyclin E with altered substrate specificity. *Nucleic Acids Res.* **28,** E101 (2000).
22. Wingate, H. *et al.* The tumor-specific hyperactive forms of cyclin E are resistant to inhibition by p21 and p27. *J Biol Chem.* **280,** 15148–57 (2005).
23. Wang, X. D., Rosales, J. L., Magliocco, A., Gnanakumar, R. & Lee, K. Y. Cyclin E in breast tumors is cleaved into its low molecular weight forms by calpain. *Oncogene*. **22,** 769–74 (2003).
24. Chung, A. S. *et al.* An interleukin-17-mediated paracrine network promotes tumor resistance to anti-angiogenic therapy. *Nat Med Sep*. **19,** 1114–23 (2013).
25. Younesi, V. & Nejatollahi, F. Induction of anti-proliferative and apoptotic effects by anti-IL-25 receptor single chain antibodies in breast cancer cells. *Int Immunopharmacol.* **23,** 624–32 (2015).
26. Duong, M. T. *et al.* LMW-E/CDK2 deregulates acinar morphogenesis, induces tumorigenesis, and associates with the activated b-Raf-ERK1/2-mTOR pathway in breast cancer patients. *PLoS Genet*. **8,** e1002538; doi: 10.1371/journal.pgen (2012).
27. Weber, C. K., Slupsky, J. R., Kalmes, H. A. & Rapp, U. R. Active Ras induces heterodimerization of cRaf and BRaf. *Cancer Res.* **61,** 3595–8 (2001).
28. Rushworth, L. K., Hindley, A. D., O'Neill, E. & Kolch, W. Regulation and role of Raf-1/B-Raf heterodimerization. *Mol Cell Biol.* **26**, 2262–72.
29. Benatar, T. *et al.* IL-17E, a proinflammatory cytokine, has antitumor efficacy against several tumor types in vivo. *Cancer Immunol Immunother.* **59,** 805–17 (2010).
30. Chin, Y. *et al.* Phenotypic analysis of tumor-infiltrating lymphocytes from human breast cancer. *Anticancer Res.* **12,** 1463–6 (1992).
31. Schmidt, M. *et al.* The humoral immune system has a key prognostic impact in node-negative breast cancer. *Cancer Res.* **68,** 5405–13 (2008).
32. Jung, J. S. *et al.* Association of IL-17RB gene polymorphism with asthma. *Chest*. **135,** 1173–80 (2009).
33. Hagn, M. *et al.* Human B cells secrete granzyme B when recognizing viral antigens in the context of the acute phase cytokine IL-21. *J Immunol.* **183,** 1838–45 (2009).
34. Wiedow, O., Schroder, J. M., Gregory, H., Young, J. A. & Christophers, E. Elafin: an elastase-specific inhibitor of human skin. Purification, characterization, and complete amino acid sequence. J *Biol Chem.* **265,** 14791–5 (1990).
35. Zhang, M., Zou, Z., Maass, N. & Sager, R. Differential expression of elafin in human normal mammary epithelial cells and carcinomas is regulated at the transcriptional level. *Cancer Res.* **55,** 2537–41 (1995).
36. Sarra, M. *et al.* IL-25 prevents and cures fulminant hepatitis in mice through a myeloid-derived suppressor cell-dependent mechanism. *Hepatology*. **58**, 1436–50.
37. Dolgachev, V., Petersen, B. C., Budelsky, A. L., Berlin, A. A. & Lukacs, N. W. Pulmonary IL-17E (IL-25) production and IL-17RB+ myeloid cell-derived Th2 cytokine production are dependent upon stem cell factor-induced responses during chronic allergic pulmonary disease. *J Immunol.* **183,** 5705–15 (2009).
38. Miyagaki, T. *et al.* IL-22, but not IL-17, dominant environment in cutaneous T-cell lymphoma. *Clin Cancer Res.* 17, 7529–38.
39. Mayer, C. *et al.* DNA repair capacity after gamma-irradiation and expression profiles of DNA repair genes in resting and proliferating human peripheral blood lymphocytes. *DNA Repair*. **1,** 237–50 (2002).

Author Contributions

J.G. and A.B. designed and supervised the study and wrote the manuscript text. S.M., S.C. and J.G. performed experiments and prepare the figures. Y.M., F.A. and J.B. contributed to the design, interpretation of experiments and to the editing of the manuscript. C.G., G.A., N.B., J.-F. E. and E.L. contributed to the interpretation of experiments and to the editing of the manuscript.

Additional Information

Supplementary information accompanies this paper at http://www.nature.com/srep

Competing financial interests: G.A., N.B., J.-F.E. and A.B are cofounders and shareholders of OREGA Biotech. J.B. is employee of OREGA Biotech and S.M., S.C., Y.M., C.G., F.A., E.L. and J.G. declare no conflict of interest.

How to cite this article: Mombelli, S. *et al.* IL-17A and its homologs IL-25/IL-17E recruit the c-RAF/S6 kinase pathway and the generation of pro-oncogenic LMW-E in breast cancer cells. *Sci. Rep.* **5**, 11874; doi: 10.1038/srep11874 (2015).

Research Paper

IL-17E synergizes with EGF and confers *in vitro* resistance to EGFR-targeted therapies in TNBC cells

Yacine Merrouche[1,2,*], Joseph Fabre[1,2,*], Herve Cure[3,4], Christian Garbar[1,2], Camille Fuselier[1,2], Jeremy Bastid[5], Frank Antonicelli[2], Reem Al-Daccak[6,7,#], Armand Bensussan[5,6,7,#], Jerome Giustiniani[1,2,#]

[1]Institut Jean Godinot, Unicancer, F-51726 Reims, France

[2]Université Reims-Champagne-Ardenne, DERM-I-C, EA7319, 51095 Reims, France

[3]CHU-Grenoble Alpes, CS 10217, 38043 La Tronche, France

[4]Institut National de la Santé et de la Recherche Médicale (INSERM) U823, Centre de Recherche (CRI), Institut Albert Bonniot, 38043, France

[5]OREGA Biotech, F-69130 Ecully, France

[6]Institut National de la Santé et de la Recherche Médicale (INSERM) UMR-S 976, Hôpital Saint Louis, 75010 Paris, France

[7]Université Paris Diderot, Sorbonne Paris Cité, Laboratoire Immunologie Dermatologie and Oncologie, UMR-S 976, F-75475, Paris, France

[*]Co-first authors, these authors contributed equally to this work

[#]These authors have contributed equally and share senior authorship

Correspondence to: Jerome Giustiniani, **email:** jerome.giustiniani@reims.unicancer.fr
Reem Al-Daccak, **email:** reem.al-daccak@inserm.fr

Keywords: *IL-17E, breast cancer, EGFR, resistance, TNBC*

Received: *May 27, 2016* ***Accepted:*** *July 13, 2016* ***Published:*** *July 23, 2016*

ABSTRACT

Estrogen receptor-, progesterone receptor- and HER2-negative breast cancers, also known as triple-negative breast cancers (TNBCs), have poor prognoses and are refractory to current therapeutic agents, including epidermal growth factor receptor (EGFR) inhibitors. Resistance to anti-EGFR therapeutic agents is often associated with sustained kinase phosphorylation, which promotes EGFR activation and translocation to the nucleus and prevents these agents from acting on their targets. The mechanisms underlying this resistance have not been fully elucidated. In addition, the IL-17E receptor is overexpressed in TNBC tumors and is associated with a poor prognosis. We have previously reported that IL-17E promotes TNBC resistance to anti-mitotic therapies. Here, we investigated whether IL-17E promotes TNBC resistance to anti-EGFR therapeutic agents by exploring the link between the IL-17E/IL-17E receptor axis and EGF signaling. We found that IL-17E, similarly to EGF, activates the EGFR in TNBC cells that are resistant to EGFR inhibitors. It also activates the PYK-2, Src and STAT3 kinases, which are essential for EGFR activation and nuclear translocation. IL-17E binds its specific receptor, IL-17RA/IL17RB, on these TNBC cells and synergizes with the EGF signaling pathway, thereby inducing Src-dependent EGFR transactivation and pSTAT3 and pEGFR translocation to the nucleus. Collectively, our data indicate that the IL-17E/IL-17E receptor axis may underlie TNBC resistance to EGFR inhibitors and suggest that inhibiting IL-17E or its receptor in combination with EGFR inhibitor administration may improve TNBC management.

INTRODUCTION

Triple-negative breast cancer (TNBC) is a heterogeneous disease comprising several biologically distinct subtypes, each of which is associated with a distinct gene ontology and drug sensitivity [1, 2]. Currently, TNBC is managed mainly with chemotherapy, because no targeted therapies have been approved for the treatment of this disease. Nevertheless, nearly 50% of TNBC tumors overexpress the epidermal growth

factor receptor (EGFR) [3, 4], thus suggesting that the EGFR may serve as a molecular marker of these tumors and that the EGFR pathway may have promise as a therapeutic target in TNBC management [4]. Agents such as monoclonal antibodies that bind the extracellular ligand-binding domain of the EGFR (e.g., Cetuximab) or small molecules that inhibit the intracellular tyrosine kinase domain of the EGFR (e.g., Gefitinib/Iressa) have shown only limited effectiveness against TNBC because resistance frequently and rapidly develops; thus, metastatic TNBC often has a poor prognosis. Only 10–20% of TNBC patients show marked clinical improvement in response to therapy [5, 6]. Thus, improving the efficacy of anti-EGFR therapy in TNBC is needed.

EGFR is a plasma membrane-bound receptor tyrosine kinase that initiates growth and survival signals but can also localize to and function from the nucleus [7–9]. Thus, TNBCs rely on two distinct types of EGFR signaling to sustain their oncogenic phenotype" classical membrane-bound EGFR signaling and nuclear EGFR (nEGFR) signaling. The actions of both types of signaling promote TNBC resistance to anti-EGFR therapeutic agents [7, 10]. One mechanism underlying these actions is crosstalk between the EGFR and other signaling proteins, such as c-met and c-Src [11]. The paracrine pathways that are active within the TNBC microenvironment and facilitate the crosstalk promoting EGFR resistance have not been fully elucidated.

IL-17E is a member of the pro-inflammatory IL-17 cytokine family, which binds the IL-17RA/IL17RB complex. It is highly expressed in certain organs, including the testis and pancreas, and is not highly expressed in other organs, such as normal breast [12, 13]. Normal mammary epithelial cells (MECs) transiently produce IL-17E during mammary gland development, and IL-17E acts in conjunction with other MEC-secreted factors in preventing malignant cell growth [14]. Consistently with these findings, our recent report has demonstrated that IL-17E is scarcely detectable in normal adult breast tissues but is expressed in some tumor tissues, including TNBC tissues, as a component of their microenvironment [15]. IL-17E causes apoptosis in breast cancer cells expressing its receptor [14], and its secretion by tumor-associated fibroblasts suppresses the growth of human mammary tumor MDA-MD-231 cells serving as a metastasis control checkpoint [16]. Paradoxically, the IL-17E receptor subunits IL17-RA and RB are overexpressed in TNBC tumors [15], and IL17-RB expression is associated with a poor prognosis [17]. Furthermore, we have shown that, similarly to IL-17A, IL-17E does not induce cell death by binding to its receptor on TNBC cells but instead activates oncogenic pathways, such as c-raf and p70S6 pathways, thus resulting in Docetaxel resistance [15]. The signaling cascades downstream of the IL-17E receptor have never been explored with respect to TNBC resistance to anti-EGFR therapeutic agents.

This study builds on our previous report [15] and explores the crosstalk between IL-17E and EGF signaling in the context of anti-EGFR-resistant TNBC tumors and the eventual contribution of this crosstalk to therapy resistance. We found that IL-17E and EGF trigger interconnected molecular signaling pathways in TNBC cells through their specific receptors, thus suggesting that EGFR/IL-17RB crosstalk promotes TNBC resistance to anti-EGFR therapeutic agents. Hence, our findings provide the first evidence of the potential of the IL-17E/IL-17RB axis as a therapeutic target in the management of TNBC tumors and eventually other EGFR and IL-17RA/RB co-expressing tumors.

RESULTS

IL-17E phosphorylates the EGFR in Iressa-resistant TNBC cell lines and potentiates their resistance

TNBC *ex-vivo*-derived IJG-1731 cells and BT20 and MDA-MB468 cells are established TNBC tumors models that exhibit pronounced resistance to a specific inhibitor of EGFR phosphorylation, Iressa, even when exposed to high concentrations (1 μM) of this inhibitor for 48 hours (Figure 1A upper panel). IJG-1731, BT-20 and MDA-MB468 cells exhibit different levels of EGFR expression and distinct Y845 EGFR and Y1086 EGFR phosphorylation patterns (Y845 EGFR is a substrate for Src kinase, and Y1086 EGFR is directly phosphorylated by EGFR) [18, 19] after treatment with EGF (10 ng/ml), thus reflecting the heterogeneity of TNBC tumors (Figure 1A lower panel). Similarly to EGF treatment, IL-17E treatment (10 ng/ml) induced the phosphorylation of both Y845 EGFR and Y1086 EGFR (Figure 1A lower panel). The intensity of IL-17E-induced EGFR phosphorylation was comparable to that of EGF-induced EGFR phosphorylation and was consistent with the basal levels of EGFR expression in the cell lines. Similarly to Iressa, IL-17E (10 ng/ml) did not induce cell death, either alone or in combination with Iressa (1 μM), in any of the cell lines; instead, it potentiated resistance to EGFR inhibitors (Figure 1B). Together, these results suggest that EGFR and IL-17E signaling may interact and together sustain TNBC resistance to EGFR inhibitors.

IL-17E promotes EGFR phosphorylation in TNBC cell lines

Previous studies have shown that STAT3, PYK-2, and Src kinase phosphorylation is essential for EGFR phosphorylation [20]. Consequently, we examined the phosphorylation statuses of these essential kinases in the three cell lines treated with IL-17E. Similarly to EGF, IL-17E induced considerable STAT3-α and β phosphorylation at Y705 in IJG-1731 and BT20 cells (Figure 2A and 2B).

The phosphorylation levels of both STAT3-α and β were in accordance with the phosphorylation levels of Y1086 and Y845 EGFR in these cell lines (Figure 1A). IL-17E-induced STAT3-α and β phosphorylation was less evident in MDA-MB468 cells (Figure 2C), probably because of elevated STAT3-α phosphorylation, but was consistent with IL-17E-induced EGFR phosphorylation levels (Figure 1A). Treatment with IL-17E also induced

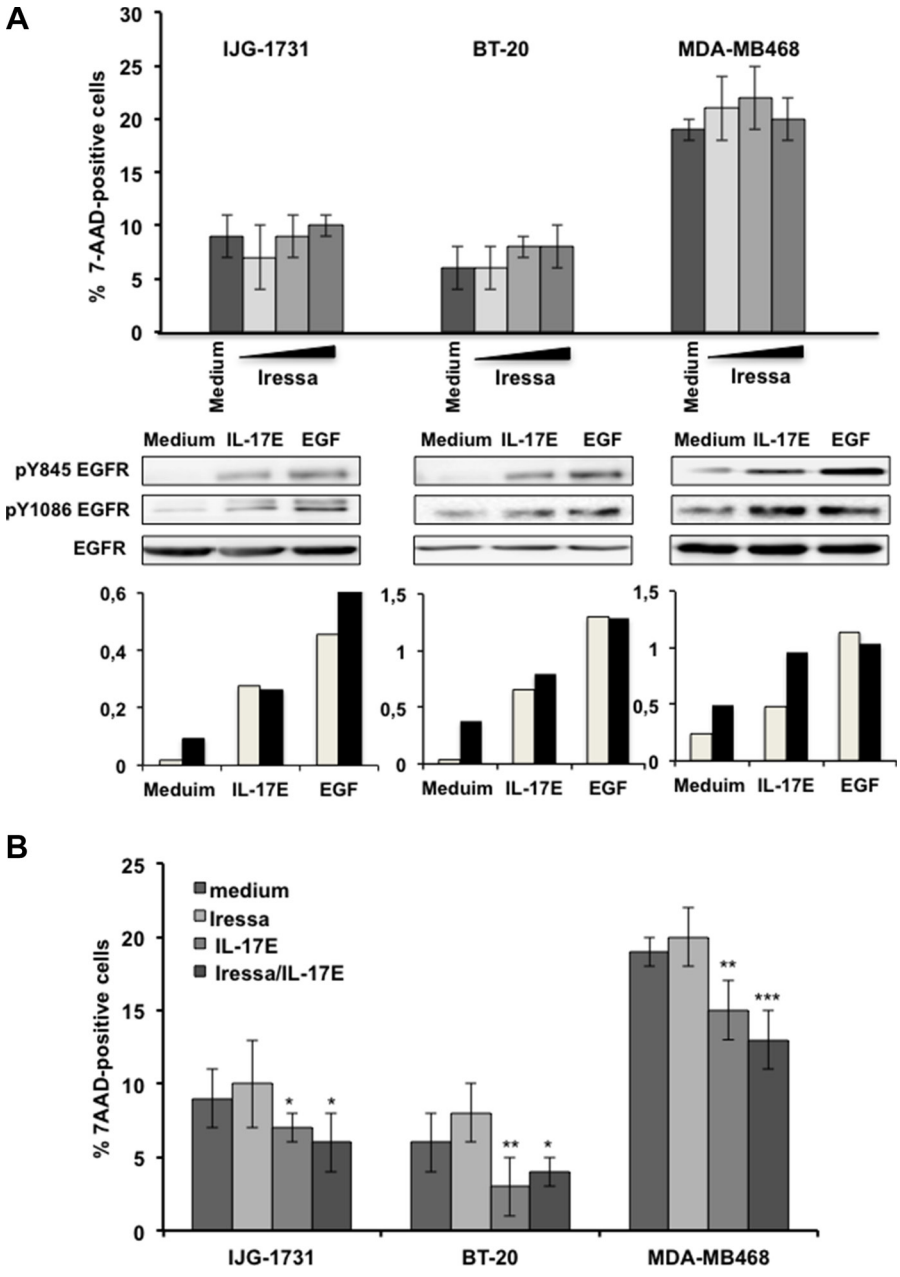

Figure 1: IL-17E phosphorylates the EGFR in Iressa-resistant TNBC cell lines. (**A**) In the upper panel, IJG-1731, BT20, and MDA-MB468 TNBC cells were cultured alone or in the presence of increasing concentrations of the EGFR inhibitor Iressa (0.25 (■), 0.5 (■), and 1 (■) μM) for 48 hours, and cell death was evaluated by determining the percentage of 7AAD-positive cells and by flow cytometry analysis. The results are presented as the mean ± SD of three independent experiments performed in triplicate. In the middle panel, TNBC cells were cultured alone or in the presence of IL-17E (10 ng/ml) or EGF (10 ng/ml), and the phosphorylation of EGFR at residues Y845 and Y1086 was assessed by western blotting. Membranes were re-blotted with anti-EGF as a loading control. Data are representative of 3 independent experiments. In the lower panel, densitometric quantification of EGFR phosphorylation, as shown in the representative blots, is expressed as the ratios of pY845 EGFR to EGFR (■) and pY1086 EGFR to EGFR (■). (**B**) IJG-1731, BT20, and MDA-MB468 TNBC cells were cultured alone or in the presence of Iressa (1 μM), IL-17E (10 ng/ml), or a combination of both for 48 hours, and the percentage of 7AAD-positive cells was determined by flow cytometry. The results are presented as the mean ± SD of three independent experiments performed in triplicate. Student *t*-test was used (*$P < 0.05$; **$P < 0.01$; ***$P < 0.001$) compared with medium alone.

PYK2 and Src kinase phosphorylation at residues Y402 and Y416, respectively, in the three cell lines at levels comparable to those induced by EGF (Figure 2).

Thus, IL-17E and EGF similarly phosphorylate the essential kinases implicated in EGFR phosphorylation; hence, IL-17E may contribute to TNBC resistance to EGFR inhibitors.

IL-17E signaling interacts with EGF signaling

To substantiate the contributions of IL-17E to TNBC resistance to EGFR inhibitors, we examined the interactions between IL-17E- and EGF-induced signaling. Sustained EGFR activity requires both Src and EGFR activation [16]. Therefore, we first determined the involvement of Src kinase in IL-17E-induced EGFR phosphorylation. TNBC tumor cell lines were pre-treated with the Src kinase-specific inhibitor AZM475271 and then stimulated with either IL-17E or EGF. Treatment with AZM475271 inhibited IL-17E- and EGF-induced Src phosphorylation but also abolished Y1086 EGFR phosphorylation in IJG-1731 and BT20 cells and, to a lesser extent, in MDA-MB468 cells (Figure 3A). Thus, similarly to EGF-induced EGFR phosphorylation, IL-17E-induced EGFR phosphorylation is also Src-dependent. This result suggests that IL-17E and EGF can transactivate the EGFR in TNBC tumors.

We then examined whether IL-17E-induced EGFR phosphorylation requires EGFR activity. TNBC cell lines were treated with Iressa, the specific inhibitor of EGFR phosphorylation, and then stimulated with IL-17E, EGF or a combination of both, and EGFR phosphorylation status was analyzed by western blotting. Treatment with Iressa elicited similar decreases in IL-17E- and EGF-induced Y1086-EGFR phosphorylation in the three cell lines (Figure 3B) and markedly decreased EGFR tyrosine phosphorylation induced by the combination of IL-17E and EGF in BT20 and MDA-MB468 cells and, to a lesser extent, in IJG-1731 cells (Figure 3B). Altogether, these data indicate that, similarly to EGF-induced phosphorylation, IL-17E-induced EGFR phosphorylation requires both Src and EGFR kinase activity; thus, EGF and IL-17E are interconnected and may synergistically activate and sustain EGFR phosphorylation in TNBC.

IL-17E synergizes with EGF through its specific receptor IL17RA/IL17RB

Src pathway activation is essential for optimal EGFR activity. Therefore, to explore the synergistic effects of IL-17E and EGF on EGFR activation, we examined the phosphorylation status of Src in TNBC cells stimulated with increasing concentrations of EGF in the presence or absence of IL-17E. Stimulation of MDA-MB468 cells with IL-17E or EGF at suboptimal concentrations of 1 ng/ml and 0.1–1 ng/ml, respectively, did not induce significant Src phosphorylation at Y416 (Figure 4). However, stimulation with 1 ng/ml IL-17E and suboptimal concentrations of EGF (0.1 and 1 ng/ml) induced a level of Y416Src phosphorylation similar to that induced by 10 mg/ml EGF alone (Figure 4). These results indicate that IL-17E and EGF synergistically activate Src kinase. The presence of the anti-IL-17E receptor (IL-17RA/RB)-blocking antibody, but not its isotype control, substantially decreased Src phosphorylation at Y416 by 0.1 and 1 ng/ml EGF in the presence of IL-17E (Figure 4). Thus, the synergistic effects of IL-17E are mediated by its recruitment to its specific receptor, IL-17RA/RB.

IL-17E facilitates pEGFR and pSTAT3 translocation to the nucleus

The translocation of phosphorylated EGFR to the nucleus is an integral component of the cascade that results in tumor resistance to EGFR therapeutic agents. Therefore, to determine the contribution of IL-17E to TNBC therapy resistance, we investigated the effect of IL-17E on EGFR nuclear translocation. Using immunofluorescence microscopy, we examined EGFR localization in TNBC cell lines stimulated with EGF, IL-17E, or both. In agreement with results from previous reports [21], EGF induced strong EGFR translocation from the membrane to the nucleus in MDA-MB468 TNBC cells (Figure 5A). Stimulation with IL-17E also induced EGFR translocation to the nucleus, but to a lesser extent than stimulation with EGF (Figure 5A upper panel). Importantly, the combination of IL-17E and EGF induced markedly increased EGFR translocation compared with that induced by each cytokine alone (Figure 5A upper panel).

To support these data, we subsequently isolated the cytoplasmic and nuclear fractions of IL-17E-, EGF- or IL-17E+EGF-stimulated MDA-MB468 cells and examined the levels of EGFR and its phosphorylated counterpart pY1086EGFR. Compared with EGF alone, IL-17E induced EGFR phosphorylation but did not induce significant EGFR nuclear translocation despite its capacity to induce non-phosphorylated EGFR nuclear translocation. Both forms of EGFR were translocated to the nucleus when MDA-MB468 cells were stimulated with the combination of IL-17E and EGF (Figure 5A lower panel and Supplementary Figure S1).

STAT3 binds the EGFR through a motif including pY1086 [22]. In addition, the correlation between pEGFR and pSTAT3α/β is well established and has been implicated in tumor resistance [23]. Therefore, we also examined STAT3 nuclear translocation and assessed the statuses of pSTAT3α and β, as well as those of their non-phosphorylated counterparts. IL-17E and EGF alone induced STAT3α and β translocation; however, the combination of the two agents triggered more significant pSTAT3α and β nuclear translocation than either agent alone.

To confirm these findings, we performed the above experiments with the BT20 cell line and obtained similar results. However, less EGFR and pSTAT3α and β translocation was induced by IL-17E and EGF in BT20 cells than in MDA-MB468 cells (Figure 5B and Supplementary Figure S2). This result is probably due to the inherent heterogeneity of TNBC tumor responses to various stimuli.

Together, these data indicate that the presence of IL-17E within the TNBC tumor microenvironment probably promotes and sustains EGFR activation and translocation and ultimately results in tumor resistance.

DISCUSSION

Strategies for efficiently combating TNBC remain to be developed. This exploratory study assessed the IL-17E/IL-17RB pathway as a potential new target for the development of more efficient therapies for TNBC. Collectively, our data demonstrate that the IL-17E/IL-17RB pathway contributes to TNBC resistance to EGFR therapeutics through a loop that amplifies and sustains the phosphorylation of the main EGFR downstream kinases implicated in tumor resistance. Thus, blocking

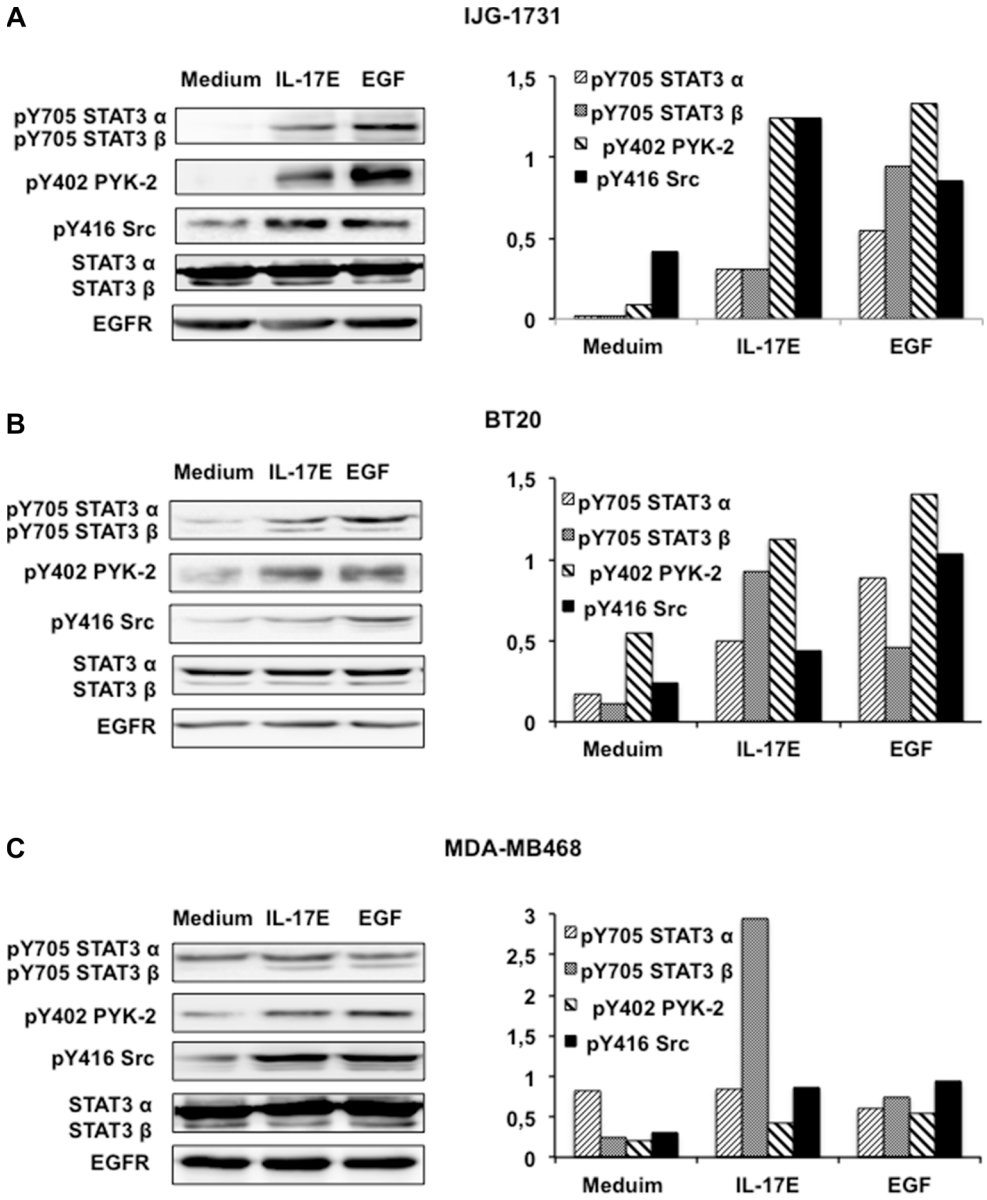

Figure 2: IL-17E phosphorylates the kinases essential for EGFR activation. IJG-1731 (**A**), BT20 (**B**), and MDA-MB468 (**C**) cells were cultured alone or in the presence of IL-17E (10 ng/ml) or EGF (10 ng/ml), and then STAT3 phosphorylation at Y705, PYK-2 phosphorylation at Y402 and Src phosphorylation at Y416 were assessed by western blotting (left panel). Membranes were re-blotted with anti-EGF or anti-STAT3α/β antibodies, which served as loading controls. Data are representative of 3 independent experiments. In the right panel, densitometric quantification of STAT3a/b, PYK-2 and Src phosphorylation, as shown in the representative blots, is expressed as the ratios of pY705 STAT3a and b to their respective un-phosphorylated forms, pY402 PYK-2, pY416 Src and EGFR, as indicated.

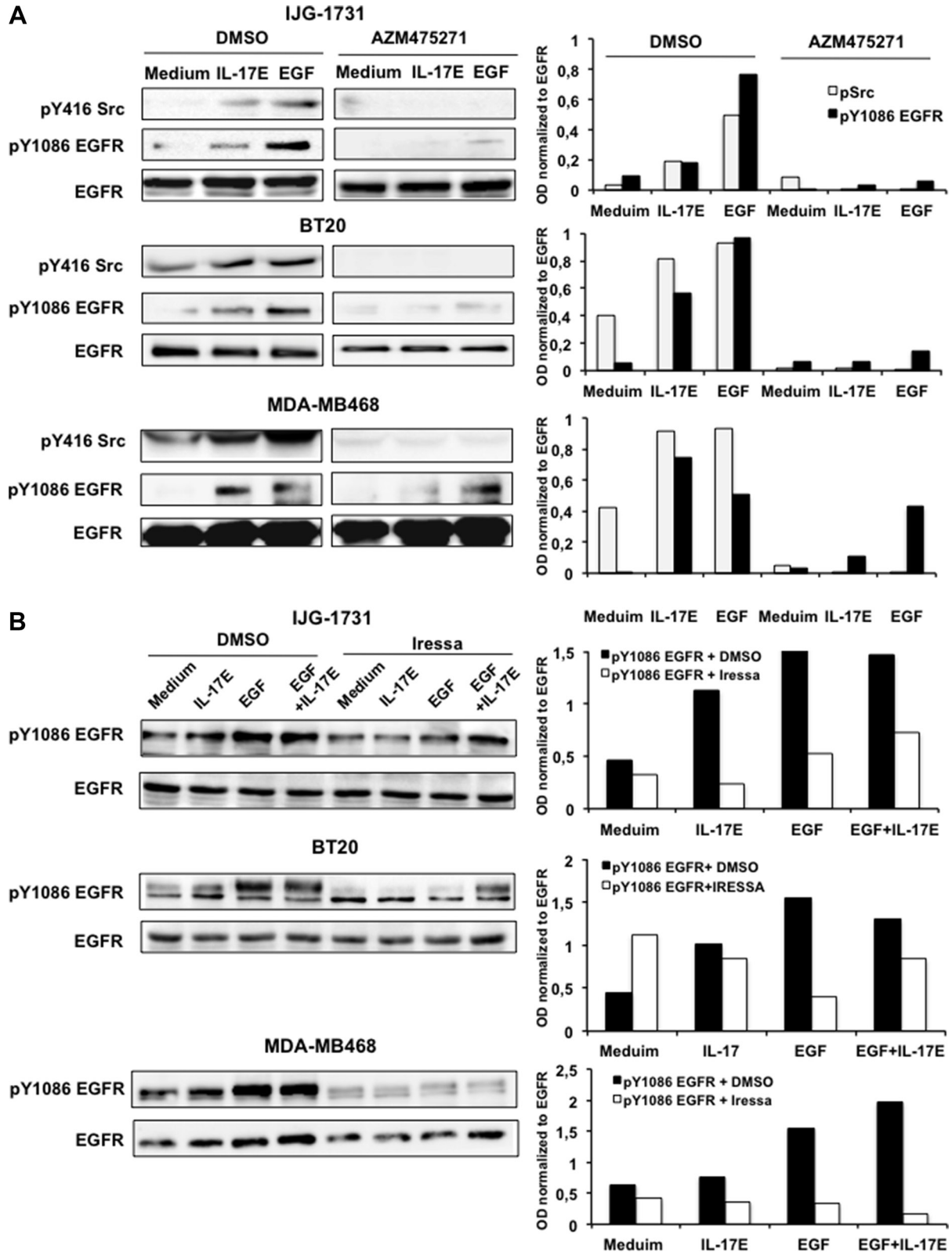

Figure 3: IL-17E-induced EGFR phosphorylation is dependent on Src and EGFR kinase activity. IJG-1731, BT20, and MDA-MB468 cells were treated with the Src specific inhibitor AZM475271 (10 μM) (**A**), Iressa (0.25 μM) (**B**), or control DMSO and then stimulated with IL-17E (10 ng/ml), EGF (10 ng/ml) or with medium alone. EGFR and Src phosphorylation was then assessed by western blotting (left panel). Loading controls were determined by re-blotting the membranes with an anti-EGFR antibody. Data are representative of at least 2 independent experiments. In the right panel, densitometric quantification of Y416 Src and Y1086 EGFR, as shown in the representative blots, is expressed as the ratios of pY416 Src to EGFR and pY1086 EGFR to EGFR, as indicated.

IL-17E or its receptor in conjunction with EGFR inhibitor administration may represent a novel strategy for treating these tumors.

We found that, consistently with the results of studies of hepatocyte growth factor (HGF) in breast cancer [11], Src and PYK2 activation also occurred downstream of the IL-17E receptor in TNBC cells. Inhibition of EGFR activation downstream of the IL-17E via administration of the Src-specific inhibitor AZM475271 supports this idea. IL-17E-induced Y1086EGFR phosphorylation in TNBC cells is dependent on EGFR kinase activity, as evidenced by the specific inhibition of this phosphorylation via administration of the EGFR kinase inhibitor Iressa. However, EGFR phosphorylation at Y1086 may also occur in the absence of EGFR kinase activity through pSrc/PYK2 crosstalk [21, 24]. The results obtained with IJG-1731 cells in this study support this idea and highlight the importance of pSrc/PYK2 crosstalk as a signaling checkpoint and molecular memory mechanism underlying tumor metastasis signaling [24].

The synergy between EGF and IL-17E is indicative of the pro-oncogenic role played by the IL-17 protein family in TNBC tumors. The presence of IL-17E in the TNBC tumor microenvironment may pre-activate the EGFR via Src/PYK2 crosstalk, thus resulting in enhanced sensitivity to EGF and potentially other EGFR ligands. Under these conditions, very low concentrations of EGFR ligands and weak expression (or accessibility) of this receptor are sufficient to activate tumor cells. Conversely, the above-mentioned increases in IL-17E-induced EGFR phosphorylation and nuclear translocation in the presence of EGF indicate that EGF also probably enhances the capacity of IL-17E to activate the EGFR and may serve as additional proof of the synergy between EGF and IL-17E with respect to sustaining EGFR activation in TNBC cells.

The EGFR is an important mediator of tumor development and progression, whereas IL-17E affects cell cycle progression, both in TNBC cells and in other breast cancer cells, such as human epidermal growth factor receptor 2 (HER2)-positive tumor cells [15]. Whether the effects of IL-17E on the cell cycle are dependent on the transactivation of EGFR or that of its family members (e.g., HER2) has not been determined. Nevertheless, the results described herein, together with those of our previous report, show the importance of IL-17A in pro-oncogenic signaling in breast cancer [25]

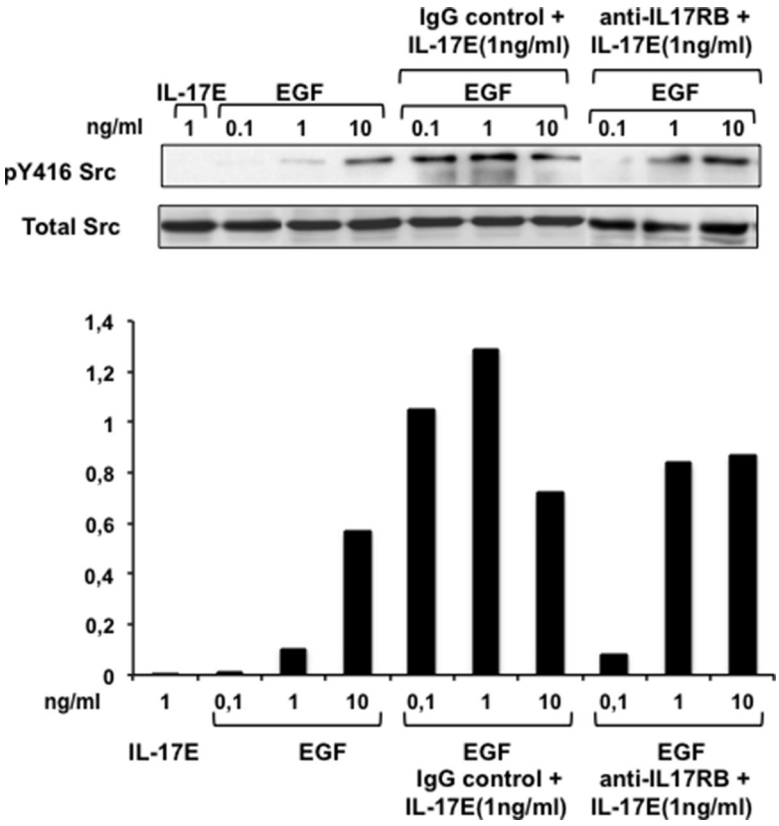

Figure 4: IL-17E synergizes with EGF in phosphorylating Src kinase. MDA-MB468 cells were left untreated or treated with anti-IL-17RB mAb (10 μg/ml) or its isotype IgG control and then stimulated with IL-17E (1 ng/ml), EGF (0.1–10 ng/ml), or a combination of IL-17E (1 ng/ml) and various concentrations of EGF (0.1–10 ng/ml). Src phosphorylation (p416Src) was then assessed by western blotting using specific anti-pSrc antibodies. Re-blotting with anti-Src antibody was performed to determine equal loading. Data are representative of 2 independent experiments. In the lower panel, densitometric quantification of Y416 Src, as shown in the representative blots, is expressed as the ratio of pY416 Src to total Src.

and are indicative of the key roles played by IL-17 family members within the TNBC microenvironment. They also reinforce the idea that inflammation is a critical component of tumor progression [26, 27].

Our results demonstrate that IL-17E, in addition to its involvement in tumor progression [15], contributes to EGFR resistance. Our results provide the first evidence of IL-17E's involvement in EGFR remodeling and subcellular localization. Physiological EGF leads to EGFR degradation through receptor-mediated endocytosis and endosomal trafficking to lysosomes [28]. Therefore, IL-17E may alter EGFR degradation in malignant cells. Importantly, the nuclear fraction of EGFR contributes to Cetuximab resistance [10] and Iressa resistance [29].

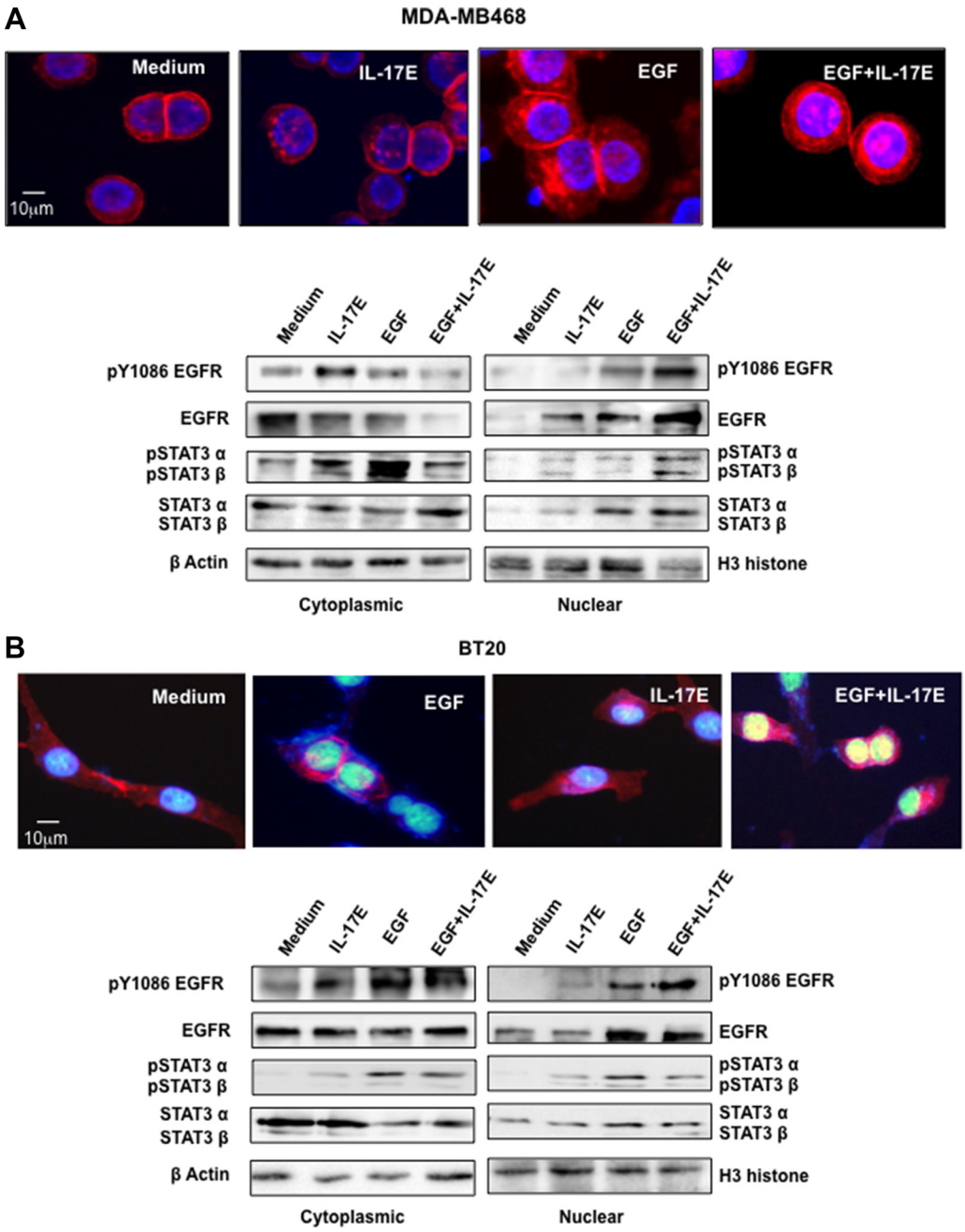

Figure 5: IL-17E facilitates pEGFR and pSTAT3 co-translocation to the nucleus. MDA-MB468 (**A**) or BT20 (**B**) cells were stimulated with IL-17E (10 ng/ml), EGF (10 ng/ml) or a combination of both. In the upper panel of (A) and (B), EGFR localization, as assessed by immunostaining with anti-EGFR antibodies (red). Nuclei were visualized with DAPI (blue). In the lower panel of (A) and (B), translocation of EGFR, STAT3α/β, and their phosphorylated counterparts from the cytoplasm to the nucleus, as assessed by western blotting using specific antibodies. Anti-β actin and H3 histone antibodies were used as loading controls for the cytoplasmic and nuclear fractions, respectively. Data are representative of 2 independent experiments. Densitometric quantifications are presented in Supplementary Figure 1 (MDA-MB468) and Supplementary Figure 2 (BT20).

IL-17E-mediated EGFR nuclear translocation, which is accompanied by pSTAT3 translocation, maintains EGFR phosphorylation and confers resistance to anti-EGFR therapeutic agents. Our data suggest that IL-17E-induced EGFR translocation facilitates the transport of pEGFR-associated pSTAT3 to the nucleus [22, 30]. In the nucleus, STAT3 activates the transcription of genes associated with tumor metastasis, as well as the transcription of anti-apoptotic and angiogenic genes, similarly to its function in various types of cancer [23, 31–33].

IL-17E-induced signaling is mediated through its specific heterodimer receptor IL17RA/IL17RB. Thus, IL-17E-induced resistance to anti-EGFR treatments conferred by Src activation and STAT3 and EGFR translocation is at least partially under the control of the IL-17E receptor, IL17RA/IL17RB, thus raising the question of whether it is involved in the treatment resistance associated with IL-17A and IL-17B, which share common co-receptors with IL-17E (IL-17RA and IL-17RB, respectively) [34]. Consistently with this idea, previous studies have shown that the IL-17RB/IL-17B signaling pathway promotes tumorigenicity and etoposide resistance in breast cancer cells through NFκB activation and Bcl-2 up-regulation [16]. Further investigation of these signaling mechanisms may improve the specificity and efficacy of biotherapies targeting these receptors.

Our findings advance the current understanding of anti-EGFR immunotherapy failures in breast cancer. IL-17E-induced signaling may also be interconnected with signaling mediated by other EGF receptor family members, such as HER2 and HER3, and contribute to their resistance to specific drugs. IL-17E is abundant in most metastatic tumors found in the brain [35, 36], liver [37] and lung [38]. However, whether IL-17E is pro-oncogenic or anti-oncogenic remains under debate.

Studies in animal models of colon cancer have demonstrated that IL-17E plays an inhibitory role with respect to the chronic inflammation associated with this disease [39]. Studies of hepatocellular carcinoma have shown that IL-17E activates the NFκB and Jak/STAT3 signaling pathways in cancer stem cells, thus resulting in tumor growth and progression and suggesting that IL-17E/IL-17RB may be a therapeutic target in the treatment of this disease [40]. In our TNBC model, direct IL-17E signaling via IL-17RB activated various signaling pathways associated with IL-17-induced tumor proliferation and progression [41, 42] and did not induce tumor cell apoptosis [15]. In contrast, Furata and colleagues have shown that IL-17E induces apoptosis in breast cancer cells [14], and Benatar and colleagues have reported that it exerts antitumor effects on xenografted tumors [43]. IL-17E is not the only member of IL-17 family that exerts contrasting effects in the setting of tumor progression. Direct or indirect Stat3 pathway activation by IL-17A promotes the proliferation and progression of various tumors, whereas IL-17A-mediated adaptive and innate immune responses exert anti-tumor effects [41, 42, 44–47]. The mechanisms underlying the contrasting roles played by members of the IL-17 family have not been fully elucidated. However, it is likely that IL-17 family members promote or suppress tumorigenesis in specific cell types and at specific stages of disease in response to specific cytokines present at the tumor site. The combination IL-17 signaling-mediated effects on tumor cell behavior at a specific stage of differentiation and various environmental factors probably determines whether tumor proliferation or apoptosis ultimately occurs.

In summary, our study provides the first evidence suggesting the possible role of IL-17E in tumor resistance to anti-EGFR therapeutic agents. Blocking either IL-17E or its receptor in combination with EGFR inhibitor administration might reduce the likelihood of tumor resistance and enhance therapeutic efficacy.

MATERIALS AND METHODS

Cell culture

BT20 and MDA-MB468 triple-negative (HER2-, ER-, PR-) cells were obtained from the American Type Culture Collection (ATCC N°HTB19 and ATCC N°HTB132, respectively). The LumB and Her2-, ER-, PR-negative IJG-1731 cell line was previously established in our laboratory, as described elsewhere [15], and was used as primary tumor cells model. Briefly, IJG-1731 were liberated from a patient LumB tumor biopsy characterized as an ypT2N1aM tumor, grown in culture media for several weeks for stabilization, and phenotyped as negative for estrogen, progesterone and HER2 receptors and positive for EGFR (HER1). BT20 and IJG-1731 cells were grown in complete RPMI-1640 medium with L-glutamine supplemented with 10% fetal calf serum (FCS) and penicillin–streptomycin solution (100 µg/ml each) (Life Technology, Saint-Aubain, France). MDA-MB468 cells were grown in a complete DMEM-F12 medium with glutamine, 10% FCS and penicillin–streptomycin. All cells were maintained in a humidified 5% CO_2 atmosphere at 37°C. All experiments were conducted with confluent cells after overnight starvation.

Antibodies and reagents

Rabbit anti-pEGFR (Y845), anti-pEGFR (Y1086), anti-pPYK2 (Y402), anti-pSTAT3 (Y705), anti-pSrc Family (Y416), anti-EGFR, anti-STAT3, anti-β-actin and Alexa 594-conjugated anti-rabbit F(ab)'2 fragment antibodies were purchased from Cell Signaling Technology (Danvers, MA, USA). Rabbit anti-Histone H3 antibodies were purchased from Thermo Scientific (Rockford, NY, USA). Isotype control IgG (MAB002) and anti-IL-17RB antibodies were purchased from R&D systems (Minneapolis, MN, USA). Iressa (Gefitinib) and the Src inhibitor AZM475271 were

obtained from Tocris Bioscience (R&D systems). 7-AAD was purchased from Beckman (Coulter, France). EverBrite mounting medium with DAPI was purchased from Biotium (Hayward, CA, USA).

Cell death

Cells (3×10^5) were seeded in 6-well plates in complete medium for 24 hours and then starved overnight. Cells were stimulated for 48 hours at 37°C with IL-17E (10 ng/ml), Iressa (0.25, 0.5 or 1 μM) or a combination of both, as indicated. The cells were then harvested with cold PBS/0.5 mM EDTA, washed and stained with 7-AAD, according to the supplier's recommendations. Cell analysis was performed on a FC500 flow cytometer.

Cellular fractionation

Cells (3×10^5) were seeded in 6-well plates in complete medium for 24 hours and then starved overnight. The cells were stimulated for 2 hours at 37°C with IL-17E (10 ng/ml), EGF (10 ng/ml), or a combination of both, as indicated. The cells were then washed with PBS and lysed in lysis buffer (10 mM HEPES, 15 mM $MgCl_2$, 10 mM KCl, 0.5 mM DTT, 0.2 mM PMSF, 1 mM Na_3VO_4, 10 mM NaF, and 0.5% Nonidet P-40). After the cells were incubated on ice for 20 minutes, the cytoplasmic fraction was obtained via centrifugation for 10 seconds at 10000 rpm at 4°C, and the nuclear pellet was washed with lysis buffer. For nuclear protein extraction, the isolated nuclei were suspended in buffer containing 20 mM HEPES, 25% glycerol, 420 mM NaCl, 15 mM $MgCl_2$ and 0.2 mM EDTA supplemented with PMSF, DTT and Na_3VO_4, as above. After incubation for 20 minutes at 4°C, the nuclear extract was collected via centrifugation for 10 minutes at 10000 rpm. Protein concentrations were determined by using the Bradford method. Samples were mixed with Laemmli buffer, heated for 10 minutes at 95°C, and then subjected to 8% SDS-PAGE. Proteins were subsequently transferred to nitrocellulose membranes, hybridized with specific anti-EGFR, anti-pY1086EGFR, anti-STAT3 or anti-pY705STAT3 antibodies, and then detected with ECL. Anti-β-actin and anti-Histone H3 antibodies were used as loading controls.

Tyrosine phosphorylation

Cells (3×10^5) were seeded in 6-well plates in complete medium for 24 hours and then starved overnight. The cells were then stimulated with IL-17E (10 ng/ml), EGF (10 ng/ml), or a combination of both for 30 min in serum-free medium. The cells were then lysed in 1% Triton ×100 buffer and left on ice for 1 hour. Protein samples were then subjected to 8% SDS-PAGE. Western blotting was performed using specific antibodies to assess the phosphorylation of various kinases. In some experiments, cells were treated with AZM475271 (10 μM) or Iressa (0.25 μM) prior to stimulation with IL-17E, EGFR, or a combination of both, as indicated.

Immunofluorescence microscopy

Cells (4.10^3) were grown on Lab-Tek chamber slides in complete culture medium for 24 hours and then starved overnight. The cells were then stimulated with IL-17E (10 ng/ml), EGF (10 ng/ml) or a combination of both for 2 hours at 37°C, washed, and fixed with 4% paraformaldehyde (PFA)-PBS solution at 4°C. Cells were then permeabilized with 0.5% Triton-X-100 in PBS, saturated with 20% FCS in PBS and incubated 18 hours with anti-EGFR (1/500) in 10% FCS-PBS. Slides were mounted with mounting medium containing DAPI and then visualized with a Leica DMRB fluorescence microscope. Image analysis was performed with Archimed software (Microvision).

CONFLICTS OF INTEREST

Y.M., C.G., J.B., R.D., A.B., J.G. hold patent EP16305540, "Combination therapy for the treatment of cancer". AB is the co-founder of OREGA Biotech, and JB is an employee of OREGA Biotech.

GRANT SUPPORT

This work was supported in part by grants from the "Agence Nationale de la Recherche" awarded to OREGA Biotech and from INSERM and Université Paris Diderot awarded to UMR-S 976.

REFERENCES

1. Marme F, Schneeweiss A. Targeted Therapies in Triple-Negative Breast Cancer. Breast Care (Basel). 10:159–166.
2. Lehmann BD, Bauer JA, Chen X, Sanders ME, Chakravarthy AB, Shyr Y, Pietenpol JA. Identification of human triple-negative breast cancer subtypes and preclinical models for selection of targeted therapies. J Clin Invest. 121:2750–2767.
3. Rakha EA, El-Sayed ME, Green AR, Lee AH, Robertson JF, Ellis IO. Prognostic markers in triple-negative breast cancer. Cancer. 2007; 109:25–32.
4. Corkery B, Crown J, Clynes M, O'Donovan N. Epidermal growth factor receptor as a potential therapeutic target in triple-negative breast cancer. Ann Oncol. 2009; 20:862–867.
5. Arteaga CL. EGF receptor as a therapeutic target: patient selection and mechanisms of resistance to receptor-targeted drugs. J Clin Oncol. 2003; 21:289s–291s.
6. Bianco R, Troiani T, Tortora G, Ciardiello F. Intrinsic and acquired resistance to EGFR inhibitors in human cancer therapy. Endocr Relat Cancer. 2005; 12:S159–171.

7. Brand TM, Iida M, Dunn EF, Luthar N, Kostopoulos KT, Corrigan KL, Wleklinski MJ, Yang D, Wisinski KB, Salgia R, Wheeler DL. Nuclear epidermal growth factor receptor is a functional molecular target in triple-negative breast cancer. Mol Cancer Ther. 13:1356–1368.
8. Han W, Lo HW. Landscape of EGFR signaling network in human cancers: biology and therapeutic response in relation to receptor subcellular locations. Cancer Lett. 318:124–134.
9. Yarden Y, Pines G. The ERBB network: at last, cancer therapy meets systems biology. Nat Rev Cancer. 12:553–563.
10. Li C, Iida M, Dunn EF, Ghia AJ, Wheeler DL. Nuclear EGFR contributes to acquired resistance to cetuximab. Oncogene. 2009; 28:3801–3813.
11. Mueller KL, Hunter LA, Ethier SP, Boerner JL. Met and c-Src cooperate to compensate for loss of epidermal growth factor receptor kinase activity in breast cancer cells. Cancer Res. 2008; 68:3314–3322.
12. Lee J, Ho WH, Maruoka M, Corpuz RT, Baldwin DT, Foster JS, Goddard AD, Yansura DG, Vandlen RL, Wood WI, Gurney AL. IL-17E, a novel proinflammatory ligand for the IL-17 receptor homolog IL-17Rh1. J Biol Chem. 2001; 276:1660–1664.
13. Kim MR, Manoukian R, Yeh R, Silbiger SM, Danilenko DM, Scully S, Sun J, DeRose ML, Stolina M, Chang D, Van GY, Clarkin K, Nguyen HQ, et al. Transgenic overexpression of human IL-17E results in eosinophilia, B-lymphocyte hyperplasia, and altered antibody production. Blood. 2002; 100:2330–2340.
14. Furuta S, Jeng YM, Zhou L, Huang L, Kuhn I, Bissell MJ, Lee WH. IL-25 causes apoptosis of IL-25R-expressing breast cancer cells without toxicity to nonmalignant cells. Sci Transl Med. 3:78ra31.
15. Mombelli S, Cochaud S, Merrouche Y, Garbar C, Antonicelli F, Laprevotte E, Alberici G, Bonnefoy N, Eliaou JF, Bastid J, Bensussan A, Giustiniani J. IL-17A and its homologs IL-25/IL-17E recruit the c-RAF/S6 kinase pathway and the generation of pro-oncogenic LMW-E in breast cancer cells. Sci Rep. 5:11874.
16. Yin SY, Jian FY, Chen YH, Chien SC, Hsieh MC, Hsiao PW, Lee WH, Kuo YH, Yang NS. Induction of IL-25 secretion from tumour-associated fibroblasts suppresses mammary tumour metastasis. Nat Commun. 7:11311.
17. Huang CK, Yang CY, Jeng YM, Chen CL, Wu HH, Chang YC, Ma C, Kuo WH, Chang KJ, Shew JY, Lee WH. Autocrine/paracrine mechanism of interleukin-17B receptor promotes breast tumorigenesis through NF-kappaB-mediated antiapoptotic pathway. Oncogene. 33:2968–2977.
18. Cooper JA, Howell B. The when and how of Src regulation. Cell. 1993; 73:1051–1054.
19. Batzer AG, Rotin D, Urena JM, Skolnik EY, Schlessinger J. Hierarchy of binding sites for Grb2 and Shc on the epidermal growth factor receptor. Mol Cell Biol. 1994; 14:5192–5201.
20. Park OK, Schaefer TS, Nathans D. *In vitro* activation of Stat3 by epidermal growth factor receptor kinase. Proc Natl Acad Sci U S A. 1996; 93:13704–13708.
21. Verma N, Keinan O, Selitrennik M, Karn T, Filipits M, Lev S. PYK2 sustains endosomal-derived receptor signalling and enhances epithelial-to-mesenchymal transition. Nat Commun. 6:6064.
22. Shao H, Cheng HY, Cook RG, Tweardy DJ. Identification and characterization of signal transducer and activator of transcription 3 recruitment sites within the epidermal growth factor receptor. Cancer Res. 2003; 63:3923–3930.
23. Bromberg JF, Wrzeszczynska MH, Devgan G, Zhao Y, Pestell RG, Albanese C, Darnell JE, Jr. Stat3 as an oncogene. Cell. 1999; 98:295–303.
24. Park SY, Avraham HK, Avraham S. RAFTK/Pyk2 activation is mediated by trans-acting autophosphorylation in a Src-independent manner. J Biol Chem. 2004; 279:33315–33322.
25. Cochaud S, Giustiniani J, Thomas C, Laprevotte E, Garbar C, Savoye AM, Cure H, Mascaux C, Alberici G, Bonnefoy N, Eliaou JF, Bensussan A, Bastid J. IL-17A is produced by breast cancer TILs and promotes chemoresistance and proliferation through ERK1/2. Sci Rep. 3:3456.
26. Fort MM, Cheung J, Yen D, Li J, Zurawski SM, Lo S, Menon S, Clifford T, Hunte B, Lesley R, Muchamuel T, Hurst SD, Zurawski G, et al. IL-25 induces IL-4, IL-5, and IL-13 and Th2-associated pathologies *in vivo*. Immunity. 2001; 15:985–995.
27. Wang YH, Angkasekwinai P, Lu N, Voo KS, Arima K, Hanabuchi S, Hippe A, Corrigan CJ, Dong C, Homey B, Yao Z, Ying S, Huston DP, et al. IL-25 augments type 2 immune responses by enhancing the expansion and functions of TSLP-DC-activated Th2 memory cells. J Exp Med. 2007; 204:1837–1847.
28. Wiley HS. Trafficking of the ErbB receptors and its influence on signaling. Exp Cell Res. 2003; 284:78–88.
29. Huang WC, Chen YJ, Li LY, Wei YL, Hsu SC, Tsai SL, Chiu PC, Huang WP, Wang YN, Chen CH, Chang WC, Chen AJ, Tsai CH, et al. Nuclear translocation of epidermal growth factor receptor by Akt-dependent phosphorylation enhances breast cancer-resistant protein expression in gefitinib-resistant cells. J Biol Chem. 286:20558–20568.
30. Lin SY, Makino K, Xia W, Matin A, Wen Y, Kwong KY, Bourguignon L, Hung MC. Nuclear localization of EGF receptor and its potential new role as a transcription factor. Nat Cell Biol. 2001; 3:802–808.
31. Niu G, Wright KL, Huang M, Song L, Haura E, Turkson J, Zhang S, Wang T, Sinibaldi D, Coppola D, Heller R, Ellis LM, Karras J, et al. Constitutive Stat3 activity up-regulates VEGF expression and tumor angiogenesis. Oncogene. 2002; 21:2000–2008.
32. Wei D, Le X, Zheng L, Wang L, Frey JA, Gao AC, Peng Z, Huang S, Xiong HQ, Abbruzzese JL, Xie K. Stat3 activation regulates the expression of vascular endothelial growth factor and human pancreatic cancer angiogenesis and metastasis. Oncogene. 2003; 22:319–329.

33. Lo HW, Hsu SC, Ali-Seyed M, Gunduz M, Xia W, Wei Y, Bartholomeusz G, Shih JY, Hung MC. Nuclear interaction of EGFR and STAT3 in the activation of the iNOS/NO pathway. Cancer Cell. 2005; 7:575–589.

34. Gaffen SL. Structure and signalling in the IL-17 receptor family. Nat Rev Immunol. 2009; 9:556–567.

35. Pan G, French D, Mao W, Maruoka M, Risser P, Lee J, Foster J, Aggarwal S, Nicholes K, Guillet S, Schow P, Gurney AL. Forced expression of murine IL-17E induces growth retardation, jaundice, a Th2-biased response, and multiorgan inflammation in mice. J Immunol. 2001; 167:6559–6567.

36. Sonobe Y, Takeuchi H, Kataoka K, Li H, Jin S, Mimuro M, Hashizume Y, Sano Y, Kanda T, Mizuno T, Suzumura A. Interleukin-25 expressed by brain capillary endothelial cells maintains blood-brain barrier function in a protein kinase Cepsilon-dependent manner. J Biol Chem. 2009; 284:31834–31842.

37. Wang AJ, Yang Z, Grinchuk V, Smith A, Qin B, Lu N, Wang D, Wang H, Ramalingam TR, Wynn TA, Urban JF, Jr., Shea-Donohue T, et al. IL-25 or IL-17E Protects against High-Fat Diet-Induced Hepatic Steatosis in Mice Dependent upon IL-13 Activation of STAT6. J Immunol. 195:4771–4780.

38. Yao X, Sun Y, Wang W. Interleukin (IL)-25: Pleiotropic roles in asthma. Respirology. 2016; 21:638–47. doi: 10.1111/resp.12707.

39. Thelen TD, Green RM, Ziegler SF. Acute blockade of IL-25 in a colitis associated colon cancer model leads to increased tumor burden. Sci Rep. 6:25643.

40. Luo Y, Yang Z, Su L, Shan J, Xu H, Xu Y, Liu L, Zhu W, Chen X, Liu C, Chen J, Yao C, Cheng F, et al. Non-CSCs nourish CSCs through interleukin-17E-mediated activation of NF-kappaB, JAK/STAT3 signaling in human hepatocellular carcinoma. Cancer Lett. 375:390–399.

41. Sun Y, Pan J, Mao S, Jin J. IL-17/miR-192/IL-17Rs regulatory feedback loop facilitates multiple myeloma progression. PLoS One. 2014; 9:e114647.

42. Wang L, Yi T, Kortylewski M, Pardoll DM, Zeng D, Yu H. IL-17 can promote tumor growth through an IL-6-Stat3 signaling pathway. J Exp Med. 2009; 206:1457–1464.

43. Benatar T, Cao MY, Lee Y, Li H, Feng N, Gu X, Lee V, Jin H, Wang M, Der S, Lightfoot J, Wright JA, Young AH. Virulizin induces production of IL-17E to enhance antitumor activity by recruitment of eosinophils into tumors. Cancer Immunol Immunother. 2008; 57:1757–1769.

44. Maniati E, Soper R, Hagemann T. Up for Mischief? IL-17/Th17 in the tumour microenvironment. Oncogene. 2010; 29:5653–5662.

45. Yang B, Kang H, Fung A, Zhao H, Wang T, Ma D. The role of interleukin 17 in tumour proliferation, angiogenesis, and metastasis. Mediators Inflamm. 2014; 2014:623759.

46. Qian X, Chen H, Wu X, Hu L, Huang Q, Jin Y. Interleukin-17 acts as double-edged sword in anti-tumor immunity and tumorigenesis. Cytokine. 2015.

47. Welte T, Zhang XH. Interleukin-17 Could Promote Breast Cancer Progression at Several Stages of the Disease. Mediators Inflamm. 2015; 2015:804347.

International Journal of
Molecular Sciences

MDPI

Review

Targeting the Tumor Microenvironment: The Protumor Effects of IL-17 Related to Cancer Type

Joseph Fabre [1,2,3,*], Jerome Giustiniani [1,2], Christian Garbar [1,2], Frank Antonicelli [2], Yacine Merrouche [1,2], Armand Bensussan [4,5,6,*], Martine Bagot [4,5] and Reem al-Dacak [5]

1 Institut Jean Godinot, Unicancer, 1 rue du Général Koenig, F-51726 Reims, France; jerome.giustiniani@gmail.com (J.G.); Christian.GARBAR@reims.unicancer.fr (C.G.); yacine.merrouche@reims.unicancer.fr (Y.M.)
2 Université Reims-Champagne-Ardenne, DERM-I-C, EA7319, 51 rue Cognacq-Jay, F-51095 Reims, France; frank.antonicelli@univ-reims.fr
3 Centre Hospitalo-Universitaire Henri Mondor, Service de Radiothérapie, 51 Avenue du Maréchal de Lattre de Tassigny, F-94010 Créteil, France
4 Institut National de la Santé et de la Recherche Médicale (INSERM) U976, Hôpital Saint Louis, F-75010 Paris, France; martine.bagot@aphp.fr
5 Université Paris Diderot, Sorbonne Paris Cité, Laboratoire Immunologie Dermatologie & Oncologie, UMR-S 976, F-75475 Paris, France; reem.al-daccak@inserm.fr
6 OREGA Biotech, 69130 Ecully, France
* Correspondence: fabrejoseph@yahoo.fr (J.F.); armand.bensussan@inserm.fr (A.B.); Tel.: +33-(0)1-4981-3513 (J.F. & A.B.)

Academic Editor: Anthony Lemarie
Received: 1 July 2016; Accepted: 24 August 2016; Published: 30 August 2016

Abstract: The inflammatory process contributes to immune tolerance as well as to tumor progression and metastasis. By releasing extracellular signals, cancerous cells constantly shape their surrounding microenvironment through their interactions with infiltrating immune cells, stromal cells and components of extracellular matrix. Recently, the pro-inflammatory interleukin 17 (IL-17)-producing T helper lymphocytes, the Th17 cells, and the IL-17/IL-17 receptor (IL-17R) axis gained special attention. The IL-17 family comprises at least six members, IL-17A, IL-17B, IL-17C, IL-17D, IL-17E (also called IL-25), and IL-17F. Secreted as disulfide-linked homo- or heterodimers, the IL-17 bind to the IL-17R, a type I cell surface receptor, of which there are five variants, IL-17RA to IL-17RE. This review focuses on the current advances identifying the promoting role of IL-17 in carcinogenesis, tumor metastasis and resistance to chemotherapy of diverse solid cancers. While underscoring the IL-17/IL-17R axis as promising immunotherapeutic target in the context of cancer managing, this knowledge calls upon further in vitro and in vivo studies that would allow the development and implementation of novel strategies to combat tumors.

Keywords: interleukin 17 (IL-17); cancer; tumor microenvironment; immunotherapy

1. Introduction

Tumor cells have enhanced capacities of proliferation, neo-angiogenesis development and distance seeding under the form of metastases [1,2]. The tumor microenvironment (TME), which comprises malignant and non-malignant cells distinguished by specific markers and interacting in a dynamic fashion, is an important aspect of cancer biology that contributes to tumor initiation, tumor progression and responses to therapy [3–5]. Cells and molecules of the immune system are a fundamental component of the TME. Although critical for anti-tumor responses, cells of the immune system including macrophages, neutrophils, mast cells, dendritic cells (DCs) and lymphocytes can also promote the development and progression of almost every solid tumor [6–8]. Tumor cells counterattack

the host's immune cells detouring them to their own profit and evading elimination [9]. They often secrete a variety of cytokines and mediators creating a self-entertaining inflammation of the TME that is favorable to tumor development and progression [10].

Recently, a subset of T helper (Th) lymphocytes secreting mainly the pro-inflammatory IL-17 cytokines, the Th17 cells, has gained considerable attention, given their contribution to infectious, auto-, and cancer immunity [11]. Consequently, the IL-17 pro-inflammatory cytokines have become a key therapeutic target in a variety of chronic inflammatory diseases. Because inflammation is also tightly correlated to cancer development [12], these cytokines have been also intensively investigated in the context of cancer development and progression. Recent research provided substantial insights into the mode of action of Th17 and IL-17 cytokines in a variety of tumors. Lessons are learned and paradigms are changing: IL-17 cytokines are double-edged agents acting in a cancer-type depending manner as anti- and protumor cytokines. If respectively targeted, the IL-17/IL-17R axis could be part of the dynamic and durable mechanisms that might promote tumor regression. We discuss the hurdles, lessons, and advances accomplished in the field through the progressive journey of IL-17 family toward tumor immunotherapy.

2. The IL-17/IL-17R Axis

2.1. Tumor Infiltrating Lymphocytes and Th 17 Cells

Tumor infiltrating lymphocytes present a minor population of healthy and cancer patients' pool of peripheral and lymph nodes T lymphocytes but are found at a high concentration in the microenvironment of diverse types of cancers [13–15]. The intensity of TIL infiltration to tumors often correlates with the stage of the disease [16]. TIL comprise various subsets of T lymphocytes, among which is the subset of Th17 lymphocytes.

Th17 cells have been extensively studied over the last five years. They are an independent lineage of Th lymphocytes and are characterized by a specific cytokine secretion profile, transcription regulation and immune functions [17]. Th17 play important role in infection since they repel against diverse microbes and are key mediators of inflammation in a variety of inflammatory and autoimmune disorders including psoriasis, rheumatoid arthritis and inflammatory bowel diseases [18]. The development of Th17 lineage is controlled by RORγt, STAT3 and IFN regulatory factor-4 transcription factors and necessitates the exposure to a variety of cytokines [19]. In mouse, lymphocyte engagement in the Th17 pathway needs the exposure to TGF-β plus IL-6 or IL-21 [20] as well as IL-23 [21]. In human, IL-1 is the cornerstone of human Th17 cells differentiation, and can be potentiated by a combination of IL-23, IL-6 and TGF-β [22,23]. Besides cytokines, the activation of antigen-presenting cells, the DCs, through the Toll-like receptor (TLR) and bacterial sensor nod2 programs them to polarize human memory T cells towards the Th17 lineage [24].

Similar to other T lymphocytes subsets, Th17 cells also infiltrate cancers. Within the tumor microenvironment, the infiltrating Th17 cells are often abundant at a proximity to the tumor mass. Phenotypically, these cells, to which we will refer to as TIL-Th17 cells, express memory-like markers (CD45RA−CD45RO+), CD49 integrins, and surface receptors allowing their traffic to peripheral tissues including CXCR4, CCR6 and C-type lectin CD161 [25,26]. However, TIL-Th17 cells do not express CCR2, CCR5 and CCR7, which limit their capacity to access the lymph nodes [27]. This configuration may be responsible for Th17 lymphocytes stagnation in the tumor microenvironment where the levels of CCL20 and CXCL12 are high [28]. CCL20 can be also produced by Th17 [29], which could self-consolidate their adhesion to the tumor site.

Compared to conventional effector T cells, Th17 phenotype comprised low levels of granzyme B and activation markers HLA-DR and CD25. This observation is in favor of an impossibility to initiate cytotoxic killing. Besides, Th17 express minimal PD-1 and forkhead box P3 (FOXP3), which make them distinct from immune-suppressive regulator T cells (Treg) [30].

2.2. IL-17 and IL-17 Receptor Family

Early studies with rodent models described in T cell hybridoma a cDNA sequence coding for a mRNA sharing characteristics with cytokines [31]. Primarily designated as CTLA8, it was termed interleukin-17 (IL-17) after its cloning from a cDNA library [11]. Today, the IL-17 is a family of pro-inflammatory cytokines implicated in a variety of immune responses and is composed of six members, from IL-17A to IL-17F.

IL-17A and -F share 50% homology and are the closest members [32]. They are secreted as IL-17A and IL-17F homodimers and also as IL-17A/F heterodimers [33]. In term of activity, IL-17F is less potent than IL-17A, and the heterodimer has an intermediate efficacy [34]. The functions of IL-17B, IL-17C and IL-17E are less defined. Nonetheless, IL-17E (also referred to as IL-25), which shares the lowest homology with IL-17A, was involved in allergy reactions and in immunity against parasites [35]. Although their production is the hallmark of Th17 cells, both IL-17A and -F can also be produced by γδT cells, natural killer T (NKT) cells, neutrophils and eosinophils [36].

The receptor of IL-17 (IL-17R) is a transmembrane protein composed of a 27 amino acid (aa) N-terminal signal peptide, a 293 aa extracellular domain, a 21 aa transmembrane domain and a cytoplasmic tail of 525 aa [37]. Particular motives have been identified within these domains: fibronectin type III (FnIII) regions in the extracellular portion of the protein and similar expression to fibroblast growth factor genes (SEFIR) motif inside the cytoplasmic tail. Five members of the IL-17R family have been identified so far and designated as IL-17RA, IL-17RB, IL-17RC, IL-17RD and IL-17RE (Figure 1). Each of these members is a subunit that needs to associate with another one to form the functional receptor [38]. The subunit IL-17RA is ubiquitous, and is encoded by a gene situated on chromosome 22, while others are encoded by a cluster on chromosome 3 [23,33]. It is also a common co-receptor subunit for other members of the IL-17 family. Conversely, IL-17RC subunit was an obligate co-receptor for IL-17RA to mediate IL-17A, IL-17F and IL-17A/F signaling [39]. Other members of the IL-17 family, IL-17B, IL-17C, and IL-17E respectively bind IL-17RB, IL-17RA/RC, and IL-17RA/RB [40]. IL-17D as well as IL-17RD matches remain unfound yet [36]. In any case, ligand fixation activates IL-17RA and transduces signal through the phosphorylation of Mitogen Activated Protein Kinases (MAPK) and Nuclear Factor-κB (NF-κB) via TNF Receptor Associated Factor-6 (TRAF6). Interaction with NF-κB protein (Act1) has also been reported [41]. To comfort this, Act1 knockdown experiences showed abrogation of IL-17 induced inflammatory gene expression and NF-κB activation [42]. The structural data about SEFIR domains of IL-17RA, IL-17RB and IL-17RC are accumulating and suggest a key role of the αC-helix in the SEFIR-SEFIR interactions with Act1 [43]. Secondary to Act1 and TRAF6 activation, Iκβ kinase (IKK) phosphorylates p105, which releases Tumor Progression locus 2 (TPL2). TPL2 then phosphorylates MEK1, which activates ERK1 and ERK2 and ultimately leads to transcription factors phosphorylation and gene expression modulation [44].

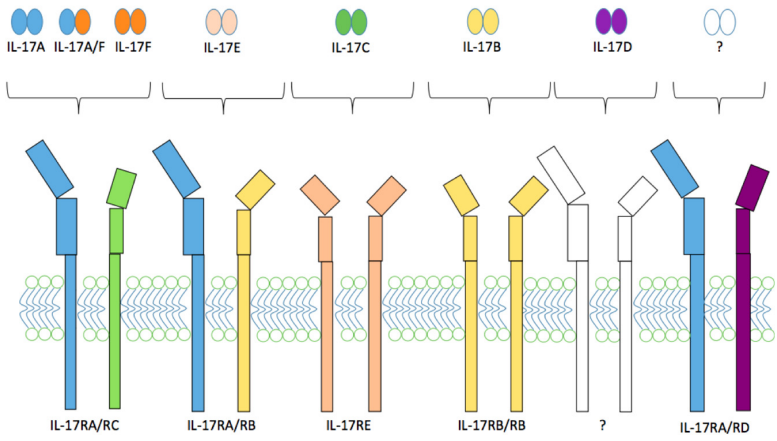

Figure 1. Interleukin 17 and interleukin 17 receptor family members.

2.3. IL-17 and Cancer

If the efficacy of IL-17 pathway inhibiting therapies in inflammatory disease like rheumatoid arthritis or psoriasis has been clearly established [45], it still has to be validated as a target for cancer treatment given its double-edged role in cancer. Indeed, since its primary detection in human cancers including breast, gastric and prostate cancer [46–51], the role of IL-17 in oncology has been highly debated and controversial [52].

2.3.1. IL-17 and Cervical Cancer

One of the earliest publications arguing in favor of a deleterious tumor enhancing effect of IL-17 was the study from Tartour et al. [53]. They observed that cervical cancer cell cultured with IL-17 had an increased production of both IL-6 and IL-8 mRNA and proteins levels. Although no direct effect on proliferation had occurred in vitro, the tumor size was increased when nude mice were transplanted with two cell lines transfected with IL-17-encoding-cDNA as compared to the parent tumor. Of note, IL-6 level and macrophage number was raised at the tumor site. Punt et al. also reported cell index-stimulating effects of IL-17 and observed it was present mainly in neutrophils (66%), mast cells (23%) and at a lesser level in innate lymphoid cells (8%). From patients' tissue samples, they observed that a higher number of neutrophils was correlated with a poorer survival [54].

2.3.2. IL-17 and Breast Cancer

Several articles brought evidence for a protumor role of IL-17. Lyon et al. confronted the blood levels of diverse cytokines from 35 patients newly diagnosed with breast cancer (BC) to patients with negative breast biopsy [55]. They observed that IL-17, IL-6 and GCS-F were significantly more elevated in breast cancer patients than in control though no correlation with prognosis was made. Zhu et al. were the first to propose a study to analyze the expression in situ of IL-17 in BC. On immunostaining, IL-17 was located particularly to the peritumoural area concomitantly to a macrophage infiltration. Then, they evaluated Four BC cell lines (MDA-MB231, MDA-MB435, MCF7 and T47D) on matrigel invasion assay. IL-17, as well as TNF, markedly increased invasion for MDA-MB231 and MDA-MB435. When adding matrix metalloproteinase (MMP) inhibitors to cell cultures, the IL-17-dependent invasion was inhibited [56]. Other authors suggested that tumor favoring effects of IL-17 may occur via an increase in suppressive functions of myeloid-derived suppressor cells (MDSCs) through the CXCL1/5–CXCR2 axis. In this study, anti IL-17-blocking antibodies were reported to dramatically decrease tumor growth and the number of MDSCs in mice [13]. Angiogenesis-promoting effects of IL-17 in breast tumor cell grafts in vivo as measured by microvascular density has also been reported [57]. In contrast with these results, some authors reported anti-tumor activity of the IL-17 family members. Furuta et al. observed caspase-dependent pro-apoptosis effects of IL-17E on culture cells as well as xenografts [58].

Nevertheless, our team also observed that human breast cancer cell lines expressed IL-17RA and IL-17RC, and stimulation with IL-17A recruited the MAPK pathway by upregulating phosphorylated ERK1/2 as reported in previous studies [59]. This mechanism lead to enhanced migration, invasion and resistance to chemotherapy, and was abrogated by anti-IL17A antibodies [60].

Our next step was to further assess the molecular signaling after stimulation of human breast cancer cell lines with IL-17A and IL-17E. The result was an induction by both cytokines of the phosphorylation of c-RAF, ERK1/2 and p70 S6 Kinase, which are known to be involved in the proliferation and survival of tumor cells [61]. Besides, unlike findings by other authors [58,62,63], IL-17A or IL-17E did not induce apoptosis in IL-17RB-expressing human breast cancer cells but conversely exacerbated cell resistance to docetaxel [61]. Another argument in favor of a protumor impact of IL-17A and -E was the detection of an enhanced generation of low molecular weight forms of cyclin E (LMWE) in the four different cell lines (MCF7, T47D, MCF10A and IJG-1731) [61], which has been described as a negative factor in cancer [64].

2.3.3. IL-17 and Prostate Cancer

Chronic inflammation and eventually atrophy are implicated in prostate cancer [65]. The first report of the presence of an IL-17R-like receptor in prostate cells was in 2002 [46]. The year after, another study confirmed that IL-17 expression was low in normal prostate cells, whereas it was elevated in 58% of cancer cells and 79% in benign prostatic hypertrophy cells. Concerning IL-17 receptor, it was ubiquitously detected [47]. Only years later, You et al. identified the reported transmembrane protein to be IL-17-RC of which they reported several isoforms both in hormone-dependent and independent prostate cancers [66]. Moreover, a study analyzed cell signaling mediated by IL-17A ex vivo, and found that ERK pathway and NF-κB were activated but cell growth was not modified. Besides, several chemokines (CXCL1, CXCL2, CCL2, and CCL5) and IL-6 expression level were increased [67].

Liu et al. investigated whether obesity played a role in prostate cancer (PC) development [68]. In a mice model of obesity they found a higher rate of PC [69]. Obese subjects developed a chronic inflammatory state with increased serum levels of IL-17, insulin, and insulin-like growth factor 1 (IGF1). They also observed that hyperinsulinemia reinforced IL-17-induced expression of downstream proinflammatory genes with increased levels of IL-17RA, resulting in the development of more invasive prostate cancer. Glycogen synthase kinase 3 (GSK3) is constitutively attached to the phosphorylation of IL-17RA at T780 and its activation leads to ubiquitination and proteasome-mediated destruction of IL-17RA, which ultimately blocks IL-17-mediated inflammation [68]. Concordantly, phosphorylated IL-17RA was decreased, and its IL-17RA mRNA levels were raised in the proliferative human prostate cancer cells compared to the normal cells. Besides, Insulin and IGF1 enhanced IL-17-induced inflammatory responses through suppressing GSK3 in cultured cell lines and in obese mouse models of prostate cancer indicating crosslink between the insulin receptor pathway and IL-17 signaling [68]. From a therapeutic point of view, GSK3-targeting may lead to the suppression of IL-17-mediated inflammation and could prevent appearance of prostate cancer in obese men. The same authors very recently added evidences from murine experiences that IL-17-mediated prostate cancer promotion may occur through epithelial to mesenchymal transition via MMP7 enhancement [70]. This mechanism is concordant with a progressive transformation of prostate cancer cells exposed to chronic inflammation via IL-17-recruiting of inflammatory cells and ultimately a loss of adhesion. The improved invasiveness through metalloproteinase expression allows them to digest extracellular matrix as well as the basal membrane and thus expand.

2.3.4. IL-17 and Gastric Cancer

Only a few studies evaluated IL-17 in gastric cancer. Zhou et al. investigated the immortalized AGS human gastric adenocarcinoma cell line. They demonstrated that IL-17A and possibly IL-17F could initiate transduction pathways, increase expression of MAPKs and recruit neutrophils participation in gastric inflammation and thus promote cancer progression through IL-17R docking. These effects were significantly abrogated by disrupting IL-17RA or IL-17RC signaling, therefore evocating their participation in gastric cancer [71]. Interleukin-17B acts in a paracrine fashion since it has also been detected locally in gastric cancer but only at low levels, whereas the expression of its receptor IL-17RB was increased and correlated with poor prognosis. Surprisingly, IL-17E expression was absent in the stomach. Evaluation of the IL-17B/17-RB axis in gastric cancer cells, reported that it promoted proliferation and migration as well as stemness phenotype as assessed by the detection of stem cells markers Oct4, Nanog, Lgr5, Sall4 [72]. The mechanism was an activation of the AKT/GSK-3β/β-catenin pathway.

2.3.5. IL-17 and Colon Cancer

Colorectal cancers develop from normal colonic epithelium in a four-step progression of gene alterations [73]. The study by Cui et al. evaluated the dynamic variations of the expression of IL-17A in the tumor microenvironment during the colorectal adenoma-carcinoma sequence. Results are in

favor of a progressive increase of IL-17 mRNA level throughout the sequence which was correlated with dysplasia severity. By immunohistochemistry (IHC), they confirmed these results by observing that Th17 presence was growing gradually in both stroma and adenomatous/cancerous epithelium. Th17-stimulating factors like IL-1β, IL-6, IL-23, TGF-β and housekeeping gene β-actin were also increased in real-time PCR, which indirectly reflects an activation of Th17 cells along the sequence [74]. To complete this observation, Al-Samadi et al. reported an increased level of IL-17B in CRC in both epithelial and stromal compartments, while IL-17F was decreased. Concerning IL-17E, no difference was noted between altered and healthy tissues [75]. For IL-17C the expression pattern was dependent on the grade of the differentiation.

In 2016, Housseau et al. reported a redundant role for adaptive and innate γδT17 cell-derived IL-17 in a model of bacteria induced colon carcinogenesis [76]. Notably, they observed that knocking out STAT3 in CD4+ T cells delayed tumorigenesis but failed to definitely suppress colonic tumors appearance. IL-17 appeared critical for the emergence of colonic tumors, although this cytokine is secreted by another source than cancer cells. The source responsible for this relay of IL-17 secretion may be mucosal γδT17 cells because genetic ablation in ETBF-colonized Th17 deficient mice prevented the late emergence of colonic tumors. When they examined human colon cancer samples, both Th17 and γδT17 cells were found. Finally, when they inoculated MC38 colon cancer cell line in IL-17$^{-/-}$ mice, it had an enhanced growth and developed metastases to the lungs more frequently than nondeficient mice. The explanation could be a reduction in IFNγ producing NK and CD8+ cells [27].

2.3.6. IL-17 and Lung Cancer

In 2015, Pan et al. investigated the impact of IL-17 in non-small cell lung cancer (NSCLC) [77,78]. Ex vivo, they observed that IL-17 could induce VEGF secretion in cancer cell lines. This effect was dependent of the STAT3-Gα–Interacting Vesicle-associated protein (GIV) pathway and was abolished when cells where exposed to small interfering RNA (siRNA) [77]. In patients, they observed that those with increased levels of serum IL-17 had a poorer survival and an enhanced angiogenesis compared to healthy control [78]. To comfort that, exposure of three different NSCLC cell lines to IL-17 has also been reported to increase neoangiogenesis and to promote in vivo tumor growth in SCID mice through a CXCR-2-dependent mechanism. IL-17 up-regulated several pro-angiogenic CXC chemokines including CXCL1, CXCL5, CXCL6 and CXCL8. Inhibition of IL-17 with monoclonal antibodies abolished this up-regulation. Noteworthy, direct stimulating effect on cell cultures was not observed [79].

2.3.7. IL-17 and Skin Cancer

Several studies reported effects of IL-17 on tumor progression, growth and migration in skin cancer cell culture as well as in mice [80,81]. Both basal and squamous cell cancer cell types were responsive to IL-17 stimulation. Similar to other cell types, cytoplasmic adaptor Act1 has been reported as critical for IL-17R signaling and ultimately tumor formation [82]. The authors also described a novel IL-17-mediated cascade starting from IL-17R and leading to ERK5 activation via recruitment of Act1, TRAF4 and MEKK3. At a genetic level, the metalloreductase Steap4 and transcription factor p63 were reported to be overexpressed at the end of the cascade and to create a positive feedback through p63-mediated TRAF4 expression.

Wang et al. studied the role of IL-17 in cell lines growth of melanoma (B16) and bladder carcinoma (MB49) [83]. Both had a reduced expansion in IL-17$^{-/-}$ mice, and were enhanced in IFNγ$^{-/-}$ mice as a consequence of an elevated intra-tumor IL-17 level. IFNγ probably plays a minor or an upstream role since double knockout (KO) mice are resistant to tumor cell growth like IL-17$^{-/-}$. In vitro, the cell proliferation promoting-effect was modest. In each cell line, IL-6 production was stimulated by signal transducer and activator of transcription (Stat3). The same was observed in tumor associated stromal cells such as fibroblasts, endothelial cells and dendritic cells. The pro-angiogenic effects of IL-17 such as angiogenic factor secretion by endothelial cells and improved cell migration were also dependent of STAT3 activation. In absence of IFNγ, tumors were characterized by an important

production of IL-17 and IL-6 by tumor infiltrating cells and tumor cells. When blocking IL-6, tumor progression was partially reversed indicating that the protumor activity of IL-17 needs IL-6 in a STAT3-dependent pathway.

2.3.8. IL-17 and Brain Tumors

IL-17 has not been suggested to play a role in brain tumors except for gliomas. A clinical study compared blood levels of IL-17 in 80 brain tumors versus 26 healthy patients and found it was elevated in 30% of gliomas, 4% of meningioma, 5.5% of schwannoma, and none of the control group [84]. When exposed to IL-17, diverse glioma cell lines showed an increased expression of IκB-α mRNA and IκB-α protein degradation. Besides, IL-17 also stimulated IL-6 and IL-8 alone and in a potentiated fashion when combined with IL-1β [85]. In vivo, the presence of Th17 lymphocytes and IL-17A mRNA was demonstrated in glioma from mouse and human yet without assessing their impact in that situation [86]. The presence of Th17 cells in the glioma microenvironment was further investigated by Cantini et al. [87]. The authors reported Th17 and Treg cells infiltration in mouse glioma to be time-dependent. Then, they injected spleen-derived Th17 from naive (nTh17) or glioma-bearing mice (gTh17) concomitantly to GL261 glioma cell lines in immune-competent mice. All Th17 lymphocytes showed high levels of IL-17mRNA, variable levels of IL-10 and IFNγ but lacked Foxp3. Survival was significantly shorter and tumor size larger in mice injected with gTh17 than nTh17. Analysis of the microenvironment showed that in tumors co-injected with nTh17, high expression of IFNγ and TNF was present, whereas, in comparison to gTh17 IL-10 and TGF-β, were at least two times more expressed. Note that direct exposure of glioma cell lines to IL-17 did not stimulate cell growth. Hu et al. suggested indirect tumor-promoting effects of IL-17 via accelerated angiogenesis [88]. Glioma graft growth in mice transfected with an IL-17 vector was superior to the mock vector, as was the mRNA expression levels of CD31 in tumor tissues.

Some authors reported tumor-protective effects of Tregs in glioma. IL-17+ Tregs were identified in abundance in surgically removed high-grade glioma, and co-culture provoked an inhibition of CD8+ T cells proliferation. Tregs suppressive effects are probably mediated by TGF-β and IL-17 because selective antibodies against each of the cytokine blocked the inhibition of CD8+ and when both IL-17 and TGF-β were targeted, the effect was potentiated [89].

Recently, functional IL-17R has been detected in glioma stem cells and suggested as an interesting target [90].

2.4. IL-17 and Hepatocarcinoma

Zhang et al. observed in 2009 that IL-17+ cells were strongly represented in human hepatocellular carcinoma (HCC) and their level was correlated with both microvessel density in tissues and poor survival for patients [91]. They also reported that most of these IL-17+ cells were Th17 (CD4+) and a significant number amongst them were CD8+ T cells. Later, the same team found that tumor-activated monocytes could enhance the proliferation of these CD8+ T cells [92].

2.5. IL-17 and Sarcoma

The activation of IL-17R at the surface of synovial sarcoma cells by IL-17A [64] was found to recruit ERK1/2, p38 MAPK and c-Jun N-terminal kinases (JNKs), and then to activate AP-1, finally leading to an increase of MMP-3 mRNA and protein expression, which has been shown to stimulate tumor development in breast and lung [93,94]. On the other hand, an intact IL-17/IL-17R axis has been reported to improve immunogenic cell death after chemotherapy [95]. Another study by O'Sullivan et al. also regroups experiments on sarcoma cells lines among other cancer types with a focus on IL-17E [96]. They observed that the cytokine mediated tumor rejection through the recruitment of NK cells probably by stimulating the production of chemokine MCP-1.

3. Conclusions

Very soon after its discovery, researchers have been exploring the relationships between the IL-17 pathway and cancer development and progression. The presence of IL-17 and Th17 cells has been confirmed in almost all types of invasive cancers rare or frequent. Taken together, our data support cell proliferation, tumor growth and progression and treatment resistance through cell IL-17R signaling activation and probably crosslinks with other receptors such as EGFR, or IGFR. Analysis of patients' blood or tissue samples was more often reported in favor of a negative impact of high values of IL-17 and IL-17-secreting cells. Nevertheless, a few studies have also reported anti-tumor activity. The presence of regulator T lymphocytes, as well as cytokines other than IL-17 present in the microenvironment modulate the immune response and orientate the balance towards cancer immunogenicity or immunosuppression. Our present work underscore IL-17/IL-17R axis as a promising immunotherapeutic target, and calls upon further in vitro and in vivo studies that would allow the development of novel strategies to combat tumors.

Author Contributions: Joseph Fabre wrote most of the manuscript, draw the figure and made corrections. Jerome Giustianiani, Christian Garbar, Martine Bagot and Yacine Merrouche provided bibliography and councelling during the writing. Armand Bensussan elaborated the title and the plan, and provided instructions about the articles' objectives as well as reviews. Frank Antonicelli and Reem Al-Dacak wrote parts of the manuscripts and gave reviews.

Conflicts of Interest: The authors declare no conflict of interest.

References

1. Joyce, J.A.; Fearon, D.T. T cell exclusion, immune privilege, and the tumor microenvironment. *Science* **2015**, *348*, 74–80. [CrossRef] [PubMed]
2. He, D.; Li, H.; Yusuf, N.; Elmets, C.A.; Li, J.; Mountz, J.D.; Xu, H. IL-17 promotes tumor development through the induction of tumor promoting microenvironments at tumor sites and myeloid-derived suppressor cells. *J. Immunol.* **2010**, *184*, 2281–2288. [CrossRef] [PubMed]
3. De la Cruz-Merino, L.; Barco-Sanchez, A.; Henao Carrasco, F.; Nogales Fernandez, E.; Vallejo Benitez, A.; Brugal Molina, J.; Martinez Peinado, A.; Grueso Lopez, A.; Ruiz Borrego, M.; Codes Manuel de Villena, M.; et al. New insights into the role of the immune microenvironment in breast carcinoma. *Clin. Dev. Immunol.* **2013**, *2013*, 785317–785328. [CrossRef] [PubMed]
4. Quail, D.F.; Joyce, J.A. Microenvironmental regulation of tumor progression and metastasis. *Nat. Med.* **2013**, *19*, 1423–1437. [CrossRef] [PubMed]
5. Quail, D.F.; Bowman, R.L.; Akkari, L.; Quick, M.L.; Schuhmacher, A.J.; Huse, J.T.; Holland, E.C.; Sutton, J.C.; Joyce, J.A. The tumor microenvironment underlies acquired resistance to CSF-1R inhibition in gliomas. *Science* **2016**. [CrossRef] [PubMed]
6. Bowman, R.L.; Joyce, J.A. Therapeutic targeting of tumor-associated macrophages and microglia in glioblastoma. *Immunotherapy* **2014**, *6*, 663–666. [CrossRef] [PubMed]
7. Dunn, G.P.; Old, L.J.; Schreiber, R.D. The immunobiology of cancer immunosurveillance and immunoediting. *Immunity* **2004**, *21*, 137–148. [CrossRef] [PubMed]
8. Beyer, M.; Schultze, J.L. Regulatory T cells in cancer. *Blood* **2006**, *108*, 804–811. [CrossRef] [PubMed]
9. Dunn, G.P.; Bruce, A.T.; Ikeda, H.; Old, L.J.; Schreiber, R.D. Cancer immunoediting: From immunosurveillance to tumor escape. *Nat. Immunol.* **2002**, *3*, 991–998. [CrossRef] [PubMed]
10. Mantovani, A.; Romero, P.; Palucka, A.K.; Marincola, F.M. Tumour immunity: Effector response to tumour and role of the microenvironment. *Lancet* **2008**, *371*, 771–783. [CrossRef]
11. Yao, Z.; Painter, S.L.; Fanslow, W.C.; Ulrich, D.; Macduff, B.M.; Spriggs, M.K.; Armitage, R.J. Human IL-17: A novel cytokine derived from T cells. *J. Immunol.* **1995**, *155*, 5483–5486. [PubMed]
12. Maniati, E.; Soper, R.; Hagemann, T. Up for mischief? IL-17/Th17 in the tumour microenvironment. *Oncogene* **2010**, *29*, 5653–5662. [CrossRef] [PubMed]
13. Novitskiy, S.V.; Pickup, M.W.; Gorska, A.E.; Owens, P.; Chytil, A.; Aakre, M.; Wu, H.; Shyr, Y.; Moses, H.L. TGF-β receptor II loss promotes mammary carcinoma progression by Th17 dependent mechanisms. *Cancer Discov.* **2011**, *1*, 430–441. [CrossRef] [PubMed]

14. West, N.R.; Kost, S.E.; Martin, S.D.; Milne, K.; Deleeuw, R.J.; Nelson, B.H.; Watson, P.H. Tumour-infiltrating FOXP3+ lymphocytes are associated with cytotoxic immune responses and good clinical outcome in oestrogen receptor-negative breast cancer. *Br. J. Cancer* **2013**, *108*, 155–162. [CrossRef] [PubMed]
15. Su, X.; Ye, J.; Hsueh, E.C.; Zhang, Y.; Hoft, D.F.; Peng, G. Tumor microenvironments direct the recruitment and expansion of human Th17 cells. *J. Immunol.* **2010**, *184*, 1630–1641. [CrossRef] [PubMed]
16. Miyashita, M.; Sasano, H.; Tamaki, K.; Hirakawa, H.; Takahashi, Y.; Nakagawa, S.; Watanabe, G.; Tada, H.; Suzuki, A.; Ohuchi, N.; et al. Prognostic significance of tumor-infiltrating CD8+ and FOXP3+ lymphocytes in residual tumors and alterations in these parameters after neoadjuvant chemotherapy in triple-negative breast cancer: A retrospective multicenter study. *Breast Cancer Res.* **2015**, *17*, 124–137. [CrossRef] [PubMed]
17. Gu, C.; Wu, L.; Li, X. IL-17 family: Cytokines, receptors and signaling. *Cytokine* **2013**, *64*, 477–485. [CrossRef] [PubMed]
18. Tesmer, L.A.; Lundy, S.K.; Sarkar, S.; Fox, D.A. Th17 cells in human disease. *Immunol. Rev.* **2008**, *223*, 87–113. [CrossRef] [PubMed]
19. Yang, X.O.; Pappu, B.P.; Nurieva, R.; Akimzhanov, A.; Kang, H.S.; Chung, Y.; Ma, L.; Shah, B.; Panopoulos, A.D.; Schluns, K.S.; et al. T helper 17 lineage differentiation is programmed by orphan nuclear receptors RORα and RORγ. *Immunity* **2008**, *28*, 29–39. [CrossRef] [PubMed]
20. Zhou, L.; Ivanov, I.I.; Spolski, R.; Min, R.; Shenderov, K.; Egawa, T.; Levy, D.E.; Leonard, W.J.; Littman, D.R. IL-6 programs T_H-17 cell differentiation by promoting sequential engagement of the IL-21 and IL-23 pathways. *Nat. Immunol.* **2007**, *8*, 967–974. [CrossRef] [PubMed]
21. Cua, D.J.; Sherlock, J.; Chen, Y.; Murphy, C.A.; Joyce, B.; Seymour, B.; Lucian, L.; To, W.; Kwan, S.; Churakova, T.; et al. Interleukin-23 rather than interleukin-12 is the critical cytokine for autoimmune inflammation of the brain. *Nature* **2003**, *421*, 744–748. [CrossRef] [PubMed]
22. Wilson, N.J.; Boniface, K.; Chan, J.R.; McKenzie, B.S.; Blumenschein, W.M.; Mattson, J.D.; Basham, B.; Smith, K.; Chen, T.; Morel, F.; et al. Development, cytokine profile and function of human interleukin 17-producing helper T cells. *Nat. Immunol.* **2007**, *8*, 950–957. [CrossRef] [PubMed]
23. Yang, X.O.; Chang, S.H.; Park, H.; Nurieva, R.; Shah, B.; Acero, L.; Wang, Y.H.; Schluns, K.S.; Broaddus, R.R.; Zhu, Z.; et al. Regulation of inflammatory responses by IL-17F. *J. Exp. Med.* **2008**, *205*, 1063–1075. [CrossRef] [PubMed]
24. Van Beelen, A.J.; Zelinkova, Z.; Taanman-Kueter, E.W.; Muller, F.J.; Hommes, D.W.; Zaat, S.A.; Kapsenberg, M.L.; de Jong, E.C. Stimulation of the intracellular bacterial sensor NOD2 programs dendritic cells to promote interleukin-17 production in human memory T cells. *Immunity* **2007**, *27*, 660–669. [CrossRef] [PubMed]
25. Kryczek, I.; Wei, S.; Gong, W.; Shu, X.; Szeliga, W.; Vatan, L.; Chen, L.; Wang, G.; Zou, W. Cutting edge: IFNγ enables APC to promote memory Th17 and abate Th1 cell development. *J. Immunol.* **2008**, *181*, 5842–5846. [CrossRef] [PubMed]
26. Martin-Orozco, N.; Muranski, P.; Chung, Y.; Yang, X.O.; Yamazaki, T.; Lu, S.; Hwu, P.; Restifo, N.P.; Overwijk, W.W.; Dong, C. T helper 17 cells promote cytotoxic T cell activation in tumor immunity. *Immunity* **2009**, *31*, 787–798. [CrossRef] [PubMed]
27. Kryczek, I.; Banerjee, M.; Cheng, P.; Vatan, L.; Szeliga, W.; Wei, S.; Huang, E.; Finlayson, E.; Simeone, D.; Welling, T.H.; et al. Phenotype, distribution, generation, and functional and clinical relevance of Th17 cells in the human tumor environments. *Blood* **2009**, *114*, 1141–1149. [CrossRef] [PubMed]
28. Ghadjar, P.; Rubie, C.; Aebersold, D.M.; Keilholz, U. The chemokine CCL20 and its receptor CCR6 in human malignancy with focus on colorectal cancer. *Int. J. Cancer* **2009**, *125*, 741–745. [CrossRef] [PubMed]
29. Muranski, P.; Boni, A.; Antony, P.A.; Cassard, L.; Irvine, K.R.; Kaiser, A.; Paulos, C.M.; Palmer, D.C.; Touloukian, C.E.; Ptak, K.; et al. Tumor-specific Th17-polarized cells eradicate large established melanoma. *Blood* **2008**, *112*, 362–373. [CrossRef] [PubMed]
30. Kryczek, I.; Liu, R.; Wang, G.; Wu, K.; Shu, X.; Szeliga, W.; Vatan, L.; Finlayson, E.; Huang, E.; Simeone, D.; et al. FOXP3 defines regulatory T cells in human tumor and autoimmune disease. *Cancer Res.* **2009**, *69*, 3995–4000. [CrossRef] [PubMed]
31. Rouvier, E.; Luciani, M.F.; Mattei, M.G.; Denizot, F.; Golstein, P. CTLA-8, cloned from an activated T cell, bearing AU-rich messenger RNA instability sequences, and homologous to a herpesvirus saimiri gene. *J. Immunol.* **1993**, *150*, 5445–5456. [PubMed]
32. Kolls, J.K.; Linden, A. Interleukin-17 family members and inflammation. *Immunity* **2004**, *21*, 467–476. [CrossRef] [PubMed]

33. Moseley, T.A.; Haudenschild, D.R.; Rose, L.; Reddi, A.H. Interleukin-17 family and IL-17 receptors. *Cytokine Growth Factor Rev.* **2003**, *14*, 155–174. [CrossRef]
34. Xu, S.; Cao, X. Interleukin-17 and its expanding biological functions. *Cell. Mol. Immunol.* **2010**, *7*, 164–174. [CrossRef] [PubMed]
35. Jin, W.; Dong, C. IL-17 cytokines in immunity and inflammation. *Emerg. Microbes Infect.* **2013**, *2*, 60–65. [CrossRef] [PubMed]
36. Song, X.; Qian, Y. The activation and regulation of IL-17 receptor mediated signaling. *Cytokine* **2013**, *62*, 175–182. [CrossRef] [PubMed]
37. Chen, Z.; O'Shea, J.J. Regulation of IL-17 production in human lymphocytes. *Cytokine* **2008**, *41*, 71–78. [CrossRef] [PubMed]
38. Kirkham, B.W.; Kavanaugh, A.; Reich, K. Interleukin-17A: A unique pathway in immune-mediated diseases: Psoriasis, psoriatic arthritis and rheumatoid arthritis. *Immunology* **2014**, *141*, 133–142. [CrossRef] [PubMed]
39. Toy, D.; Kugler, D.; Wolfson, M.; Vanden Bos, T.; Gurgel, J.; Derry, J.; Tocker, J.; Peschon, J. Cutting edge: Interleukin 17 signals through a heteromeric receptor complex. *J. Immunol.* **2006**, *177*, 36–39. [CrossRef] [PubMed]
40. Rickel, E.A.; Siegel, L.A.; Yoon, B.R.P.; Rottman, J.B.; Kugler, D.G.; Swart, D.A.; Anders, P.M.; Tocker, J.E.; Comeau, M.R.; Budelsky, A.L. Identification of functional roles for both IL-17RB and IL-17RA in mediating IL-25-induced activities. *J. Immunol.* **2008**, *181*, 4299–4310. [CrossRef] [PubMed]
41. Shalom-Barak, T.; Quach, J.; Lotz, M. Interleukin-17-induced gene expression in articular chondrocytes is associated with activation of mitogen-activated protein kinases and NF-κB. *J. Biol. Chem.* **1998**, *273*, 27467–27473. [CrossRef] [PubMed]
42. Chang, S.H.; Park, H.; Dong, C. Act1 adaptor protein is an immediate and essential signaling component of interleukin-17 receptor. *J. Biol. Chem.* **2006**, *281*, 35603–35607. [CrossRef] [PubMed]
43. Zhang, B.; Liu, C.; Qian, W.; Han, Y.; Li, X.; Deng, J. Structure of the unique SEFIR domain from human interleukin 17 receptor A reveals a composite ligand-binding site containing a conserved α-helix for Act1 binding and IL-17 signaling. *Acta Crystallogr. D Biol. Crystallogr.* **2014**, *70*, 1476–1483. [CrossRef] [PubMed]
44. Sun, F.; Qu, Z.; Xiao, Y.; Zhou, J.; Burns, T.F.; Stabile, L.P.; Siegfried, J.M.; Xiao, G. NF-κB1 p105 suppresses lung tumorigenesis through the Tpl2 kinase but independently of its NF-κB function. *Oncogene* **2016**, *35*, 2299–2310. [CrossRef] [PubMed]
45. Fabre, J.; Giustinniani, J.; Antonicelli, F.; Merrouche, Y.; Bagot, M.; Bensussan, A. A focus on IL-17 targeting treatments in psoriasis. *J. Dermatol. Res.* **2016**, *2*, 1–5.
46. Haudenschild, D.; Moseley, T.; Rose, L.; Reddi, A.H. Soluble and transmembrane isoforms of novel interleukin-17 receptor-like protein by RNA splicing and expression in prostate cancer. *J. Biol. Chem.* **2002**, *277*, 4309–4316. [CrossRef] [PubMed]
47. Steiner, G.E.; Newman, M.E.; Paikl, D.; Stix, U.; Memaran-Dagda, N.; Lee, C.; Marberger, M.J. Expression and function of pro-inflammatory interleukin IL-17 and IL-17 receptor in normal, benign hyperplastic, and malignant prostate. *Prostate* **2003**, *56*, 171–182. [CrossRef] [PubMed]
48. Sfanos, K.S.; Bruno, T.C.; Maris, C.H.; Xu, L.; Thoburn, C.J.; DeMarzo, A.M.; Meeker, A.K.; Isaacs, W.B.; Drake, C.G. Phenotypic analysis of prostate-infiltrating lymphocytes reveals Th17 and Treg skewing. *Clin. Cancer Res.* **2008**, *14*, 3254–3261. [CrossRef] [PubMed]
49. Zhang, B.; Rong, G.; Wei, H.; Zhang, M.; Bi, J.; Ma, L.; Xue, X.; Wei, G.; Liu, X.; Fang, G. The prevalence of Th17 cells in patients with gastric cancer. *Biochem. Biophys. Res. Commun.* **2008**, *374*, 533–537. [CrossRef] [PubMed]
50. Derhovanessian, E.; Adams, V.; Hahnel, K.; Groeger, A.; Pandha, H.; Ward, S.; Pawelec, G. Pretreatment frequency of circulating IL-17+ CD4+ T-cells, but not Tregs, correlates with clinical response to whole-cell vaccination in prostate cancer patients. *Int. J. Cancer* **2009**, *125*, 1372–1379. [CrossRef] [PubMed]
51. Horlock, C.; Stott, B.; Dyson, P.J.; Morishita, M.; Coombes, R.C.; Savage, P.; Stebbing, J. The effects of trastuzumab on the CD4+ CD25+ FOXP3+ and CD4+ IL17A+ T-cell axis in patients with breast cancer. *Br. J. Cancer* **2009**, *100*, 1061–1067. [CrossRef] [PubMed]
52. Qian, X.; Chen, H.; Wu, X.; Hu, L.; Huang, Q.; Jin, Y. Interleukin-17 acts as double-edged sword in anti-tumor immunity and tumorigenesis. *Cytokine* **2015**. [CrossRef] [PubMed]

53. Tartour, E.; Fossiez, F.; Joyeux, I.; Galinha, A.; Gey, A.; Claret, E.; Sastre-Garau, X.; Couturier, J.; Mosseri, V.; Vives, V.; et al. Interleukin 17, a T-cell-derived cytokine, promotes tumorigenicity of human cervical tumors in nude mice. *Cancer Res.* **1999**, *59*, 3698–3704. [PubMed]
54. Punt, S.; Fleuren, G.J.; Kritikou, E.; Lubberts, E.; Trimbos, J.B.; Jordanova, E.S.; Gorter, A. Angels and demons: Th17 cells represent a beneficial response, while neutrophil IL-17 is associated with poor prognosis in squamous cervical cancer. *Oncoimmunology* **2015**, *4*, e984539. [CrossRef] [PubMed]
55. Lyon, D.E.; McCain, N.L.; Walter, J.; Schubert, C. Cytokine comparisons between women with breast cancer and women with a negative breast biopsy. *Nurs. Res.* **2008**, *57*, 51–58. [CrossRef] [PubMed]
56. Zhu, X.; Mulcahy, L.A.; Mohammed, R.A.; Lee, A.H.; Franks, H.A.; Kilpatrick, L.; Yilmazer, A.; Paish, E.C.; Ellis, I.O.; Patel, P.M.; et al. IL-17 expression by breast-cancer-associated macrophages: IL-17 promotes invasiveness of breast cancer cell lines. *Breast Cancer Res.* **2008**, *10*, 95–106. [CrossRef] [PubMed]
57. Du, J.W.; Xu, K.Y.; Fang, L.Y.; Qi, X.L. Interleukin-17, produced by lymphocytes, promotes tumor growth and angiogenesis in a mouse model of breast cancer. *Mol. Med. Rep.* **2012**, *6*, 1099–1102. [CrossRef] [PubMed]
58. Furuta, S.; Jeng, Y.M.; Zhou, L.; Huang, L.; Kuhn, I.; Bissell, M.J.; Lee, W.H. IL-25 causes apoptosis of IL-25R-expressing breast cancer cells without toxicity to nonmalignant cells. *Sci. Transl. Med.* **2011**. [CrossRef] [PubMed]
59. Kim, G.; Khanal, P.; Lim, S.C.; Yun, H.J.; Ahn, S.G.; Ki, S.H.; Choi, H.S. Interleukin-17 induces AP-1 activity and cellular transformation via upregulation of tumor progression locus 2 activity. *Carcinogenesis* **2013**, *34*, 341–350. [CrossRef] [PubMed]
60. Cochaud, S.; Giustiniani, J.; Thomas, C.; Laprevotte, E.; Garbar, C.; Savoye, A.M.; Cure, H.; Mascaux, C.; Alberici, G.; Bonnefoy, N.; et al. IL-17A is produced by breast cancer TILs and promotes chemoresistance and proliferation through ERK1/2. *Sci. Rep.* **2013**, *3*, 3456–3466. [CrossRef] [PubMed]
61. Mombelli, S.; Cochaud, S.; Merrouche, Y.; Garbar, C.; Antonicelli, F.; Laprevotte, E.; Alberici, G.; Bonnefoy, N.; Eliaou, J.F.; Bastid, J.; et al. IL-17A and its homologs IL-25/IL-17E recruit the c-RAF/S6 kinase pathway and the generation of pro-oncogenic LMW-E in breast cancer cells. *Sci. Rep.* **2015**, *5*, 11874–11884. [CrossRef] [PubMed]
62. Benatar, T.; Cao, M.Y.; Lee, Y.; Lightfoot, J.; Feng, N.; Gu, X.; Lee, V.; Jin, H.; Wang, M.; Wright, J.A.; et al. IL-17E, a proinflammatory cytokine, has antitumor efficacy against several tumor types in vivo. *Cancer Immunol. Immunother.* **2010**, *59*, 805–817. [CrossRef] [PubMed]
63. Benatar, T.; Cao, M.Y.; Lee, Y.; Li, H.; Feng, N.; Gu, X.; Lee, V.; Jin, H.; Wang, M.; Der, S.; et al. Virulizin induces production of IL-17E to enhance antitumor activity by recruitment of eosinophils into tumors. *Cancer Immunol. Immunother.* **2008**, *57*, 1757–1769. [CrossRef] [PubMed]
64. Duong, M.T.; Akli, S.; Wei, C.; Wingate, H.F.; Liu, W.; Lu, Y.; Yi, M.; Mills, G.B.; Hunt, K.K.; Keyomarsi, K. LMW-E/CDK2 deregulates acinar morphogenesis, induces tumorigenesis, and associates with the activated b-Raf-ERK1/2-mTOR pathway in breast cancer patients. *PLoS Genet.* **2012**, *8*, e1002538. [CrossRef] [PubMed]
65. De Marzo, A.M.; Marchi, V.L.; Epstein, J.I.; Nelson, W.G. Proliferative inflammatory atrophy of the prostate: Implications for prostatic carcinogenesis. *Am. J. Pathol.* **1999**, *155*, 1985–1992. [CrossRef]
66. You, Z.; Dong, Y.; Kong, X.; Zhang, Y.; Vessella, R.L.; Melamed, J. Differential expression of IL-17RC isoforms in androgen-dependent and androgen-independent prostate cancers. *Neoplasia* **2007**, *9*, 464–470. [CrossRef] [PubMed]
67. You, Z.; Ge, D.; Liu, S.; Zhang, Q.; Borowsky, A.D.; Melamed, J. Interleukin-17 induces expression of chemokines and cytokines in prostatic epithelial cells but does not stimulate cell growth in vitro. *Int. J. Med. Biol. Front.* **2012**, *18*, 629–644. [PubMed]
68. Liu, S.; Zhang, Q.; Chen, C.; Ge, D.; Qu, Y.; Chen, R.; Fan, Y.M.; Li, N.; Tang, W.W.; Zhang, W.; et al. Hyperinsulinemia enhances interleukin-17-induced inflammation to promote prostate cancer development in obese mice through inhibiting glycogen synthase kinase 3-mediated phosphorylation and degradation of interleukin-17 receptor. *Oncotarget* **2016**, *7*, 13651–13666. [PubMed]
69. Zhang, Q.; Liu, S.; Ge, D.; Zhang, Q.; Xue, Y.; Xiong, Z.; Abdel-Mageed, A.B.; Myers, L.; Hill, S.M.; Rowan, B.G.; et al. Interleukin-17 promotes formation and growth of prostate adenocarcinoma in mouse models. *Cancer Res.* **2012**, *72*, 2589–2599. [CrossRef] [PubMed]
70. Zhang, Q.; Liu, S.; Parajuli, K.R.; Zhang, W.; Zhang, K.; Mo, Z.; Liu, J.; Chen, Z.; Yang, S.; Wang, A.R.; et al. Interleukin-17 promotes prostate cancer via MMP7-induced epithelial-to-mesenchymal transition. *Oncogene* **2016**. [CrossRef] [PubMed]

71. Zhou, Y.; Toh, M.L.; Zrioual, S.; Miossec, P. IL-17A versus IL-17F induced intracellular signal transduction pathways and modulation by IL-17RA and IL-17RC RNA interference in AGS gastric adenocarcinoma cells. *Cytokine* **2007**, *38*, 157–164. [CrossRef] [PubMed]
72. Bie, Q.; Sun, C.; Gong, A.; Li, C.; Su, Z.; Zheng, D.; Ji, X.; Wu, Y.; Guo, Q.; Wang, S.; et al. Non-tumor tissue derived interleukin-17B activates IL-17RB/AKT/β-catenin pathway to enhance the stemness of gastric cancer. *Sci. Rep.* **2016**, *6*, 25447–25459. [CrossRef] [PubMed]
73. Li, B.; Shi, X.Y.; Liao, D.X.; Cao, B.R.; Luo, C.H.; Cheng, S.J. Advanced colorectal adenoma related gene expression signature may predict prognostic for colorectal cancer patients with adenoma-carcinoma sequence. *Int. J. Clin. Exp. Med.* **2015**, *8*, 4883–4898. [PubMed]
74. Cui, G.; Yuan, A.; Goll, R.; Florholmen, J. IL-17A in the tumor microenvironment of the human colorectal adenoma-carcinoma sequence. *Scand. J. Gastroenterol.* **2012**, *47*, 1304–1312. [CrossRef] [PubMed]
75. Al-Samadi, A.; Moossavi, S.; Salem, A.; Sotoudeh, M.; Tuovinen, S.M.; Konttinen, Y.T.; Salo, T.; Bishehsari, F. Distinctive expression pattern of interleukin-17 cytokine family members in colorectal cancer. *Tumour Biol.* **2016**, *37*, 1609–1615. [CrossRef] [PubMed]
76. Housseau, F.; Wu, S.; Wick, E.C.; Fan, H.; Wu, X.; Llosa, N.J.; Smith, K.N.; Tam, A.; Ganguly, S.; Wanyiri, J.W.; et al. Redundant innate and adaptive sources of IL17 production drive colon tumorigenesis. *Cancer Res.* **2016**, *76*, 2115–2124. [CrossRef] [PubMed]
77. Pan, B.; Che, D.; Cao, J.; Shen, J.; Jin, S.; Zhou, Y.; Liu, F.; Gu, K.; Man, Y.; Shang, L.; et al. Interleukin-17 levels correlate with poor prognosis and vascular endothelial growth factor concentration in the serum of patients with non-small cell lung cancer. *Biomarkers* **2015**, *20*, 232–239. [CrossRef] [PubMed]
78. Pan, B.; Shen, J.; Cao, J.; Zhou, Y.; Shang, L.; Jin, S.; Cao, S.; Che, D.; Liu, F.; Yu, Y. Interleukin-17 promotes angiogenesis by stimulating VEGF production of cancer cells via the STAT3/GIV signaling pathway in non-small-cell lung cancer. *Sci. Rep.* **2015**, *5*, 16053–16066. [CrossRef] [PubMed]
79. Numasaki, M.; Watanabe, M.; Suzuki, T.; Takahashi, H.; Nakamura, A.; McAllister, F.; Hishinuma, T.; Goto, J.; Lotze, M.T.; Kolls, J.K.; et al. IL-17 enhances the net angiogenic activity and in vivo growth of human non-small cell lung cancer in SCID mice through promoting CXCR-2-dependent angiogenesis. *J. Immunol.* **2005**, *175*, 6177–6189. [CrossRef] [PubMed]
80. He, D.; Li, H.; Yusuf, N.; Elmets, C.A.; Athar, M.; Katiyar, S.K.; Xu, H. IL-17 mediated inflammation promotes tumor growth and progression in the skin. *PLoS ONE* **2012**, *7*, e32126. [CrossRef] [PubMed]
81. McAllister, F.; Kolls, J.K. Th17 cytokines in non-melanoma skin cancer. *Eur. J. Immunol.* **2015**, *45*, 692–694. [CrossRef] [PubMed]
82. Wu, L.; Chen, X.; Zhao, J.; Martin, B.; Zepp, J.A.; Ko, J.S.; Gu, C.; Cai, G.; Ouyang, W.; Sen, G.; et al. A novel IL-17 signaling pathway controlling keratinocyte proliferation and tumorigenesis via the TRAF4-ERK5 axis. *J. Exp. Med.* **2015**, *212*, 1571–1587. [CrossRef] [PubMed]
83. Wang, L.; Yi, T.; Kortylewski, M.; Pardoll, D.M.; Zeng, D.; Yu, H. IL-17 can promote tumor growth through an IL-6-STAT3 signaling pathway. *J. Exp. Med.* **2009**, *206*, 1457–1464. [CrossRef] [PubMed]
84. Doroudchi, M.; Pishe, Z.G.; Malekzadeh, M.; Golmoghaddam, H.; Taghipour, M.; Ghaderi, A. Elevated serum IL-17A but not IL-6 in glioma versus meningioma and schwannoma. *Asian Pac. J. Cancer Prev.* **2013**, *14*, 5225–5230. [CrossRef] [PubMed]
85. Kehlen, A.; Thiele, K.; Riemann, D.; Rainov, N.; Langner, J. Interleukin-17 stimulates the expression of IκB-α mRNA and the secretion of IL-6 and IL-8 in glioblastoma cell lines. *J. Neuroimmunol.* **1999**, *101*, 1–6. [CrossRef]
86. Wainwright, D.A.; Sengupta, S.; Han, Y.; Ulasov, I.V.; Lesniak, M.S. The presence of IL-17A and T helper 17 cells in experimental mouse brain tumors and human glioma. *PLoS ONE* **2010**, *5*, e15390. [CrossRef] [PubMed]
87. Cantini, G.; Pisati, F.; Mastropietro, A.; Frattini, V.; Iwakura, Y.; Finocchiaro, G.; Pellegatta, S. A critical role for regulatory T cells in driving cytokine profiles of Th17 cells and their modulation of glioma microenvironment. *Cancer Immunol. Immunother.* **2011**, *60*, 1739–1750. [CrossRef] [PubMed]
88. Hu, J.; Ye, H.; Zhang, D.; Liu, W.; Li, M.; Mao, Y.; Lu, Y. U87MG glioma cells overexpressing IL-17 acclerate early-stage growth in vivo and cause a higher level of CD31 mRNA expression in tumor tissues. *Oncol. Lett.* **2013**, *6*, 993–999. [PubMed]

89. Liang, H.; Yi, L.; Wang, X.; Zhou, C.; Xu, L. Interleukin-17 facilitates the immune suppressor capacity of high-grade glioma-derived CD4+ CD25+ Foxp3+ T cells via releasing transforming growth factor β. *Scand. J. Immunol.* **2014**, *80*, 144–150. [CrossRef] [PubMed]
90. Parajuli, P.; Anand, R.; Mandalaparty, C.; Suryadevara, R.; Sriranga, P.U.; Michelhaugh, S.K.; Cazacu, S.; Finniss, S.; Thakur, A.; Lum, L.G.; et al. Preferential expression of functional IL-17R in glioma stem cells: Potential role in self-renewal. *Oncotarget* **2016**, *7*, 6121–6135. [PubMed]
91. Zhang, J.P.; Yan, J.; Xu, J.; Pang, X.H.; Chen, M.S.; Li, L.; Wu, C.; Li, S.P.; Zheng, L. Increased intratumoral IL-17-producing cells correlate with poor survival in hepatocellular carcinoma patients. *J. Hepatol.* **2009**, *50*, 980–989. [CrossRef] [PubMed]
92. Kuang, D.M.; Peng, C.; Zhao, Q.; Wu, Y.; Zhu, L.Y.; Wang, J.; Yin, X.Y.; Li, L.; Zheng, L. Tumor-activated monocytes promote expansion of IL-17-producing CD8+ T cells in hepatocellular carcinoma patients. *J. Immunol.* **2010**, *185*, 1544–1549. [CrossRef] [PubMed]
93. Sternlicht, M.D.; Lochter, A.; Sympson, C.J.; Huey, B.; Rougier, J.P.; Gray, J.W.; Pinkel, D.; Bissell, M.J.; Werb, Z. The stromal proteinase MMP3/stromelysin-1 promotes mammary carcinogenesis. *Cell* **1999**, *98*, 137–146. [CrossRef]
94. Stallings-Mann, M.L.; Waldmann, J.; Zhang, Y.; Miller, E.; Gauthier, M.L.; Visscher, D.W.; Downey, G.P.; Radisky, E.S.; Fields, A.P.; Radisky, D.C. Matrix metalloproteinase induction of Rac1b, a key effector of lung cancer progression. *Sci. Transl. Med.* **2012**. [CrossRef] [PubMed]
95. Ma, Y.; Aymeric, L.; Locher, C.; Mattarollo, S.R.; Delahaye, N.F.; Pereira, P.; Boucontet, L.; Apetoh, L.; Ghiringhelli, F.; Casares, N.; et al. Contribution of IL-17-producing γ delta T cells to the efficacy of anticancer chemotherapy. *J. Exp. Med.* **2011**, *208*, 491–503. [CrossRef] [PubMed]
96. O'Sullivan, T.; Saddawi-Konefka, R.; Gross, E.; Tran, M.; Mayfield, S.P.; Ikeda, H.; Bui, J.D. Interleukin-17D mediates tumor rejection through recruitment of natural killer cells. *Cell Rep.* **2014**, *7*, 989–998. [CrossRef] [PubMed]

MUC/EGFR/IL17 et l'autophagie sont associés à la résistance à la chimiothérapie ou aux thérapies ciblées dans les cancers du sein triple négatif.

Le cancer du sein triple négatif (TN) est un cancer présentant des résistances aux agents de chimiothérapie. Malgré la forte expression de l'EGFR, il est aussi résistant aux agents anti-EGFR. Ces mécanismes de résistance ne sont pas connus. MUC1 est une protéine transmembranaire largement glycosylée. Sa fonction extracellulaire est impliquée dans la régulation des récepteurs membranaires, dont l'EGFR. Comme les autres glycoprotéines membranaires, son unité extracellulaire (MUC1-N) peut moduler la réponse cellulaire immune par hypersialylation. Son unité intracellulaire (MUC1-C) possède des sites de phosphorylation impliqués dans plusieurs voies de signalisation telles que PI3K/AKT/mTOR ou RAS/RAF/MEK/ERK. Ces dernières régulent l'autophagie qui est un mécanisme de survie cellulaire associé à la résistance aux agents de chimiothérapie. Nous avons démontré que les TN présentaient des modifications quantitatives et qualitatives de l'expression de MUC1, altérant probablement les régulations des voies associées à MUC1/EGFR dont l'autophagie. L'activation de l'autophagie explique la résistance aux traitements des agents de chimiothérapie. L'IL17 est un facteur pro-inflammatoire secrété par du microenvironnement tumoral et associé également à la résistance des agents de chimiothérapie des TN, par activation de la voie MEK/ERK, suggérant son implication à activer l'autophagie. En conclusion, nos travaux permettent d'émettre l'hypothèse que l'inhibition de l'autophagie et/ou MUC1 et/ou IL17 pourrait augmenter la sensibilité aux traitements de chimiothérapie ou des thérapies ciblées dirigées contre les TN.

Mots-clés : MUC1, EGFR, IL17, autophagie, triple-négatif, sein, cancer

MUC1/EGFR/IL17 and autophagy are associated in resistance of chemiotherapy or targeted therapy in triple negative breast cancer.

Triple negative breast cancer (TN) is often associated to chemioresistance. Despite an EGRF over-expression, TN is also resistant to anti-EGFR drugs. These resistance mechanisms are not known yet. MUC1 is a transmembrane broadly glycosylated protein. Its extracellular unit (MUC-N) is involved to membrane receptor regulations, as EGFR. As other membrane glycoproteins, MUC1 could modulate, by over-sialylation, the immune cellular response. Its intracellular unit (MUC-C) presents phosphorylation sites involved in numerous signal pathways such as PI3K/AKT/mTOR or RAS/RAF/MEK/ERK. Both pathways regulate autophagy which is a survival cellular mechanism associated to resistance of chemiotherapy drugs. We showed that TN presents quantitative and qualitative MUC1 alterations, likely associated with dys-regulation of autophagy/MUC1/EGFR pathways. The activation of autophagy explains the chemiotherapy resistance. IL17 is a proinflammatory interleukin secreted by the tumor microenvironment. In TN, IL17 is also associated to chemiorestistance throughout the MEK/ERK pathways, suggesting its involving activating autophagy.In conclusion, our work allows us to hypothesize that inhibition of autophagy and/or MUC1 and/or IL17 could be increasing the sensibility to chemiotherapy or targeted therapies against TN.

Key words : MUC1, EGFR, IL17, autophagie, triple-negative, breast, cancer

Discipline : SCIENCES DE LA VIE ET DE LA SANTE

Spécialité : Médecine - STS

Université de Reims Champagne-Ardenne

ICA - EA 7319

Pôle Santé, 51 rue Cognacq-Jay, 51095 Reims